In vivo analysis of RNA polymerase I elongation and termination in *Saccharomyces cerevisiae*

vorgelegt von

Alarich Reiter

aus

Temeschburg

im Juni 2011

Promotionsgesuch eingereicht am: 15. Juni 2011

Die Arbeit wurde angeleitet von: Prof. Dr. Herbert Tschochner

Prüfungsausschuss:

      Vorsitzender: Prof. Dr. Reinhard Wirth
      1. Prüfer: Prof. Dr. Herbert Tschochner
      2. Prüfer: Prof. Dr. Michael Thomm
      3. Prüfer: Prof. Dr. Reinhard Sterner

Tag der mündlichen Prüfung: 26. Juli 2011

Die vorliegende Arbeit wurde in der Zeit von April 2007 bis Juni 2011 am Lehrstuhl Biochemie III des Instituts für Biochemie, Genetik und Mikrobiologie der Naturwissenschaftlichen Fakultät III der Universität Regensburg unter Anleitung von Prof. Dr. Herbert Tschochner angefertigt.

Ich erkläre hiermit, dass ich diese Arbeit selbst verfasst und keine anderen als die angegebenen Quellen und Hilfsmittel verwendet habe.
Diese Arbeit war bisher noch nicht Bestandteil eines Prüfungsverfahrens.
Andere Promotionsversuche wurden nicht unternommen.

Regensburg, den 15. Juni 2011

Alarich Reiter

Table of Contents

1 INTRODUCTION

1.1 RNA polymerases

In 1960, Sam Weiss, Audrey Stevens, and Jerard Hurwitz independently discovered a RNA polymerase. One year before the Nobel Prize in Medicine had been awarded to Severo Ochoa and Arthur Kornberg for their discovery of the mechanisms in the biological synthesis of RNA and DNA by the identification of a DNA polymerase. Interestingly, another Nobel Prize was awarded to the polymerase research field in 2006, emphasizing general importance of these kind of enzymes. Roger Kornberg, Arthur Kornberg`s son, was awarded for describing the molecular mechanism of elongating RNA polymerase II.

The DNA-dependent RNA polymerase (RNAP) is an enzyme which catalyzes the synthesis of ribonucleic acids (RNAs) in a process called transcription. RNAP is a nucleotidyl transferase that polymerizes ribonucleotides in a 5´-3´-direction on a DNA gene template.

In general, RNA polymerases can initiate transcription at specific DNA sequences known as promoters. It then produces an RNA chain which is complementary to the template DNA strand. The process of adding nucleotides to the RNA strand is called elongation. The release of its RNA transcript at specific DNA sequences, encoded at the end of genes is known as termination.

RNAPs are essential for growth and are found in all organisms and many viruses.

Most information on viral RNA polymerases is available from the RNAP of the bacteriophage T7. The single-subunit T7 RNA polymerase is related to that found in mitochondria and chloroplasts (Hedtke et al., 1997), and shares considerable homology to DNA polymerases. It is suggested that most viral polymerases therefore evolved from a DNA polymerase and are not directly related to the multi-subunit RNA polymerases.

In bacteria, one RNA polymerase catalyzes the synthesis of the three major RNAs (rRNA, mRNA, and tRNA). The core enzyme consists of 5 subunits whereas the complete holoenzyme contains 6 subunits: $\alpha_2\beta\beta'\sigma\omega$ (~480 kDa). The sigma factor (σ) greatly reduces the affinity of RNAP for nonspecific DNA while increasing specificity for certain promoter regions to assure correct transcription initiation.

Archaea also have a single RNAP that synthesizes all three major RNAs. However, it is closely related in structure and function to the three main eukaryotic RNA polymerases (Hirata et al., 2008). Thus, it has been speculated that the archaeal RNA polymerase and the three specialized eukaryotic RNA polymerases evolved from a common ancestor.

Initially only one single RNA polymerase had been characterized in extracts from different eukaryotic organisms varying from mammals to yeast (Weiss, 1960). A decade later the

purification of the polymerase over an anion exchange column resulted in three different fractions, namely RNA polymerase I, II, and III (Roeder and Rutter, 1969). RNAPI synthesizes the precursor of ribosomal RNA (rRNA). RNAPII synthesizes precursors of mRNAs, most small nuclear RNAs (snRNA), and microRNAs (Lee et al., 2004). RNAPIII synthesizes tRNAs, 5S rRNA and other small RNAs found in the nucleus and cytosol (Willis, 1993). In plants, two additional RNAPs were identified. RNAPIV and RNAPV are related to siRNA metabolism (Herr et al., 2005; Wierzbicki et al., 2009). Other RNAPs exist in mitochondria and chloroplasts.

Additionally, RNA-dependent RNA polymerases are involved in RNA interference (Makeyev and Bamford, 2002).

It is unclear yet, why a specialization of RNA synthesis occured during evolution and what are the molecular basics of this specialization. One of the features of this specialization in RNA production is the association of the different RNAPs with different nuclear sub-domains. This correlation may suggest that spatial separation of the transcription apparatuses in the nucleus provides an advantage for eukaryotic cells.

An example of a complex interplay between all three nuclear RNAPs is the synthesis of ribosomes. All nuclear RNAPs are involved to assure that ribosomal components are available in stoichiometric amounts. This process needs to be well adapted to the proliferation state of a cell, and it was suggested that the RNA polymerases need to be tightly coregulated (Warner, 1999).

1.2 RNA polymerase I transcription

1.2.1 Cellular localization and structure of ribosomal RNA genes

Ribosomal RNA genes are localized in the nucleolus, which is the major site of RNA polymerase I transcription in eukaryotic cells. The nucleolus denotes a specialized sub-compartment of the nucleus. In yeast, only one single nucleolus is found. Under the electron microscope (EM), three morphologically different regions of the nucleolus can be distinguished, namely fibrillar centers (FC), a dense fibrillar component (DFC), and a granular component (GC) (Figure 1). Fibrillar centers are detected near the nuclear envelope and contain the rDNA (Schwarzacher and Wachtler, 1993). These fibrillar centers are surrounded by a dense fibrillar component, where the nascent rRNA transcripts accumulate (Cmarko et al., 2000). Transcripts extend as a network throughout the nucleolar volume and contain the Pol I transcription machinery. This arrangement of rDNA in the FCs and nascent transcript in the DFC suggests a model, where rRNA transcription from the rDNA occurs just at the interface between FC and DFC. The granular component is dispersed throughout the rest of the nucleolus and contains the maturing pre-ribosomes (Léger-Silvestre et al., 1999).

2
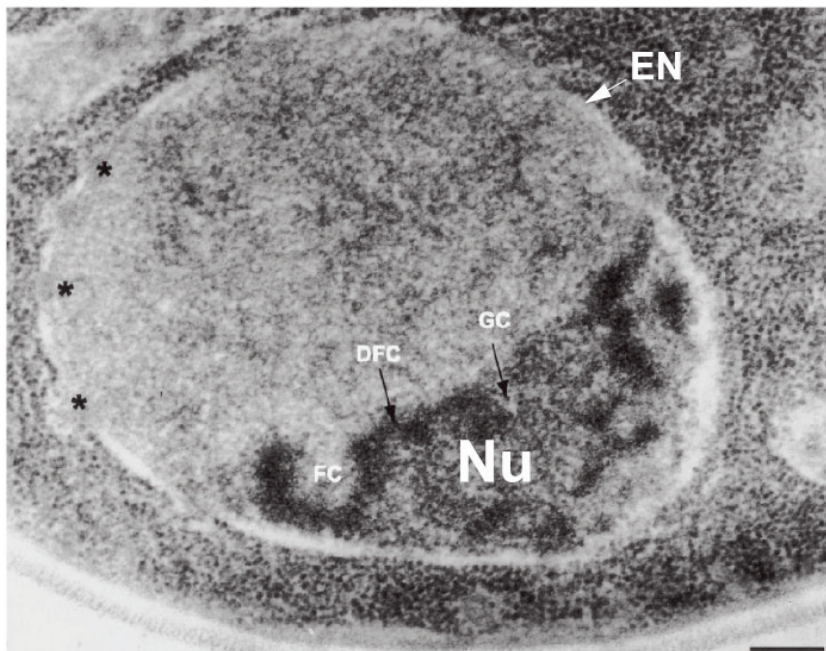
Figure 1. Nucleolar structure of *Saccharomyces cerevisiae*
Electron micrograph of a yeast nucleus. Nuclear pore complexes are marked (*). The nucleolus (Nu) can be seen as an electron dense structure next to the nuclear envelope (EN). The nucleolus is sub-structured into 3 sub-compartments visible in EM: the fibrillar center (FC), the dense fibrillar component (DFC) and the granular component (GC). Scale bar is 0.2μm. (from Léger-Silvestre et al., 1999)

In *S. cerevisiae* the rRNA genes are located on the right arm of Chromosome XII and consist of about 150-200 transcription units arranged in a tandem array (Schweizer and Halvorson, 1969; Petes, 1979). Each rDNA copy has a size of 9.1-kilobase pairs (kb) (Figure 2). The number of repeats is dynamic and can vary due to unequal meiotic and mitotic recombination events (Warner, 1989). Each of the repeated rDNA units is composed of the Pol I transcribed 35S rRNA gene and the gene for the 5S rRNA, which is transcribed in the opposite direction by Pol III (Philippsen et al., 1978). The presence of the 5S rRNA gene within the rDNA unit in *S. cerevisiae* is different from the situation in other eukaryotes where the 5S rRNA repeats are separated from the nucleolar rRNA repeats (Rubin and Sulston, 1973; Drouin and de Sá, 1995; Geiduschek and Kassavetis, 2001). The 35S rRNA is transcribed as a precursor which is processed into the mature 18S, 5.8S, and 25S rRNAs. Different elements important for the regulation of rDNA transcription have been identified within the 35S rRNA gene (Kulkens et al., 1991; Musters et al., 1989). The upstream element (UE) and the core element (CE) are located on the 5´ end of the 35S rDNA within the intergenic spacer region 2 (IGS2). These elements span about 170 bp and constitute the 35S rDNA promoter.

A third element, called enhancer (ENH), is located at the 3´ end of the 35S transcription unit. This element has been shown to exhibit a stimulatory effect on RNA synthesis by Pol I, using Pol I reporter templates, either *in vitro* or *in vivo* (Elion and Warner, 1984, 1986). The ENH region also contains two terminators for 35S rDNA transcription (Reeder et al., 1999).
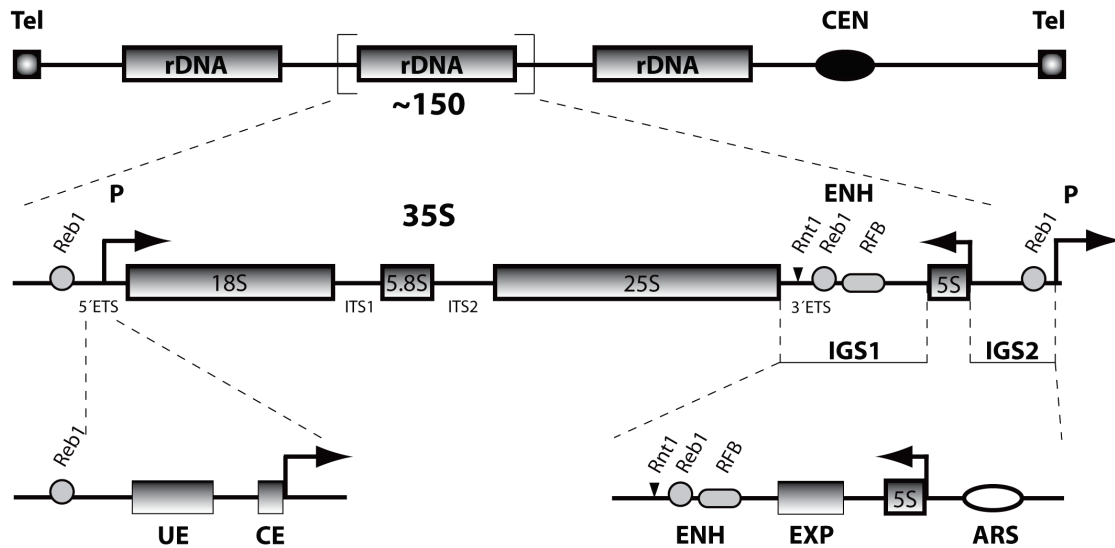
Figure 2. Schematic representation of the rDNA locus in *S. cerevisiae*

The position of the rDNA repeat cluster on chromosome XII with respect to the centromere (CEN) and telomeres (Tel) is shown. Each rDNA repeat consists of the Pol I transcribed 35S rRNA gene (precursor for the 18S, 5.8S, and 25S rRNAs), the RNA Pol III transcribed 5S rRNA gene and two intergenic spacer regions IGS 1 and 2. Arrows mark the transcription start sites and direction. The positions of several DNA elements like the 5` and 3` external transcribed spacers (ETS), the internal transcribed spacers (ITS) 1 and 2, as well as the Reb1 binding site (Reb1), the RNAse III (Rnt1) cleavage site, and the replication fork barrier (RFB) are indicated. The upstream element (UE) and core element (CE) constitute the Pol I promoter (P). Termination occurs at the Reb1 binding site which is located within a region called enhancer (ENH). Sites of autonomous replication sequence (ARS) and a region required for repeat expansion (EXP), harboring a bidirectional Pol II promoter, are depicted.

Several other *cis*-regulatory elements unrelated to 35S rDNA transcription are located within IGS1 and IGS2. During S-phase, bidirectional replication is initiated at the ribosomal autonomous sequence (rARS) (Linskens and Huberman, 1988). A replication fork barrier (RFB) site is located near the enhancer element and allows the progression of the replication fork in the direction of 35S rDNA transcription but not in the opposite direction (Brewer and Fangman, 1988; Brewer et al., 1992; Fangman and Brewer, 1992; Kobayashi et al., 1992). The replication fork blocking protein (Fob1) binds to the RFB and is required for this activity (Kobayashi and Horiuchi, 1996). In addition, Fob1 is required for expansion and contraction of rDNA repeats (Kobayashi et al., 1998). These repeat expansion and contraction events require recombination which is triggered by double strand breaks introduced into the rDNA by Fob1-dependent pausing of the DNA replication machinery at RFB sites (Burkhalter and Sogo, 2004; Kobayashi et al., 1998, 2004). In addition to the RFB, the adjacent region (EXP) has also been shown to be required for repeat expansion (Kobayashi et al., 2001). This region harbors a bidirectional Pol II promoter which drives the transcription of non-coding RNAs (Ganley et al., 2005; Houseley et al., 2007).

1.2.2 RNA polymerase I structure and subunit composition

The yeast enzyme RNA polymerase I is a multi-protein complex consisting of 14 different subunits as revealed by the analyses of Pol I complexes purified by diverse methods (Keener et al., 1998; Carles et al., 1991; Kuhn et al., 2007; Paule, 1999). Their designation in the common Pol I nomenclature is composed of the letter A, B and/or C indicating the appearance of the subunit in RNA polymerase I, II and/or III, respectively, and of a number denoting the respective molecular weight in kDa as determined by SDS-PAGE (Table 1). All but four of the Pol I subunits are essential proteins (Mémet et al., 1988; Yano and Nomura, 1991; Thuriaux et al., 1995; Mann et al., 1987; Woychik et al., 1990; Dequard-Chablat et al., 1991; Treich et al., 1992).

Table 1. Subunit composition of RNA polymerases

Eukaryotes			Archaea	Bacteria	Subunit type
Pol I	Pol II	Pol III			
A190	Rpb1	C160	A´+A´´	β´	core/homolog
A135	Rpb2	C128	B (B´+B´´)	β	core/homolog
AC40	Rpb3	AC40	D	α	core/homolog
AC19	Rpb11	AC19	L	α	core/homolog
ABC27	ABC27 (Rpb5)	ABC27	H	ω	core/common
ABC23	ABC23 (Rpb6)	ABC23	K	-	common
ABC14.5	ABC14.5 (Rpb8)	ABC14.5	-	-	common
ABC10α	ABC10α (Rpb10)	ABC10α	N	-	common
ABC10β	ABC10β (Rpb12)	ABC10β	P	-	common
A12.2*	Rpb9	C11	X	-	homolog
A14*	Rpb4	C17	F	-	counterpart
A43	Rpb7	C25	E	-	counterpart
A49*	-	C37	-	-	Pol I/III specific
A34.5*	-	C53	-	-	Pol I/III specific
-	-	C82	-	-	Pol III specific
-	-	C34	-	-	Pol III specific
-	-	C31	-	-	Pol III specific

Non-essential Pol I subunits are marked with a *

Molecular details of multisubunit RNA polymerases have been revealed by the crystal structures of the bacterial RNA polymerase from *Thermus aquaticus* (Zhang et al., 1999; Vassylyev et al., 2002). To date most progress in structural studies for eukaryotic polymerases was achieved for RNA polymerase II, culminating in the atomic structure of the 10-subunit core

enzyme (Cramer et al., 2001) and the complete 12-subunit enzyme structure (Armache et al., 2005). As suggested by the high degree of conservation between the polymerase subunits, it resembles the general architecture of multisubunit RNA polymerases (Bischler et al., 2002; Cramer, 2002; Kuhn et al., 2007).

The Pol I structure has been intensively investigated by EM, immuno-EM and cryo-EM analyses (Schultz et al., 1993; Klinger et al., 1996; Bischler et al., 2002; De Carlo et al., 2003; Kuhn et al., 2007). The Pol II crystal structure could be fitted into the Pol I cryo-EM maps (Bischler et al., 2002; Kuhn et al., 2007). Based on the structural similarities, sequence alignments and a new crystal structure of the Pol I subunits A43 and A14, it was only possible to construct a 12 subunit Pol I homology model (Kuhn et al., 2007) with the absence of A49 and A34.5 as their counterparts in Pol II are missing in the model. However, their position in the complex could be derived from the difference between cryo-EM maps of the complete Pol I and of a variant lacking the A34.5/A49 heterodimer (Huet et al., 1975; Kuhn et al., 2007) (Figure 3).
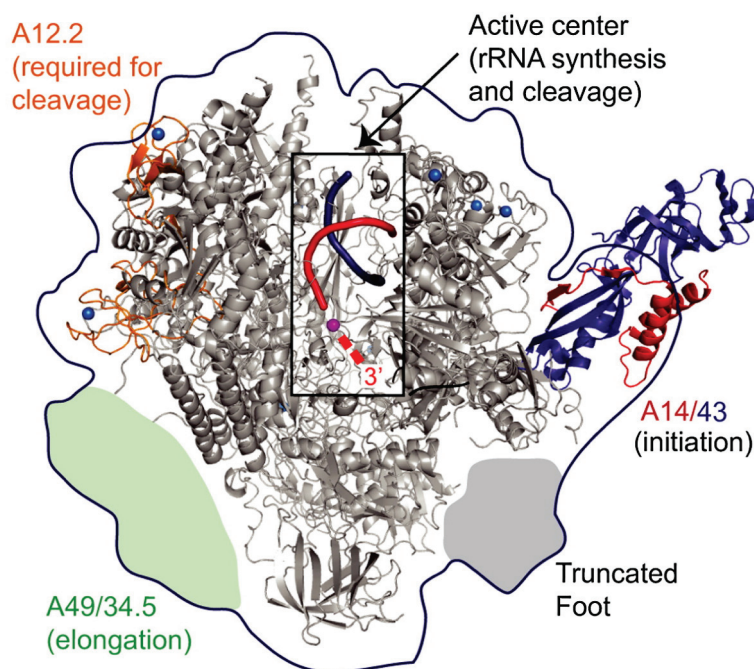
Figure 3. RNA polymerase I structure

Hybrid structure and functional architecture of Pol I. The EM envelope is shown as a blue line, the Pol I core ribbon model in gray with Rpb9 (A12.2) highlighted in orange, and the A14/43 crystal structure in red/blue. The position of the A49/34.5 heterodimer is indicated in green. The window shows a cut-away view of the active center containing a modeled DNA-RNA hybrid. Red dashes indicate the RNA 3' end extruded into the pore. (from Kuhn et al., 2007)

The two large Pol I subunits A190 and A135 form the central mass of the RNA polymerase I complex and are localized on the opposite sites of the cleft (Bischler et al., 2002). Derived from homology studies with the respective Pol II counterparts Rpb1 and Rpb2 (Mémet et al., 1988) they comprise the active center, coordinating a Mg^{2+} ion required for the enzymatic mechanism of the enzyme.

6

The two subunits AC40 and AC19 are common in Pol I and Pol III and share homologies with Rpb3 and Rpb11, the corresponding subunits of RNA polymerase II (Lalo et al., 1993). These two subunits are the counterparts of the two identical α-subunits of the bacterial enzyme and play a role in the first steps of RNA polymerase assembly (Ishihama, 1981).

The subunits ABC27, ABC23, ABC14.5, ABC10β, and ABC10α are identical in all three nuclear polymerases (Carles et al., 1991). Interestingly, ABC23 is the only common subunit with a homolog in the bacterial RNA polymerase. In Pol I it forms the main interaction interphase between the core polymerase and the two `stalk` subunits (A43, A14) and therefore plays a role in polymerase assembly (Smid et al., 1995; Lanzendörfer et al., 1997).

The subunits A14 and A43 form a heterodimer constituting the protruding `stalk`, which is distantly related to Rpb4/Rpb7 in Pol II and Rpc17/Rpc25 in Pol III (Peyroche et al., 2002; Geiger et al., 2008). The structure of these subcomplexes within the three nuclear RNA polymerases has been solved with high resolution (Armache et al., 2003; Jasiak et al., 2006; Geiger et al., 2008). Structures of A43 and its counterparts Rpb7, C25, and the archaeal RpoE can be separated into two distinct domains: the N-terminal part, involved in the binding to ABC23 (called 'tip domain'), and the C-terminal half, forming the most outer part of the stalk (called 'OB-domain') (Kuhn et al., 2007). A43 plays an important role in transcription initiation through contact formation with the respective basal transcription factor Rrn3 (Peyroche et al., 2000). However, the molecular details of this A43-Rrn3 complex formation and regulatory mechanisms controlling this interaction are still unclear and under current investigation.

Subunit A12.2 is homologous to subunit Rpb9 in Pol II and C11 in Pol III. It is non-essential under normal growth conditions, but required for growth at elevated temperatures (Nogi et al., 1993). This is consistent with its Pol II homolog Rpb9 (Woychik et al., 1991), while the homologous Pol III subunit C11 is an essential protein (Chédin et al., 1998). The A12.2 C-terminal domain contains a highly conserved motif (Q.RSADE..T.F; only Rpb9 contains variations), which is also present in the Pol II elongation factor TFIIS (Figure 4). Thus, A12.2, Rpb9, C11, and the archaeal factor TFS are sometimes referred to as TFIIS-like RNA polymerase subunits and are linked to transcript elongation (see section 1.2.4.2). However, this homology is limited to the C-terminal domain of A12.2 and the C-terminal zinc binding domain of the much larger Pol II transcript cleavage factor TFIIS (Mullem et al., 2002; Chédin et al., 1998).
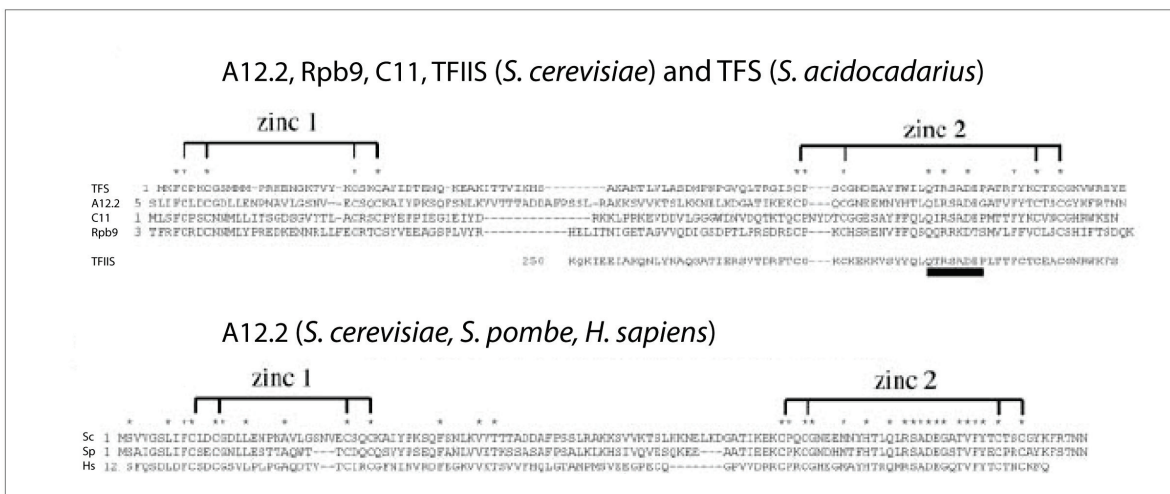
Figure 4. Homology of A12.2, Rpb9, C11, TFIIS, and TFS

Top: Sequence alignment of *S. cerevisiae* A12.2, Rpb9, C11, TFIIS, and of the archeal TFS factor (*Sulfolobus acidocaldarius*). Alignments were made using a BLOSUM 62 matrix. Stars indicate the invariant amino acids. The black bar denotes the invariant Q.RSADE..T.F motif shared by these polypeptides except Rpb9.
Bottom: Sequence alignment of *S. cerevisiae*, *S. pombe,* and *Homo sapiens* A12.2 homologues. Stars indicate the invariant amino acids shared by all three polypeptides. (modified from Mullem et al., 2002)

The TFIIS-like polymerase subunits are also involved in the transcription termination processes (Chédin et al., 1998; Landrieux et al., 2006; Prescott et al., 2004). Yeast strains lacking *RPA12* (the gene encoding A12.2) were shown to accumulate Pol I molecules in the IGS regions of the rDNA locus (Prescott et al., 2004). In the case of Pol III, C11 was identified as a termination factor, but the associated intrinsic RNA cleavage activity does not seem to be necessary (Landrieux et al., 2006).

The analysis of deletion mutants lacking either the N-terminal (A12.2 ΔN) or C-terminal half of the protein (A12.2 ΔC) revealed, that the ΔN-mutant is not able to bind to the polymerase, and thus was phenotypically indistinguishable from a strain with a full *RPA12* knock-out (Mullem et al., 2002). In the obtained Pol I structure A12.2 binds to the jaw region of the largest subunit (Figure 3). In contrast yeast strains expressing the A12.2 ΔC mutant, lacking the highly conserved domain, do not show the temperature sensitive (ts) phenotype and grow like wild-type arguing for a non-essential function of this domain. Most probably, the binding of the N-terminal half of A12.2 is required to assure the correct conformation of A190 (Mullem et al., 2002). As depicted above, A12.2 seems to play a role in several transcription processes. However, some discrepancy between *in vitro* and *in vivo* data concerning *e.g.* transcript cleavage and termination can be observed.

No counterparts in other polymerases have been found for subunits A49 and A34.5 (Gadal et al., 1997; Liljelund et al., 1992). However, local homologies were detected between these two proteins and the Pol II-associated factors TFIIF and TFIIE, respectively. It was shown *in vitro* that these subunits form a TFIIF-like heterodimer which could provide a built-in elongation factor for RNA polymerase I (Kuhn et al., 2007; Geiger et al., 2010). Whether this described function

can also be applied *in vivo* is still unclear. Genetic analyses of the deletion strains for each of the two subunits revealed synthetic lethal effects with deletions of *RPA14*. Furthermore synthetic growth defects of *Δrpa34* with the deletion of DNA Topoisomerase I (*TOP1*) and *HMO1* (Gadal et al., 1997; Berger et al., 2007) and of *Δrpa49* with deletions of DNA Topoisomerase III (*TOP3*) and *HMO1* were found (Gadal et al., 1997; Berger et al., 2007). Recently it was reported that these two subunits control the binding and release of Rrn3 during transcription and play a role in initiation and polymerase loading rate (Beckouet et al., 2008; Albert et al., 2011).

1.2.3 Assembly of RNA polymerase I

The assembly of single subunits into a RNA polymerase complex is best studied for the five subunit RNA polymerase of *E. coli*. Assembly of the polymerase core of eukaryotic enzymes seems to follow the same mechanism. The homodimerization of the bacterial α-subunits is the first step in the assembly of the RNA polymerase in *E. coli*, followed by the subsequent binding of the β- and β′-subunit (A135 and A190 Pol I counterparts, see Table 1) (Ishihama, 1981). The heterodimerization of AC40 and AC19, the α-subunit counterparts in Pol I and Pol III, has been demonstrated *in vivo* (Lalo et al., 1993; Flores et al., 1999). ABC23 (Rpb6) is the eukaryotic counterpart of the bacterial RNAP ω-subunit (Minakhin et al., 2001) whose function seems to be related to the assembly of the enzyme (Nouraini et al., 1996; Minakhin et al., 2001). In the proposed mechanism ABC23 latches the C-terminus of the largest polymerase subunit to a more N-terminal region of the protein, thus inducing a conformational change, which promotes the binding to the $\alpha_2\beta$-like intermediate complex (Minakhin et al., 2001; Lanzendörfer et al., 1997; Ghosh et al., 2001). Furthermore it forms the main interaction interphase between the core polymerase and the A14/A43 heterodimer in Pol I (Peyroche et al., 2002). Additionally the subunits ABC10α, ABC10β seem to be crucial for the assembly of the eukaryotic enzyme (Gadal et al., 1999; Rubbi et al., 1999). They form a subcomplex with the α-like polymerase subunits and seem to be involved in interactions with the large subunits (Cramer et al., 2000). The binding of the N-terminal half of A12.2 is required to assure the correct conformation and assembly of A190, increasing polymerase stability (Mullem et al., 2002).

This is consistent with the observation, that the ts-phenotype of a *Δrpa12* strain can be suppressed by overexpression of A190 (Nogi et al., 1993).

It is not easy to distinguish between effects due to the lacking activity of A12.2 or an incorrect folding of A190. For instance the 6AU-sensitivity described for *RPA12* deletion strains could also be suppressed by the overexpression of A190 (Mullem et al., 2002). The instability of A190 is probably also the cause for an observed synthetic lethal defect of *Δrpa12* when combined with either *Δrpa14* (Gadal et al., 1997) or *Δhmo1* (Berger et al., 2007).
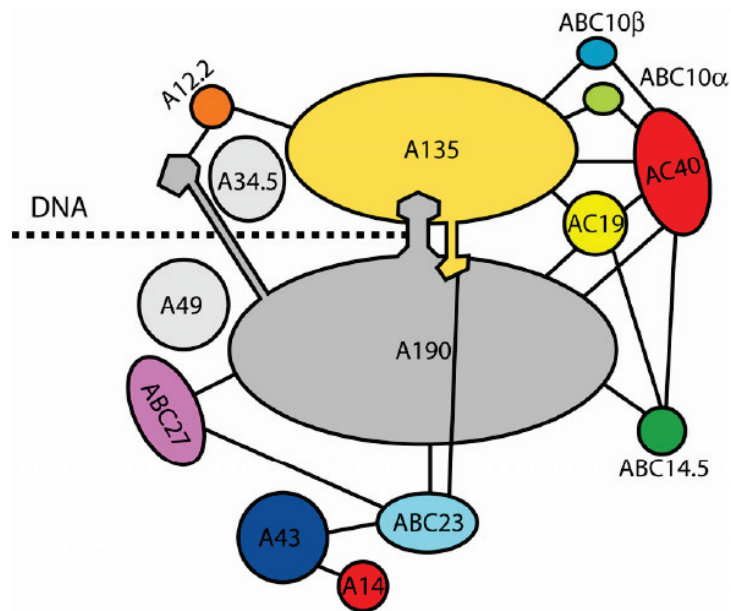
Figure 5. Interaction diagram for the Pol I subunits

The scheme was derived from interaction diagrams of the 10 subunit Pol II (Cramer et al., 2000, 2001) and represents the top view. Approximate positions of Pol I specific subunits A49, A34.5, A43, and A14 are indicated using information described by (Bischler et al., 2002). Downstream DNA bound in the cleft is also shown. (from Gerber, 2008)

1.2.4 The RNA polymerase I transcription cycle

1.2.4.1 Initiation

Pol I requires four major transcription factors to transcribe its substrate. These transcription factors are TBP, Rrn3 and two protein complexes, termed UAF for upstream activating factor and CF for core factor. The latter bind to two promoter sequences, the upstream element (UE) and the core element (CE), respectively. The UE is situated from -146 to -51 bp with respect to the transcription start site (Kulkens et al., 1991; Musters et al., 1989) and is bound by the UAF protein complex (Keys et al., 1996) which consists of the six subunits Rrn5, Rrn9, Rrn10, Uaf30, and the histones H3 and H4 (Keener et al., 1997; Keys et al., 1996; Siddiqi et al., 2001). Uaf30 was demonstrated to be important for UAF recruitment to the UE (Hontz et al., 2009), whereas the functions of the other factors, besides mediating specific protein-protein interactions (Steffan et al., 1996), are still unknown. The histones H3 and H4 are targets for multiple posttranslational modifications (Pazin and Kadonaga, 1997; Li et al., 2007a). However, it is not known if they are modified in the context of UAF. Further proximal to and including the transcription start site locates the CE at position -28 to +8 bp (Kulkens et al., 1991; Musters et al., 1989), targeted by the core factor (Keys et al., 1994; Lalo et al., 1996). CF consists of three proteins, namely Rrn6, Rrn7, and Rrn11 (Keys et al., 1994; Lalo et al., 1996). The TATA-binding protein (TBP) participates in Pol I initiation by bridgeing between UAF and CF through interaction with both complexes (Steffan et al., 1998). Rrn3 interacts directly with Pol I forming

10

an active Pol I-Rrn3 complex via interaction with the A43 subunit (Yamamoto et al., 1996; Peyroche et al., 2000). Less than 2% of Pol I is associated with Rrn3 in whole cell extracts, which is the fraction competent for initiation (Milkereit and Tschochner, 1998). In addition, Rrn3 binds to the CF subunit Rrn6 suggesting that Rrn3 may act as a bridge between CF and Pol I (Peyroche et al., 2000). Promoter assembly studies draw the current picture as follows: UAF is first recruited to the UE. TBP binds to the UAF and recruits / stabilizes the CF onto the CE. UAF and CF form a stable complex. This assembly onto the yeast ribosomal DNA (rDNA) promoter forms the pre-initiation complex (PIC), to which the initiation competent, Rrn3-associated, Pol I is recruited.

The two Pol I subunits A49 and A34.5 also seem to influence interaction properties between Rrn3 and Pol I and are essential for nucleolar assembly and for the high polymerase loading rate associated with frequent contact between adjacent enzymes (Beckouet et al., 2008; Albert et al., 2011).
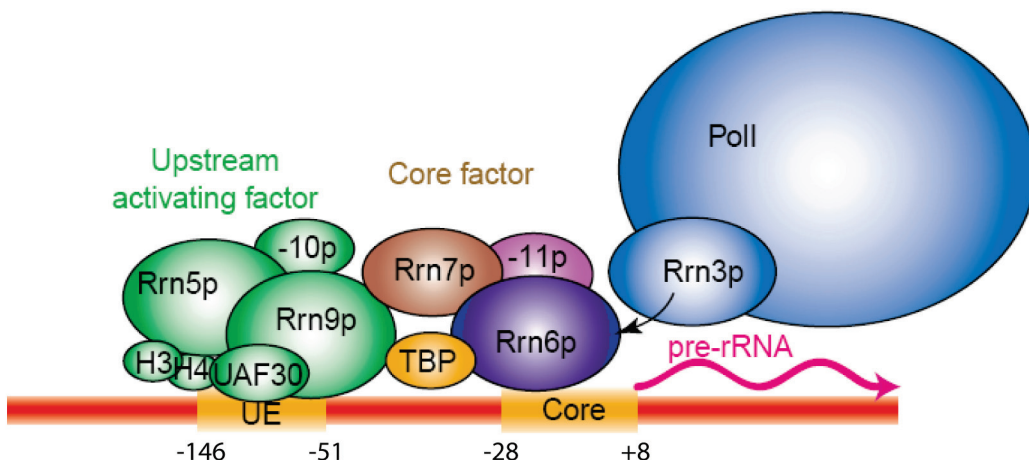
Figue 6. The Pol I pre-initiation complex (PIC)

Yeast PIC. The six subunit containing upstream activating factor (green) binds the upstream element (UE). The core factor (composed of Rrn6, Rrn7, and Rrn11) binds the core element (`core`). The two complexes are bridged via the TATA-binding protein (TBP). Initiation competent Pol I, associated with Rrn3, interacts with the Rrn6 subunit of the core factor. (from Moss, 2004)

After transcription initiation Rrn3 dissociates from the template during or immediately after Pol I switched from initiation to elongation (Bier et al., 2004). The mechanism of this transition is not completely understood yet, since dissociation of Rrn3 from Pol I does not seem to be vital in a strain expressing an A43-Rrn3 fusion protein (Laferté et al., 2006).

It is likely that (de-)phosphorylation of Pol I subunits is involved in the regulation of this transition step, since it was shown that Rrn3 bound Pol I exhibits a different phosphorylation pattern than the bulk of Pol I (Fath et al., 2001).

1.2.4.2 Elongation

Most knowledge about RNA elongation comes from studies with RNA Pol II (Shilatifard, 2004; Reinberg and Sims, 2006; Svejstrup, 2007) and bacterial polymerases (Borukhov and Nudler, 2008).

Eukaryotic or bacterial elongation factors like TFIIS or GreA/GreB, respectively, allow the transcription complex to pass through physical barriers (Reines and Mote, 1993; Toulmé et al., 2000). TFIIS induces the hydrolytic cleavage of the nascent RNA chain from the 3` end of a backtracked Pol II after encountering a transcriptional block (Fish and Kane, 2002; Sigurdsson et al., 2010). The two acidic residues (DE) in the conserved C-terminal motif were shown to be crucial for the mechanism of TFIIS-induced RNA cleavage (Jeon et al., 1994; Kettenberger et al., 2003). Other factors like FACT and Elongator facilitate transcription from chromatin templates (Reinberg and Sims, 2006). However, it is unclear how these factors contribute to efficient transcription through chromatin *in vivo*, especially since many of them (like TFIIS, Elongin, Paf1) are dispensable for cell viability under physiological conditions (Archambault et al., 1992; Yamazaki et al., 2003). Our understanding about elongation in the Pol I cycle is rather low compared to the regulation of initiation events since RNA Pol I elongation has only been marginally investigated *in vitro* (Stefanovsky et al., 2006; Schneider et al., 2007). In fact, there is a need to establish a system for *in vivo* analysis of Pol I elongation.

The recently reported interactions of Pol I with transcription elongation factors previously described to be involved in Pol II transcription like Spt4/5 and Paf1 (Schneider et al., 2006; Zhang et al., 2009, 2010; Anderson et al., 2011; Viktorovskaya et al., 2011) suggests common principles in RNA chain elongation. As in the case for Pol II it is concluded that it is not the elongation rate (nucleotide addition per minute) that is increased by Spt4/Spt5, but rather the processivity of the polymerase (nucleotide addition per initiation event) (Mason and Struhl, 2005).

Moreover, it was shown in bacteria that trailing RNA Pols transcribing the same gene have anti-arrest and anti-pause effects due to forward translocation of leading complexes. This effect could also be transferred to the Pol I system where several polymerases, approximately one polymerase every 70 bp, are transcribing one rDNA gene as seen in Miller chromatin spreads (Figure 7). The cooperation of RNA Pols may explain why elongation can still be fast and processive *in vivo* even without anti-arrest factors (Epshtein and Nudler, 2003; Epshtein et al., 2003).
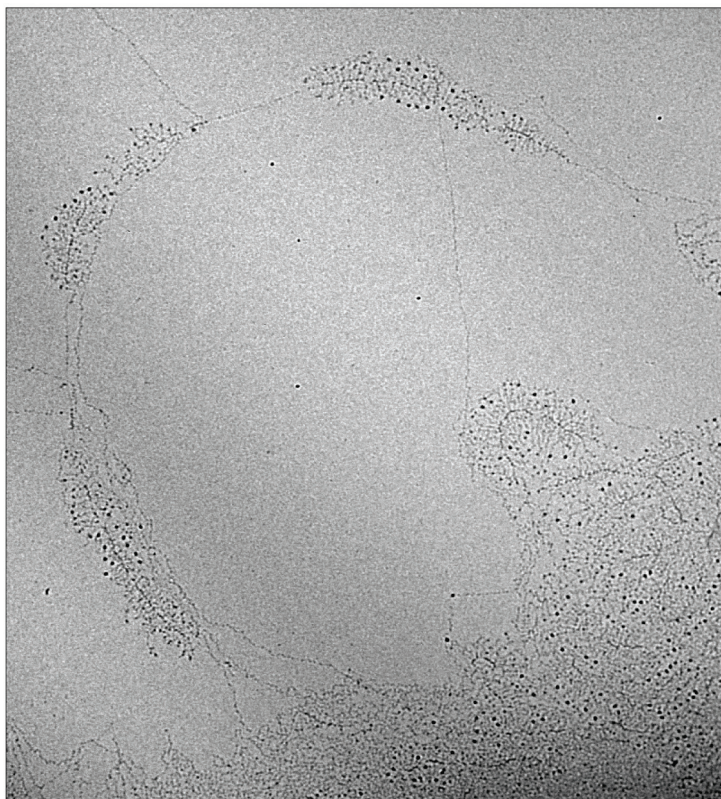
Figure 7. Miller chromatin spread of yeast rDNA

Electron microscopic image of a Miller chromatin spread of yeast strain y1599 (WT) with a 20000 fold magnification, obtained from Dr. Isabelle Léger-Silvestre, University of Toulouse. The tandemly repeated and transcriptionally active rRNA genes are especially noticeable in the chromatin mass due to their relatively dark appearance, which is due to multiple nascent RNA transcripts extending from the DNA backbone.

No specific Pol I elongation factors are known so far. However, the idea of a A49/A34.5 heterodimer acting as a 'built-in' Pol I elongation factor, derived from *in vitro* studies, exists (Kuhn et al., 2007; Geiger et al., 2010). Furthermore the function of the Pol I subunit A12.2 is linked to transcription elongation (Mullem et al., 2002). It has only been shown *in vitro*, that Pol I exhibits an intrinsic RNA cleavage activity which is dependent on the C-terminal domain of A12.2, capable of shortening the RNA from the 3` end in an artificially stalled ternary complex (Kuhn et al., 2007). Similar to TFIIS deletion mutants, yeast strains lacking the gene coding for A12.2 are sensitive to the NTP-pool depleting drug 6-azauracil (6AU), a phenotype often associated with defects in transcription elongation (Archambault et al., 1992; Exinger and Lacroute, 1992; Hampsey, 1997; Mullem et al., 2002).

1.2.4.3 Termination

Transcription termination requires specific DNA sites which are recognized by the respective RNA polymerase machinery. Termination of transcription shows common features in all nuclear transcription machineries (Richard and Manley, 2009). It depends on pausing of the RNA polymerase at a specific site and is followed by destabilization and dissociation of the

stalled polymerase. Two terminators for 35S rDNA transcription reside within the ENH region of yeast (Reeder et al., 1999). Approximately 90% of all transcripts terminate at a T1 site located 93 nucleotides downstream of the 3` end of mature 25S rRNA. The remaining transcripts terminate at a T2 failsafe termination site composed of a thymine-rich DNA stretch located 250 nucleotides downstream of the 3` end of the mature 25S rRNA (Reeder et al., 1999). The T1 terminator site contains two elements: one binding site for the Pol I enhancer binding protein Reb1 and an upstream T-rich element that encodes the last 10-12 nucleotides of the terminated transcript (Reeder and Lang, 1997). There are some similarities to the mouse terminator, where the Reb1 homolog TTF-I cooperates with PTRF, a transcript release factor, in combination with a T-rich upstream DNA sequence to terminate and dissociate Pol I and the nascent transcript from the template DNA (Kuhn et al., 1990; Jansa and Grummt, 1999). Homologies within the terminator structure as well as in the amino acid sequences of the Myb-like DNA binding domains at the C-terminal regions of the terminator proteins, suggest a high conservation of the mechanism of Pol I termination throughout eukaryotes (Jeong et al., 1995). However, two models of termination are currently discussed due to a discrepancy of *in vitro* and *in vivo* data. These are *a)* Termination of transcription by `pause and release` mechanism or *b)* a `torpedo-like` model, similar to Pol II termination.

Ad a) In vitro reconstitution of termination from purified yeast factors revealed that Reb1 both pauses Pol I and supports the release of the generated transcripts at the T1 site (Lang and Reeder, 1993). In addition, a T-rich DNA element at this site supports termination by destabilizing the pausing Pol I through a resulting A-U heteroduplex (Lang and Reeder, 1995). *In vivo* studies on ribosomal minigenes using S1 nuclease protection analysis strongly support this *in vitro* data (Reeder et al., 1999). However, Reb1 binding *in vivo* can only be detected at its binding site near the Pol I promoter but not at the terminator and a fourfold reduction of Reb1 *in vivo* had no effect on termination (Kawauchi et al., 2008). Non-terminated transcripts are extended either to a `failsafe` terminator (T2), which resides about 250 nt downstream of the 25S 3` end (Prescott et al., 2004; Reeder et al., 1999) or to the replication fork barrier (RFB), which is located about 300 bp downstreams (El Hage et al., 2008). Fob1, a protein which blocks DNA replication forks binds to RFB (Huang et al., 2006; Takeuchi et al., 2003) and was suggested to be involved in efficient termination (El Hage et al., 2008).

Ad b) For efficient Pol I termination, accoding to the `torpedo`-model (Kawauchi et al., 2008; El Hage et al., 2008), cleavage of the nascent pre-rRNA by the RNase III-like endonuclease Rnt1, which acts across a stem-loop structure within the 3` ETS, is required (Kufel et al., 1999; Henras et al., 2004; Prescott et al., 2004). The generated 5` end of the cleaved transcript then serves as a substrate for the exonuclease Rat1 which progressivly degrades the Pol I-bound transcripts with the help of the helicase Sen1 and, thus, finally releases Pol I from the template by destabilization of the transcription complex. This model is based on *in vivo* analyses of yeast mutants deficient in the endonuclease Rnt1, resulting in accumulated transcripts beyond the

T1 termination site (Prescott et al., 2004; Reeder et al., 1999). Additionally, inactivation of the nuclear exonuclease Rat1 and the RNA helicase Sen1 leads to accumulation of extended pre-rRNAs and increased Pol I occupancy in the region downstream of the T1 terminator (Kawauchi et al., 2008; El Hage et al., 2008). Very recent studies introduce the RNA/DNA kinase Grc3, which is proposed to control the phosphorylation status of the downstream Rnt1 cleavage product and thereby regulates its accessibility to the torpedo Rat1, in Pol I termination (Braglia et al., 2010a). Interestingly, inactivation of Rat1 alone is insufficient to display a full termination defect (Kawauchi et al., 2008). ChIP analyses of a *Δfob1* strain showed increased Pol I occupancy 3` of the RFB when Rat1 is depleted. This is pointing towards an additional role of the RFB as an extra barrier for Pol I transcription and a Fob1-dependent terminator to avoid collisions of Pol I complexes with rDNA replication forks moving in opposite direction (El Hage et al., 2008). In an approach by Braglia et al. from 2010 the effects of Rnt1 deletion, already leading to slow growth, on termination were observed *in vivo* on a plasmid based Pol I minigene. In their analysis a torpedo-like termination mechanism was suggested to function even in the absence of the Rnt1-dependent cleavage. In cells carrying Pol I minigenes, which lack the Rnt1-cleavage site, a second - `failsafe` - cleavage site at the T-rich region of T1 by a not yet identified endonuclease was proposed. Alternative cleavage at the T-rich element and the presence of an intact Reb1 binding site are crucial for efficient transcription termination. Cleavage at this site should allow co-transcriptional recruitment of the exonuclease Rat1 (Braglia et al., 2010b). Additionally the Pol I subunit A12.2 seems to play a role in termination (Prescott et al., 2004).

Taken together, there is a discrepancy between the rather conclusive *in vitro* data about Reb1 and the *in vivo* termination analyses. Furthermore, it is difficult to distinguish between transcription termination and processing events at the proposed second - `failsafe` - cleavage site at the T-rich region since 5` and 3` ends of the resulting transcripts were not mapped.

To clarify these controversies, the establishment of an *in vivo* system consisting of several DNA *cis*-elements will help to study termination in more detail.

1.2.5 Pre-rRNA processing and maturation of ribosomes

Three of the four ribosomal RNA species in yeast (18S, 5.8S, and 25S) are transcribed by RNA polymerase I as a single polycistronic precursor, the 35S pre-rRNA. This precursor is subsequently matured in a complex series of co- and post-transcriptional processing steps to yield the mature RNAs. In yeast, a subset of ribosomal proteins and ribosomal biogenesis factors along with diverse small nucleolar ribonucleoprotein particles (snoRNPs) assemble to the precursor rRNA in the course of transcription to establish the initial 90S pre-ribosomal particle. The first detectable pre-rRNA transcript (35S) is thought to be co-transcriptionally cleaved at site B_0 (Henras et al., 2004). U3 snoRNP dependent endonucleolytic cleavages at

sites A_0, A_1, and A_2 occur next. These processing events are strongly coupled and involve base pairing of U3 snoRNA with ETS1 and 18S rRNA sequences (Hughes and Ares, 1991; Beltrame and Tollervey, 1992). Processing at site A_2 finally leads to separation of the pre-40S and pre-60S particle containing either the 20S or the $27SA_2$ pre-rRNA species, respectively. The pre-40S particle is exported to the cytoplasm where it is converted into the mature small ribosomal subunit by cleavage of the 20S pre-rRNA at site D, producing the 18S rRNA. Further, processing of the $27SA_2$ pre-rRNA into the mature 5.8S and 25S rRNAs through several exo- and endonucleolytic digestion steps occurs by two alternative pathways (Figure 8). For comprehensive and detailed description of each processing step see (Nazar, 2004; Henras et al., 2008) and references therein.
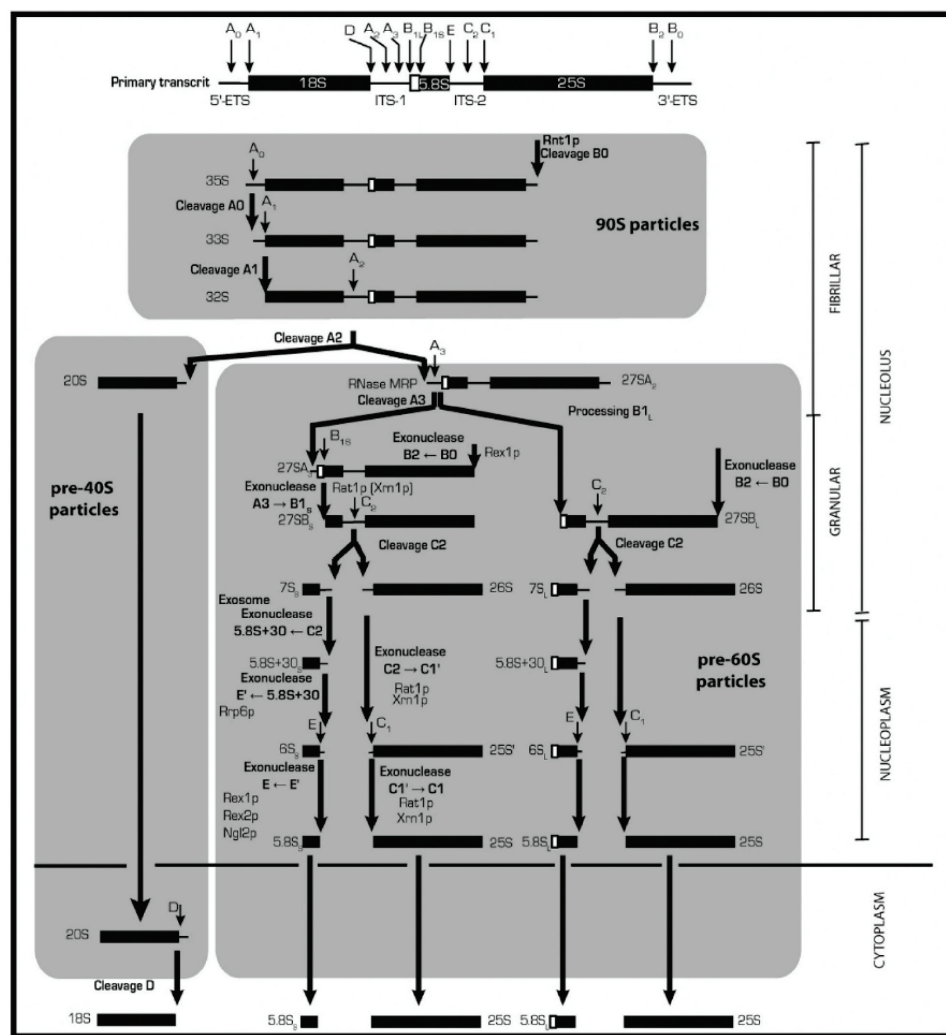
Figure 8. Pre-rRNA processing scheme in *Saccharomyces cerevisiae*

The upper panel shows a schematic drawing of the 35S pre-rRNA transcript with the locations of the respective processing sites. The central panel depicts the successive processing steps from the 35S to the 32S pre-rRNA within the pre-90S particle. An endonucleolytic cleavage event separates the processing pathways of the pre-40S and the pre-60S particle, both of which are illustrated in the two lower panels. Subsequent conversion of the 20S pre-rRNA and the $27SA_2$ pre-rRNA into the mature rRNA species is shown. The intermediate rRNA species and the implications of diverse exo- and endonucleolytic cleavage activities are depicted, as are the cell compartments where the respective processing steps occur. (from Henras et al., 2008)

Contrary to the pre-40S particle, all rRNA species of the pre-60S particle are matured completely before the particle is exported to the cytoplasm (Figure 8) (Venema and Tollervey, 1995; Tschochner and Hurt, 2003; Fromont-Racine et al., 2003; Henras et al., 2008). Although there are differences in the pre-rRNA processing and modification pathways between yeast and mammals, the overall sequence of maturation events in eukaryotes seems very related, since *trans*-acting factors involved in ribosome biogenesis are highly conserved (Henras et al., 2008). The modifications like cytosine-methylation or pseudouridylation are most probably important for ribosome function, rather than for ribosome biogenesis. However, the modifications could be structural checkpoints, since the binding sites for some r-proteins of biogenesis factors might be formed only if the modification mark is set (Song and Nazar, 2002).

Importantly, continuous availability of ribosomal proteins in at least stoichiometric amounts with the rRNA is crucial for proper maturation of ribosomal subunits. Reduced production of individual ribosomal proteins due to conditional depletion or r-protein gene haploinsufficiency rapidly leads to severe pre-rRNA processing defects (Lucioli et al., 1988; Song et al., 1996; Deutschbauer et al., 2005; Ferreira-Cerca et al., 2005; Pöll et al., 2009).

Although RNA polymerase I transcription proceeds in some cases unabated until the 3` ETS is synthesized, the nascent transcript could also be modified and cleaved co-transcriptionally in the ITS1, thereby immediately releasing a pre-40S particle without prior pre-90S particle formation (Osheim et al., 2004; Kos and Tollervey, 2010). Indeed, accurate transcription elongation by RNA Pol I is a prerequisite for efficient pre-rRNA processing and pre-ribosome assembly (Schneider et al., 2007). Similarly, two independent studies revealed a subset of early assembling non-ribosomal proteins to be implicated not only in accurate pre-rRNA processing but also in efficient rDNA transcription (Gallagher et al., 2004; Prieto and McStay, 2007). Additionally, depletion of the Pol II elongation factor Spt4, which is similarly involved in the Pol I system, results in pre-rRNA processing defects (Schneider et al., 2006). These observations indicate that efficient rRNA elongation and rRNA processing are closely linked and therefore have to be tightly regulated (Granneman and Baserga, 2005).

1.2.6 Regulation of Pol I transcription and ribosome biogenesis

Survival of a cell critically relies on its ability to respond to environmental signals. Consequently, living organisms sense and react to the availability of nutrients. Ribosome biogenesis is an energetically very costly process in the cell that has to be tightly regulated in response to nutrient and energy conditions. Prokaryotic cells mainly regulate ribosome synthesis at the level of rDNA transcription and translational feedback mechanisms (Wagner, 2002; Magnusson et al., 2005; Suthers et al., 2007). Each prokaryotic cell has to deal with fast changing environmental conditions. Nutrient depletion, in particular amino acid starvation triggers the so-called `stringent response` on ribosome biogenesis.

The common pathway in eukaryotes of sensing nutrient availability and other environmental conditions, is mediated by the TOR (target of rapamycin) kinase (Powers and Walter, 1999; Lempiäinen and Shore, 2009). TOR kinase is found in two structural and functional diverse complexes termed TORC1 and TORC2 (TOR kinase complex 1 or 2). The TORC1 is sensitive to stress and lack of nutrients (mimicked by the drug rapamycin). The main functions of TORC2 are the regulation of the cytoskeleton dynamics and the AGC kinase family (protein kinase A, G, C) (Cybulski and Hall, 2009).

TOR signaling has been shown to affect the complex process of ribosome biogenesis on the levels of transcriptional regulation of the polymerases, translation initiation, RNA processing, and internuclear and nucleo-cytoplasmic transport processes.

For example, nutrient deprivation or rapamycin treatment of eukaryotic cells results in a rapid decrease in Pol I transcription rates (Grummt et al., 1976; Zaragoza et al., 1998; Powers and Walter, 1999). Therefore, the activity of RNA polymerase I and thus ribosome biogenesis is apparently strictly regulated in a TOR-dependent manner. In yeast cells following rapamycin-induced TOR inactivation, the amount of Pol I-Rrn3 complexes is decreased as is the association of Pol I with both the promoter and the transcribed region of the rDNA locus, nicely resembling the situation in stationary phase (Claypool et al., 2004; Philippi et al., 2010). This suggests that in yeast the rate of Pol I transcription is strongly dependent on the formation of Pol I-Rrn3 complexes.

Since in yeast Rrn3 as well as Pol I are described to be phosphorylated *in vivo* (Bell et al., 1976; Buhler et al., 1976a; Bréant et al., 1983; Fath et al., 2001), TOR signaling was speculated to influence the formation of Pol I-Rrn3 complexes via phosphorylation-dephosphorylation cascades in a growth-dependent manner. Indeed, *in vitro* experiments suggest that Pol I needs to be phosphorylated for binding to Rrn3, whereas the latter is able to bind to Pol I in its unphosphorylated form (Fath et al., 2001). The level of Rrn3 was recently reported to gradually decrease in rapamycin treated yeast cells due to the combination of proteasome-dependent degradation and a reduction in the neo-synthesis rate of this factor (Philippi et al., 2010). The decrease in Pol I occupancy at the rDNA locus following rapamycin treatment could be further attenuated in a mutant strain expressing an A43-Rrn3 fusion protein, thereby preventing not only the degradation of Rrn3 but also its dissociation from Pol I. This strain termed **CARA** for **C**onstitutive **A**ssociation of **R**rn3 and RP**A**43, was largely insensitive to rapamycin treatment and TORC1 inhibition. Concomitantly, the decline in 35S pre-rRNA synthesis is also significantly retarded in these cells (Laferté et al., 2006). Although all these observations suggest distinct roles for Rrn3-levels and for the phosphorylation status of both Rrn3 and Pol I in the regulation of Pol I-Rrn3 complex formation and thus Pol I transcription, little is known about the underlying regulatory mechansims.

However, TOR inactivation affects ribosome biogenesis in yeast not only at the level of Pol I transcription initiation but also the elongation rate of the polymerase seems to be regulated in

a growth-dependent manner (Zhang et al., 2009, 2010). It is suggested that the elongation factor Paf1C plays a TOR-dependent role in the modulation of rRNA production. Besides Pol I transcription, TOR inactivation was also shown to specifically and rapidly down-regulate the RNA polymerase II-dependent transcription of ribosomal protein (RP) genes (Powers and Walter, 1999; Cardenas et al., 1999). Transcription by Pol II is similarly decreased following impaired TOR signaling in the Ribi-regulon consisting of the ribosome biogenesis (Ribi) genes coding for auxiliary ribosome biogenesis factors (Jorgensen et al., 2002, 2004). Consecutive analysis revealed several transcription regulators and transcription factors such as Sch9, Sfp1, Fhl1, and Ifh1 whose activity or binding to RP and Ribi gene promoters, respectively, is controlled by TOR signaling via alterations in their cellular localization or abundance (Jorgensen et al., 2004; Marion et al., 2004; Schawalder et al., 2004; Rudra et al., 2005). Another factor which may be directly involved in downregulation of RNA Pol I and RNA Pol III transcription following rapamycin treatment is TORC1 itself. A nuclear fraction of TORC1 associates with the rRNA gene promoter and the 5S rRNA gene locus under normal growth conditions but leaves the nucleus in the presence of rapamycin or upon nutrient deprivation (Li et al., 2006). TOR inactivation obviously mediates the transcriptional downregulation of all components required for ribosome biogenesis. However, the activity of RNA polymerase I seems to play a superior role in this process, since the artificial stabilization of Pol I transcription in rapamycin-treated CARA mutant cells attenuates the decrease in the level of both r-protein mRNAs and 5S rRNAs produced by Pol II and Pol III, respectively (Laferté et al., 2006). In addition to transcription, general translation is also severely compromised upon TOR inactivation due to the impaired function of various translation factors (Barbet et al., 1996). One downstream consequence of rapamycin treatment is the activation of Gcn2 kinase which, in turn, phosphorylates the α-subunit of eukaryotic initiation factor 2 (eIF2α), thus inhibiting translation initiation (Cherkasova and Hinnebusch, 2003). TOR inactivation further affects translation initiation by the degradation of eIF4G, an essential protein required for mRNA translation via the 5` cap-dependent pathway in yeast (Berset et al., 1998).

Strikingly, it was shown that not only Pol I transcription is repressed following rapamycin treatment, but also 35S pre-rRNA processing is severely and rapidly affected, thereby nearly abolishing the production of mature ribosomal RNAs (Powers and Walter, 1999). This could be due to direct TOR-dependent inactivation of ribosome biogenesis factors and/or to the transcriptional downregulation of genes controlled by the Ribi regulon, leading to rapid depletion of protein factors involved in rRNA maturation. Another example for TOR-mediated effects on RNA metabolism is the specific inhibition of r-protein mRNA splicing, induced by amino acid starvation (Pleiss et al., 2007). Finally, evidence exists suggesting that TOR signaling is involved in the control of pre-ribosomal transport processes. TOR inactivation leads to a rapid nucleolar entrapment of various ribosome biogenesis factors, thereby causing cessation

of late rRNA maturation steps and defects in the nuclear-cytoplasmic translocation of pre-ribosomal particles (Honma et al., 2006; Vanrobays et al., 2008).

During eukaryotic ribosome biogenesis, misfolded or misassembled precursors are detected, polyadenylated by the TRAMP (**Tr**f4p-**A**ir1/2p-**M**tr4p **p**olyadenylation) complex and subsequently degraded by the exosome (Dez et al., 2006; Schneider et al., 2007; Wery et al., 2009). The absence of the non-essential nuclear exosome component Rrp6 conferres RNA stabilization and leads to hyperadenylation (Dez et al., 2006).

1.2.7 Posttranslational modifications of RNA polymerase I

Protein phosphorylation-dephosphorylation is often seen as as a mechanism of modulating the activity of enzymes (Fischer and Krebs, 1955; Cohen, 2002). The importance of this reversible posttranslational modification as a common regulatory concept emerged already in the early 1970s (Holzer and Duntze, 1971).

In 1976, two research groups identified, independently from one another, five RNA polymerase I subunits (A190, A43, A34.5, ABC23 and ABC19) as *in vivo* phosphorylated proteins (Bell et al., 1976; Buhler et al., 1976b). Considerable *in vitro* data argue for a regulatory role of Pol I phosphorylation by modulating the enzyme at the different stages of the transcription cycle (Fath et al., 2001, 2004; Bier et al., 2004).

Since Pol I is phosphorylated *in vivo*, TOR signaling was speculated to influence the Pol I-Rrn3 complexe formation via phosphorylation-dephosphorylation.

Up to date, detailed analyses of phosphorylation sites and their function in eukaryotic RNA polymerases have been largely limited to the carboxy-terminal domain (CTD) of the largest Pol II subunit, which was subject to many investigations due to its importance for Pol II transcription (Phatnani and Greenleaf, 2006). Recently Jochen Gerber identified 13 RNA polymerase I specific phosphorylation sites through chemical derivatization of phosphopeptides and mass spectrometry (Gerber et al., 2008). Furthermore, additional Pol I phosphosites are described in the proteome-wide approaches by Ficarro *et al.* (2002) and Li *et al.* (2007). These findings served as a starting point for the mutant-analysis of these phosphosites to investigate their role in regulation. A list of all identified phosphosites is shown in Table 2.

Table 2. Identified RNA polymerase I phosphorylation sites

Subunit	Phosphosite	Reference
A190	S354	(Gerber et al., 2008)
	S685	(Gerber et al., 2008)
	S936 or S941	(Gerber et al., 2008)
	S1413 or S1415 or S1417	(Ficarro et al., 2002)
	S1636	(Li et al., 2007b)
A43	S208	(Gerber et al., 2008)
	S220	(Gerber et al., 2008)
	S262 or S263	(Gerber et al., 2008)
	S285	(Gerber et al., 2008)
A34.5	S10 or S12 or S14	(Li et al., 2007b)
ABC23	S102	(Gerber et al., 2008)
AC19	T33	(Gerber et al., 2008)
	T51 or T54 or T55	(Li et al., 2007b)

Additionally to the posttranslational modification by phosphorylation, A190 was shown to be a substrate for sumoylation in yeast (Panse et al., 2004).

The largest Pol II subunit Rpb1 was found to be a substrate for the E3 ubiquitin-protein ligase Rsp5 (Huibregtse et al., 1997; Crews, 2003). The mapped ubiquitination-sites are conserved in A190 (Somesh et al., 2005; Kuhn et al., 2007), but as Rpb1 ubiquitination seems to depend on the CTD-domain (Huibregtse et al., 1997; Somesh et al., 2007) it is unclear whether a similar mechanism exists for Pol I.

1.3 Objectives

Several objectives covering the Pol I transcription cycle and its regulation have been set.

First, it is difficult to distinguish between primary and secondary effects after inactivation of the TOR pathway in eukaryotic cells since the multiple processes leading to mature ribosomes appear to be intimately linked. Following rapamycin treatment or nutrient deprivation, transcription by all three RNA polymerases, general translation, as well as pre-rRNA processing are substantially down-regulated or exhibit severe defects (see 1.2.6). In order to timely resolve the response of transcription and pre-rRNA processing to rapamycin treatment, we investigated effects on both processes shortly after TOR inactivation (after 15 min).

Second, our laboratory data suggested that the phosphorylation pattern of Pol I is crucial for association and dissociation of the Pol I-Rrn3 complex (Fath et al., 2001, 2004). However, all phosphorylation sites identified so far in Pol I and Rrn3 turned out not to be required for this

process (Gerber et al., 2008). To elucidate common principles and specific features in eukaryotic transcription, the further characterization of the created phosphosite mutants, the identification and functional analysis of additional Pol I mutants, namely the synthetic lethal mutant (*rpa190* S685D / *Δrpa12*), the putative A43-Rrn3 interaction mutant (A43 S141/143D) as well as the lethal mutant of the non essential Pol I subunit A12.2 (A12.2 DE/AA), *in vivo* and *in vitro* should be tackled in this work.

Third, most knowledge about RNA elongation comes from studies with RNA Pol II and bacterial polymerases (Stefanovsky et al., 2006; Schneider et al., 2007). Specific elongation factors, first described for Pol II, allow the transcription complex to pass physical barriers. Other factors facilitate transcription from chromatin templates *in vitro*. Furthermore, the termination factor Reb1 which was described to bind to the terminator *in vitro* does not bind to the terminator *in vivo*. It is unclear yet how and if these factors contribute to efficient Pol I transcription *in vivo*. Therefore an *in vivo* system should be established which should allow to analyse elongation and termination of RNA polymerase I in more detail.

Furthermore, a major aim of this work was to set up an *in vivo* screen to identify and characterize Pol I specific elongation- and termination factors. The established *in vivo* screen should be suitable to further characterize the Pol I mutants mentioned above with the focus on elongation and termination. In the long term this system should help both to determine the requirements for transcription elongation and termination and to screen for putative Pol I specific elongation and termination factors.

2 RESULTS

2.1 *In vivo* analysis for RNA polymerase I mutants

2.1.1 Functional analysis of RNA polymerase I phosphomutants

The functions of the many Pol I phosphosites are unknown. Primary analysis of single mutations of the Pol I phosphosites to either alanin or aspartic acid, to mimic constitutively dephosphorylated or phosphorylated states, showed no apparent impact on the growth behavior *in vivo* (Gerber, 2008). Creating clusters of Pol I phosphomutants or looking for genetic interaction partners of these phosphomutants in a synthetic lethal screen are strategies to further investigate the *in vivo* role of these phosphosites and to obtain more information about their contribution in the regulation of Pol I. Furthermore, additional Pol I phosphorylation sites might still exist since it is possible that only the constitutive, but not the transient phosphosites were detected in Jochen Gerber´s approach.

For further analysis of the Pol I phosphomutants, Johannes Felixberger and I continued the mutagenesis to generate strains with several mutated Pol I phosphosites. A list of the created Pol I phosphomutants is shown in Table 3.

The mutant yeast strains were obtained by introducing the vectors with the mutated genes into the corresponding plasmid-shuffle strain for the respective five Pol I subunit genes, using either canavanine- or 5-FOA-counterselection (depending on the genotype of the strain) (Sikorski and Boeke, 1991). Since A34.5 is a non-essential protein, the vectors containing mutant alleles of this gene were simply transformed into a *Δrpa34* strain.

Several to all phosphosites of one subunit were mutated and tested for complementation of the wild-type subunit (for A190 mutants see Felixberger, 2009). A43 phosphomutants were generated by splicing by overlap extension-PCR (SOE-PCR) (Horton et al., 1989; Pogulis et al., 1996) (see Figure 45 for schematic mutagenesis strategy).

Table 3. RNA polymerase I phosphorylation site mutations

Pol I subunit	Mutation
A190	S354A
	S354D
	S685A
	S685D
	S936/941A
	S936/941D
	S936D
	S941D
	S936E
	S941E
	S1413/1415/1417A
	S1413/1415/1417D
	S1636A
	S1636D
	S936/941A S1413/1415/1417A
	S354A S936/941A S1413/1415/1417A
	S354A S685A S936/941A S1413/1415/1417A
	S354A S685A S936/941A S1413/1415/1417A S1636A
	S354D S685D
	S1413/1415/1417D S1636D
	S936/941D S1413/1415/1417D S1636D
	S354D S685D S936/941D S1413/1415/1417D S1636D
A43	S208A
	S208D
	S220A
	S220D
	S208/220A
	S208/220D
	S262A
	S262D
	S263D
	S262/263/265A
	S262/263D
	S285A
	S285D
	S208A S220A S262/263A
	S208A S220A S262/263A S285A
	S220D S262/263D
	S208D S220D S262/263D
	S208D S220D S262/263D S285D
A34.5	S10/12/14A
ABC23	S102A
	S102D
AC19	T33A

The capability of the Pol I A43 phosphosite mutants to complement the loss of their wild-type subunits was checked in the plasmid-shuffle strains on full media YPD agar plates at 16°C, 24°C, 30°C, and 37°C (Figure 9). Plasmid-shuffling was controlled on appropriate synthetic media plates to check for the presence of the mutant copy vector, the loss of the wild-type vector, and the maintenance of the original RPA-gene deletion. Isogenic wild-type strains carrying the same plasmid without mutations of the respective RPA-gene served as a control in each case. All A43 mutants fully complement the loss of the wild-type subunit and show no significant growth phenotype (Figure 9).
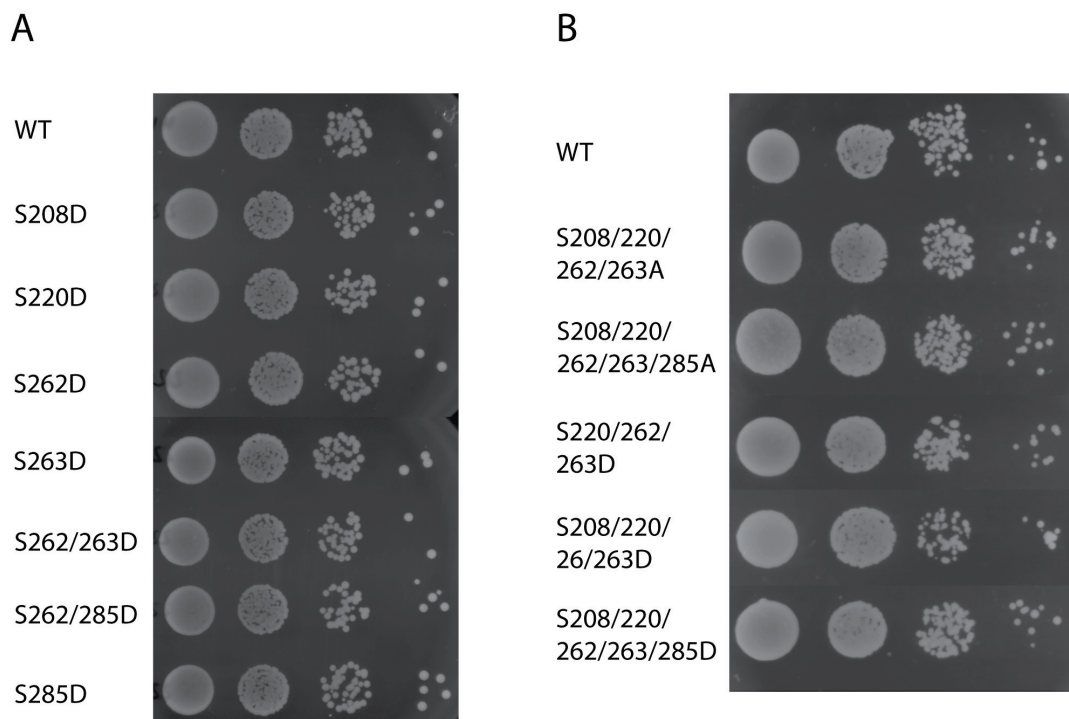
Figure 9. Single and combined mutations of the phosphorylated amino acids of A43 have no effect on growth
Experiments were performed with the strain D101-I2 transformed with the respective phosphosite mutation vectors. Plasmid-shuffling and maintenance of the chromosomal deletion was controlled via the respective auxotrophic markers. The 5-FOA-shuffle system was used for the creation of the Pol I phosphosite mutants of A43. Strains were spotted in serial dilutions on YPD plates and grown at different temperatures for 2-3 days before pictures were taken. Growth on YPD plates at 30°C is shown as an example. **(A)** Single and **(B)** combined RPA43 mutations.

Additionally, Johannes Felixberger created A190 mutant strains with all A190 phosphosites either mutated to alanin or aspartic acid using a variation of the site-specific mutagenesis-strategy by Muhlrad (Muhlrad et al., 1992). All of the created mutants could complement the wild-type A190 subunit and showed no significant growth defect on 6AU plates (Felixberger, 2009). 6AU, which lowers the free pool of UTP and GTP by interfering with their biosynthesis pathways, is commonly used to test for defects in transcription elongation (Hampsey, 1997; Schneider et al., 2007).

Furthermore, the sensitivity of phosphomutant strains to DNA damaging agents such as methyl methanesulfonat (MMS), causing double stranded DNA breaks, and ultraviolet (UV) radiation, causing thymine dimers in DNA (Ide et al., 2010), was addressed. Using different concentrations of MMS (from 0% to 0,01%) and different UV doses (from 0 J/m^2 to 400 J/m^2) no significant growth-phenotype of the phosphomutants compared to wild-type cells was detected by spotting serial dilutions of the cultures on YPD (MMS)- or YPD-plates prior to UV-treatment, respectively (data not shown).

Interestingly, the mutation *rpa190* S685D was found to be synthetic lethal (SL) with a deletion of the non-essential Pol I subunit A12.2 (Reiter, 2007). In a continuative approach the newly created mutations of A43 phosphoserines to aspartic acid were tested for genetic interaction with selected non essential yeast genes (see Reiter, 2007 for detailed description of the synthetic lethal (SL) screen). Results of the small-scale SL screen are depicted in Table 4.

Table 4. No phenotype was detected in a small-scale SL screen for mutations of A43 phosphoserines to aspartic acid in combination with selected gene deletions (blue field indicates the absence of a growth phenotype)

	WT	S208D	S220D	S262D	S263D	S262/263D	S262/285D	S285D
Δtop1								
Δtop3								
Δuaf30								
Δasf1								
Δrpa49								
Δrpa34								
Δrpa14								
Δrpa12								
Δrps6A								
Δrps30B								

Since no synthetic lethal phenotype was detected, a large scale screen for genetic interactions of the A43 phosphosite/A or phosphosite/D mutants (all phosphosites are mutated either to alanin or aspartic acid) with a library of all non-essential yeast genes according to the slightly modified GIM-method (<u>G</u>enetic <u>I</u>nteraction <u>M</u>apping) (Decourty et al., 2008) was carried out. This screen was performed by Johannes Felixberger in collaboration with Christophe Normand from the lab of Olivier Gadal in Toulouse in the course of the PICS program. No genetic interaction partner of the A43 phosphomutants could be identified in this approach (Felixberger, 2009).

Thus, it appears that the so far identified phosphosites do not primarily contribute to the regulation of Pol I since no phenotype was detected yet.

2.1.2 Characterization of a putative A43-Rrn3 interaction mutant

It is possible that transient phosphorylation is required for the regulation of Pol I. Such regulatory transient phosphosites are often found within the contact surface of interacting proteins. Mutant analysis of A43 revealed a highly conserved region in A43 which is probably important for the interaction with Rrn3 (Peyroche et al., 2000). Furthermore, the structural data of the A14/A43 subcomplex could show that most of the conserved amino acids are located on the upstream surface region of A43 (Kuhn et al., 2007; Geiger et al., 2008). These data suggests the presence of a putative A43-Rrn3 interaction surface. Therefore, selected serine residues within or nearby the conserved surface region, which could be putative phosphorylation sites, were mutated to alanin and aspartic acid, respectively. Mutagenesis was done by SOE-PCR on the plasmid pRS314-*RPA43* (pGP5). A list of the mutated residues and the location of the chosen residues in the A43 structure can be seen in Figure 10A-C.

Complementation of the loss of the wild-type protein by the mutated Pol I subunit was checked in the *RPA43* plasmid-shuffle strain. Wild-type strains carrying the same vector without mutations of the *RPA43* gene as well as strains carrying an empty vector served as controls. Interestingly, only cells with the *rpa43* S141/143D but not the *rpa43* S141/143A mutation are unable to grow because they cannot complement the loss of the wild-type subunit, resulting in a lethal phenotype (Figure 10D).

A

Mutated A43 residues
S48
S141
S143
S141/143
S156
S213
S244

B

C

D
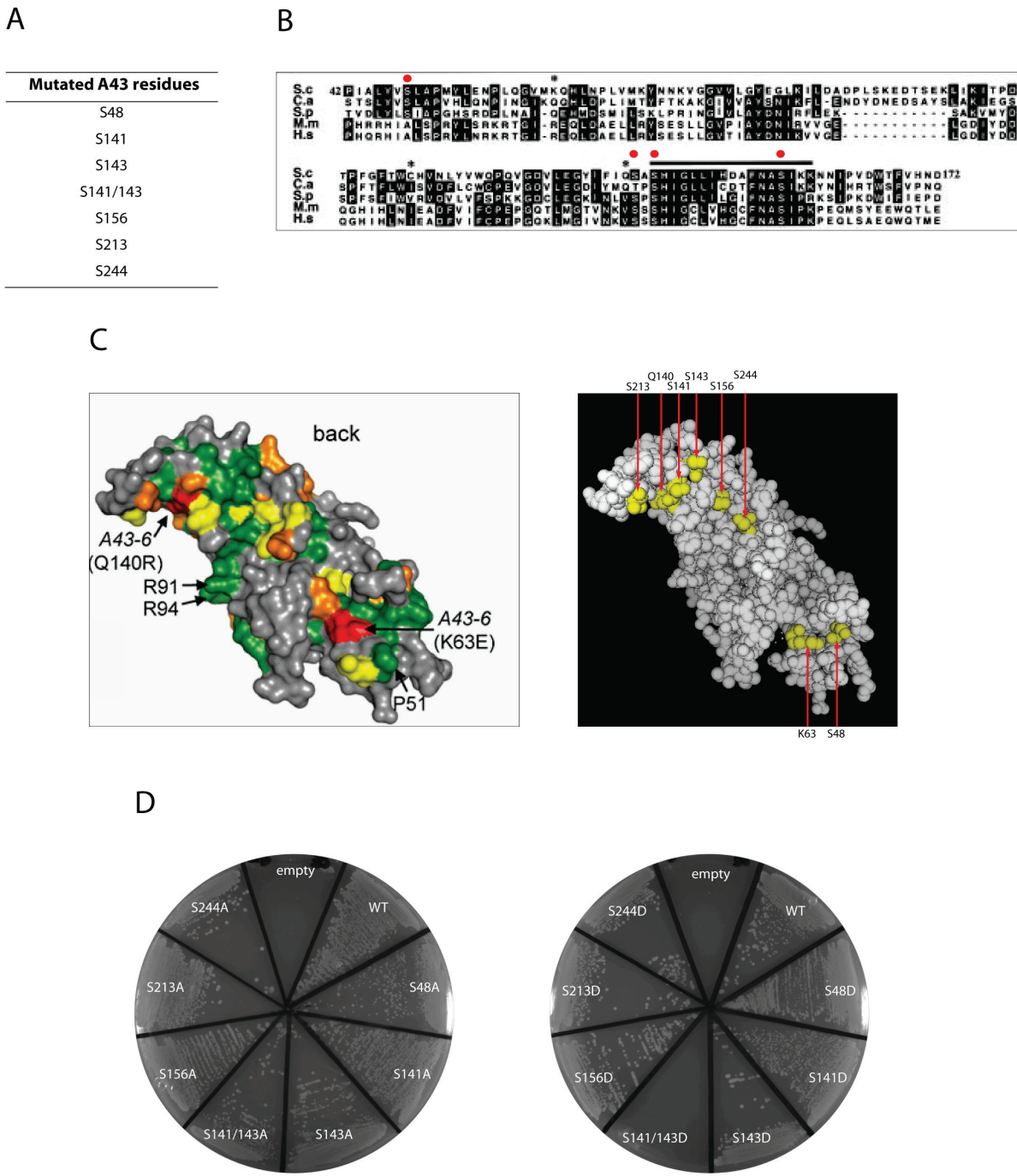
Figure 10. A mutation in the putative A43-Rrn3 interaction site leads to a lethal phenotype

(A) Mutated serines in the putative A43-Rrn3 interaction site. **(B)** Sequence alignment of the conserved domain between orthologues of the A43 subunit. S.c., *Saccharomyces cerevisiae*; C.a., *Candida albicans*; S.p., *Schizosaccharomyces pombe*; M.m., *Mus musculus*; H.s., *Homo sapiens*. Black boxes indicate the residues identical in at least three sequences. The black line localizes a 15 residue motif highly conserved from yeast to human. The asterisks indicate the three residues mutated in the protein encoded by the *rpa43-6* allele. The red dots indicate the mutated S48, S141, S143 and S156 residues within the conserved A43 domain. (from Peyroche et al., 2000) **(C)** Left: Surface representation of the A14/43 complex. Residues conserved among eight selected *Saccharomycotinae* are colored in green, orange, and yellow, according to decreasing conservation. Residues affected by the A43-6 mutations (Peyroche et al., 2000) are in red. (from Kuhn et al., 2007) Right: Position of the mutated serines on the surface representation of the A14/43 complex. Mutated serines as well as the mutated Q140, K63 residues in the A43-6 mutant are shown in yellow. **(D)** Growth of *RPA43* shuffle strain D101-I2 transformed with an empty vector as well as wild-type (WT) vector and mutated *RPA43* vectors is shown on SDC + 5-FOA plates incubated at 30°C. Plasmid shuffling and maintenance of the chromosomal deletion was controlled via the respective auxotrophic markers. Strains were grown at different temperatures for 2-3 days before pictures were taken.

In vitro and *in vivo* experiments were carried out to further analyse this A43 mutant with regard to A43-Rrn3 complex formation or Pol I recruitment to the promoter.

For *in vitro* analyses the serine residues 141/143 were mutated either to alanin or aspartic acid in the expression-vector pET21b A14/A43, kindly provided by Sebastian Geiger from the laboratory of Patrick Cramer. Protein expression and purification from *E. coli* BL21 (DE3) cells, except for the thrombin-cleavage step, were performed as described (Kuhn et al., 2007). A silver-stained SDS-gel of the purified A14/A43 heterodimers (A43 WT, A43 S141/143A, A43 A141/143D) is shown in Figure 11.
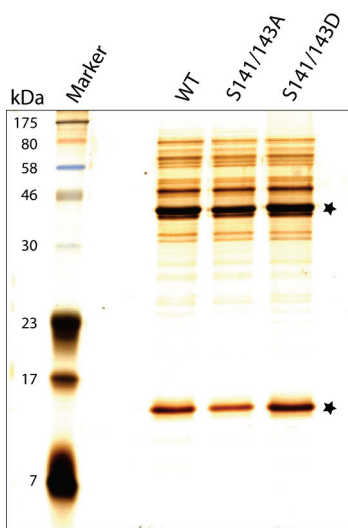
Figure 11. Silver-stained SDS-gel of purified recombinant yeast A14/A43 heterodimers containing either wild-type A43 (WT) or the A43 mutants (S141/143A and S141/143D)

Expression of recombinant proteins and purification via a Ni-NTA column was performed as described in (Geiger et al., 2008) from the expression vector pET21b A14/A43. An internal ribosomal entry site was introduced before A43 to enable bicistronic expression.1µg of total protein of each preparation was loaded and separated on a NuPAGE® 4-12% gradient gel. The corresponding bands for A14 and A43 on the silver-stained gel are marked with a star.

Initial experiments to test the recombinant A14/A43 (WT/A/D) heterodimer for Rrn3 complex formation with immunopurified Rrn3 from yeast were carried out but could not give any conclusive results (data not shown).

Parallel to these studies with recombinant proteins, *in vivo* studies with wild-type and mutant A43 were performed (Felixberger, 2009). Therefore C- and N-terminally FLAG-tagged as well as untagged versions of A43 wild-type, A43 S141/143A and A43 S141/143D were cloned in the YCplac22-pGAL vector. Plasmids were transformed in *RPA43* shuffle-strains D101-I2, D101-I2 A135-TEV-ProtA and D101-I2 Rrn3-TEV-ProtA. A wild-type version of A43 is co-expressed in these strains. Incorporation of the mutated subunits in the polymerase as well as interaction of the mutants with Rrn3 was checked by co-immunoprecipitation. The Co-IP experiments of the mutant A43 subunits and the polymerase performed with ANTI-FLAG M2 beads show that the mutated A43 subunits are incorporated into the polymerase to the same extent as the wild-type subunit (Felixberger, 2009). This result excludes that the lethal phenotype of the

A43 S141/143D mutation originates from incorrect assembly of the subunit to the polymerase. Occupancy of the mutated Pol I at the rDNA promoter and throughout the rDNA was analysed by ChIP in which the FLAG-tagged A43 subunit (wild-type and mutants) was co-immunoprecipitated with rDNA chromatin. One could emphasize that the mutant polymerase co-precipitates only about 40-50% of rDNA chromatin at the promoter and that general Pol I occupancy throughout the rDNA gene is lowered compared to wild-type (Felixberger, 2009). Whether this is due to a disturbance in A43-Rrn3 interaction still remains unclear. The detailed findings of this work are summarized in the diploma thesis of Johannes Felixberger (Felixberger, 2009).

Taken together, it should be noted that conclusive statements on the interaction of the mutated A43 subunits with Rrn3 could not be drawn since, in the performed experiments, the co-expressed untagged A43 wild-type version from the constitutive endogenous promoter is in direct competition with the FLAG tagged A43 versions for Pol I incorporation and Rrn3 interaction. Furthermore it remains unclear whether the mutated serine residues are *in vivo* phosphorylated. *In vivo* and *in vitro* experiments to further characterize these lethal mutations should be carried out.

2.1.3 Analysis of the Pol I synthetic lethal mutant *rpa190* S685D / *Δrpa12*

As mentioned earlier (see 2.2), one phosphosite mutant showed a synthetic lethal phenotype in combination with the deletion of the non-essential Pol I subunit A12.2 (Gerber et al., 2008). Deletion of *RPA12* alone leads to a temperature-sensitive growth phenotype. It is suggested that in the absence of A12.2, the assembly of A190 into a stable Pol I structure is partially defective and the free A190 subunit is subject to proteolytic degradation (Nogi et al., 1993). Increased synthesis of A190 increases the amount of Pol I containing A190 to some extent, leading to partial suppression of growth defects at higher temperatures.

For further analysis of the *rpa190* S685D / *Δrpa12* SL-mutant, conditional yeast strains were established revealing the SL phenotype after shifting the cells from galactose to glucose. Therefore vectors were constructed containing the genes for *RPA190* wild-type or S685 mutants (S/A or S/D), respectively, as well as the gene for *RPA12* expressed from a galactose-inducible promoter. Vectors were transformed in the A190 shuffle strain deleted in *RPA12* and cells were grown in YPG medium after plasmid-shuffling. Shuffling was controlled on different synthetic media to check for presence of the mutant vector, the loss of the wild-type plasmid, and the maintenance of the original RPA-gene deletion. A schematic view of the established yeast strains and serial dilutions of conditional strains with A190 wild type, A190 S685A and A190 S685D mutations on YPG and YPD plates at 30°C are shown in Figure 12A. An isogenic wild-type strain carrying the same vector with a wild-type copy of *RPA190* served as a control. All, wild-type and mutated Pol I subunits, could complement the

loss of the wild-type protein on YPG plates where A12.2 is expressed. However, shift of the cells to glucose, which results in a depletion of A12.2, leads to a severe growth phenotype of the strain expressing the A190 S685D mutant which can be seen in Figure 12B.
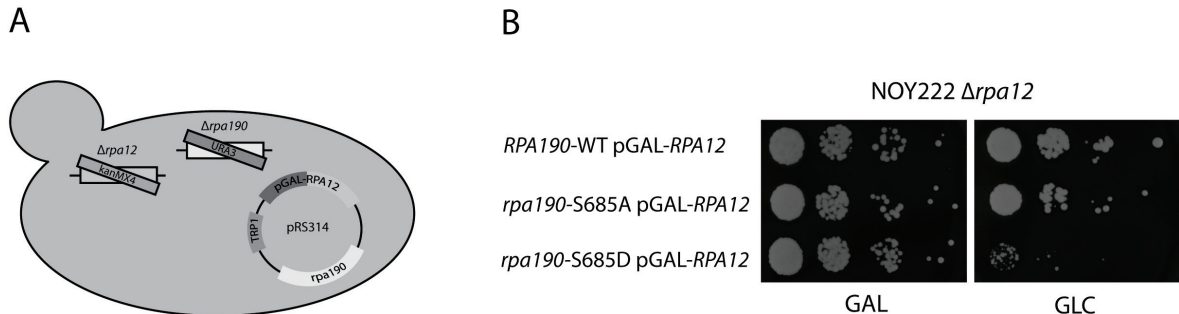
Figure 12. Combination of *rpa19*0 S685D and *Δrpa12* mutations is synthetic lethal

(A) Schematic view of established conditional strains exemplified for an *rpa190* mutant. Endogenous *RPA190* and *RPA12* are deleted by *URA*3- or *KanMX4*-genes, respectively. Cells of the A190-shuffle strain (NOY222 *Δrpa12)* grow on galactose containing media by expressing the wild-type *RPA12* from a galactose-inducible promoter and wild-type or mutant A190 subunit, respectively, from the same low copy plasmid. Shifting of cells from galactose- to glucose containing media leads to a depletion of A12.2 and subsequently emerges the SL-phenotype of the *rpa190* S685D/*Δrpa12* mutations. **(B)** Serial dilutions of the respective wild-type (y1600) and mutant strains (y1601 (S685A), y1602 (S685D)) on galactose and glucose-plates at 30°C are shown as an example. Strains were grown at different temperatures for 2-3 days before pictures were taken.

In growth curves an effect of the SL mutations can be detected 14-16h after shift to glucose (data not shown). Since both mutations are in Pol I, we wanted to confirm that the SL-phenotype is due to impaired Pol I activity. Thus, we performed pulse experiments in which logarithmically growing yeast cells were pulsed with [^{3}H]-uracil for 30 min before shifting to glucose as well as 8h, 10h, 12h, 14h, and 16h after the shift, respectively. RNA was extracted and seperated on a denaturing TBE/urea/acrylamide gel to distinguish the small 5.8S from the 5S rRNAs. Since the 5.8S rRNA derives from the Pol I transcribed 35S rRNA precursor and the 5S rRNA is transcribed by Pol III, changes in transcription activity of the two polymerases in the mutants can be directly compared after the shift to glucose (Figure 13A). After 12-14h the signals for the processed Pol I transcripts 25S, 18S, and 5.8S rRNA get weaker compared to the signal of the Pol III transcribed 5S rRNA in the *rpa190* S685D / *Δrpa12* mutant in comparison to the wild-type. This indicates that the two mutations lead to a non-functional Pol I. As a consequence of this, cell growth is heavily impaired leading to the synthetic lethal phenotype.

A

B
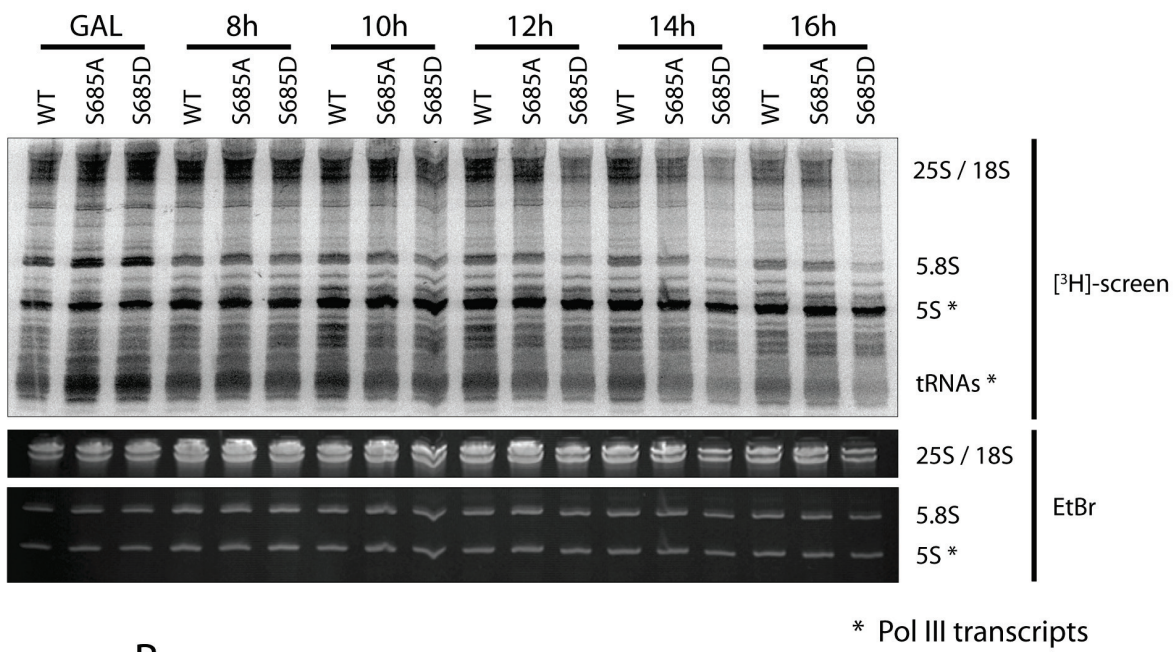
* Pol III transcripts
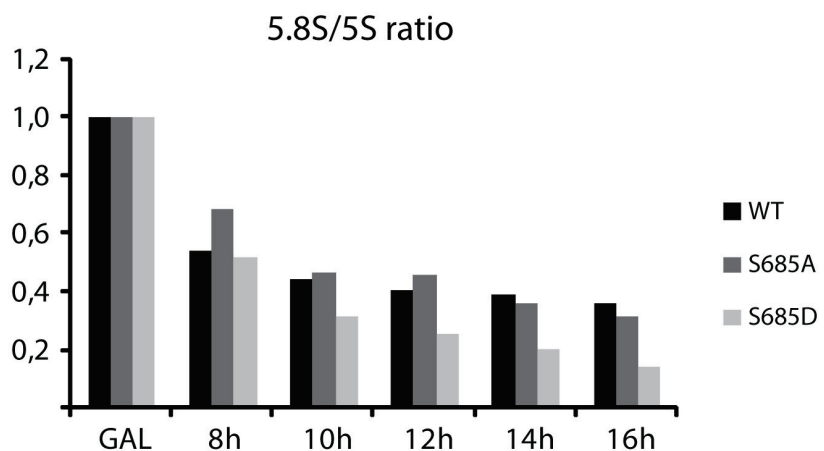
Figure 13. Pol I but not Pol III transcription is impaired in the conditional SL mutant *rpa190* S685D / *Δrpa12* after shift to glucose for 12-14h

Experiments were performed in yeast strains y1600 (WT), y1601 (S685A) and y1602 (S685D). **(A)** [³H]-uracil metabolic labeling of newly synthesized RNA. Cells were pulsed for 30 minutes at 30°C before and at the indicated times after shift to glucose containing media. Total RNA was extracted and separated by gel electrophoresis. RNA was blotted on a positively charged nylon membrane and a [³H]-imaging-screen (FUJI) was applied for 2 days before signals were detected with the FLA-3000 imaging system (FUJI). Signals for 25S-, 18S-, 5.8S-, and 5S rRNA as well as for smaller tRNAs are indicated. Pol III transcripts are marked by an asterisk. Ethidium bromide (EtBr) staining of RNA serves as a loading control. **(B)** Quantification of the 5.8S/5S ratio at the indicated times after shift to glucose in the three analysed strains normalized to the ratio of the corresponding non-shifted strain which was arbitrarily set to 1. Signal intensities for quantification of the obtained 5.8S and 5S signals were determined with the MultiGauge software (FUJI).

Keeping the temperature-sensitive phenotype of the *RPA12* deletion in mind, which is probably caused by partially defective assembly of the A190 subunit into a stable polymerase (Nogi et al., 1993), one could imagine that the *rpa190* S685D phosphosite mutation could enhance this ts-phenotype. Since Van Mullem and co-workers reported that the N-terminal

zinc domain is sufficient to cure the ts-phenotype (Mullem et al., 2002), we created a conditional system for the expression of wild-type A12.2 as well as for N-terminally (aa69-125) and C-terminally (aa1-69) truncated A12.2 variants to verify if the presence of the N-terminal domain of A12.2 rescues the SL-phenotype. For this purpose the Tet-Off expression system was used. The Tet-system was originally developed for mammalian cells (Gossen and Bujard, 1992) and is based on a tetracycline-controlled transactivator protein (tTA), which is composed of the Tet repressor DNA binding protein (TetR) from *E. coli* fused to the strong transactivating domain of VP16 from Herpes simplex virus. It regulates expression of a target gene that is under transcriptional control of a tetracycline-responsive promoter element (TRE). The TRE is made up of Tet operator (tetO) sequence concatemers fused to a minimal promoter. In the absence of tetracycline (Tc) or its analogon doxycyclin (Dox), tTA binds to the TRE and activates transcription of the target gene. In the presence of Tc or Dox, tTA can not bind to the TRE, and expression from the target gene remains inactive (Baron and Bujard, 2000). One advantage of this expression system is that expression can be precisely regulated via the concentration of Tc or Dox in the media. In *S. cerevisiae* this system is mainly used to characterize essential proteins, which can be done either by using yeast-specific expression vectors, containing the tTA-gene and the tetO-promoter, or by direct integration of these two elements into the yeast genome through homologous recombination. In our case we used a slightly modified version of the pCM182 yeast expression vector (Garí et al., 1997) in which the *TRP1* marker was replaced by a *LEU2* marker from YCplac111 to make it compatible with the markers used in the analysed yeast strain. *RPA12* wild-type, *rpa12-ΔC* (aa1-69), and *rpa12-ΔN* (aa69-125) were PCR-amplified and cloned into the MCS of the modified pCM182-LEU2. The obtained vectors and an empty vector control were transformed in the wild-type and mutant strains, and serial dilutions were spotted on GAL, GLC, GAL + Dox and GLC + Dox plates (final Dox concentration 10 µg/ml). A schematic overview of the used strains and expected results exemplified for the N-terminally truncated A12.2 version as well as the results from the serial dilutions are depicted in Figure 14B-C. This data shows that the N-terminal domain of A12.2 alone is sufficient to rescue the SL phenotype which could argue for a destabilized Pol I as the main reason for the growth inhibition.
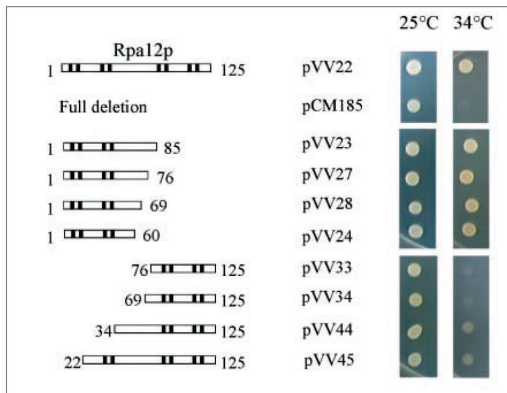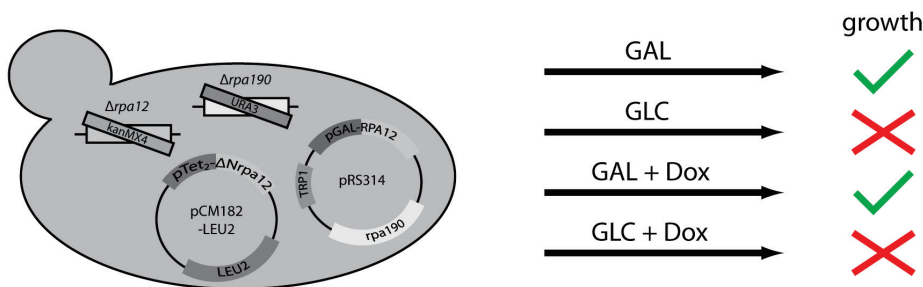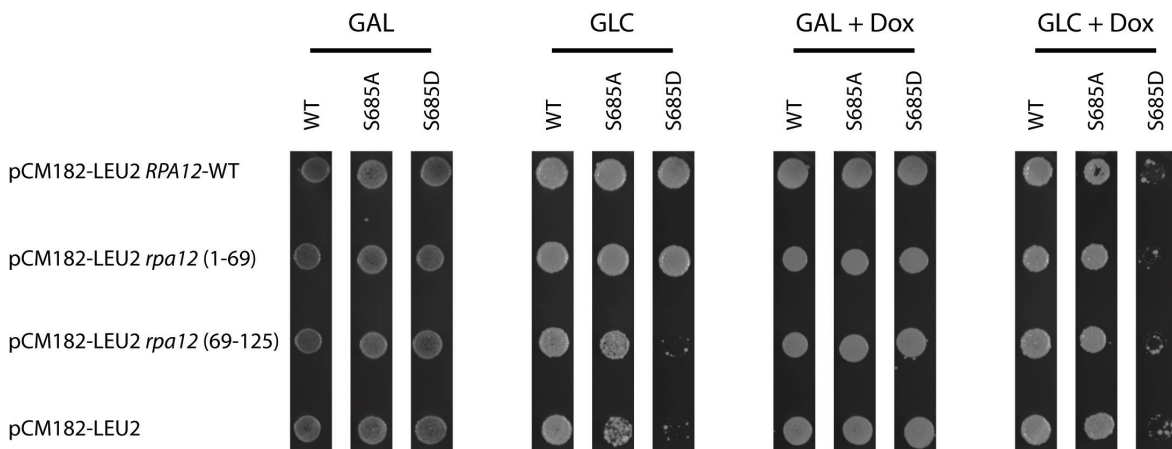
Figure 14. Expression of the A12.2 N-terminus rescues the SL phenotype of the *rpa190* S685D / *Δrpa12* mutant

(A) Partial deletions of A12.2. Growth pattern: strain SL9-6b (*Δrpa12*) was transformed with pCM185 derivatives bearing wild type or partly deleted *RPA12* mutants. Cells were spotted and incubated at 25°C and 34°C for 4–5 days. A12.2 fragments are symbolized by open boxes. The black boxes denote invariant cysteines (from Mullem et al., 2002). **(B)** Schematic representation of the conditional yeast strain with galactose-dependent expression of wild-type A12.2 and an N-terminally truncated A12.2 (69-125) version expressed from a doxycyclin (Dox)-repressed promoter, when Dox is missing. Expected survival on different growth conditions for the N-terminally truncated A12.2 (aa69-125) version is shown to the right. **(C)** Experiments were performed in yeast strains y1600 (WT), y1601 (S685A) and y1602 (S685D). Spots of respective strains transformed with the indicated Tet-Off vectors (left) on different SC-leu plates (GAL, GLC, GAL + Dox, GLC + Dox) are shown. Plates were incubated for 3-4 days at 24°C before pictures were taken, to exclude possible ts-effects caused by A12.2 variants.

To confirm that the mutations cause a Pol I assembly phenotype we wanted to compare the amount of co-precipitated Pol I subunits in wild-type and mutant strains (Pilsl, 2010). A semi-quantitative mass spectrometry approach (iTRAQ®, Applied Biosystems) was used. 16h after shift to glucose, the polymerases were purified via the TEV-ProtA-tagged A135 subunit in the corresponding yeast strains. The associated proteins were digested with trypsin, labeled with the iTRAQ reagents, and analysed by mass spectrometry (MALDI TOF/TOF). A135 is the second largest Pol I subunit and part of the core polymerase. Early Pol I assembly defects should be detected by different subunit stoichiometry of the co-purified Pol I complexes. Indeed, these preliminary results indicate that subunit assembly is affected in the SL mutant, since A190 and associated subunits like A43, ABC27, ABC23, and A14 seem to be partially depleted from the complex (Figure 15), arguing for an impaired assembly of A190 and subsequently associated subunits in the SL mutant polymerase (Nogi et al., 1993; Lanzendörfer et al., 1997). However, this experiment should be repeated to confirm these results.
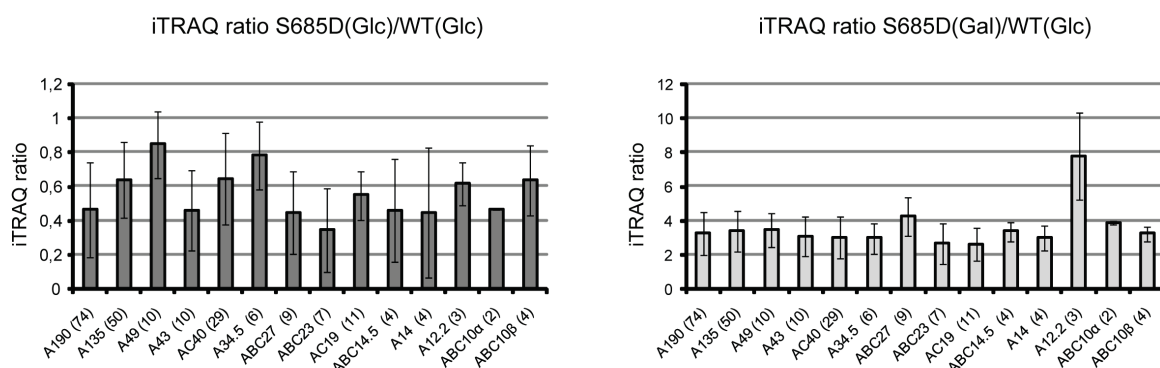
Figure 15. The synthetic lethal phenotype is probably caused by impaired assembly of A190 and subsequently associated subunits

Semi-quantitative mass spectrometric comparison of co-purified Pol I subunits from mutant and WT cells shifted to glucose (left panel) as well as mutant cells overexpressing A12.2 and WT cells (right panel). Experiments were performed in yeast strains y2043 (WT), y2044 (S685A) and y2045 (S685D). RNA polymerase I was purified via its TEV-ProtA tag on subunit A135 from cell lysates of both, wild-type strain and respective mutant strains depleted for *RPA12,* as well as for a control strain y2045 not depleted for *RPA12.* For a detailed description of iTRAQ labeling see 5.2.6. The relative iTRAQ ratio of purified Pol I subunits for both, shifted SL-mutant (S685D) and shifted corresponding wild-type (WT), indicating an enrichment or depletion of co-purified subunits is shown in the left panel. The relative iTRAQ ratio of purified Pol I subunits for both, non-shifted SL-mutant (S685D) and shifted corresponding wild-type (WT) showing the depletion of A12.2 is depicted in the right panel. A mean value, with the corresponding standard deviation of all identified peptides of a single protein is depicted. The name of the respective yeast protein is given below each bar followed by the number of identified peptides in parentheses.

2.1.4 Characterization of a dominant negative A12.2 mutation

The Pol I subunit A12.2 seems to be not only involved in Pol I assembly and complex stability but was also reported to play a role in RNA cleavage, transcript elongation and termination (Kuhn et al., 2007; Mullem et al., 2002; Prescott et al., 2004). Although deletion of the C-terminal domain does not lead to a temperature-sensitive phenotype as found for the N-terminus, it contains a highly conserved motif (Q.RSADE..T.F), which is also present in the Pol II elongation factor TFIIS (see 1.2.2).

The two acidic residues (DE) in the conserved motif were shown to be crucial for the mechanism of TFIIS-induced RNA cleavage (Jeon et al., 1994; Kettenberger et al., 2003). Mutation of the same residues in C11 (the Pol III counterpart) is lethal (Chédin et al., 1998). An intrinsic RNA cleavage activity which was shown to be dependent on the C-terminal domain of A12.2 is responsible for shortening the RNA from the 3` end in an artificially stalled ternary complex *in vitro* (Kuhn et al., 2007).

In collaboration with the laboratory of Patrick Cramer, Jochen Gerber created a mutant of the Pol I subunit A12.2 to investigate the role of this subunit in the intrinsic Pol I RNA cleavage activity. The two above mentioned acidic residues in the conserved C-terminal motif were replaced by alanines in A12.2, resulting in the mutant *rpa12* D105A E106A (A12.2 DE/AA) (Gerber, 2008). Paradoxically, the mutation of these two amino acids in a dispensable part of a non-essential protein leads to a lethal phenotype. To further investigate this phenomenon, plasmids were constructed in which the genes for the wild-type A12.2 and the mutant A12.2 DE/AA are expressed from a galactose-inducible promoter. Under the repressing glucose conditions all strains behaved like the *RPA12* deletion strain showing the described ts-phenotype (Nogi et al., 1993). On galactose plates, the knock-out was complemented by the wild-type A12.2 as judged by the ability to grow at 37°C. In contrast, after induction of A12.2 DE/AA mutant-expression, no colonies were formed at any incubation temperature (Figure16), confirming the observation that this mutation apparently results in a lethal phenotype.
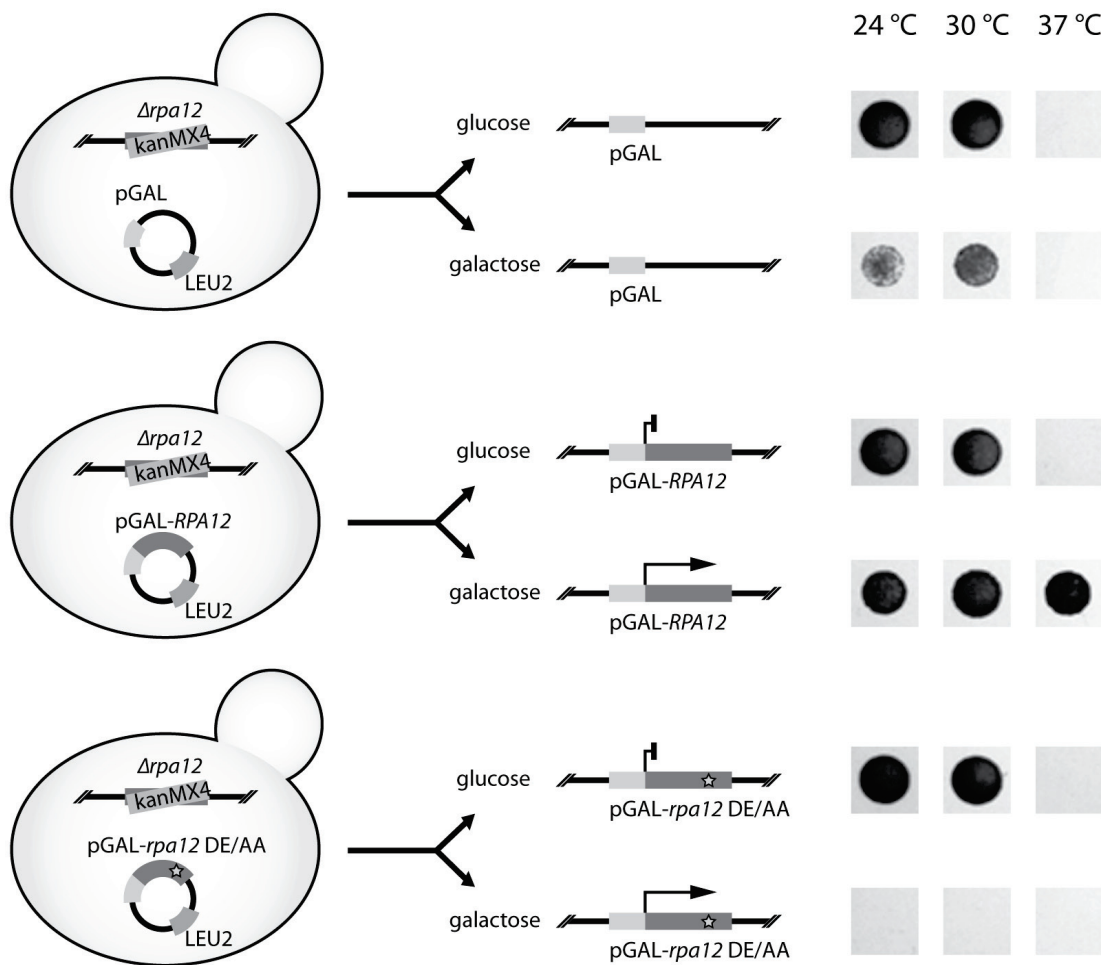
Figure 16. Overexpression of the mutated Pol I subunit A12.2 D105A E106A, containing the mutations in the highly conserved C-terminal motif (Q.RSA<u>DE</u>..T.F), is lethal

Experiments were performed with the strain y601 (BY4741 *Δrpa12)* transformed with the vectors YCplac111-pGAL, YCplac111-pGAL-*RPA12*, or YCplac111-pGAL-*rpa12* DE/AA. Strains were spotted on plates containing either glucose (no expression) or galactose (expression) and grown at different temperatures for 2-3 days before pictures were taken. (from Gerber, 2008)

The phenotype of the *rpa12* DE/AA mutation is suppressed at higher temperatures. The constructed plasmids (YCplac111-pGAL, YCplac111-pGAL-*RPA12* or YCplac111-pGAL-*rpa12* DE/AA) were transformed in the EUROSCARF wild-type strain BY4741 and A12.2 versions were co-expressed with endogenous A12.2 wild-type. Serial dilutions of the corresponding strains were spotted on glucose- and galactose containing plates, respectively (Figure 17).
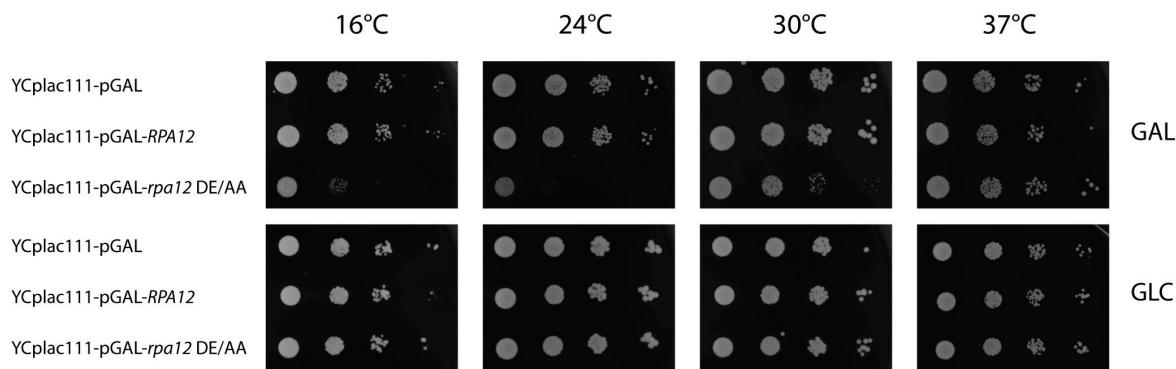
Figure 17. The dominant negative phenotype of the *rpa12* DE/AA mutation is suppressed at higher temperatures in wild-type strains

Experiments were performed with the strain y206 (BY4741) transformed with the vectors YCplac111-pGAL, YCplac111-pGAL-*RPA12*, or YCplac111-pGAL-*rpa12* DE/AA. Strains were spotted in serial dilutions on plates containing either glucose (no expression) or galactose (expression) and grown at different temperatures for 2-3 days before pictures were taken.

Note that the phenotype of the *rpa12* DE/AA mutation is attenuated in strains endogenously expressing wild-type A12.2 at low temperatures and disappears at higher temperatures.

Interestingly, the N-terminal FLAG-tag on A12.2 shows no effect on the lethal phenotype of the DE/AA mutation, whereas the C-terminal FLAG-tag suppresses the lethal phenotype and additionally rescues the *Δrpa12* ts-phenotype at 37°C (Figure 18), indicating, that the lethal phenotype is suppressed most probably by sterical hindrance introduced by the C-terminal FLAG-tag.
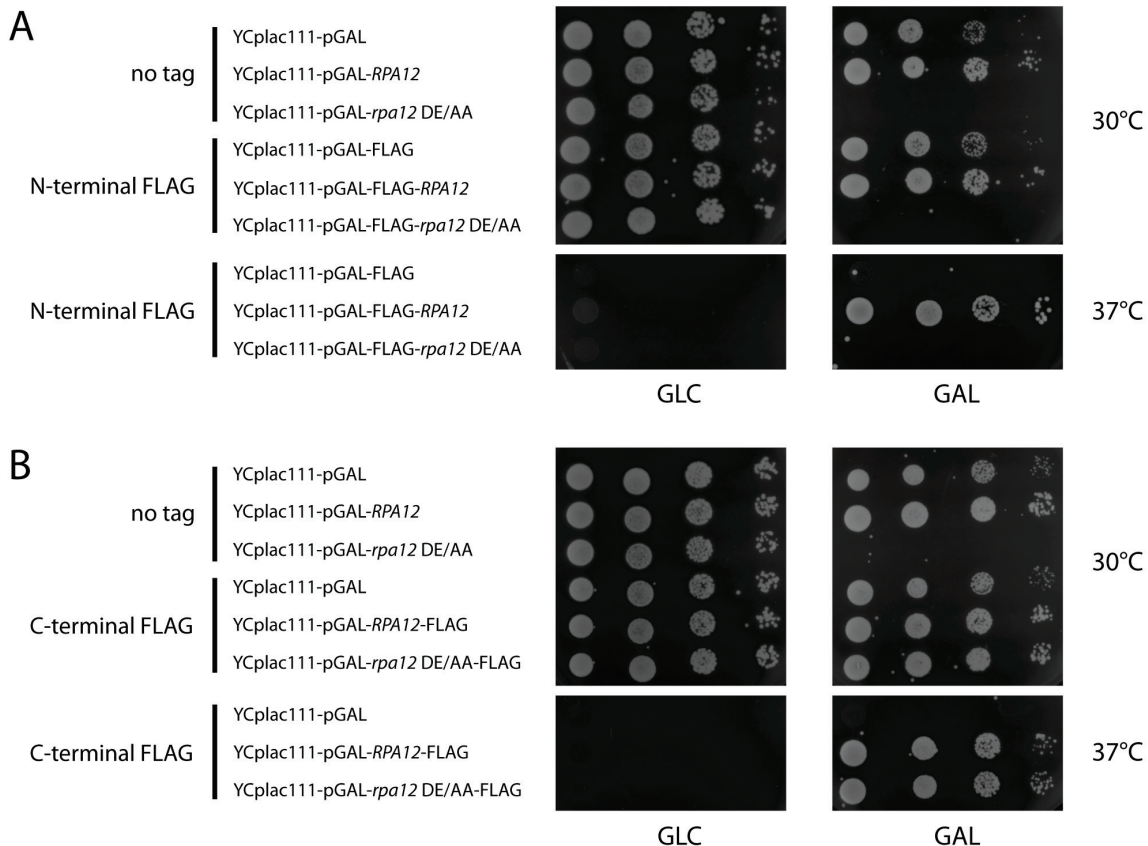
Figure 18. C-Terminal FLAG-tag rescues the lethal phenotype induced by the A12.2 DE/AA mutant

Experiments were performed with the strain y601 (BY4741 *Δrpa12*) transformed with the vectors YCplac111-pGAL, YCplac111-pGAL-*RPA12*, YCplac111-pGAL-*rpa12* DE/AA, YCplac111-pGAL-FLAG, YCplac111-pGAL-FLAG-*RPA12*, or YCplac111-pGAL-FLAG-*rpa12* DE/AA) **(A)** and with the vectors YCplac111-pGAL, YCplac111-pGAL-*RPA12*, YCplac111-pGAL-*rpa12* DE/AA, YCplac111-pGAL-*RPA12*-FLAG, or YCplac111-pGAL-*rpa12* DE/AA-FLAG) **(B)**. Strains were spotted in serial dilutions on plates containing either glucose (no expression) or galactose (expression) and grown at different temperatures for 2-3 days before pictures were taken.

To investigate whether these mutations impair Pol I transcription and do not induce general toxicity, we performed RNA pulse labeling experiments in BY4741 *Δrpa12* (y601) transformed with YCplac111-pGAL, YCplac111-pGAL-*RPA12*, or YCplac111-pGAL-*rpa12* DE/AA before, as well as 2h, 4h, and 8h after shifting the cells to galactose. Logarithmically growing yeast cells were pulsed with [^{3}H]-uracil for 15 min. RNA was extracted and separated by denaturing agarose gel electrophoresis to resolve the larger rRNAs as well as on a denaturing TBE/urea/acrylamide gel to resolve the smaller 5.8S rRNA and the Pol III transcribed 5S rRNA. An autoradiograph of the blotted RNA is shown in Figure 19.
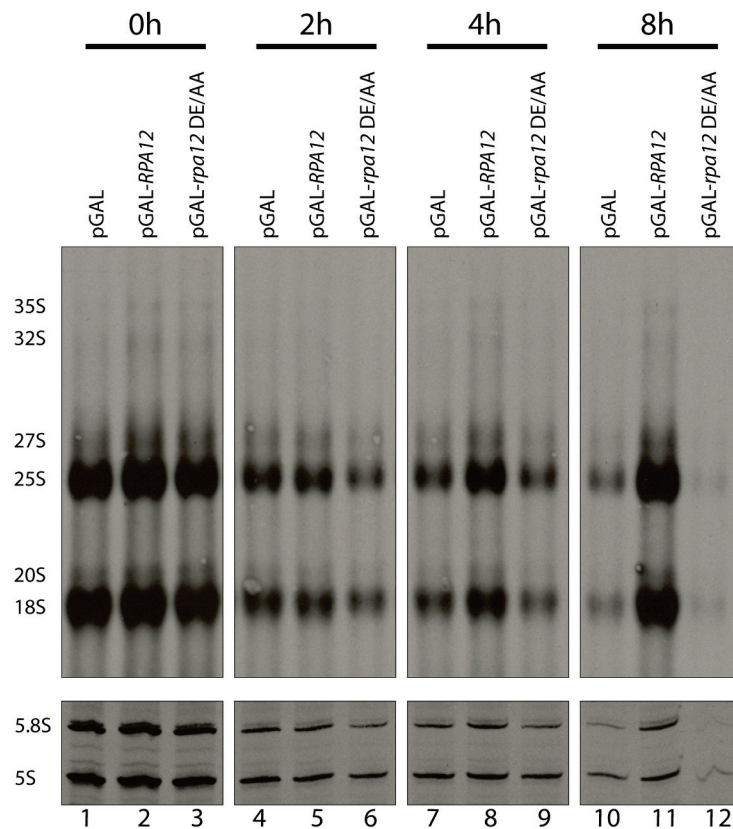
Figure 19. The lethal A12.2 DE/AA mutant affects primarily Pol I transcription

Experiments were performed with the strain y601 (BY4741 *Δrpa12*) transformed with the vectors YCplac111-pGAL, YCplac111-pGAL-*RPA12*, or YCplac111-pGAL-*rpa12* DE/AA. Cells were grown overnight in selective media containing glucose before shift to YPG to induce expression of A12.2 variants. One OD_{600} of cells was withdrawn at the indicated times for $[^3H]$-uracil metabolic labeling of newly synthesized RNA. Cells were pulsed for 15 min at 30°C. Total RNA was extracted and separated by gel electrophoresis. Radio-labeled RNA was visualized by fluorography.

It appears that Pol I transcription, but not pre-rRNA processing is severely affected after shift to galactose for 8h since no signal accumulation of a rRNA precursor over the mature rRNA is detected. Signal intensity and thus transcription is generally reduced in the mutant compared to wild-type (Figure 19, compare lane 12 to lane 11). It is also apparent that Pol I transcription is primarily affected compared to Pol III transcription (Figure 19, compare 5.8S rRNA to 5S rRNA in lanes 10-12). The signal intensity for the Pol III transcribed 5S rRNA also declines 8h after the shift. This is probably due to secondary effects of the lethal phenotype. By creating single mutants of the acidic residues D105 and E106 to alanin via SOE-PCR we tried to dissect the lethal mutation. Vectors were transformed in BY4741 *Δrpa12* (y601) and corresponding strains were spotted in serial dilutions on glucose- and galactose containing plates (Figure 20). The single mutations alone also generate a severe growth phenotype (D105A more severe than E106A) but no lethality.
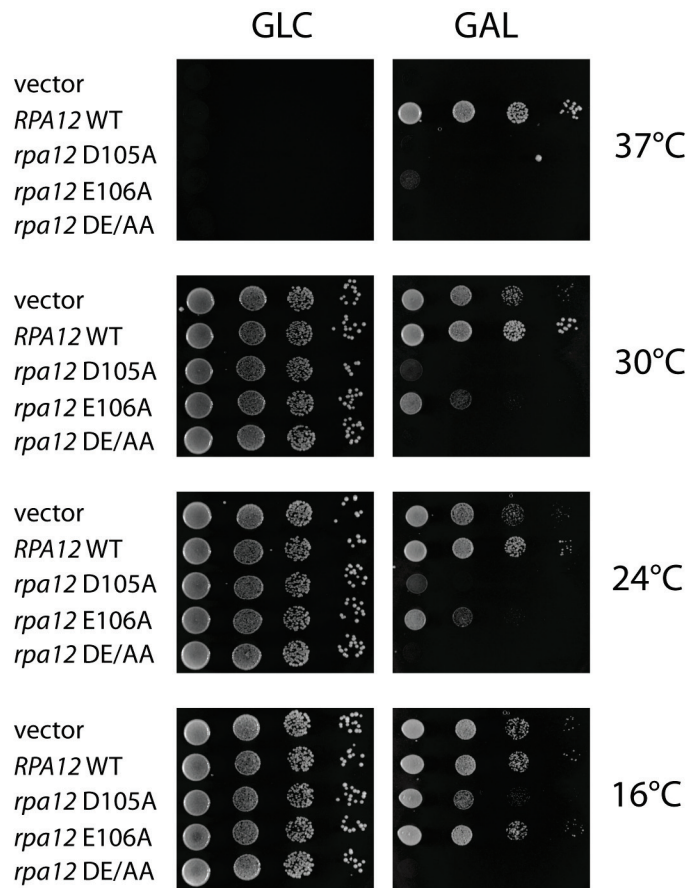
Figure 20. Overexpression of the single mutants A12.2 D105A and A12.2 E106A exhibits a severe growth phenotype but is not lethal

Experiments were performed with the strain y601 (BY4741 *Δrpa12)* transformed with the vectors YCplac111-pGAL, YCplac111-pGAL-*RPA12*, YCplac111-pGAL-*rpa12* D105A, YCplac111-pGAL-*rpa12* E106A, or YCplac111-pGAL-*rpa12* DE/AA. Strains were spotted in serial dilutions on plates containing either glucose (no expression) or galactose (expression) and grown at different temperatures for 2-3 days before pictures were taken.

In RNA pulse labeling experiments, effects on Pol I transcription compared to Pol III transcription are evident in all mutant strains (Figure 21, compare 5.8S rRNA to 5S rRNA). Only slight differences are detectable among the mutants (Figure 21, compare lane 6, 8, and 10) after 8h of induction.

As the control strain with the transformed empty vector also shows comparable defects after shift to galactose, it seems that the EUROSCARF yeast strain BY4741 *Δrpa12* (y601) generally acts sensitive upon shift to galactose.
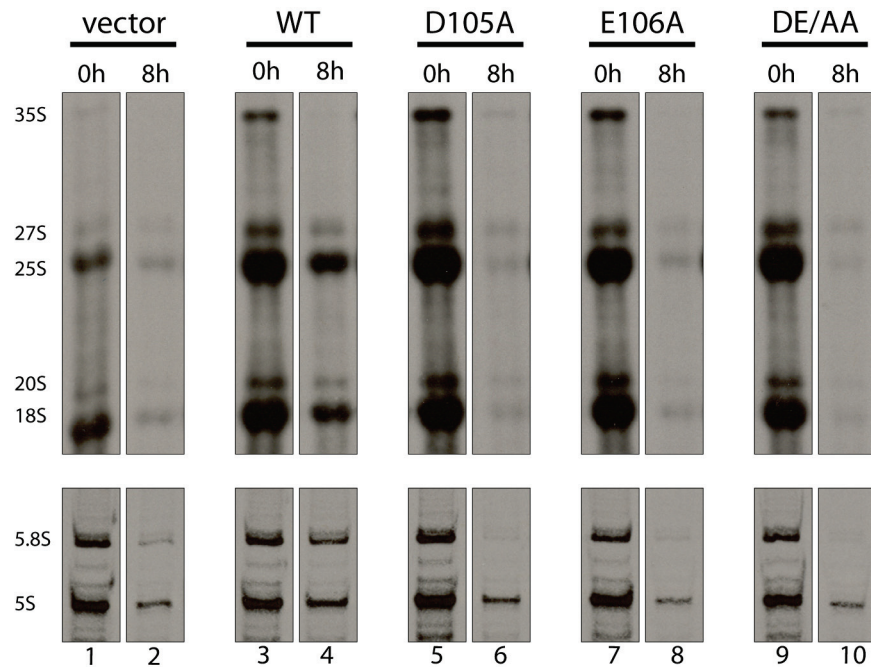
Figure 21. The single mutants A12.2 D105A, A12.2 E106A and the double mutant A12.2 DE/AA impair Pol I but not Pol III transcription

Experiments were performed with the strain y601 (BY4741 *Δrpa12)* transformed with the vectors YCplac111-pGAL, YCplac111-pGAL-*RPA12*, YCplac111-pGAL-*rpa12* D105A, YCplac111-pGAL-*rpa12* E106A, or YCplac111-pGAL-*rpa12* DE/AA. Cells were grown overnight in selective media containing glucose before shift to YPG for expression of A12.2 variants. One OD_{600} of cells was withdrawn at the indicated times for [^{3}H]-uracil metabolic labeling of newly synthesized RNA. Cells were pulsed for 15 min at 30°C. Total RNA was extracted and separated by gel electrophoresis. Radio-labeled RNA was visualized by fluorography.

Therefore all following experiments were carried out in the yeast strain background W303-1a, which is commonly used in shift experiments. Vectors were transformed in W303-1a and W303-1a *Δrpa12* (y1597) to test for the above described phenotypes after shift to galactose in the new strain backgrounds by spotting serial dilutions of the corresponding strains on glucose and galactose containing plates.

The growth phenotype of the *rpa12* D105A, E106A and DE/AA mutations is attenuated in strains endogenously expressing wild-type A12.2 at low temperatures and disappears at higher temperatures whereas the lethal effect prevails in the *Δrpa12* genetic background (data not shown). Occurring phenotypes are as described in the BY4741 and BY4741 *Δrpa12* (y601) strain background.

To investigate correct subunit incorporation of the wild-type and mutated A12.2 subunits into the polymerase, the A135 subunit was TEV-ProtA-tagged as described in (Knop et al., 1999). Since no antibody detecting the A12.2 subunit is available in the lab, N-terminal FLAG-tagged versions of the A12.2 wild-type and mutants were cloned. Vectors were transformed in W303-1a *Δrpa12* RPA135-TEV-ProtA to test for the presence of the described phenotypes after shift to galactose by spotting serial dilutions of the corresponding strains on glucose and galactose containing plates. A135-TEV-ProtA-tagging and N-terminal FLAG-tagging of A12.2

wild-type and mutants did not affect the described phenotypes (data not shown). A co-immunoprecipitation of the FLAG tagged A12.2 mutants in the Pol I complex via IgG-coupled magnetic beads immunoprecipitating the A135 subunit was performed to analyse assembly of the mutant subunits to the enzyme. However, correct integration could not be clearly shown in this preliminary experiment (Pilsl, 2010). Yet, it can be assumed that a correct incorporation takes place since strains carrying the N-terminal FLAG-tag show the same phenotype as untagged strains. For example, the galactose induced expression of tagged A12.2 rescues the ts-phenotype of a deletion strain at 37°C. Furthermore, Michael Pilsl used chromatin-immunoprecipitation (ChIP) experiments to determine whether the association of the polymerase with the rDNA varies in the different mutants. First indications that Pol I is less associated to rDNA in the mutants, pointing to problems in Pol I initiation or early elongation, could be detected. For more detailed information see (Pilsl, 2010). Nevertheless, these experiments should be repeated to reproduce the obtained results.

Taken together, in the performed Pol I mutant analyses no phenotype could be detected in the investigated Pol I phosphomutants. Furthermore a putative Pol I-Rrn3 interaction mutant could be generated and initially characterized. Analysis of the described Pol I synthetic lethal mutant (Reiter, 2007) could give indications for the possible role of the A190 S685 phosphosite in enzyme assembly, and the characterization of a lethal A12.2 mutant could reveal the possible role of the A12.2 C-terminus in transcript cleavage and/or early elongation. However, to elucidate at which exact stages the mutations affect the Pol I transcription process further *in vivo* analyses of the mutant enzymes are necessary.

2.2   Regulation of ribosome synthesis upon environmental changes

The activity of RNA polymerase I and thus ribosome biogenesis is apparently strictly regulated in a TOR-dependent manner. As a cause of rapamycin-induced TOR inactivation, the amount of Pol I-Rrn3 complexes is decreased as is the association of Pol I with both the promoter and the transcribed region of the rDNA locus (Claypool et al., 2004; Philippi et al., 2010). This suggests that in yeast the rate of Pol I transcription is strongly dependent on the formation of Pol I-Rrn3 complexes.

Since in yeast Rrn3 as well as Pol I is described to be phosphorylated *in vivo* (Bell et al., 1976; Buhler et al., 1976a; Bréant et al., 1983; Fath et al., 2001), TOR signaling was speculated to influence the formation of Pol I-Rrn3 complexes via phosphorylation-dephosphorylation cascades in a growth-dependent manner.

However, the dramatic reduction of rRNA synthesis in the immediate cellular response to impaired TOR signalling cannot be explained by the simple down-regulation of Rrn3 and Pol I–Rrn3 levels (Philippi et al., 2010).

As indicated in the introduction (1.2.6) TOR inhibition appears to affect ribosome biogenesis on many different levels: (a) transcriptional regulation of all three polymerases, (b) translation initiation, (c) RNA processing, and (d) internuclear and nucleo-cytoplasmatic transport processes.

It has become increasingly difficult to distinguish between primary and secondary effects on ribosome biogenesis in the yeast *Saccharomyces cerevisiae* since the multiple processes leading to mature ribosomes appear to be intimately linked. To determine the target mediating the fast response to TOR inactivation we performed an in-depth analysis of yeast cellular phenotypes after 15 min of rapamycin treatment. Rapamycin treatment mimics nutrient starvation of cells by specifically inactivating the kinase activity of TORC1. Since the inhibition of translation by cycloheximide treatment leads to very similar pre-rRNA processing defects (de Kloet, 1966; Udem and Warner, 1972; Warner and Udem, 1972), this drug can be used as a tool to directly compare the effects of short-term rapamycin treatment and cycloheximide treatment on rRNA neo-synthesis in pulse-chase experiments. Therefore, yeast strains RRN3-TAP-A43-3xHA (y658), and a wild-type BY4741 (y206) were grown in YPD at 30°C to mid-log phase before cultures were split in three parts and further cultivated in YPD either in the absence or in the presence of rapamycin or cycloheximide, respectively. After 15 min of treatment, same amounts of cells were pulsed for 5 min with [^{3}H]-uracil and chased with an excess of unlabeled uracil for 4 min, 8 min, and 16 min. Total RNA was isolated and analysed by denaturing agarose gel electrophoresis with subsequent Northern blotting and autoradiography (Figure 22A-B). To exclude effects of rapamycin or cycloheximide on the cellular [^{3}H]-uracil uptake, experiments were performed after pulse labeling where samples were taken twice for untreated cells (black) and three times after 15 min treatment (gray) (Figure 22C). Note, that the [^{3}H]-uracil uptake was only moderately affected after 15 min rapamycin or cycloheximide treatment.
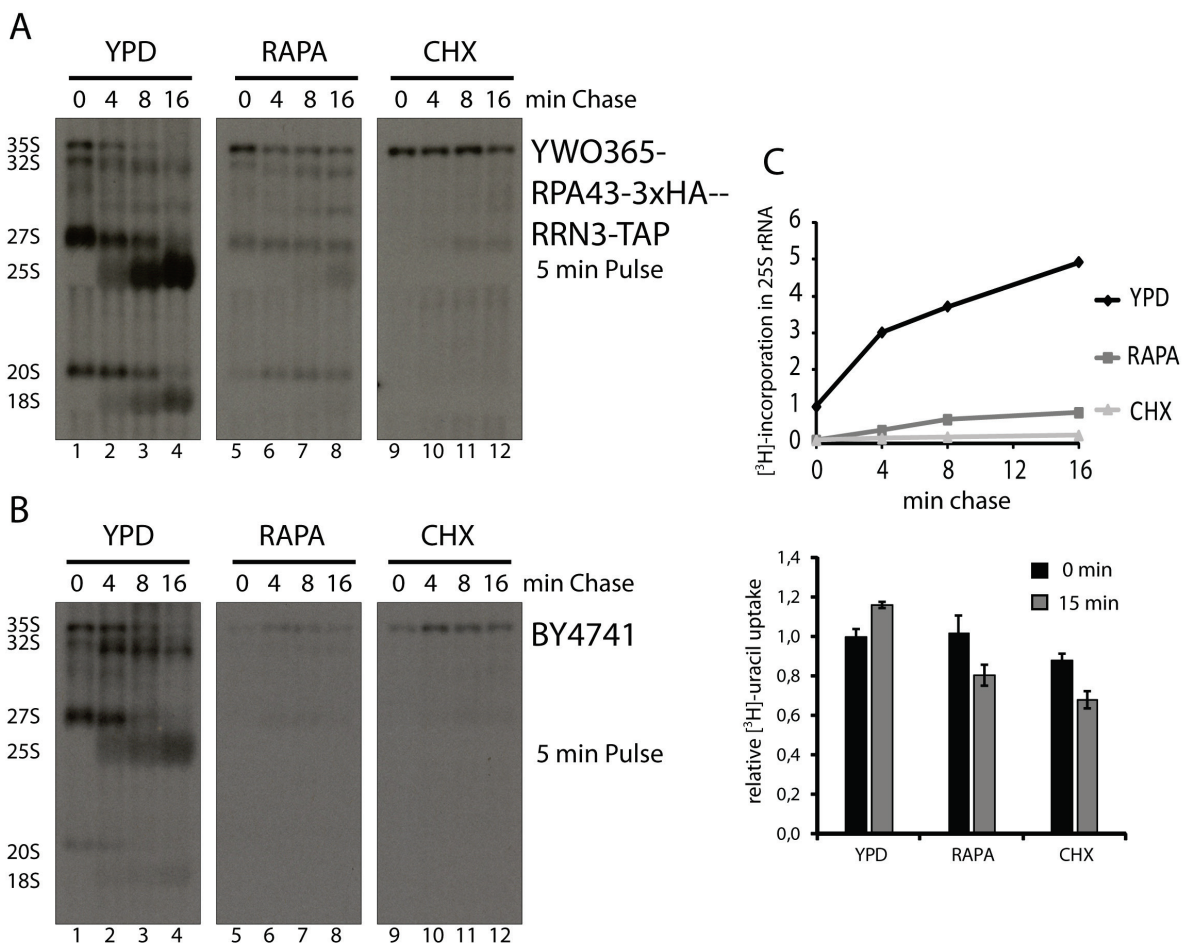
Figure 22. Short-term rapamycin or cycloheximide treatment lead to severe pre-rRNA processing defects while [³H]-uptake is only moderately affected after 15 min treatment

Experiments were performed with yeast strains y658 **(A)**, and y206 **(B)**. Strains y658 (expressing 3xHA-tagged Pol I subunit A43 and TAP-tagged Rrn3), and y206 (BY4741) were grown in YPD at 30°C to mid-log phase before the cultures were split in three parts and further cultivated in YPD either in the absence or in the presence of rapamycin (200 ng/ml) or cycloheximide (100 µg/ml) for 15 min. Pulse labeling with [³H]-uracil was performed for 5 min followed by a chase with an excess of unlabeled uracil (final concentration 1 mg/ml) for the times indicated above the panel. RNA was isolated, separated in a denaturing agarose gel, and transferred to a positively charged nylon membrane. The autoradiogram shown was obtained after exposure of the membrane treated with EN³HANCE solution. Positions of the different rRNA processing products are indicated on the left. **(C)** Data for y685 is depicted as an example. Quantitative analysis of [³H]-uracil incorporation into 25S rRNA (top) was determined by excision of the 25S rRNA bands from an identical blot and analysis by liquid scintillation counting. The values obtained were normalized to the value after 5 min pulse (0) of the culture grown for 15 min in YPD, which was arbitrarily set to 1, and plotted against the time of the chase. Cellular [³H]-uracil uptake moderately decreases upon rapamycin and cycloheximide treatment for 15 min (bottom). Exponentially growing yeast strains were cultured in the absence (YPD) or presence of rapamycin (200 ng/ml) or cycloheximide (100 µg/ml) for the times indicated. Pulse-labeling with [³H]-uracil was performed for 5 min. The cell-associated [³H]-label was determined. The values obtained were normalized to the value after 5 min pulse (0 min) of the culture grown in YPD, which was arbitrarily set to 1. The experiment was performed twice for untreated cells (black bars) and in triplicate for cells after 15 min treatment (gray bars).

Untreated cells showed wild-type levels of newly synthesized 35S pre-rRNA, which was subsequently processed to the intermediate 27S and 20S rRNA and finally to the mature 25S and 18S rRNA (Figure 22A-B, lanes 1-4). Strikingly, in both rapamycin and cycloheximide treated cells, strong maturation defects could be detected resulting in the relative accumulation of labeled 35S pre-rRNA. Although the initial 35S pre-rRNA levels were

45

comparable to those observed in untreated cells, the amounts of intermediate rRNA and mature rRNA were strongly reduced in rapamycin-treated cells and almost completely lost in cycloheximide-treated cells (Figure 22A-B, lanes 5-12). Furthermore, the incorporation of [^{3}H]-uracil into the mature 25S rRNA was quantified for all strains as a measure of ribosome neo-production (Figure 22C). 15 min of TOR inactivation were sufficient to decrease the neo-synthesis of 25S rRNA to less than 10%, whereas the effect in cells inhibited in translation for the same time was even stronger. These results suggest that inhibition of translation by cycloheximide for 15 min leads to severe defects in pre-rRNA maturation comparable to those observed after short-term TOR inactivation by rapamycin.

Since the pool of "free" ribosomal proteins is limited due to their fast turnover rate and rapid assembly into pre-ribosomal particles (Gorenstein and Warner, 1977; Kruiswijk et al., 1978; Wittekind et al., 1990) and since ribosome biogenesis defects are observed after conditional shutdown of individual r-proteins (Ferreira-Cerca et al., 2005, 2007; Pöll et al., 2009), we compared neosynthesis of r-proteins upon short-term rapamycin treatment and treatment with different concentrations of cycloheximide. Experiments were performed by Robert Steinbauer. To this end, yeast strains were cultured in either the absence or presence of rapamycin or cycloheximide for 15 min prior to pulse-labeling of proteins with [^{35}S] methionine-cysteine. After extraction, [^{35}S]-incorporation into total protein was determined. Proteins were separated in 16% urea gels and analysed by Coomassie staining and autoradiography.

Total protein production decreased to around 50% to 60% of the value in the untreated sample after 15 min of rapamycin treatment (Figure 23B). Downregulation of protein synthesis was virtually identical when cells were treated with 0.1 µg/ml cycloheximide, the lowest concentration used in the experiment (Figure 23B). However, when we analysed [^{35}S]-incorporation into specific polypeptides after urea gel electrophoresis and autoradiography, we found that neosynthesis of a group of small proteins was specifically affected upon the addition of rapamycin but not in the presence of 0.1 µg/ml cycloheximide (Figure 23C, compare lanes 8 and 9 in top panels; the region of interest is marked by a black bar on the left side of the autoradiogram, enlarged in the bottom panels). Most of these proteins migrated with the same velocity as r-proteins derived from an affinity-purified 80S ribosome (Figure 23C, bottom panels, compare lane 1 with lanes 2 and 8). We focused on the apparent level of neosynthesized proteins in two prominent bands (Figure 23C, bottom panels, asterisks), for which we unambiguously identified further r-proteins as major components by mass spectrometry. We found that production of these proteins was only moderately affected in the presence of 0.1 µg/ml cycloheximide, whereas they were no longer detectable in the rapamycin-treated sample (Figure 23C, lanes 8 to 10 in the bottom panels). [^{35}S]-labeling of these proteins was similar, however, in cells treated with concentrations of 1 to 10 µg/ml cycloheximide (Figure 23C, bottom panels; compare lanes 9, 11, and 12).
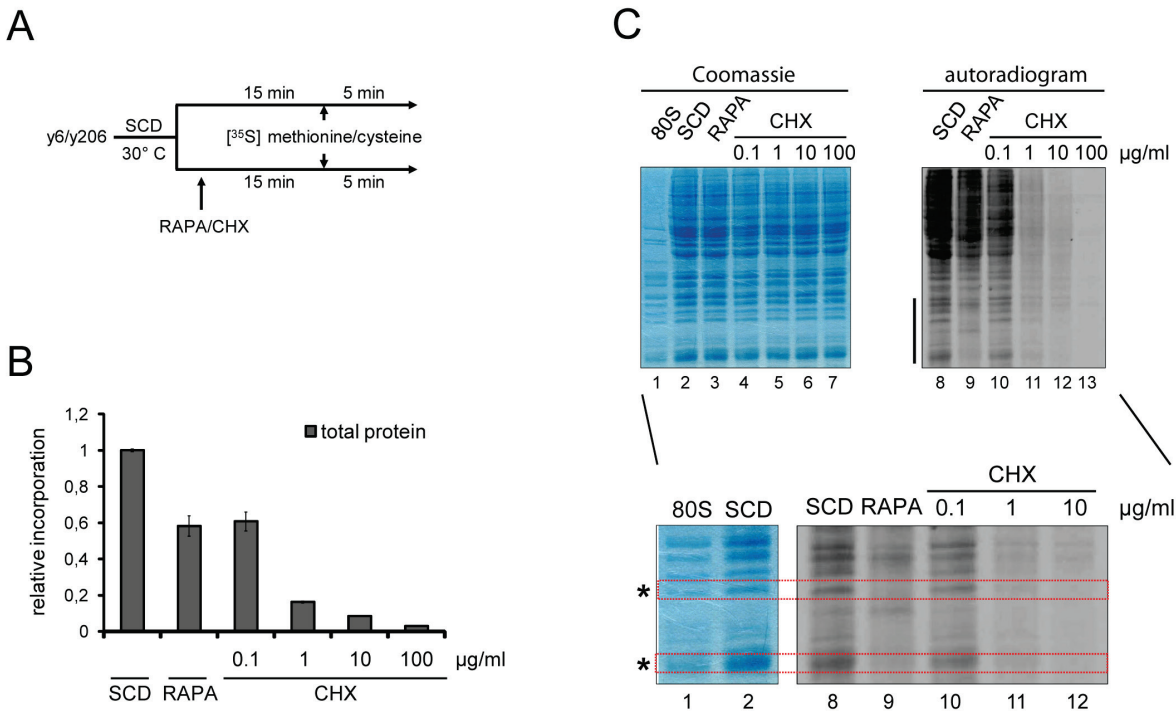
Figure 23. The defect in ribosomal subunit synthesis upon TOR inactivation correlates with shutdown of r-protein production (experiments performed by Robert Steinbauer)

(A to C) r-protein production is severely and specifically affected shortly after rapamycin treatment. Panel **(A)** shows a flow chart of the experiment presented in panel (C). Two wild-type yeast strains (y6 (W303-1a) and y207 (BY4742)) were grown to exponential phase (OD_{600} of 0.5) at 30°C in SCD medium lacking methionine and cysteine (SCD-Met-Cys). Each culture was split in six parts, and rapamycin (200 ng/ml; RAPA), or cycloheximide (0.1, 1, 10 or 10μg /ml; CHX) was added, with one of the samples remaining untreated. After another 15 min at 30°C, pulse-labeling with [^{35}S] methionine-cysteine was performed for 5 min. **(B)** Protein was isolated, and relative [^{35}S]-incorporation was determined. Values were normalized to the value obtained for the untreated cells growing in SCD-Met-Cys medium. The average and standard deviation of two independent biological replicates of strain y6 are shown. **(C)** Protein from the different samples described above, as well from affinity-purified 80S ribosome (80S), was separated in a 16% polyacrylamide urea gel. Total protein was detected with Coomassie blue, whereas neosynthesized proteins were detected after autoradiography of the gel. The position of a subset of proteins whose neosynthesis is specifically inhibited in the presence of rapamycin is marked by a bar on the left side of the autoradiogram. This area is enlarged for lanes 1 and 2 and 8 to 12 in the lower panels. Two asterisks mark protein bands whose major components have been unambiguously identified as r-proteins by mass spectrometry. The experiment shown is from an analysis of strain y6. Identical results were obtained for strain y207 (modified from Reiter et al., 2011).

Thus, upon rapamycin treatment the production of r-proteins is specifically inhibited, which might be caused by the combination of downregulation of general translation (Barbet et al., 1996) and the strong reduction in r-protein mRNA levels (Powers and Walter, 1999; Warner and Gorenstein, 1978).

It was recently postulated that the transcriptional activity of RNA polymerase I is a key determinant for the level of all ribosome components (Laferté et al., 2006). A yeast mutant strain was described whose RNA polymerase I molecules remain constitutively competent for initiation of transcription under stress conditions due to the expression of an A43-Rrn3 fusion protein (Laferté et al., 2006). In this CARA mutant, the downregulation of Pol I transcription upon rapamycin treatment is attenuated, resulting concomitantly in a derepression of Pol II transcription that is restricted to the genes encoding ribosomal proteins. To estimate the

influence of the described CARA phenotype and to analyse whether this attenuated decrease in the mRNA levels of ribosomal proteins leads to increased neo-synthesis of these proteins, [^{35}S]-pulse experiments including the corresponding wild-type strain YPH500 as an appropriate control were performed under the same rapamycin and cycloheximide conditions by Robert Steinbauer (Steinbauer, 2010). In both cases the same reduction in the expression levels of ribosomal proteins was detected as observed for strain y6 (W303-1a) and y207 (BY4742) (Steinbauer, 2010). To directly correlate the reduction in r-protein production with the reduction in ribosome production, pulse-chase experiments with [^{3}H]-uracil were performed in the same strains used for the protein analysis (Figure 24).
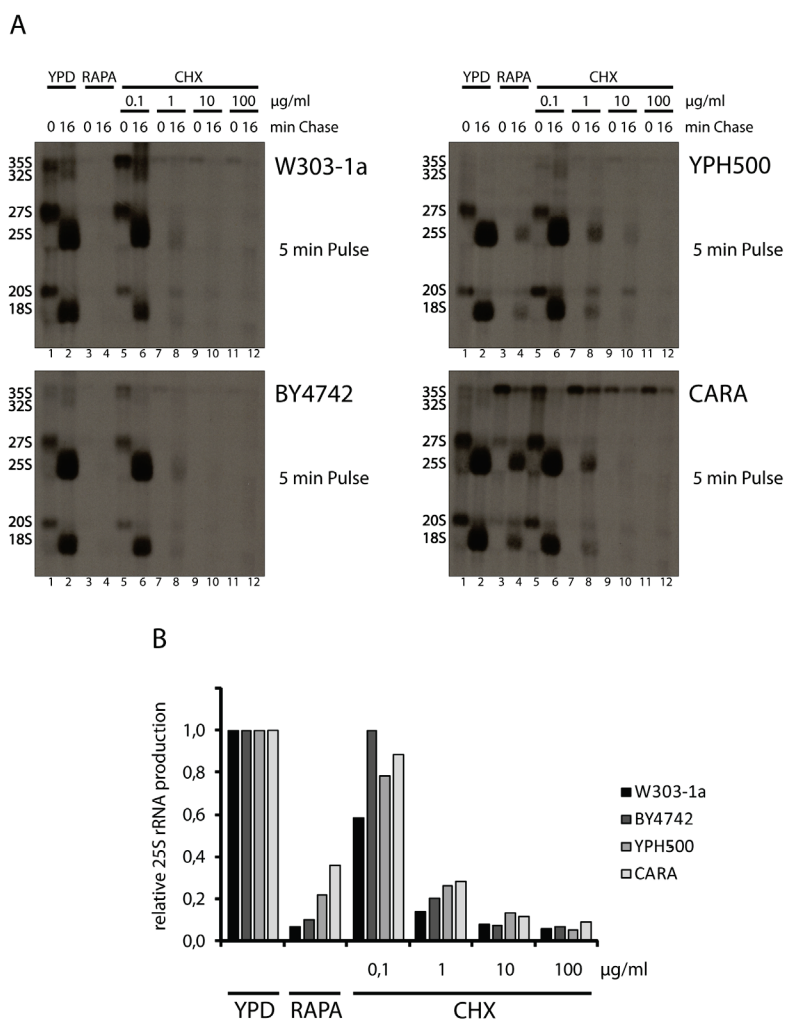
Figure 24. Neosynthesis of r-proteins correlates with production of mature rRNAs

(A) Experiments were performed in strains y6 (W303-1a), y207 (BY4742), y2172 (YPH500), and y2171 (CARA). For [^{3}H]-uracil pulse-chase experiments strains were grown in YPD at 30°C to mid-log phase before the cultures were split in six parts and further cultivated in YPD either in the absence or in the presence of rapamycin (200 ng/ml) or cycloheximide (0,1-100 μg/ml as indicated) for 15 min. Pulse labeling with [^{3}H]-uracil was performed for 5 min followed by a 16 min chase with an excess of unlabeled uracil (final concentration 1 mg/ml). RNA was isolated, separated in a denaturing agarose gel, and transferred to a positively charged nylon membrane. The autoradiogram shown was obtained after exposure of the membrane treated with EN^{3}HANCE solution. Positions of the different rRNA processing products are indicated on the left. **(B)** The relative [^{3}H]-incorporation in 25S rRNA was determined by excision of the 25S rRNA bands from an identical blot and analysis by liquid scintillation counting. The values obtained after a 5 min pulse followed by a 16 min chase were normalized to the value obtained for the cultures grown for 15 min in YPD medium, which were arbitrarily set to 1.

As expected, production of mature rRNAs was severely impaired upon rapamycin treatment (Figure 24B). In the presence of 0.1 µg/ml cycloheximide, a concentration that reduces total protein production (but not r-protein production) to the level observed after rapamycin treatment (Figure 23B), robust 25S rRNA synthesis could still be observed (Figure 24B). In contrast, the defect in 25S rRNA production was virtually identical in rapamycin-treated cells and cells incubated at concentrations of 1 to 10 µg/ml cycloheximide (Figure 24B), in which r-protein production was similarly affected (Figure 23B). Thus, there is a very good correlation between r-protein production and rRNA synthesis.

Since the imbalance of structural components of the ribosome is then presumably adjusted by rapid degradation of misassembled, excess rRNA precursors and since the exosome is one of the most important protein complexes involved in maintaining correct RNA levels in eukaryotic cells (Mitchell et al., 1997), we constructed a *Δrrp6* mutant to see whether there is an enrichment of polyadenylated rRNAs after rapamycin or cycloheximide treatment. Rrp6 is a non-essential exosome subunit which conferres RNA stabilization and leads to hyperadenylation (Dez et al., 2006).

Pules-chase experiments with the strain y1697 (BY4741 *Δrrp6*) revealed no significant differences in rRNA synthesis after rapamycin or cycloheximide treatment compared to its corresponding wild-type strain BY4741 (see Figure 25).
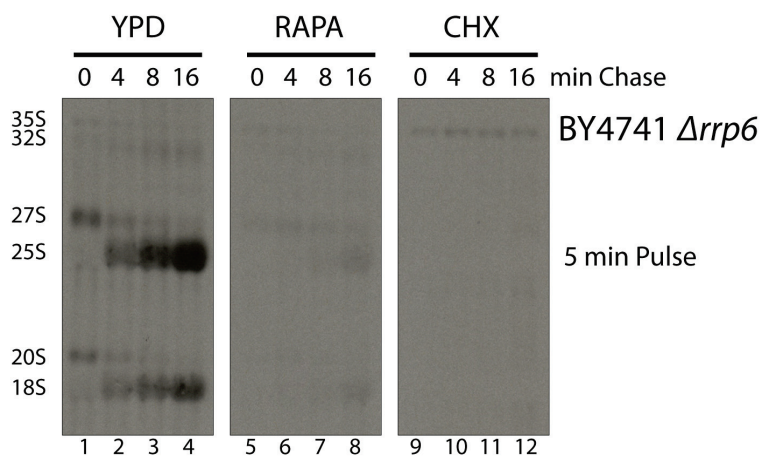
Figure 25. Short-term rapamycin or cycloheximide treatment leads to severe pre-rRNA processing defects in strain BY4741 *Δrrp6*

Strain y1697 (BY4741 *Δrrp6*) was grown in YPD at 30°C to mid-log phase before the culture was split in three parts and further cultivated in YPD either in the absence or in the presence of rapamycin (200 ng/ml) or cycloheximide (100 µg/ml) for 15 min. Pulse labeling with [^{3}H]-uracil was performed for 5 min followed by a chase with an excess of unlabeled uracil (final concentration 1 mg/ml) for the times indicated above the panel. RNA was isolated, separated in a denaturing agarose gel, and transferred to a positively charged nylon membrane. The autoradiogram shown was obtained after exposure of the membrane treated with EN^{3}HANCE solution. Positions of the different rRNA processing products are indicated on the left.

Furthermore, no difference was detected in an isolation of polyadenylated RNAs in the strain BY4741 *Δrrp6*, using biotinylated oligo-T primers, after rapamycin or cycloheximide treatment compared to untreated cells (data not shown). Our experiments indicate that in addition to Rrp6 other RNases participate in pre-rRNA degradation after TOR inactivation.

We conclude that rapid depletion of the endogenous pool of "free" r-proteins is sufficient to explain the observed defects in rRNA processing and other prominent phenotypes observed in the quick response to TOR inactivation.

2.3 Establishment of an *in vivo* system to study Pol I elongation

To identify and characterize Pol I mutants or factors involved in transcription elongation we tried to establish an *in vivo* Pol I elongation assay. Our primary goal was to use this *in vivo* elongation assay to characterize the above mentioned Pol I mutants (section 2.1.1 – 2.1.4). The idea was to generate an artificial roadblock for Pol I which reduces elongation efficiency, but does not completely block transcription, and therefore leads to a reduced growth rate. This reduced growth rate was expected to be further affected if Pol I elongation is impaired due to the lack of an elongation factor or a deficient Pol I subunit. The roadblock should be generated by integration of a DNA sequence for a protein binding site in each of the 150 to 200 rDNA repeats. This could be done by the genetic manipulation of yeast strains. To this end, different DNA binding sites for DNA binding proteins such as LacI, LexA, TTF-I, the 601 nucleosome positioning sequence (Lowary and Widom, 1998) were integrated at the AflII restriction site between the 18S rRNA and 5.8S rRNA gene in every rDNA copy (Figure 26B).
For details in strain construction see 5.2.1.6.
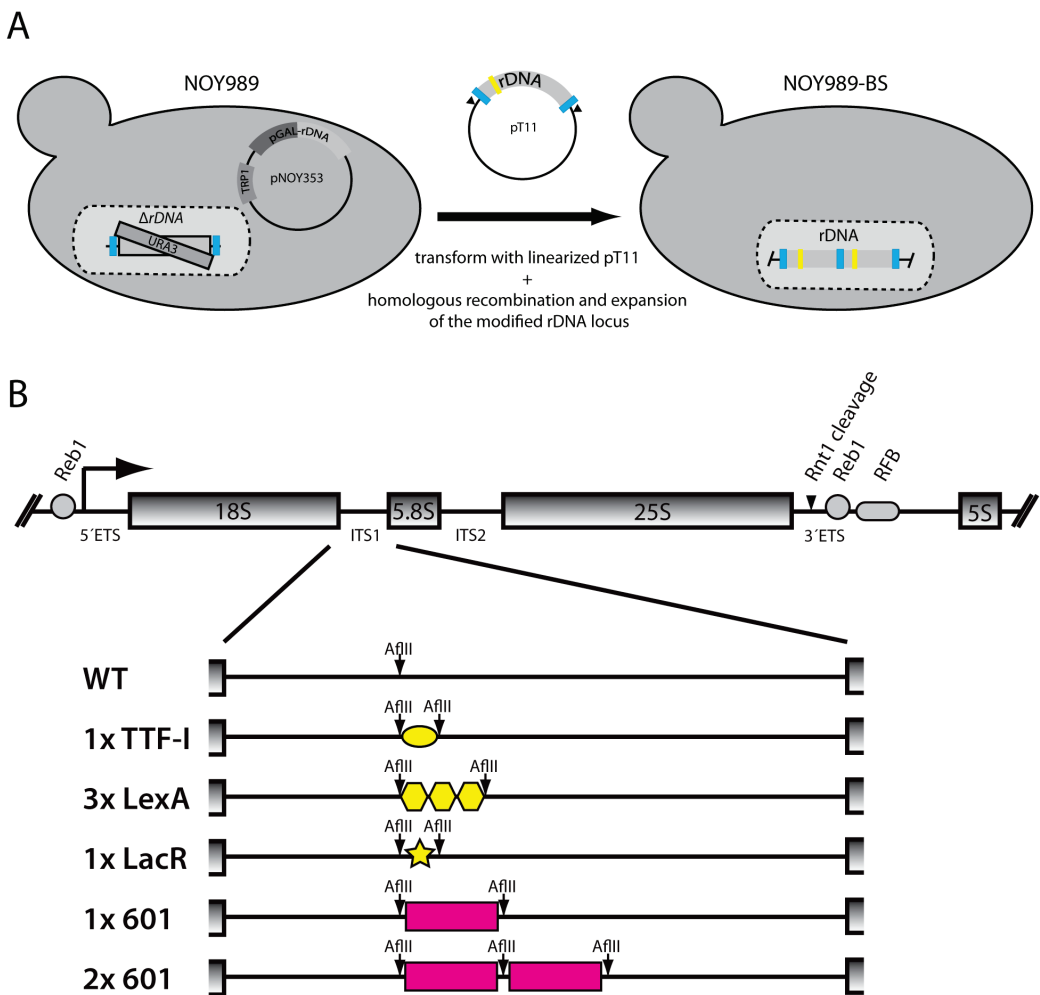
Figure 26. Generated strains with genetically modified 35S rRNA coding sequences

(A) Schematic scetch of yeast rDNA manipulation. Linearized vector pT11 containing a modification of the rDNA locus (yellow) and flanking sites for homologous recombination (blue) is transformed in the yeast strain NOY989 for recombination and expansion of the modified rDNA. Restriction sites for linearization of pT11 are marked as black triangles. **(B)** Cartoon of a yeast rDNA repeat. The positions of the 5S rRNA gene and the 35S rRNA gene including the 5` and 3` external transcribed spacers (ETS), the internal transcribed spacers (ITS) 1 and 2 and the coding sequences for the mature 18S, 5.8S, and 25S rRNAs, as well as several *cis* elements (rDNA enhancer binding protein binding site (Reb1), the RNase III (Rnt1) cleavage site, and the replication fork barrier (RFB)) are indicated. An arrow depicts the Pol I transcription initiation site. Either one TTF-I binding site, three LexA binding sites, a binding site for the Lac-repressor protein as well as one or two 601 nucleosome positioning sequences were introduced at the AflII restriction site in ITS1 of the 35S rRNA gene. Yellow: DNA binding sites for non-yeast proteins. Pink: nucleosome positioning sequences.

Furthermore, for modified strains with binding sites for non-yeast proteins (TTF-I, LexA, and LacI), vectors with wild-type and C-terminally MNase-tagged versions of these binding proteins were cloned.

Experiments with TTF-I were performed with an N-terminally truncated version (TTF-IΔN348) of the protein which showed a higher affinity to its binding site (Németh et al., 2004). Expression of these proteins is galactose-dependent, creating a conditional system in which protein binding and the thereby generated effects can be induced by shifting cells from glucose to galactose containing media. To avoid repressing effects by residual amounts of glucose, cells

were shifted from raffinose to galactose. Expression of binding proteins after shift to galactose is shown in Figure 27B. A growth phenotype is detected in spot tests with serial dilutions for strains carrying the TTF-I binding site on galactose containing plates when TTF-I is expressed. In contrast, no effect is detected on SCG-*leu* plates in strains carrying integrated 3xLexA binding sites or the binding site for the Lac repressor (Figure 27C).
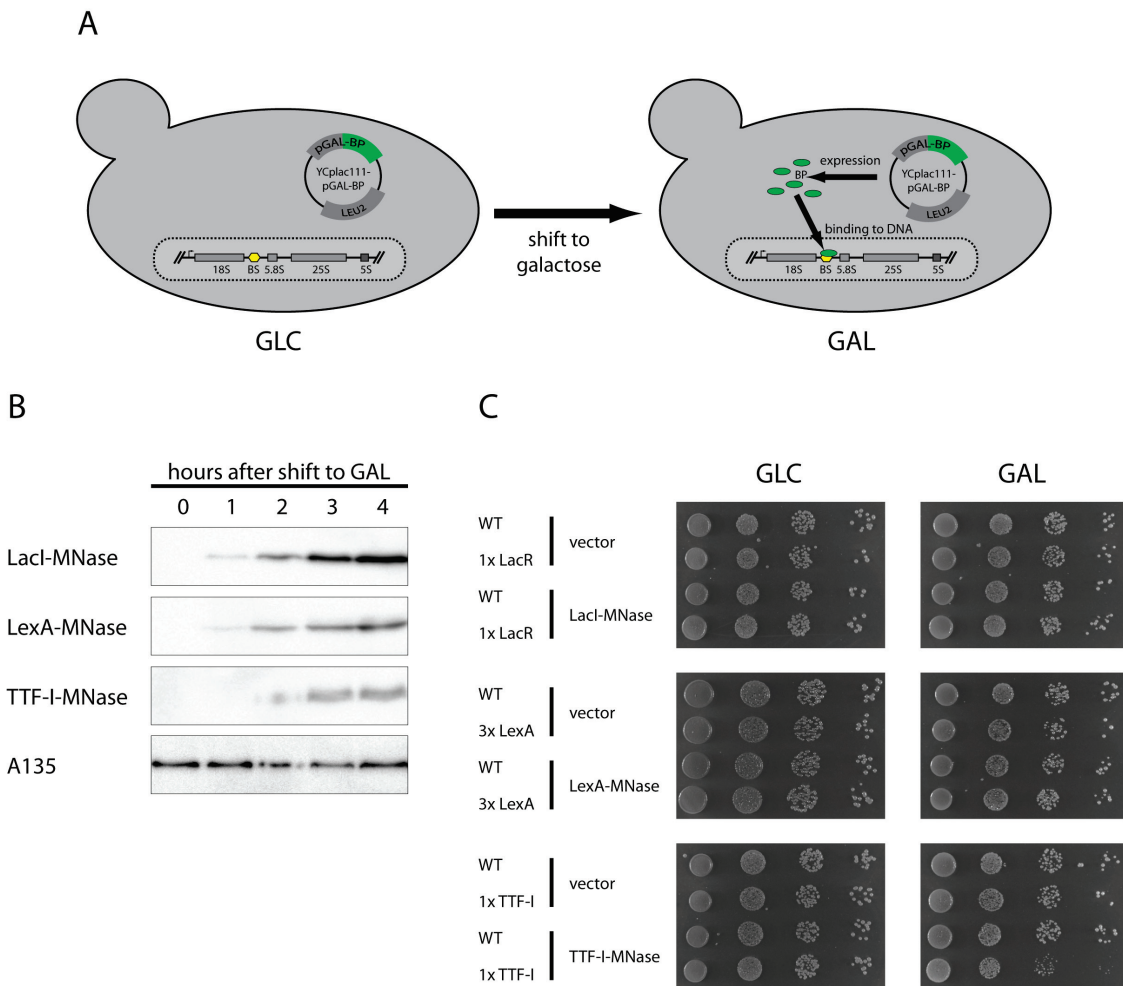
Figure 27. TTF-I expression causes a growth phenotype in the strain carrying an integrated TTF-I binding site in ITS1

(A) Schematic representation of the artificial elongation-block for non-yeast DNA binding proteins (BP). Yeast strains with integrated protein binding sites in the ITS1 rDNA sequence are transformed with YCplac111-pGAL-BP vectors expressing the non-yeast DNA binding protein (BP) from a galactose-inducible promoter. After shift to galactose, the wild-type or C-terminally MNase-tagged versions of these binding proteins are expressed and presumably bind to their respective binding site. **(B)** Expression of the C-terminally MNase-tagged binding proteins. Yeast strains y1599 (WT), y2034 (1x LacR), y1598 (3x LexA) and y2038 (1x TTF-I) were transformed with the vector for expression of the respective binding protein and cultured to early exponential growth phase in SCR-leu at 30°C before galactose was added to a final concentration of 2% and cells were further grown for 4 hours. Samples were taken at the indicated times and denaturing protein extraction was performed from two OD_{600} of cells. 1/8 of the extracts was separated by SDS-PAGE in a 10% polyacrylamide gel and transferred to a PVDF membrane. Signal for the MNase-3xHA-tagged binding proteins and for the Pol I subunit A135, which served as loading control, were detected in Western blot analysis using antibodies α-HA (3F10) and α-A135, respectively. **(C)** Experiments were performed with strains y1599 (WT), y2034 (1x LacR), y1598 (3x LexA) and y2038 (1x TTF-I) transformed with an empty vector or with the respective plasmids for expression of the MNase-tagged binding proteins (YCplac111-pGAL, YCplac111-pGAL-*LacI-MNase*, YCplac111-pGAL-*LexA-MNase*, YCplac111-pGAL-*TTF-I-MNase*). Strains were spotted in serial dilutions on plates containing either glucose (no expression) or galactose (expression) and grown at 30°C for 2-3 days before pictures were taken.

To analyse whether the DNA binding proteins are able to bind to their introduced binding site *in vivo* we performed ChEC assays (Schmid et al., 2004). The factor of interest (TTF-I, LacI, or LexA) is expressed as a fusion protein with a C-terminal Micrococcal nuclease (MNase)-tag from a plasmid under the control of the galactose-inducible promoter. Cells were treated with formaldehyde to crosslink the DNA-bound proteins to the DNA after a shift of 4h to galactose for expression of the MNase-tagged binding proteins. Nuclei are prepared and incubated in a calcium-containing buffer to activate the MNase which should cleave the genomic DNA in the vicintiy of the binding site of the MNase fusion protein. After DNA isolation, the cleavage site introduced by the MNase can be mapped precisely to the DNA sequence by Southern blot analysis. Chromatin was digested with KpnI and a probe detecting fragments upstream from the KpnI restriction site in the 25S rDNA was used for indirect endlabeling. After induction of the MNase fusion protein expression DNA cleavage is detected at the expected position 3` of the 18S rRNA gene for TTF-I-MNase as well as for LexA-MNase (Figure 28). LacI-MNase showed no cleavage at the expected site, meaning that the MNase-fusion protein does not bind to the Lac-repressor binding site.
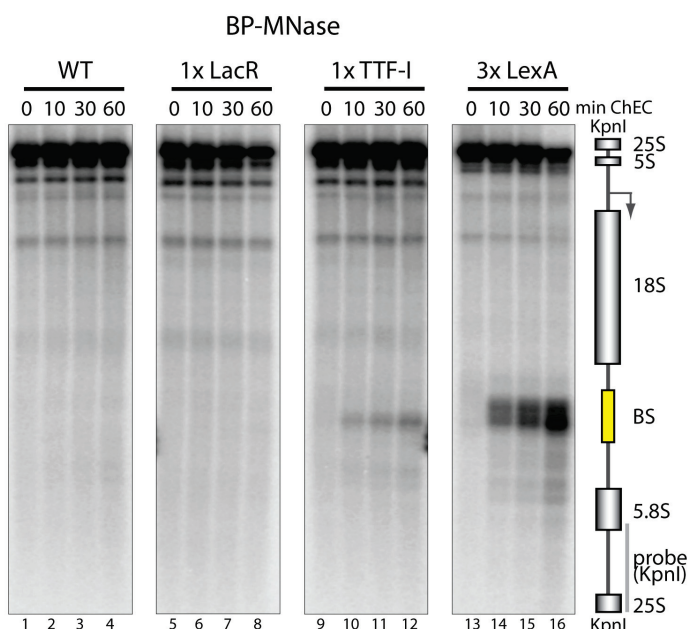
Figure 28. *In vivo* **binding of TTF-I- MNase, LacI- MNase and LexA-MNase to binding sites within the genetically modified 35S rRNA coding sequence**

Yeast strains y1599 (WT), y2034 (1x LacR), y1598 (3x LexA) and y2038 (1x TTF-I) transformed with vectors expressing either LacI-MNase, LexA-MNase, or TTF-I-MNase fusion proteins from a galactose-inducible promoter were cultured to early exponential growth phase in SCR-leu at 30°C before galactose was added to a final concentration of 2% and cells were further grown for 4h. After formaldehyde crosslinking for 15 min at 30°C cells were harvested and crude nuclei were isolated. The nuclei suspension was incubated in the absence (0) or presence of calcium thereby activating DNA cleavage by MNase fusion proteins for the times indicated on top of the panels (min). DNA was isolated, linearized with the restriction endonuclease KpnI, separated in an agarose gel, and analysed in a Southern blot by indirect endlabeling using an rDNA specific probe. The cartoon on the right shows a map of the corresponding KpnI rDNA fragment to localize the cleavage events mediated by the MNase fusion proteins. The positions of the rRNA coding sequences (18S, 5.8S, 25S, 5S), of the integrated protein binding sites (BS) (yellow) and of the target sequence of the radiolabeled probe (light gray) are depicted.

In summary, all DNA binding proteins are expressed as MNase fusion proteins but only TTF-I-MNase and LexA-MNase can bind to their respective introduced binding site. Furthermore, only in strains with an integrated TTF-I binding site a growth defect was detected after protein expression.

We next investigated whether Pol I is paused as a consequence of TTF-I binding. To assess this, the Pol I subunit A190 was MNase-tagged and ChEC was performed. We observed a specific accumulation of Pol I (A190-MNase) upstream of the TTF-I binding site in strain y2056 (1x TTF-I / A190-MNase), after induction of TTF-I and binding to its respective binding site, which indicates that Pol I is paused (Figure 29). This effect was not observed in strains with a 3xLexA binding site and induction of LexA (data not shown).
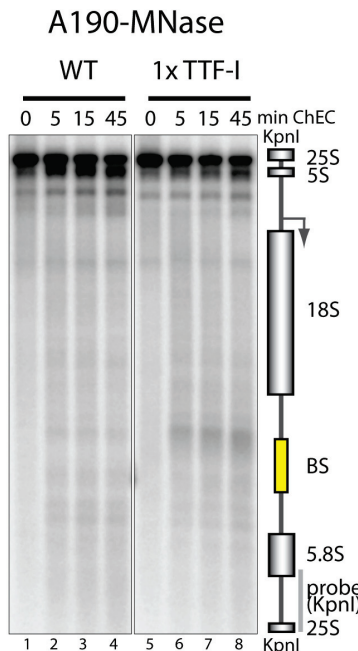
Figure 29. TTF-I binding accumulates Pol I upstream of the introduced TTF-I binding site *in vivo*

Experiments were performed with strains y1620 (WT) and y2056 (1x TTF-I) carrying either wild-type 35S rRNA gene or one TTF-I binding site introduced into ITS1 of the rRNA gene. Corresponding strains expressing TTF-I from a plasmid based galactose-inducible promoter and A190-MNase fusion protein from its endogenous promoter were cultured to early exponential phase in SCR-leu at 30°C before galactose was added to a final concentration of 2% and cells were further grown for 4 hours. ChEC was performed as described in Figure 28.

Next, we wanted to know if an intact TTF-I binding site in its natural orientation is required for termination of transcription. This was already shown *in vitro* in mammals (Henderson and Sollner-Webb, 1986; Gerber et al., 1997). We wanted to test whether this hypothesis is true *in vivo* and created a yeast strain carrying an inverted TTF-I binding site in the ITS1 sequence.

A
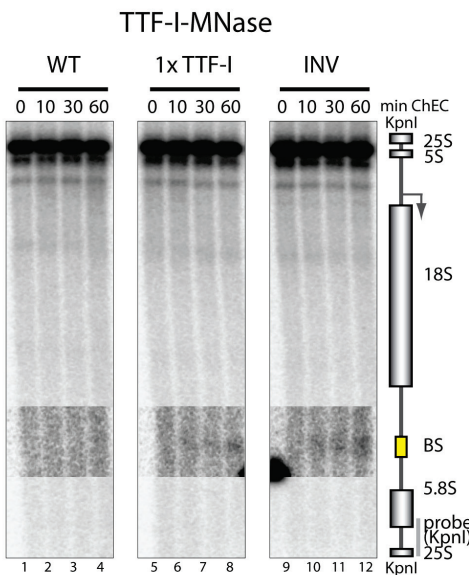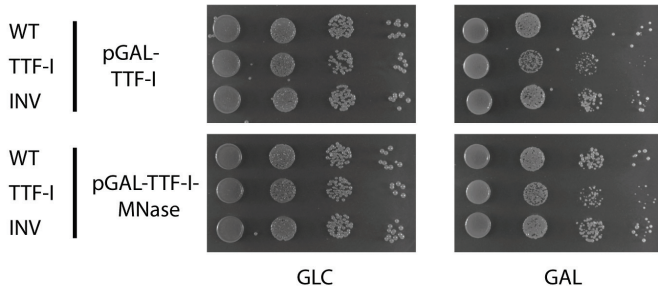
Figure 30. Inversion of the TTF-I binding site still leads to TTF-I binding but has no effect on cell growth *in vivo*
Experiments were done with strains y1599 (WT), y2038 (1x TTF-I) and y2039 (1x TTF-I INV) transformed with vectors expressing TTF-I from a galactose-inducible promoter (YCplac111-pGAL-*TTF-I*, YCplac111-pGAL-*TTF-I-MNase*). **(A)** No binding site (WT), one TTF-I binding site in its natural orientation (TTF-I) or one TTF-I binding site in its inverse orientation (INV) were introduced into ITS1 of the rRNA gene. Yeast strains were cultured to early exponential phase in SCR-leu at 30°C before galactose was added to a final concentration of 2% and cells were further grown for 4h. ChEC was performed as described in Figure 28. Signals surrounding the area of the artificial binding site are enhanced. **(B)** Strains transformed with the indicated vectors were spotted in serial dilutions on plates containing either glucose (no expression) or galactose (expression) and grown at 30°C for 2-3 days before pictures were taken.

Although the cleavage-signal is very weak, binding of TTF-I-MNase can be detected at the naturally orientated and at the inverted TTF-I binding site (Figure 30A). Interestingly, upon induction of TTF-I expression from a galactose-inducible promoter, a growth phenotype is detected only in strains carrying the correctly orientated TTF-I binding site integrated in the ITS1 region (Figure 30B) indicating that efficient Pol I pausing/termination *in vivo* is dependent on the right orientation of the DNA-bound termination factor.

Furthermore, in a preliminary approach, we tried to find out whether the Pol I subunits A49 and A12.2 are involved to pass the artificial barrier. Therefore *RPA49* deletions and *RPA12* deletions were created in strains carrying the manipulated rDNA sequence with integrated TTF-I binding sites (correct and inverse orientation), Lac repressor binding site, 3x LexA binding site, aside from a wild-type control with no integrated binding site. Growth tests by serial dilutions of strains transformed with empty vectors as well as vectors expressing the DNA binding proteins from a galactose-inducible promoter are shown in Figure 31.
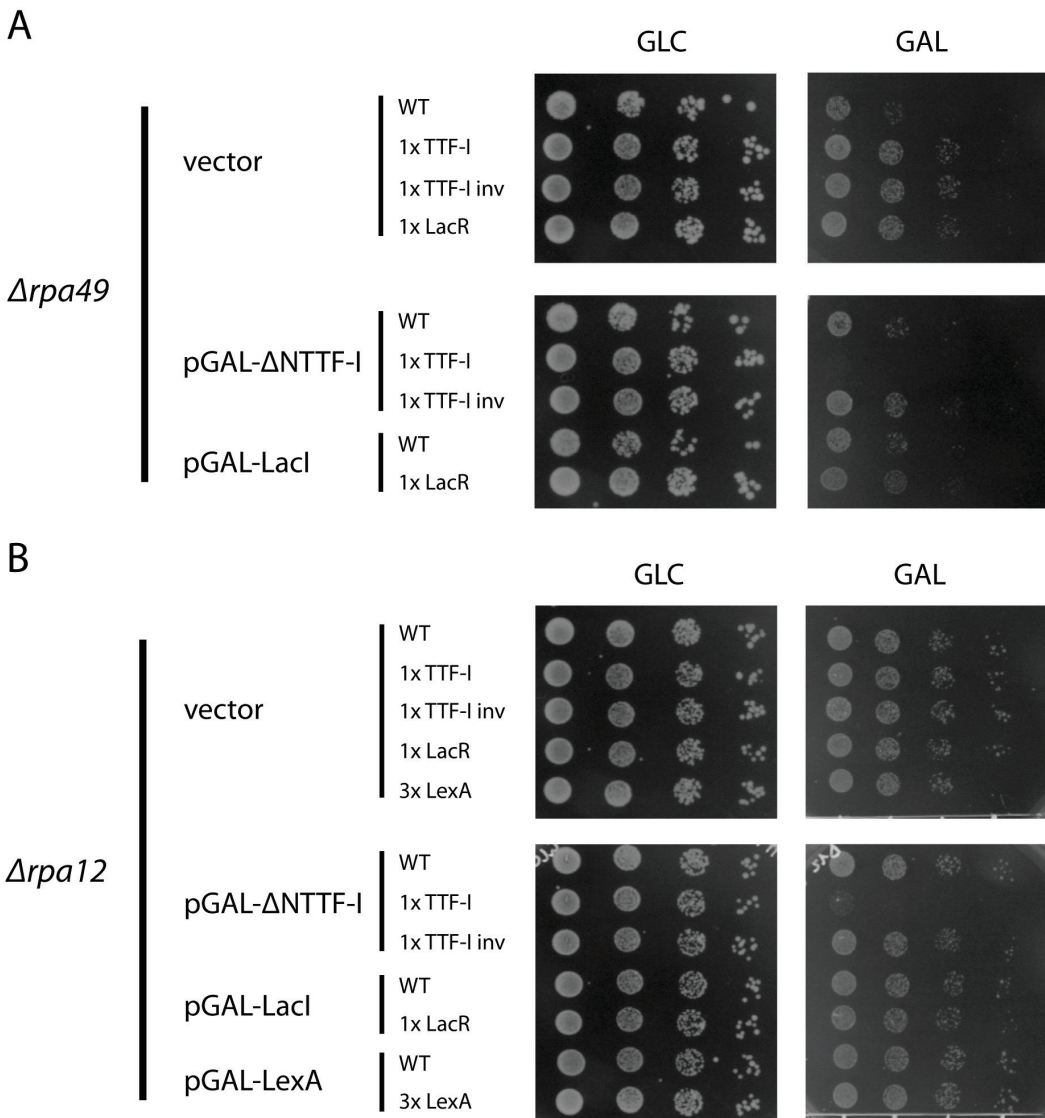
Figure 31. Deletion of *RPA12* as well as *RPA49* reinforces the observed growth phenotype in strains carrying the TTF-I binding site

Experiments were performed in strains y1615 (WT), y2288 (1x TTF-I), y2290 (1x TTF-I INV), and y2286 (1x LacR) carrying a *RPA49* deletion **(A)** and in strains y1618 (WT), y2287 (1x TTF-I), y2289 (1x TTF-I INV), y2285 (1x LacR), and y1612 (3x LexA) carrying a *RPA12* deletion **(B)**. Strains transformed with the indicated vectors were spotted in serial dilutions on SC-leu plates containing either glucose (no expression) or galactose (expression) and grown at 30°C for 2-3 days before pictures were taken. Strains carrying a 3x LexA binding site and a *RPA49* deletion were not included in this experiment. For the wild-type strain carrying the *RPA49* deletion and an empty vector control, less cells were spotted in general.

Interestingly, TTF-I binding in the strain carrying the TTF-I binding site in its natural orientation in the *Δrpa49* as well as in the *Δrpa12* genetic background causes an even stronger growth reduction. For all other strains tested, neither the deletion of *RPA49* nor *RPA12* has an effect on growth.

In summary, TTF-I binding to its introduced binding site, which is in its natural orientation, is able to accumulate Pol I upstream of the binding site and thereby causes a growth reduction. The effect on growth is enhanced if either the Pol I subunit A49 or A12.2 is missing. Both subunits are discussed to play a role in Pol I elongation (Kuhn et al., 2007).

2.4 *In vivo* characterization of Pol I termination

2.4.1 Identification of Ydr026c as yeast Pol I termination factor

In another related approach we wanted to establish an artificial rDNA termination region into the ITS1 sequence of every yeast rDNA unit. Therefore strains were constructed as described in 5.2.1.6, containing a terminator element covering the Reb1 binding site and the replication fork barrier (RFB) sequence with Fob1 binding sites (Figure 32A). Since the DNA binding proteins are yeast proteins and constitutively expressed from their wild-type promoters, no galactose-inducible expression is needed and growth related effects of their binding can be directly analysed on glucose plates (Figure 32B).
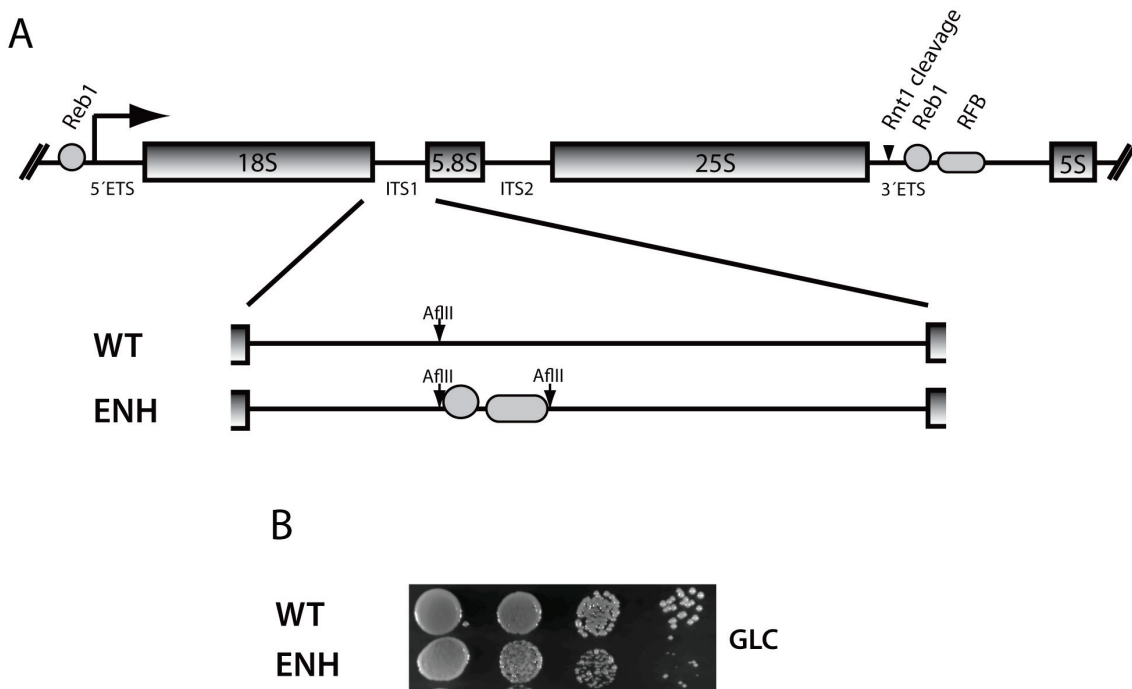
Figure 32. Integration of the enhancer region in ITS1 causes growth reduction

(A) Cartoon of the modified yeast rDNA with integrated enhancer region in ITS1. The positions of the 5S rRNA gene and the 35S rRNA gene including the 5` and 3` external transcribed spacers (ETS), the internal transcribed spacers (ITS) 1 and 2 and the coding sequences for the mature 18S, 5.8S, and 25S rRNAs, as well as several *cis* elements (rDNA enhancer binding protein binding site (Reb1), the RNase III (Rnt1) cleavage site, and the replication fork barrier (RFB)) are indicated. An arrow depicts the Pol I transcription initiation site. Integrated enhancer sequence contains the Reb1 binding site and the RFB, but not the Rnt1 cleavage site. **(B)** Strains carrying either no protein binding site y1599 (WT) or the enhancer sequence y2042 (ENH) in ITS1 were spotted in serial dilutions on YPD plates and grown at 30°C for 2-3 days before pictures were taken.

A growth phenotype was detected in the strain carrying the enhancer sequence. We next wanted to know whether this growth defect is the result of protein binding to the introduced enhancer sequence.

Interestingly, the uncharacterized protein Ydr026c, which was identified as a potential DNA binding protein in a monohybrid assay and which appeared to bind to the terminator region of yeast rDNA, interacts physically with Fob1 (Mohanty and Bastia, 2004). *In vivo* binding of the designated terminator binding proteins (Reb1, Fob1 and Ydr026c) was measured with the ChEC method as described above. Weak cleavage at the integrated enhancer element was observed in ChEC experiments with Reb1-MNase, whereas a clear distinct cleavage band is detected for Ydr026c-MNase. Presumably Ydr026c associates to the Reb1 binding site. Fob1-MNase also cleaves the DNA at the RFB 3` of the terminator region (Figure 33).
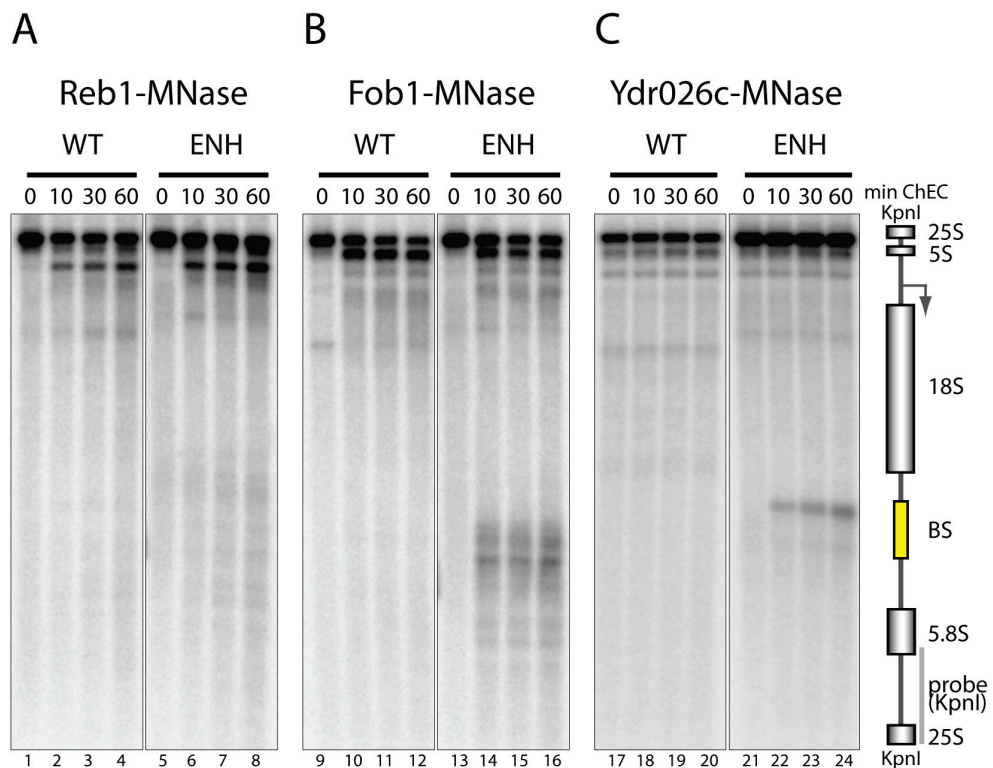
Figure 33. *In vivo* binding of putative terminator proteins to the integrated enhancer element in ITS1
ChEC-experiments were performed in strains y2050 (WT) and y2054 (ENH) **(A)**, y2051 (WT) and y2055 (ENH) **(B)**, y2090 (WT) and y2093 (ENH) **(C)** with endogenously MNase-3xHA-tagged Reb1, Fob1 or Ydr026c respectively. Either no binding site (WT) or the rDNA enhancer region (ENH) were introduced into ITS1 of the rRNA gene. Yeast strains endogenously expressing the indicated MNase fusion proteins were grown in YPD to mid-log phase. ChEC was performed as described in Figure 28.

To determine whether Ydr026c also binds to the wild-type terminator at the Reb1 binding site, we performed ChEC with MNase-tagged Reb1 and Ydr026c at the terminator and the promoter, respectively. The wild-type yeast strain was tested in this approach. Reduced Reb1-MNase mediated DNA cleavage is observed at the terminator compared to the promoter as seen in Figure 34, which is in agreement with ChIP data from HA-tagged Reb1 reported by (Kawauchi et al., 2008). Interestingly, Ydr026c-MNase mediated DNA cleavage shows the opposite pattern with strong cleavage events at the Pol I terminator and no cleavage at the promoter (Figure 34).

58
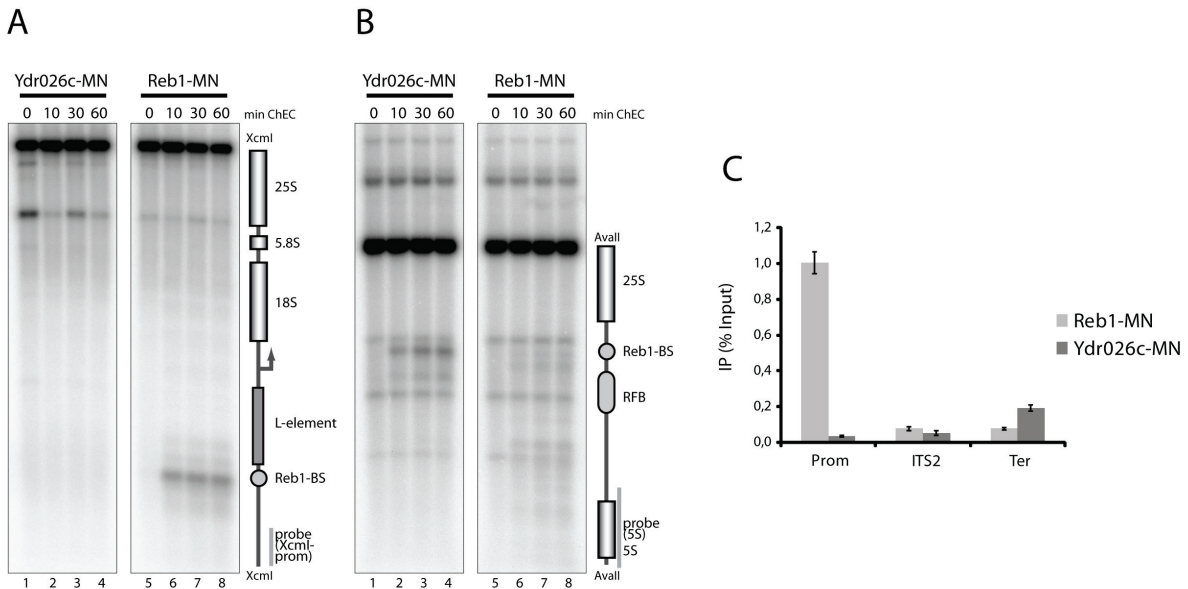
Figure 34. ChEC and ChIP analyses show that Reb1 binds preferentially to the promoter and Ydr026c to the terminator *in vivo*

ChEC- and ChIP-experiments were performed in strains y2090 (WT Ydr026c-MN) and y2050 (WT Reb1-MN). **(A)** ChEC at rDNA promoter: Wild-type yeast strains endogenously expressing the indicated MNase fusion proteins were grown in YPD to mid-log phase. ChEC was performed as described in Figure 28 except that DNA was linearized with the restriction endonuclease XcmI and analysed in a Southern blot by indirect endlabeling using an rDNA promoter specific probe. The cartoon on the right shows a map of the corresponding XcmI rDNA fragment to localize the cleavage events mediated by the MNase fusion proteins. The positions of the rRNA coding sequences (18S, 5.8S, 25S), of the Reb1 protein binding sites (Reb1-BS) at the promoter, and of the target sequence of the radiolabeled probe (light gray) are depicted. In the strains used for the experiment an artificial L-element (used for homologous recombination of the rDNA locus) of about 500bp is introduced between the promoter Reb1 binding site and the Pol I transcription start site in every rDNA copy. **(B)** ChEC at rDNA terminator: Wild-type yeast strains were treated as described in (A) except for linearization of prepared DNA with restriction endonuclease AvaII and a 5S specific probe was used for indirect endlabeling. The cartoon on the right shows a map of the corresponding AvaII rDNA fragment to localize the cleavage events mediated by the MNase fusion proteins. The positions of the rRNA coding sequences (25S, 5S), of the Reb1 protein binding sites (Reb1-BS) at the terminator as well as the sequence for the replication fork barrier (RFB), and of the target sequence of the radiolabeled probe (light gray) are depicted. **(C)** ChIP of Ydr026c and Reb1, respectively, at Reb1 binding sites at the promoter, terminator, and in ITS2 serving as an internal background control. The data presented in the bar diagram is the average of two independent ChIP experiments each analysed in triplicate quantitative PCR reactions. The percentage of the total input DNA recovered after ChIP for the different rDNA regions is depicted. For experimental procedure see 5.2.7.1.

For more quantitative statements on the binding of those two factors to the promoter or terminator, a chromatin immunoprecipitation (ChIP) experiment was applied. With ChIP we could reproduce the observed ChEC data showing that Reb1 binds preferentially to the promoter and Ydr026c to the terminator region (Figure 34C). Since the sequence surrounding of the Reb1 binding sites differ at the promoter and terminator but the binding site itself is almost identical, the affinity for Reb1 or Ydr026c, respectively, to the binding sites might be altered in a sequence specific way causing a preferential binding of Ydr026c at the terminator. While the core consensus sequence for Reb1 binding has been identified as CGGGTAA (Liaw and Brandl, 1994), substantial flexibility is permissible and the adjacent nucleotides influence the binding affinity of Reb1 or Ydr026c (Wang and Warner, 1998).

Taken together, the presented data suggests that Ydr026c rather than Reb1 binds to the wild-type yeast rDNA terminator region and to the artificially introduced terminator in ITS1 indicating that Ydr026c could be the yeast Pol I terminator.

2.4.2 Pol I accumulates in front of an artificially introduced termination site

Due to the observed growth defect in strains with an integrated enhancer sequence, we were interested whether Pol I pausing is a consequence of Reb1- or Ydr026c binding. As described for TTF-I, the Pol I subunit A190 was MNase-tagged and ChEC was performed using the KpnI-probe to detect Pol I pausing in the ITS1 region. When compared to wild-type strains, A190-MNase mediated DNA cleavage of accumulated Pol I at the expected region is detected only in strains with integrated enhancer (Figure 35A).

If less polymerase is bound to the 3` rDNA region in strains with an integrated artificial termination site one would expect changes in the chromatin structure since polymerase free rDNA will eventually be packed into nucleosomes (Wittner et al., 2011). To detect changes in the chromatin state of the rDNA as a result of Pol I pausing at the introduced binding sites, psoralen analysis was performed (Conconi et al., 1989). It is possible to distinguish transcribed (open) from non-transcribed (closed) templates by this method. Psoralen is incorporated and crosslinked only in transcribed rDNA repeats whereas nucleosome-covered rDNA is much less crosslinked, resulting in a faster migrating `f-band` in native agarose gels. Heavily crosslinked nucleosome-free rDNA produces a slow-migrating `s-band`. When psoralen treated chromatin is EcoRI digested and separated on an agarose gel, 18S and 25S fragments can be obtained with the 25S-18S-probe which detects a 3.4 kb rDNA fragment. Interestingly, in strains containing the integrated enhancer element, the s- and f-band of the 25S rDNA fragment seem to merge compared to the wild-type situation, suggesting that only the 5` part of the rDNA is transcribed by Pol I in the mutant strain (Figure 35B). Profile analyses of this blot-region supports this observation, indicating that less polymerases can enter the 25S rRNA gene due to efficient pausing of Pol I at the Reb1 site, thus leading to impaired opening of 3` rDNA fragments (Wittner et al., 2011).

In another approach, we used electron microscopy (EM) to analyse Miller spreads of actively transcribed rDNA in strains with integrated enhancer regions and wild-type strains (French et al., 2003). Apparently, the length of the Miller trees was shorter in the mutant strain compared to the wild-type strain. Quantification of this observation was done by measuring the Pol I occupied length of the 5` rDNA gene region using the ImageJ software on EM images with 40000 fold magnification. Representative examples of wild-type and mutant EM images of actively transcribing Pol I genes and a quantification of the average length of more than 30 Miller spreads in wild-type and mutant, respectively, are depicted in Figure 35C.

A significant discrepancy in Pol I occupied 5` and 3` rDNA regions is detected in the observed strains.

These three analyses indicate that there exists a different Pol I density before and after the artificial termination site which suggests transcription termination at this region.
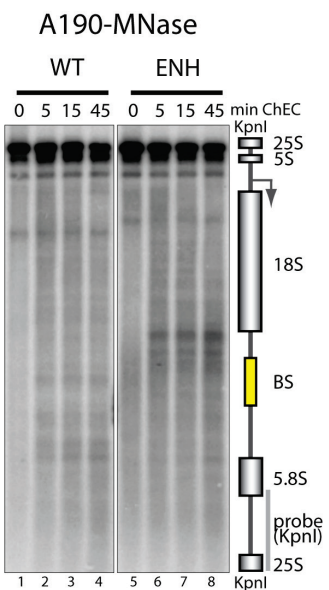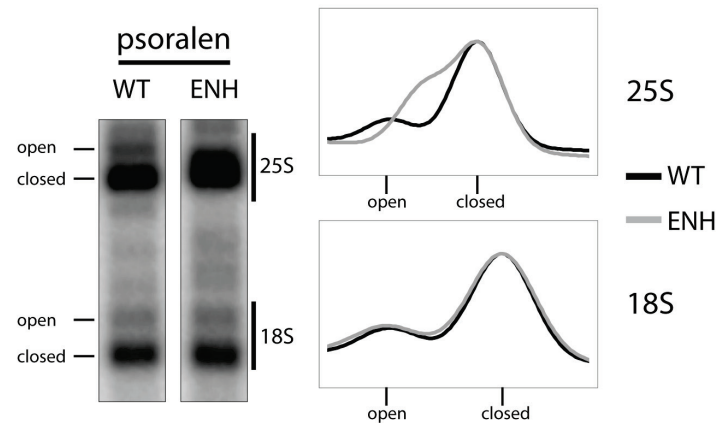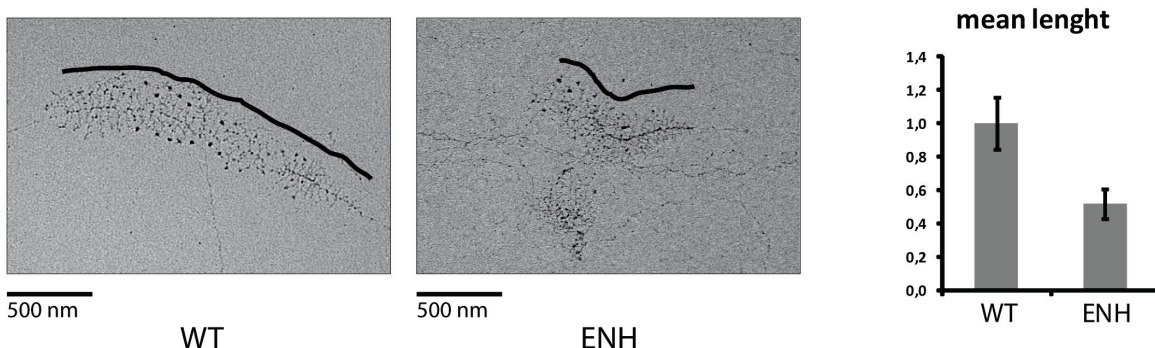
Figure 35. RNA Pol I accumulates upstream of the introduced enhancer element in ITS1 leading to a changed chromatin state in the 25S rDNA region

(A and B) Experiments were performed in strains y1620 (WT) and y2094 (ENH) with endogenously MNase-3xHA-tagged Pol I subunit A190. **(A)** Yeast strains endogenously expressing the indicated MNase fusion proteins were grown in YPD to mid-log phase. ChEC was performed as described in Figure 28. **(B)** Psoralen cross-linking was performed with yeast strains y1620 (WT) and y2094 (ENH). DNA was isolated, digested with EcoRI and analysed in a Southern blot with the 25S-18S-probe detecting a 3.4 kb rDNA fragment encompassing regions of the 18S and 25S rRNA gene. Graphs to the right depict profiles of open and closed 18S and 25S rDNA for wild-type (black) and ENH (gray) (see 5.2.7.3 for details). **(C)** Miller spread of a representative 35S rRNA gene from wild-type (left) and ENH (right) (y1599, y2042) at 40000x magnification. Length of Pol I occupied regions are retraced as depicted and measured with the ImageJ software. Statistical average length of more than 30 Miller trees in wild-type and ENH are shown in the table to the right. Averaged length of wild-type Miller spreads was arbitrarily set to 1.

2.4.3 Ydr026c binding is sufficient to terminate at an artificially introduced termination site

To elucidate which *trans*-acting binding factor is responsible for the described phenotypes we created knock-outs of *FOB1*- and *YDR026c*-genes to rescue the growth defect. Since *REB1* is essential and linked to many different targets, definitive conclusions of its role in this whole process are hard to state (Ju et al., 1990). Surprisingly, both *FOB1* and *YDR026c* knock-outs are able to cure the growth phenotype to some extent, whereas galactose dependent overexpression of only Ydr026c restores and even enforces slow growth in all strains containing the integrated enhancer element, including the knock-out strains (Figure 36A-B). This observation was rather surprising since Fob1 seemed to have no direct effect on termination. Possible unknown secondary effects of *FOB1* deletion could contribute to the rescue of the growth phenotype. Recruitment of Fob1 to DNA in a *Δydr026c* genetic background and *vice versa* is not impaired as shown in Figure 36C, arguing for no cooperativeness of these factors with regard to binding to their proposed sites.
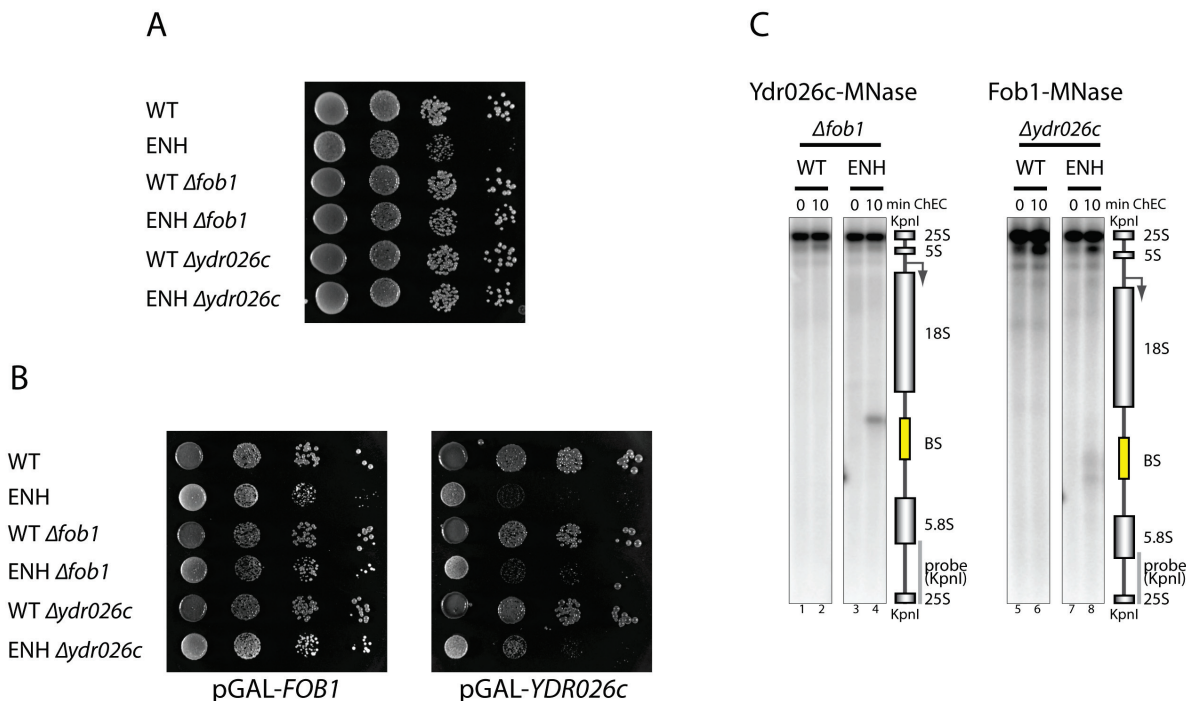
Figure 36. Ydr026c significantly contributes to Pol I terminaton *in vivo*

(A) Spot tests of strains y1599 (WT), y2042 (ENH), y2275 (WT *Δfob1*), y2280 (ENH *Δfob1*), y2276 (WT *Δydr026c*), and y2281 (ENH *Δydr026c*). Serial dilutions of above mentioned strains were spotted on YPD plates and incubated at 30°C for 2-3 days before pictures were taken. **(B)** Spot tests of strains y1599 (WT), y2042 (ENH), y2275 (WT *Δfob1*), y2280 (ENH *Δfob1*), y2276 (WT *Δydr026c*), and y2281 (ENH *Δydr026c*) either transformed with plasmid YCplac111-pGAL-*FOB1* (left) or plasmid YCplac111-pGAL-*YDR026c* (right). Serial dilutions of above mentioned strains were spotted on SCG-leu plates and incubated at 30°C for 2-3 days before pictures were taken. **(C)** Yeast strains (y2231, y2236) with a *FOB1* deletion and (y2232, y2237) with a *YDR026c* deletion, respectively, expressing the indicated MNase fusion proteins from their endogenous locus were grown in YPD to mid-log phase. ChEC was performed as described in Figure 28.

However, we cannot exclude cooperative effects of these factors concerning efficient Pol I pausing and termination. Therefore, we created yeast strains with only the Reb1 binding site or the RFB inserted 3` of the 18S rRNA gene to uncouple possible cooperativity. Additionally, strains with an inverted orientation of the above mentioned binding sites were created to differentiate between orientation-dependent effects of DNA binding. An overview of the created strains is shown in Figure 37A.

Serial dilutions of strains (y1599 (WT), y2042 (ENH), y2323 (5`-ENH fwd), y2327 (5`-ENH rev), y2331 (3`-ENH fwd), y2335 (3`-ENH rev)) on YPD plates are shown in Figure 37B. A growth phenotype is detected only for the strain containing the 5` enhancer sequence with the Reb1 binding site in the natural orientation. Inverting the orientation of the Reb1 binding site as well as inserting the RFB or an inverted RFB does not result in a detectable growth phenotype. However, the growth phenotype detected for strains with just the 5` enhancer is not as pronounced as for strains containing the whole terminator region (compare lane ENH with lane 5`-ENH fwd on serial dilution plate Figure 37B). Whether this is due to cooperative effects of Ydr026c and Fob1 remains unclear since the `failsafe`-terminator (a T-rich stretch between the Reb1 binding site and the RFB), which could also contribute to a more efficient termination in the ENH strain, is missing in the 5`-ENH fwd strain (see Figure 37A).

To clarify whether Fob1 binding is detected in the 5`-ENH strains or Ydr026c binding is detected in the 3`-ENH strains, which would argue for a strong direct interaction and possibly cooperation in termination of these two factors, ChEC with MNase-tagged Ydr026c and Fob1, respectively, was performed in the above mentioned strains.

Strong cleavage signals are detected only for Ydr026c binding to the region containing the 5`-ENH in the natural orientation. Neither Ydr026c binding nor Fob1 binding can be detected to a significant extent in strains which are not harboring the respective binding site, indicating that no or very little cooperativity exists between these factors with respect to transcription termination.

A
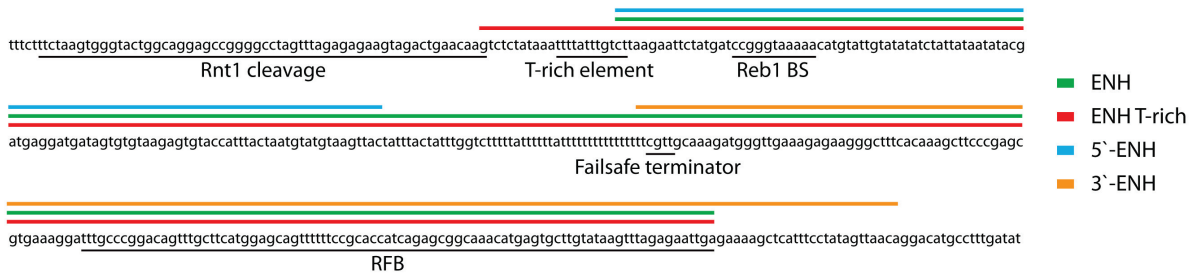
B
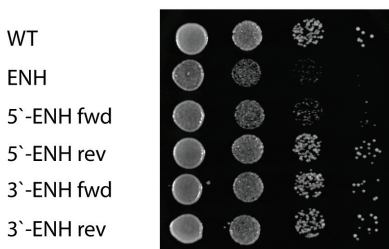
C
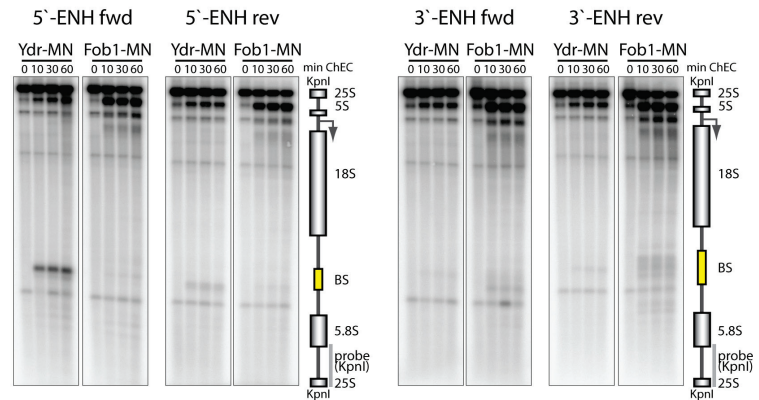
Figure 37. The Reb1 binding site in its natural orientation and Ydr026c binding is sufficient to cause a growth phenotype

(A) Sequence of the 3` end of the rRNA coding region beginning 6bp 3` of the 25S rRNA gene. Gray bars below the sequence indicate the location of the Rnt1 cleavage site, the T-rich element, the Reb1 binding site, the Failsafe terminator (Reeder et al., 1999), and the replication fork barrier (RFB). Colored bars above the sequence indicate the different DNA fragments used for integration in ITS1 (see color-code for respective strains). **(B)** Spot tests of strains y1599 (WT), y2042 (ENH), y2323 (5`-ENH fwd), y2327 (5`-ENH rev), y2331 (3`-ENH fwd) and y2335 (3`-ENH rev). Serial dilutions of above mentioned strains were spotted on YPD plates and incubated at 30°C for 2-3 days before pictures were taken. **(C)** Binding of respective binding proteins analysed by ChEC. Yeast strains y2325 and y2326 (5`-ENH fwd), y2329 and y2330 (5`-ENH rev), y2333 and 2334 (3`-ENH fwd), y2337 and 2338 (3`-ENH rev) expressing the indicated MNase fusion proteins from their endogenous locus were subjected to ChEC analysis. Strains were grown in YPD to mid-log phase. ChEC was performed as described in Figure 28.

Taken together, the Reb1 binding site in its natural orientation and Ydr026c binding significantly contribute to Pol I termination *in vivo* at the artificial terminator and Ydr026c binding is sufficient to cause the described growth phenotype.

2.4.4 Characterization of the DNA element required for termination

In addition to the Reb1 binding site it was reported that the presence of a T-rich region 5` of the terminator protein binding site is required for efficient termination in yeast and mammals (Lang and Reeder, 1995; Mason et al., 1997a). To assay the effects of this stretch of thymidine nucleotides *in vivo*, strains were created containing the whole enhancer element with the T-rich sequence integrated 3` of the 18S rRNA gene (ENH T-rich). Spot tests on YPD plates

demonstrate that a combination of the T-rich element with the Reb1 binding site enforces the obtained growth defect in ENH strains (Figure 38B).

In *in vitro* studies which characterized Reb1 as termination factor, mutations in the binding site were generated to test for better or no Reb1 binding. A mutated Reb1 binding site in which two guanine residues are replaced by thymines (ENH mut1) (Figure 38A) eliminates Reb1 binding as assayed by gel-shift analysis and concurrently prevents Pol I termination *in vitro* (Lang and Reeder, 1993). Additionally, a Reb1 binding site mutant (ENH mut2), where AAA is substituted for CCC in the 3` part of the Reb1 binding site (see Figure 39A) increases Reb1 binding about 10-fold *in vitro* and thereby increased overall termination efficiency (Lang and Reeder, 1993; Reeder et al., 1999). To test whether these mutations also affect Ydr026c – and Reb1 binding *in vivo*, strains carrying the enhancer element with the mutated Reb1 binding sites were created. For ENH mut1, the created mutations at these sites restored wild-type growth (Figure 38B). This observation is in agreement with other *in vivo* data of Pol I termination on a ribosomal minigene (Reeder et al., 1999). ChEC experiments with MNase-tagged binding proteins show Ydr026c-MNase and Fob1-MNase binding in the ENH T-rich strain, whereas Ydr026c-MNase binding is abolished in the strain with the mutated Reb1 binding site (ENH mut1) (Figure 38C).
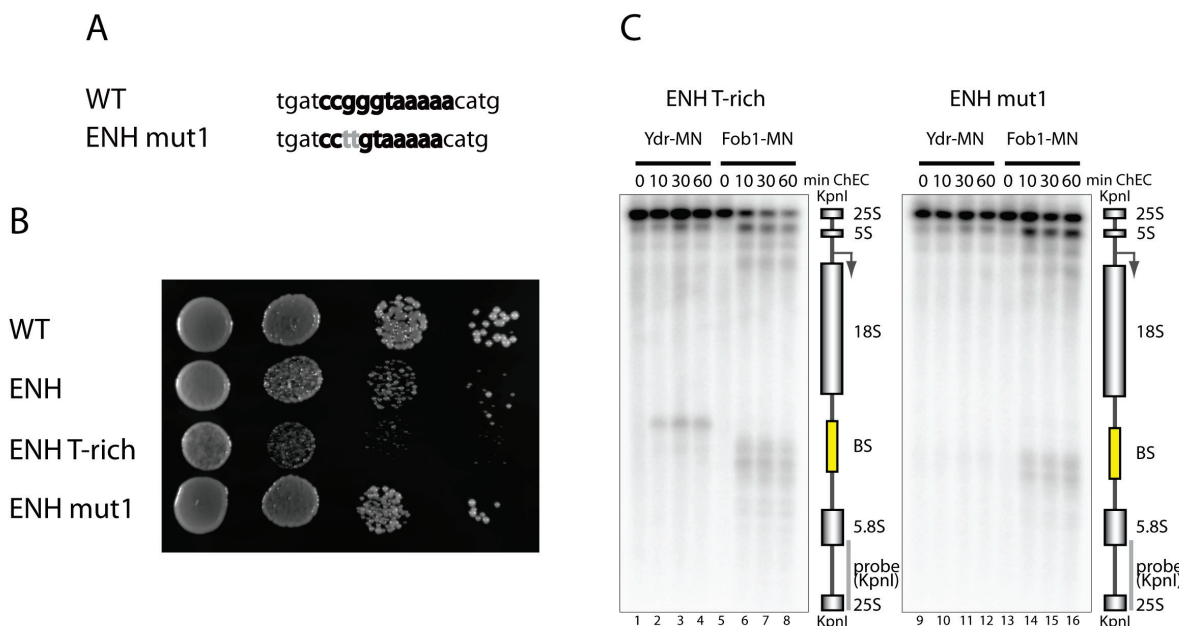
Figure 38. A T-rich element upstream of the Pol I terminator and a correct Reb1 binding site are needed for efficient termination

(A) Representation of WT and mutated Reb1 binding sites. Consensus sequence for the Reb1 binding site at the Pol I terminator is shown in bold black (WT) and mutated nucleotides are shown in bold gray (ENH mut1). ENH mut1 contains a two-base substitution in the Reb1 site that abolishes Reb1 binding (Lang and Reeder, 1993). **(B)** Spot tests of strains y1599 (WT), y2042 (ENH), y2273 (ENH T-rich), and y2274 (ENH mut1). Serial dilutions of above mentioned strains were spotted on YPD plates and incubated at 30°C for 2-3 days before pictures were taken. **(C)** Yeast strains y2239 and y2238 (ENH T-rich), y2241 and y2240 (ENH mut1) expressing the indicated MNase fusion proteins from their endogenous locus were subjected to ChEC analysis. Strains were grown in YPD to mid-log phase. ChEC was performed as described in Figure 28.

No difference in growth was detected in the strain carrying the mutated Reb1 binding site (ENH mut2) for better binding compared to the non-mutated strain in spot tests (Figure 39B). Reb1 binding and Ydr026c binding was measured by ChEC in this strain. Clear cleavage signals are detected for both fusion proteins at the indicated binding site (Figure 39C) but no significantly enhanced growth phenotype is detected due to significantly better Reb1 binding compared to strains with a wild-type terminator (Figure 39B).
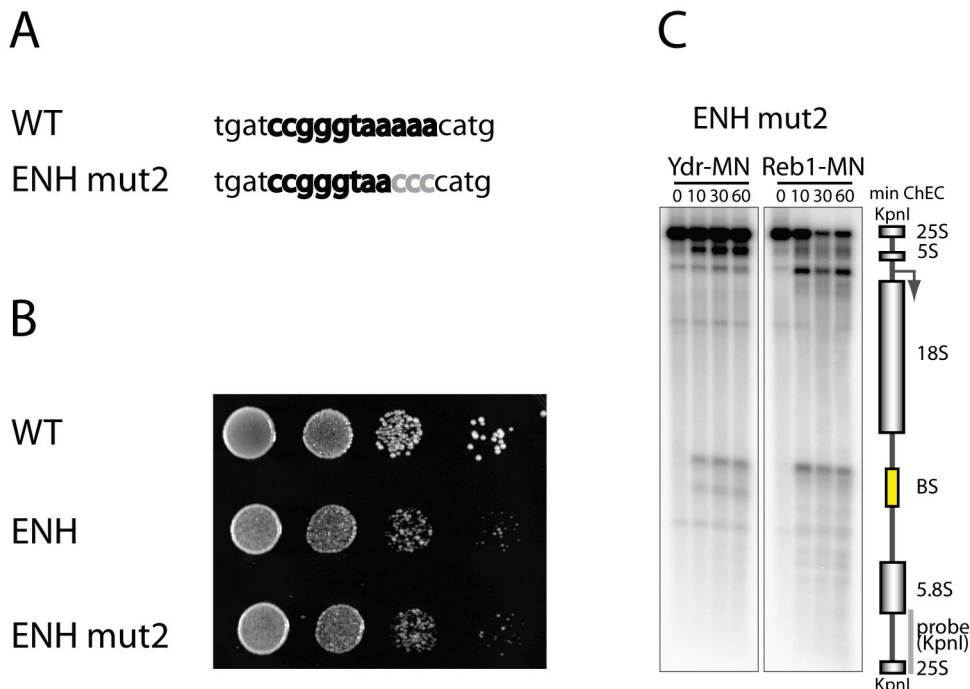
Figure 39. A mutation in the Reb1 binding site leads to better Reb1 binding but to no difference in growth

(A) Representation of WT and mutated Reb1 binding sites. Consensus sequence for the Reb1 binding site at the Pol I terminator is shown in bold black (WT) and mutated nucleotides are shown in bold gray (ENH mut2). ENH mut2 contains a three-base substitution in the Reb1 site that increases Reb1 binding about 10-fold (Lang and Reeder, 1993). **(B)** Spot tests of strains y1599 (WT), y2042 (ENH) and y2339 (ENH mut2). Serial dilutions of above mentioned strains were spotted on YPD plates and incubated at 30°C for 2-3 days before pictures were taken. **(C)** Experiments were performed with strains y2341 (ENH mut2) and y2342 (ENH mut2) with endogenously MNase-3xHA-tagged Ydr026c or Reb1, respectively (Ydr026c-MN, Reb1-MN). Yeast strains expressing the indicated MNase fusion proteins were grown in YPD to mid-log phase. ChEC was performed as described in Figure 28.

In summary, a T-rich element upstream of the Pol I terminator and a correct Reb1 binding site are needed for efficient termination. Increased Reb1 binding at the artificial terminator does not lead to an enhanced growth defect.

2.4.5 Effects of premature termination on rRNA processing

If Pol I transcription is blocked at the artificial termination site, rRNA synthesis should be impaired downstream of the termination sits. This would lead to an imbalance of the 18S / 25S synthesis which can be detected in pulse experiments and Northern blotting. We wanted to

test this in our mutant strains. Therefore logarithmically growing yeast cells were pulsed with [^{3}H]-uracil for 15 min before RNA was extracted and separated by denaturing agarose gel electrophoresis. An autoradiograph with long exposure-time of the blotted RNA is shown in (Figure 40A). According to the insertion of an additional DNA sequence 5` of the A$_2$-processing site an up-shift of the 20S pre-rRNA band should be observed in strains with integrated enhancer sequences. This up-shift can be seen in the pulse experiment in Figure 40A (compare lane 1 (WT) with lane 4 (ENH mut1)). An additional band (marked by an arrow) appears in ENH and ENH T-rich strains migrating with a higher molecular weight than the 20S+ rRNA (see Figure 40A, compare lane 2 and 3 with lane 4). Furthermore, the quantification of several Northern blot signals for 25S and 18S shows an even more drastic effect on the 25S/18S imbalance in a steady state situation than observed in the pulse experiments for strains ENH and ENH T-rich (Figure 40, compare quantification from panel B to A). Transcription and processing seem to be generally affected in these two strains. Since prevention of Ydr026c binding to the Reb1 site in ENH mut1 cures this phenotype, secondary effects are likely to be the reason for the impairment of efficient transcription/processing in these strains. Whether these effects are due to defective processing or initiation remains unclear and has not been further investigated. The appearance of this additional band as well as the detected imbalance in the 25S/18S ratio observed in ENH and ENH T-rich strains (Figure 40A) point towards an unprocessed and not degraded termination product.

To further characterize this unexpected band, we analysed rRNA of the above described strains by Northern hybridization (Figure 40C). For rRNA detection we used probes identifying the very 5` region of the 35S rRNA (1), as well as probes recognizing ITS1 sequences upstream of the A$_2$-processing site either 5` or 3` of the integrated enhancer region (2 and 3) (for probe positions see schematic sketch in Figure 40C). The additional band can be detected with probes 1 and 2 but is absent when probe 3 is used arguing for an unprocessed termination product (Figure 40C). Signal intensity of this band appears to be significantly stronger in the ENH T-rich strain compared to the ENH strain indicating increased termination efficiency due to the T-rich sequence.

Taken together, pulse experiments and Northern hybridization with strains carrying an integrated terminator sequence in ITS1 revealed an imbalance in the 25S/18S rRNA ratio. Furthermore, an additional band, which could represent an unprocessed termination product, appears in these strains.
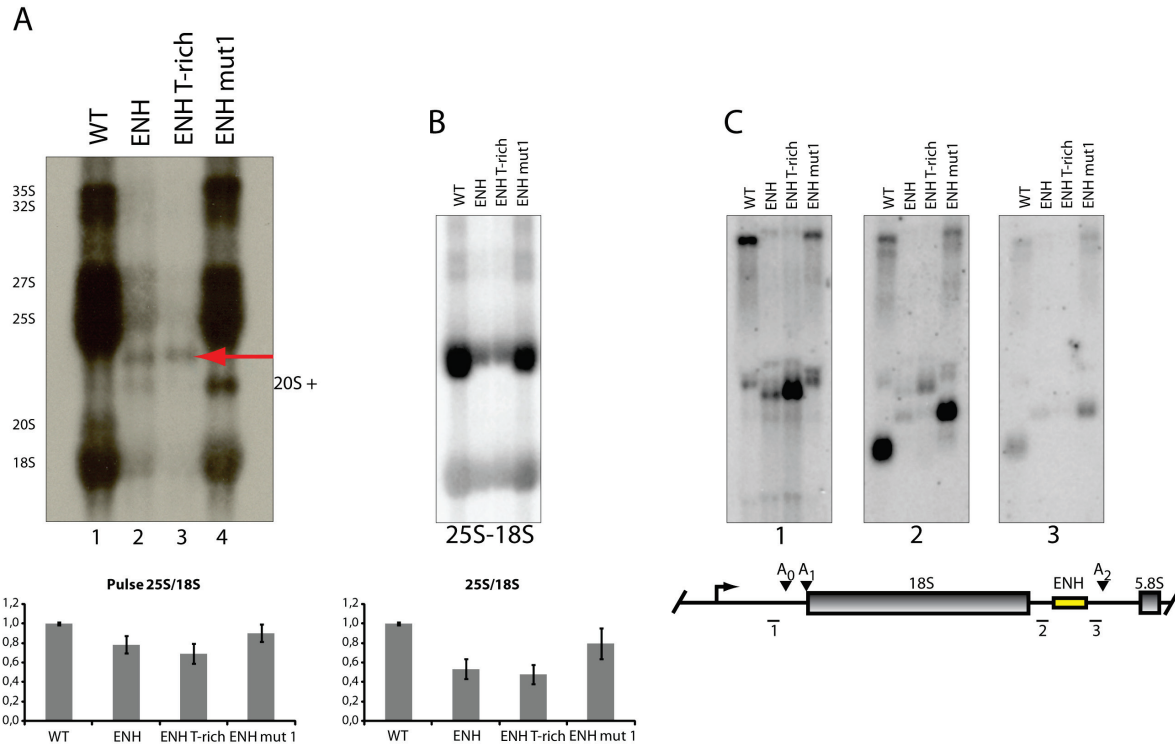
Figure 40. A termination product is detected in [³H]-pulse experiments and Northern analyses

(A) [³H]-uracil pulse. Top: [³H]-uracil metabolic labeling of newly synthesized RNA in strains y1599 (WT), y2042 (ENH), y2273 (ENH T-rich), and y2274 (ENH mut1). Cells were pulsed for 15 min at 30°C. Total RNA was extracted and separated by gel electrophoresis. Radio-labeled RNA was visualized by fluorography. Bottom: [³H]-uracil incorporation in 18S and 25S rRNA was determined by excision of the 18S and 25S rRNA bands from an identical blot and analysis by liquid scintillation counting. The 25S/18S ratio of the obtained values was calculated and normalized to wild-type, which was arbitrarily set to 1. **(B)** Top: Northern hybridization with 25S and 18S probes. RNA of yeast strains y1599 (WT), y2042 (ENH), y2273 (ENH T-rich), and y2274 (ENH mut1) was extracted, separated by gel electrophoresis, and Northern blotting was performed. Bottom: The calculated 25S/18S ratio was obtained by quantification of 25S and 18S signals of several Northern blots as described in 5.2.4.5. The 25S/18S ratio was normalized to wild-type, which was arbitrarily set to 1. **(C)** Northern hybridization to analyse the additional band. RNA of yeast strains y1599 (WT), y2042 (ENH), y2273 (ENH T-rich), and y2274 (ENH mut1) was extracted, separated by gel electrophoresis, and Northern blotting was performed as described in 5.2.4.5. The used probe is depicted below the blot. The position of the probes, as well as the location of the A_0, A_1, and A_2 processing sites and the artificially introduced enhancer site are indicated on a schematic sketch below.

2.4.6 Ydr026c is a *bona fide* Pol I transcription termination factor

So far, the role of Ydr026c was analysed only at the artificial termination site. It remains unclear whether Pol I can read through the natural termination site when Ydr026c is missing. To analyse this, we performed chromatin immunoprecipitation (ChIP) experiments in strains y1620 (WT), y2094 (ENH), y2229 (WT *Δydr026c*), and y2234 (ENH *Δydr026c*) expressing an endogenously MNase-3xHA-tagged Pol I subunit (A190). The results of the ChIP analysis are shown as the percentage of the total input DNA recovered after ChIP for the different rDNA regions (Figure 41). Deletion of *YDR026c* (strains y2229 (WT *Δydr026c*), y2234 (ENH *Δydr026c*)) shows significantly increased Pol I occupancy downstream of the Reb1 binding site and the RFB (amplicon 7 and 8) in strains with and without integrated enhancer sequences 3` of the

18S rRNA gene. This underlines that Ydr026c is required for efficient termination of rDNA transcription. We also analysed the Pol I occupancy in strains carrying the artificial terminator and no *YDR026c* knock-out. Pol I occupancy at the promoter and throughout the 18S rRNA gene is slightly affected compared to wild-type (y1620) whereas the ChIP signals from the rDNA downstream of the integrated enhancer sequence differ significantly from wild-type signals (compare amplicons 1, 2, 3 with 4, 5, 6 in Figure 41). This data is in agreement with the Miller spread data from Figure 35C. The qPCR signal at the 5S gene (amplicon 9) serves as an internal control. Pol I occupancy of the *YDR026c* deletion strains (y2229 (WT *Δydr026c*), y2234 (ENH *Δydr026c*)) is similar to wild-type except for the increase at the terminator and RFB. In particular, when signals for the two strains with integrated binding sites are compared (strain y2094 (ENH), y2234 (ENH *Δydr026c*)) it becomes obvious that Ydr026c is required for polymerase I blocking. The rescue of the growth phenotype detected in strain ENH through *YDR026c* deletion can now be entirely explained by a reconstitution of the wild type Pol I occupancy on the rDNA.
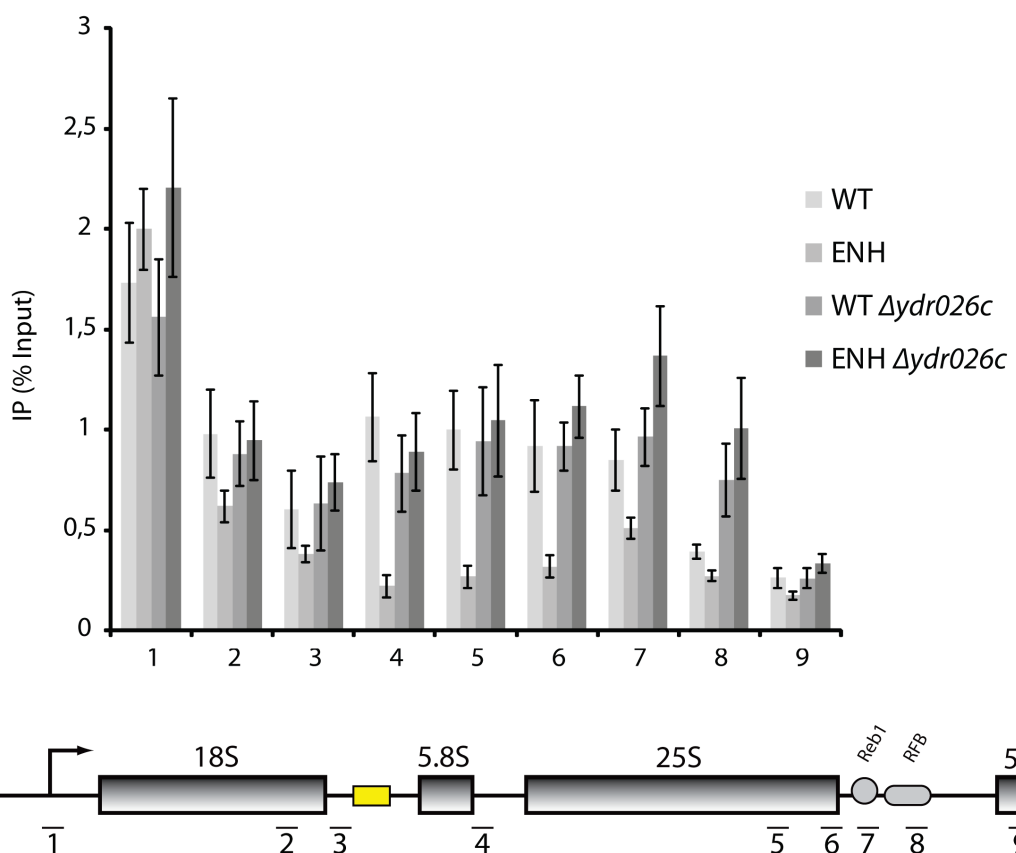
Figure 41. A deletion of *YDR026c* leads to transcription read-through of polymerases at the terminator site

Yeast strains y1620 (WT), y2094 (ENH), y2229 (WT Δydr026c), and y2234 (ENH Δydr026c) expressing the Pol I subunit A190 as a fusion protein with a C-terminal MNase-3xHA-tag were subjected to ChIP experiments as described in 5.2.7.1. The data presented in the bar diagram is the average of two independent ChIP experiments each analysed in triplicate quantitative PCR reactions. The percentage of the total input DNA recovered after ChIP for the different rDNA regions is depicted. The 5S rRNA coding sequence (9) serves as an internal control. The positions of the amplified rDNA regions are indicated in the cartoon on the bottom. Primer pairs used in ChIP experiments are listed in 5.1.4.

2.4.7 Deletion of *YDR026c* is viable and causes rDNA repeat expansion

Apparently, exact termination and ongoing transcription does not seem to be so important since *YDR026c* deletion shows no growth phenotype as already seen in Figure 36A. We started to look for other phenotypes caused by *YDR026c* deletion. Furthermore, we wanted to determine whether changes in the rDNA copy number can be detected. For this we used quantitative PCR as well as pulse-field gel electrophoresis. An expansion of the rDNA copy number was observed by qPCR in *ΔYDR026c* strains compared to wild-type strains and strains with a fixed rDNA copy number (Figure 42A). Genomic DNA was extracted and signals for 25S rDNA were compared to signals obtained from the single copy *PHO5* gene in the analysed strains. Pulse-field gel electrophoresis of yeast chromosomes was performed in collaboration with Jorge Perez-Fernandez and could confirm this result, since the rDNA carrying chromosome XII in *Δydr026c* yeast strains migrates with a significantly higher molecular weight than chromosome XII in wild-type strains or strains with a fixed rDNA copy number (NOY886 with ~40 copies; NOY1064 with ~190 copies; NOY1071 with ~25 copies) (see Figure 42B).

It is possible that the increased number of non-terminated Pol I transcription complexes interferes with a) the bidirectional Pol II promoter which is located in a region shown to be required for repeat expansion and which drives the transcription of non-coding RNAs (Ganley et al., 2005; Houseley et al., 2007) or b) the replication machinery which then might cause more uncoordinated recombination events and an extension of the rDNA locus (Kobayashi et al., 1998; Kobayashi, 2003).
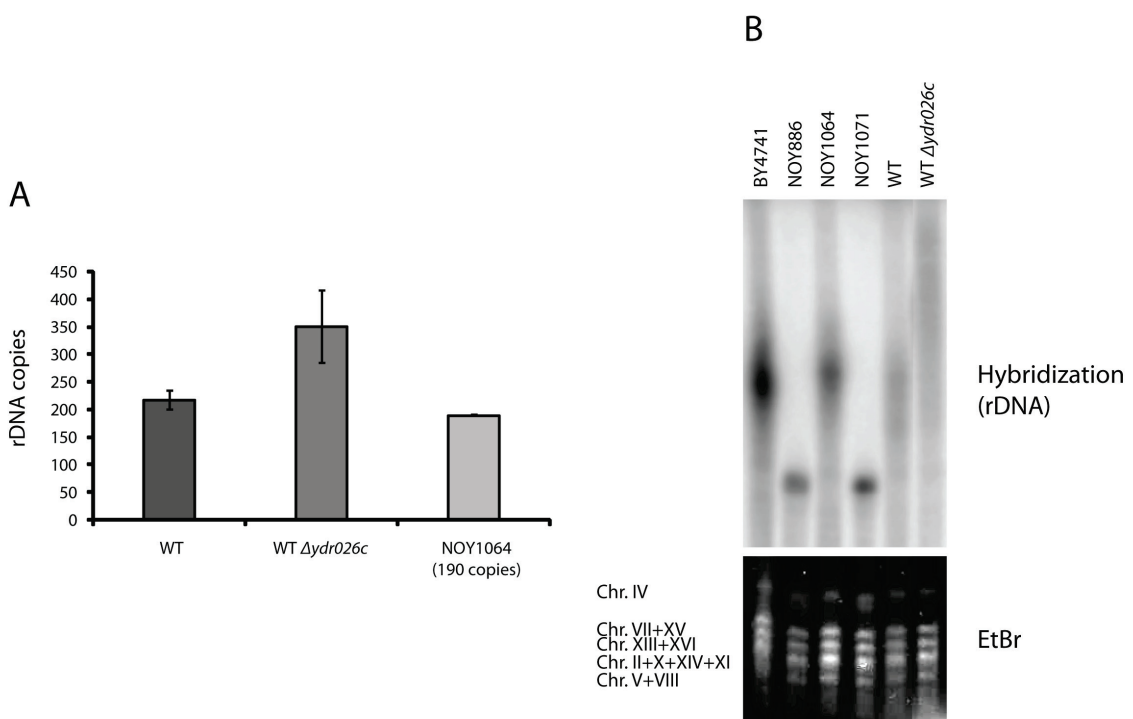
Figure 42. Expansion of rDNA copy number in *YDR026c* deletion strain

(A) Experiments were performed with strains y1599 (WT), y2276 (WT *Δydr026c*) and y352 (NOY1064). Copy number was measured by qPCR from genomic DNA. 25S signals of the indicated strains (NOY1064 with fixed copy number of 190) were compared to the signals of the single copy gene *PHO5*. Signals were normalized to 190 copies of NOY1064. **(B)** Experiments were performed with strains y206 (BY4741), y349 (NOY886), y352 (NOY1064), y353 (NOY1071), y1599 (WT), and y2276 (WT *Δydr026c*). Pulse-field gel electrophoresis of *S. cerevisiae* chromosomes of indicated strains (for detailed description see 5.2.3.4). Top: rDNA on chromosome XII determined by Southern hybridization with an rDNA specific probe in different strains. Bottom: EtBr stained agarose gel after pulse-field gel electrophoresis. Yeast chromosomes are depicted on the left. (Experiments were performed by Jorge Perez-Fernandez)

3 DISCUSSION

3.1 Possible roles of Pol I phosphorylation

The identified phosphosites apparently belong to the major phosphorylated sites in the Pol I complex. *In vivo* analysis of mutants which mimic a constitutive unphosphorylated or phosphorylated state of these phosphosites (Table 3) showed that all Pol I phosphorylations analysed are non-essential posttranslational modifications. Furthermore, the mutations have no apparent effect on cell growth. Mutants have been further characterized with regard to drug- (MMS, 6AU) and UV-sensitivity. Additionally, a large scale screen for synthetic lethality of the A43 phosphomutants was performed in collaboration with the lab of Olivier Gadal from the CNRS in Toulouse. None of the experiments resulted in a detectable growth phenotype or genetic interaction for the investigated phosphomutants. Thus, none of the phosphosites seems to play a crucial role in the regulation of Pol I transcription, which was quite unexpected since previous results indicate that Pol I activity is linked to its phosphorylation state (Fath et al., 2001, 2004). However, not all posttranslational modifications seem to play a role in regulation as seen for methylation and pseudouridinylation of rRNA (Zebarjadian et al., 1999). These modifications could be structural checkpoints, since the binding sites for some r-proteins or biogenesis factors might be formed only if the modification mark is set (Song and Nazar, 2002).

Pol I phosphorylations involved in the regulation of the RNA polymerase activity might rather contribute to the fine-tuning of the enzyme. The kinetics of an assay measuring the *in vitro* transcription activity after different time points of alkaline phosphatase treatment showed that the removal of one or few phosphorylations has little effect or even leads to an increased activity (Fath et al., 2004). Only longer phosphatase incubation and the further dephosphorylation resulted in complete inactivation.

Nevertheless, combined phosphosite mutations of the A190 and A43 subunit, respectively, resulted in no detectable growth phenotype. For further *in vivo* characterization a strain would have to be established expressing a polymerase with mutations in all identified phosphosites.

A change in the Pol I transcription activity should result in a changed rate of rRNA production, which would influence the growth rate of the cell. However, apparently other regulatory mechanisms can compensate lowered levels of rRNA production, one of which could be the increase of actively transcribed rDNA copies and/or a denser polymerase loading on these genes (French et al., 2003).

Another possibility explaining the lack of growth defects in the analysed mutant strains would be a role of the corresponding phosphorylation sites in redundant functions which are not

necessarily related to the transcription activity. Possible aspects of Pol I phosphorylation in correct enzyme assembly, where it could serve as a structural checkpoint, will be discussed in section 3.4.

Plausible roles for single selected phosphosite mutants are discussed in the thesis of Jochen Gerber (Gerber, 2008). Moreover, additional sites might have escaped detection, *e.g.* sites which are required for complex formation with the transcription factor Rrn3 and which are present in only about 2% of the total Pol I population. Since overexpression of Rrn3 results in increased amounts of Pol I-Rrn3 complexes (Steinbauer, 2010), this system could be used to isolate these complexes and further identify specific, complex forming posttranslational modifications.

3.2   Formation of Pol I-Rrn3 complexes

The crucial interactions of A43 include the complex formation with Rrn3, which renders Pol I competent for transcription initiation (Peyroche et al., 2000). This complex formation is accompanied by a change in the Pol I phosphorylation pattern *in vivo* (Fath et al., 2001). Furthermore, the *in vitro* interaction seems to depend on the phosphorylation status of Pol I but not of Rrn3 (Fath et al., 2001). Most information on the putative binding site for Rrn3 came from the ts-mutant *rpa43-6* (Peyroche et al., 2000) which contains three different mutations resulting in an unstable Pol I-Rrn3 complex. The three amino acid exchanges were mapped to a conserved region of A43 spanning from amino acid 42 to 172 in the primary structure (Peyroche et al., 2000). In the solved crystal structure of a truncated A43/A14 heterodimer, two of the three *rpa43-6* mutations are located on the surface of A43 (Kuhn et al., 2007).

Only one (S220) of the four identified A43 phosphosites is included in this structure. The others are lying in flexible regions which were deleted from the recombinant proteins in order to facilitate crystallization.

However, none of the major phosphorylation sites showed an involvement in the mechanism of the binding or release of Rrn3. Only about 2% of the total cellular Pol I is present in the initiation-competent form, the rest belongs to the pools of transcribing or free polymerases and the identified phosphosites most probably originated from these latter two.

In an approach to investigate possible roles of phosphorylation in the A43-Rrn3 complex formation, serines within the conserved putative A43-Rrn3 interaction domain were mutated and tested for complementation of wild-type A43. Interestingly, the S141/143A mutation but not the S141/143D mutation is able to complement the loss of the wild-type subunit. In fact, it remains unclear whether these serine residues are *in vivo* phosphorylated. *In vivo* and *in vitro* experiments to further characterize these lethal mutations were carried out.

A conditional system, in which this A43 phenotype can be analysed in a more direct way, will be established. Therefore, vectors were constructed containing either wild-type, S141/143A or S141/143D mutant versions of A43 expressed from their endogenous promoter and either an N-terminally FLAG-tagged or untagged A43 wild-type protein expressed from a galactose-inducible promoter. This system allows the elimination of wild-type A43 expression by shifting cells from galactose to glucose.

Co-immunoprecipitation (Co-IP) experiments can be employed to compare the total amounts and the stability of Pol I-Rrn3 complexes in wild-type and mutant strains. Furthermore, the association of Rrn3 with the elongating Pol I as well as efficient promoter recruitment of the polymerase can be tested *in vivo* by chromatin immunoprecipitation (ChIP) assays.

For further *in vitro* A43-Rrn3 interaction studies, Rrn3 purified from SF21 insect cells via the baculovirus expression system can be used together with the recombinant A43/A14 mutants obtained from *E. coli*.

3.3   Uncoupling transcription and pre-rRNA processing after short-term TOR inactivation

The cellular level of the transcription factor Rrn3 significantly influences RNA polymerase I transcription and thus the rate of rRNA synthesis (Steinbauer, 2010). However, the simple down-regulation of Rrn3 and Pol I–Rrn3 levels cannot explain the dramatic reduction of rRNA synthesis in the immediate cellular response to impaired TOR signalling (Philippi et al., 2010). Rapamycin treatment leads to a fast down regulation of both cell growth and mature rRNA production (Philippi et al., 2010). These results point towards a more drastic and rapid effect of rapamycin- or starvation-induced TOR inactivation than just down regulating Pol I transcription via reducing the amount of Rrn3. Controlling the level of Rrn3 might serve as a tool for the cell to adjust the rate of ribosome synthesis in the long term (Steinbauer, 2010). At early stages of TOR inactivation, however, a target presumably downstream of Pol I transcription initiation must be affected. In order to elucidate this issue, the quick effects of TOR inactivation on Pol I transcription and rRNA production were investigated. Interestingly, neither the level of Rrn3 nor the association of Pol I with the rDNA locus was substantially decreased after 15 min of rapamycin-induced TOR inactivation (Reiter et al., 2011). Moreover, polymerase molecules engaged in transcription elongation were still able to finish their initiated rRNA synthesis. Under these conditions RNA Pol I was still mobile, giving rise to nascent 35S pre-rRNA, which does not, however, exclude the possibility that transcription elongation is partly affected (Stefanovsky et al., 2006; Zhang et al., 2010). While 35S pre-rRNA production is maintained, a drastic decrease in the level of intermediate and mature rRNAs is

already detectable after 15 min of rapamycin treatment compared to untreated cells in several strain backgrounds (see section 2.2). TOR inactivation affects not only rRNA gene transcription by Pol I, but decreases also very fast translation initiation and pre-rRNA maturation (Barbet et al., 1996; Powers and Walter, 1999). The protein synthesis inhibitor cycloheximide was used to analyse whether a significant decrease of protein production causes the observed pre-rRNA processing defects which follow TOR inactivation. In fact, 15 min of cycloheximide treatment was sufficient to generate even more severe pre-rRNA maturation defects (see section 2.2), which is consistent with diverse earlier reports (de Kloet, 1966; Udem and Warner, 1972; Warner and Udem, 1972).

In summary, TOR-dependent inhibition of r-protein expression appears to play the dominant role in the drastic down regulation of ribosome production rather than the decrease in Pol I transcription. Ribosomal proteins have to be produced in at least stoichiometric amounts to the ribosomal RNAs in the cell to support proper assembly, processing, and maturation of the ribosomal subunits (Warner, 1999). An impairment in the production of these structural components very likely provokes drastic effects on the synthesis of ribosomes, especially if ribosome assembly occurs not strictly according to hierarchical orders.

It is known that different ribosomal domains can assemble independently (Ferreira-Cerca et al., 2007). All improperly assembled subdomains result in rapid degradation (see model in Figure 43). In support of this idea, *in vivo* depletion of individual r-proteins of the large or small ribosomal subunit frequently leads to a drastic accumulation of the corresponding other subunit both in yeast and in mammals (O'Donohue et al., 2010; Pöll et al., 2009; Robledo et al., 2008). This imbalance of structural components of the ribosome is then presumably adjusted by rapid degradation of misassembled, excess rRNA precursors (Pöll et al., 2009).
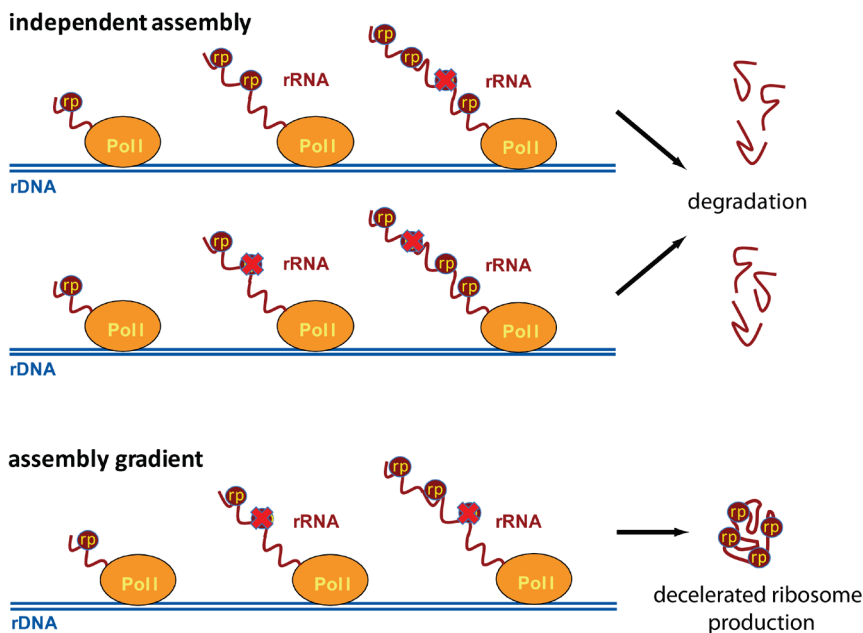
Figure 43. Two different models for ribosome assembly

Upper panel: Ribosomal proteins can assemble independently to rRNA. Shortage of individual r-proteins leads to misassembled ribosomes and rapid rRNA degradation. Lower panel: Ribosome assembly follows an assembly gradient. Shortage of individual r-proteins leads to decelerated ribosome production.

Analysis of yeast strains which exhibit severe growth defects due to a moderate reduction in the level of a single ribosomal protein in the context of gene haploinsufficiency further strengthen this point (Steinbauer, 2010). This observation was already described by others (Abovich et al., 1985; Lucioli et al., 1988; Deutschbauer et al., 2005). Interestingly, the impact of short-term rapamycin treatment is indeed predominantly directed towards the expression of ribosomal proteins, whereas cycloheximide treatment for the same time affects the overall expression of proteins in the cell. By using lower cycloheximide concentrations, which have a similar impact on the synthesis of ribosomal proteins as rapamycin treatment, a virtually identical defect in the production of mature rRNAs could be obtained (Reiter et al., 2011). Although the CARA strain, when compared to the wild-type strain, displays an attenuated decrease in the mRNA levels specifically of r-proteins upon TOR inactivation (Laferté et al., 2006), r-protein production is equally decreased in both the mutant and the wild-type cells after 15 min of rapamycin treatment (Steinbauer, 2010). It is noteworthy that the decrease in the mRNA levels of r-proteins in the CARA mutant is only slightly delayed compared to the wild-type strain after 15 min of rapamycin treatment. However, rRNA processing is also heavily affected in the CARA strain as seen in (Laferté et al., 2006). Consistent with this, similar defects in pre-rRNA processing and mature rRNA synthesis could be observed in wild-type and mutant strain in our experiments (see section 2.2). Further evidence for an early shortage of ribosomal proteins derives from a recent study showing that amino acid starvation leads to a very rapid inhibition of mRNA splicing in yeast, which predominantly affects the expression of r-protein genes (Pleiss et al., 2007). Since ribosomal protein genes account for almost 50% of the

intron-containing genes and about 90% of mRNA splicing is devoted to r-protein transcripts in yeast, a general depletion of the cellular r-protein pool was already speculated to link impairments in the nuclear pre-mRNA splicing machinery to ribosome biogenesis defects (Hartwell et al., 1970; Warner and Udem, 1972; Rosbash et al., 1981; Spingola et al., 1999; Warner, 1999). These observations indicate that the drastic reduction in ribosomal protein production following rapamycin or cycloheximide treatment is sufficient to provoke severe defects in the processing and maturation steps of pre-rRNAs, which are then obviously rapidly degraded.

In a recently described *TOR1* mutant strain, the rapamycin-induced pre-rRNA processing phenotype can be uncoupled from the inhibition of r-protein mRNA synthesis (Li et al., 2006). These observations don`t necessarily contradict the model of depleted r-proteins generating the immediate shut-off of ribosome production, as it is not clear yet whether under the conditions used in this publication rapamycin still prevents the translation of the r-protein mRNAs and thus the expression of the ribosomal proteins as it was previously observed (Barbet et al., 1996). In this regard, it would be interesting to correlate rRNA maturation with r-protein production upon TOR inactivation in these genetic backgrounds.

3.4 The importance of correct Pol I assembly and possible roles of phosphorylation in this process

The phosphorylation site A190 S685 is localized on the part of the Pore 1 domain which contributes to the backside of the polymerase complex in the vicinity of ABC14.5, the AC40/AC19 heterodimer and a conserved loop of the hybrid binding-domain of A135. Mutation of S685 to either alanine or aspartate resulted in no detectable growth defect on full media.

A striking difference between the alanine and aspartate mutations of A190 S685 is the genetic interaction with the non-essential Pol I subunit A12.2. The mutation *rpa190* S685D was found to be synthetic lethal with the deletion of *RPA12* (Reiter, 2007). In contrast, the growth behavior of the analogous *rpa190* S685A / *Δrpa12* strain was similar to a *Δrpa12* control strain. Synthetic lethality indicates a functional linkage between the two genetic interaction partners. Accordingly, reversible phosphorylation at A190 S685 seems to be linked to one of the functions of the non-essential Pol I subunit A12.2. Interaction of A12.2 with A190 seems to be important for the correct conformation of the largest subunit and its assembly into the polymerase complex (Nogi et al., 1993; Mullem et al., 2002). A deletion of *RPA12* leads to a ts-growth phenotype. Interestingly, the A12.2 binding site is localized in the jaw region of

A190, which is on the opposite side of the polymerase with respect to the phosphorylation site A190 S685 (Gerber et al., 2008). Thus, a direct interaction seems to be rather unlikely.

Phosphorylation at the A190 S685 site might allosterically induce a conformational change of the pore and the adjacent active center (Johnson and O'Reilly, 1996; Johnson and Lewis, 2001). In this conformational state, the loss of A12.2 might lead Pol I into a dead end situation resulting in synthetic lethality by reinforcing the *Δrpa12* ts-phenotype.

The 6AU sensitivity as well as the ts-phenotype of a *Δrpa12* strain can be rescued by the N-terminal domain of A12.2 (Mullem et al., 2002), indicating that the full deletion has an impact on transcription elongation. This effect is independent from the reported RNA cleavage activity of the C-terminal domain of A12.2 and most probably due to disturbed complex stability as a consequence of affected Pol I assembly. Furthermore, synthetic lethality of the *rpa190* S685D / *Δrpa12* mutant can be rescued by the expression of the N-terminal domain of A12.2 pointing towards an impaired complex stability as the possible cause of the SL phenotype.

Semi-quantitative mass spectrometric comparison of co-purified Pol I subunits revealed a Pol I complex which is partially depleted for A190 and associated subunits like A43, ABC27, ABC23, and A14 in the SL mutant strain. This observation of defective Pol I assembly could additionally indicate that the common ABC23 subunit is involved in enzyme assembly (Nouraini et al., 1996; Minakhin et al., 2001) and forms the main interaction interface of the core polymerase to its respective 'stalk' heterodimer (Peyroche et al., 2002).

Taken together, an involvement of the A190 S685 phosphosite in enzyme assembly becomes plausible. This indicates a possible hierarchical assembly order in which the phosphorylation of S685 could serve as a structural checkpoint occuring after A12.2 assembly and the thereby induced conformational changes in A190. The S685 phosphorylation might act as an energy barrier locking the achieved assembly state by impeding the backward reaction.

3.5 A12.2, a Pol I specific subunit involved in many processes

The C-terminal domain of the TFIIS-like subunit A12.2 exhibits an intrinsic Pol I cleavage activity *in vitro* (Kuhn et al., 2007). It contains the highly conserved motif Q.RSADE..T.F shared with the other members of the TFIIS-like protein family (Chédin et al., 1998; Hausner et al., 2000). Full deletion of this non-essential Pol I subunit results in a ts-phenotype and 6AU sensitivity, while truncation of the C-terminal half apparently has no consequences on cell growth (Nogi et al., 1993; Mullem et al., 2002). Thus, it was surprising that mutation of the aspartate and glutamate residues of the conserved C-terminal motif to alanines is lethal (A12.2 D105A/E106A). Apparently, the full or partial deletions of A12.2 can be compensated by the cell while the DE/AA mutation leads to a `dead end situation`.

In a similar manner the analogous mutation in the homologous but essential Pol III subunit C11 was found to be lethal (Chédin et al., 1998). The DE/AA mutation in the non-essential Pol II cleavage factor TFIIS has only been tested *in vitro* where it resulted in a loss of function (Jeon et al., 1994). Structural analysis of TFIIS bound to Pol II revealed that the two acidic amino acids of the conserved motif coordinate a metal ion in the active site required for RNA cleavage (Kettenberger et al., 2003). Moreover, significant amounts of *in vitro* data on the function of TFIIS in transcript cleavage and Pol II backtracking is contributed by the group of Jesper Svejstrup (Svejstrup, 2007; Sigurdsson et al., 2010). However, as discussed in section 3.4 the location of A12.2 in the Pol I complex could contradict an RNA cleavage mechanism analogous to the one described for TFIIS. A12.2, like its homologous Pol II subunit Rpb9, binds to the jaw region of the largest subunit. Interestingly, recent studies with chimeric fusion proteins between the N-terminal domain of Rpb9 and the C-terminal domain of the Pol III counterpart C11, which shows a higher degree of homology with the A12.2 C-terminus than with the Rpb9 C-terminus, could show that this C-terminus is more mobile, catalytic, and enters the Pol II core to induce strong RNA cleavage (Ruan et al., 2011). It is discussed that the A12.2 and C11 C-terminus may be able to swing between surface and pore locations. However, replacing the C-terminus of Rpb9 with the A12.2 C-terminus did not confer strong cleavage to Pol II.

The use of a conditional system in which the A12.2 DE/AA mutant is expressed under the control of a galactose-inducible promoter provides a useful tool to investigate the possible function of A12.2 in the intrinsic RNA cleavage activity of Pol I. In theory, the polymerase molecules apparently become trapped in the `dead end situation` upon induction.

Overexpressing the A12.2 DE/AA mutant in a wild-type strain at higher temperatures (37°C) did not result in a growth phenotype as documented at lower temperatures, probably due to greater flexibility of the C-terminal domain resolving the `dead end situation`. Additionally, the induced growth phenotype can be rescued by the presence of a C-terminal FLAG-tag which could, apparently due to sterical hinderence, prevent the possibly stuck intermediate state of the A12.2 dependent RNA cleavage process during polymerase backtracking. Since pulse experiments showed a general impairment of Pol I transcription and initial ChIP analyses could give indications for problems with Pol I initiation or early elongation (Pilsl, 2010), the hypothesis of a Pol I molecule stuck in early transcription due to affected backtracking is worth to be further discussed.

In vitro transcription assays could be used to investigate whether these `dead end situation` polymerase complexes are still active but stalled or completely inactive. Furthermore, RT-qPCR of 5` rRNA, extracted at different time points after induction of A12.2 DE/AA expression, could give more detailed information on the length of the produced RNAs and thereby reveal possible pausing sites and backtracking hotspots on the 5` rDNA gene.

3.6 *In vivo* Pol I elongation assay

We established an elaborate *in vivo* system which relies on the genetic manipulation of the entire endogenous rDNA locus (Wai et al., 2000) with each of the 150 to 200 rDNA repeats harboring the manipulated *in vivo* template of Pol I.

Thus, we introduced DNA binding sites for various DNA binding proteins including TTF-I, LacI, LexA as well as the 601 nucleosome positioning sequence into the internal transcribed spacer 1 (ITS1) in between the 18S rRNA and 5.8S rRNA within each 35S rRNA coding sequence. We are able to conditionally express the different heterologous DNA binding proteins which are under the control of a galactose-inducible promoter. DNA binding of MNase fusion proteins was detected *in vivo* by Chromatin Endogenous Cleavage (ChEC) analyses and Southern blotting (Merz et al., 2008; Schmid et al., 2004).

We could demonstrate that TTF-I- and LexA-MNase fusion proteins bind to their cognate DNA sequence within the transcribed rDNA region.

No binding could be detected for the LacI-MNase fusion protein, which could be due to sterical hinderence caused by the MNase-tag since LacI forms homotetramers and is able to bind two operators at the same time (Santillán and Mackey, 2008).

Interestingly, although TTF-I terminates transcription *in vitro* (Kuhn et al., 1990), the orientation-dependent binding of this protein interferes with, but does not inhibit Pol I elongation *in vivo* as monitored by ChEC analysis of Pol I-MNase fusion proteins.

Growth phenotypes under different conditions (different temperature, presence of 6AU, nutrient starvation, UV, and other environmental stress situations) can be monitored in the future after expression of the DNA binding protein in induced wild-type and mutant strains. Preliminary experiments in mutant strains with deletions of A49 or A12.2 showed that the growth phenotype of TTF-I binding is more pronounced in these strains. Corresponding analyses can also be performed in mutant strains in which non-essential factors of the Pol I transcription machinery like Hmo1, the remaining non-essential Pol I subunits A34.5 and A14 or factors involved indirectly or directly in elongation like Top1, Spt4, or Paf1 are impaired. Pol I distribution on the rDNA can be monitored using ChEC and ChIP analyses and by electron microscopic inspection of rDNA Miller chromatin spreads. The ability of Pol I to pass the barrier *in vivo* can be compared with the results of *in vitro* assays. This will allow a direct correlation between requirements in a defined *in vitro* system and the *in vivo* situation.

Furthermore, the described *in vivo* system can be used to identify factors which support Pol I to overcome different barriers. While binding of LexA does not change growth rate, binding of TTF-I results in a significant growth defect. The above yeast strains can be subjected to random mutagenesis. Clones can be selected which fail to grow if expression of the DNA binding protein is induced by shifting the culture from glucose to galactose. The respective mutations responsible for the growth phenotype can be identified by co-expression of a yeast expression

library in these strains and subsequent isolation of plasmids encoding complementing genes. The impact of the identified gene products on transcription elongation can be subsequently analysed in *in vitro* assays.
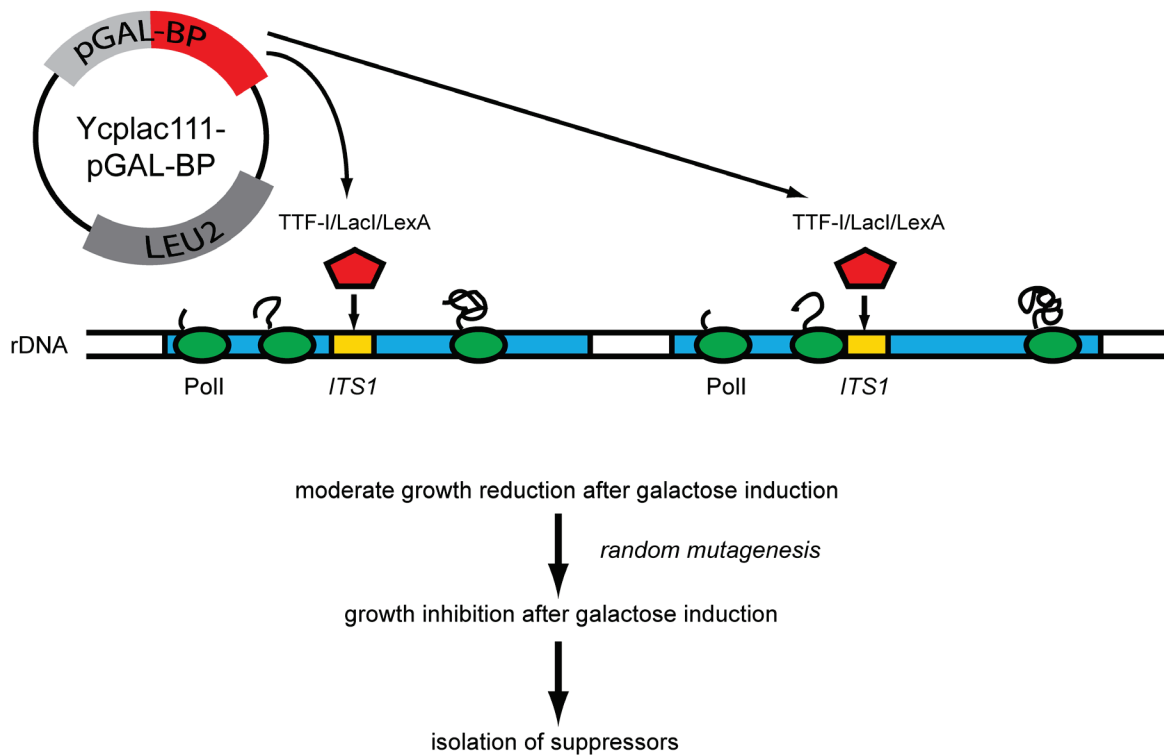
Figure 44. *In vivo* screen for Pol I specific elongation factors

TTF-I induction reduces growth rate. After random mutagenesis, galactose induction and replica plating, clones will be selected which cannot grow on galactose. Respective mutations responsible for the growth phenotype will be identified by co-expression of a yeast expression library and subsequent isolation of plasmids encoding complementing genes.

Furthermore, the random mutagenesis strategy can be used for single Pol I subunits to identify their possible role in elongation. These strains contain a shuffle-plasmid which encodes the wild-type subunit and complements the chromosomal knock-out. The mutant plasmids are transformed and after the wild-type copy is shuffled out, yeast clones are replica plated on galactose to induce the expression of the binding protein. Strains that are either impaired in growth or grow significantly better than the control strain can be isolated and the mutations within the respective Pol I subunit can be identified.

Furthermore, already described mutants, *e.g.* the Pol I phosphosite mutants, can be investigated in this elongation assay to screen for possible roles of phosphorylation in elongation.

3.7 `Torpedo termination` or not?

There exists a discrepancy between *in vitro* and *in vivo* data on Pol I termination. Reb1 has been reported to pause Pol I and to support transcript release *in vitro* (Lang and Reeder, 1993). However, Reb1 binding *in vivo* can only be detected at its binding site near the Pol I promoter but not at the terminator, and a fourfold reduction of Reb1 *in vivo* had no effect on termination (Kawauchi et al., 2008). An alternative, torpedo-like model - similar to Pol II termination - was recently proposed. This model is supported by analyses of yeast mutants deficient in the endonuclease Rnt1 which is required for 3´ end processing of 25S pre-rRNA, and which accumulates transcripts beyond the T1 termination site (Prescott et al., 2004; Reeder et al., 1999). Furthermore, inactivation of the nuclear exonuclease Rat1 and the RNA helicase Sen1 leads to accumulation of extended pre-rRNAs (Kawauchi et al., 2008). Inactivation of Rat1 also increased Pol I occupancy in the region downstream of the T1 terminator. This all leads to a model in which the nascent pre-RNA is co-transcriptionally cleaved by Rnt1. The 5´ end of the cleaved transcript serves as a substrate for the exonuclease Rat1 which progressivly degrades the Pol I bound transcripts with the help of the helicase Sen1 and, thus, finally releases Pol I from the template. Very recent studies suggest that such a torpedo-like termination mechanism functions even in the absence of the Rnt1-dependent cleavage. A second cleavage site at the T-rich region of T1 was proposed as a failsafe termination site. Cleavage at this site should allow co-transcriptional recruitment of the exonuclease Rat1 (Braglia et al., 2010b).

However, in all of these analyses it is difficult to distinguish between termination of rRNA transcription or processing since no 5` and 3` ends, which would appear after cleavage, are shown.

Therefore we decided to investigate Pol I termination *in vivo* by using a similar system as the previously described screen for Pol I specific elongation factors. Since several *cis* elements within the Pol I termination region were reported to be involved in transcription termination, we inserted various termination elements in the ITS1 spacer of the rDNA gene locus.

We examined which of these elements are required to cause growth reduction in our established *in vivo* system. Growth analyses revealed that neither the RFB nor the T2 element (failsafe terminator) significantly contributes to growth reduction. However, elimination of the T-rich element upstream of the Reb1 binding site at T1 leads to less growth inhibition. This confirms previous studies which showed that efficient *in vitro* termination depends on the presence of this T-rich element (Lang et al., 1994; Lang and Reeder, 1995) and underlines T1 function also for *in vivo* termination.

Interestingly, the Rnt1 cleavage site which was proposed as a prerequisite for `torpedo`-like termination (El Hage et al., 2008; Kawauchi et al., 2008; Reeder et al., 1999) is missing in all constructs causing growth defects. Even in the absence of the postulated failsafe cleavage site at T1 (Braglia et al., 2010b) a significant growth inhibition can be observed.

Furthermore, possible cleavage candidates like Rpa12, Dis3 (a core exosome subunit) and the NRD complex show no involvement in this postulated co-transcriptional cleavage process (Braglia et al., 2010b).

In our analysis, we identified and characterized the protein Ydr026c as the *in vivo* Pol I termination factor in yeast. The binding of Ydr026c to the introduced Reb1 binding site within ITS1 appears to be the only necessary prerequisite for growth reduction in our *in vivo* system since no growth reduction was obtained when either the direction of the Ydr026c binding site was changed or the binding site was missing.

Though Reb1 also binds to a number of Pol II genes (Remacle and Holmberg, 1992; Graham and Chambers, 1994; Carmen and Holland, 1994), Ydr026c is solely reported to bind to rDNA (Mohanty and Bastia, 2004). In a global analysis of protein localization in yeast performed with GFP-tagged proteins, Ydr026c was described to be nucleolar, whereas Reb1 is found in the nucleus (Huh et al., 2003) which would altogether argue for the specific role of Ydr026c in Pol I termination.

Considering the possibility that a factor bound to the Reb1 binding site could position the paused Pol I on top of the T-rich element, it seems rather unlikely that an unknown factor could perform the proposed failsafe cleavage at T1. However, this question could be addressed by bioinformatical protein modeling.

According to our data a `pause and release` termination model in which protein-mediated pausing of Pol I at termination sites causes backtracking of the polymerase and its release by slippage on an upstream pyrimidine-rich sequence is favoured in contrast to the above mentioned `torpedo` model (Reeder and Lang, 1997; Mason et al., 1997b).

Taken together, Ydr026c serves as an *in vivo* Pol I terminator protein and Rat1-mediated `torpedo termination` may contribute to a more efficient Pol I termination instead of playing a central role in this complex process.

The described *in vivo* system can be used to identify factors which support Pol I termination in an approach similar to the screen for Pol I *in vivo* elongation factors described in 3.6. Furthermore, the random mutagenesis strategy can also be used for single Pol I subunits to identify their possible role in termination as outlined for possible roles in elongation in section 3.6.

4 SUMMARY – ZUSAMMENFASSUNG

4.1 Summary

RNA polymerase I (Pol I) is a specialized enzyme which transcribes the ribosomal RNA (rRNA) genes in all eukaryotes. Pol I transcription is regulated by specific DNA *cis*-elements and *trans*-acting factors as well as the usage of a specific chromatin template.

Regulation and efficiency of rRNA synthesis in yeast depend on many processes including recruitment of the Pol I machinery and binding of Pol I-dependent transcription factors to the promoter, activity of the DNA-associated Pol I complexes, termination of transcription at specific sites, and co- and posttranscriptional RNA processing steps.

Analyses of molecular defects of several Pol I mutants as well as the investigation of the immediate downregulation of rRNA synthesis upon growth arrest, mediated by the TOR pathway, were part of this study. Furthermore, an *in vivo* screen to determine Pol I specific elongation and termination factors has been established and the so far uncharacterized protein Ydr026c has been identified as Pol I termination factor.

The Pol I phosphosites, identified by Jochen Gerber, were further mutated and analysed *in vivo*. All Pol I phosphorylations were found to be non-essential posttranslational modifications since none of the mutants showed a detectable, significant growth phenotype.

Transcription initiation depends on the A43-Rrn3 complex formation and (de-) phosphorylation of Pol I subunits is likely to be involved in its regulation. We have identified and initially characterized a lethal Pol I mutant which probably interferes with this essential process.

Additionally, the mutation of the A190 phosphosite S685 from serine to aspartate but not to alanine was found to be synthetic lethal with the deletion of the non-essential Pol I subunit A12.2. Our data suggest that the reversible phosphorylation at A190 S685 plays a significant role in Pol I assembly and stability.

Furthermore, a lethal phenotype resulting from a mutation in the TFIIS-like C-terminal domain of the non-essential Pol I subunit A12.2 was initially characterized *in vivo*.

Regulation of rRNA transcription by reduction of initiation competent Pol I-Rrn3 complexes after TOR inactivation seems to be too slow to explain the strong pre-rRNA processing defects. To distinguish between primary and secondary effects in the regulation of ribosome biogenesis, Pol I transcription and rRNA synthesis were investigated shortly after TOR inhibition by rapamycin. The fast downregulation of mature rRNA synthesis correlates with strong pre-rRNA processing defects and subsequent RNA degradation. The quick

downregulation of r-protein synthesis after TOR inhibition is sufficient to explain the severe pre-rRNA processing defects.

To analyse Pol I elongation *in vivo* we created possible roadblocks for Pol I transcription within every rDNA copy through genetic manipulation of the entire endogenous yeast rDNA locus. We established plasmids for inducible expression of the respective (heterologous) DNA binding proteins and we could demonstrate that many of these proteins bind to their cognate DNA sequence within the transcribed rDNA region. Although they are all blocking transcription *in vitro*, the binding of some of these proteins hampers, but does not inhibit Pol I elongation *in vivo*. The presented *in vivo* system allows the identification of factors supporting Pol I to overcome different barriers.

To identify specific factors involved in Pol I termination, we used an artificially introduced terminator region in every rDNA copy. We could identify and characterize Ydr026c as the Pol I terminator protein. Interestingly, this factor and not the previously published Reb1 is associated with the Reb1 binding site at the termination region *in vivo* and is required for *in vivo* Pol I transcription termination. Our data suggests that a `pause and release` mechanism is sufficient to support transcription termination *in vivo*, which indicates that the recently proposed `torpedo termination` model represents no necessary prerequisite for termination. Additionally, this *in vivo* system can be used to further characterize Pol I termination.

4.2 Zusammenfassung

Die RNA Polymerase I (Pol I) ist ein spezialisiertes Enzym, welches die ribosomale RNA (rRNA) in allen Eukaryonten transkribiert. In die Regulation der Polymerase I Transkription sind spezielle DNA *cis*-Elemente, *trans*-agierende Faktoren sowie der Gebrauch einer besonderen Chromatinmatrize eingebunden.

Die Effizienz und Regulation der rRNA Synthese ist bei der Hefe von vielen unterschiedlichen Prozessen abhängig. Dazu zählen die Rekrutierung der Pol I Maschinerie und die Bindung Pol I abhängiger Transkriptionsfaktoren an den Promotor, die Aktivität des DNA assoziierten Pol I Komplexes, Transkriptionstermination an genau determinierten Stellen und ko- bzw. posttranslationale RNA Prozessierungsschritte.

Ein Teil dieser Arbeit bestand aus Analysen der molekularen Defekte mehrerer Pol I Mutanten sowie der Erforschung der sofortigen Herabregulation der rRNA Synthese nach Wachstumshemmung, hervorgerufen durch Inaktivierung der TOR Signalweges. Desweiteren wurde ein *in vivo* Screen etabliert um Pol I spezifische Elongations- und Terminationsfaktoren zu ermitteln. Dabei wurde das bis dahin nicht charakterisierte Protein Ydr026c als Pol I Terminationsfaktor identifiziert.

Die von Jochen Gerber identifizierten Pol I Phosphorylierungsstellen wurden weiter mutiert und *in vivo* analysiert. Alle Pol I Phosphorylierungen wurden als nicht essenzielle posttranslationale Modifikationen eingestuft, da keine der Mutanten einen signifikantan Wachstumsphänotyp zeigte.

Die Transkriptionsinitiation ist entscheidend von der Bildung des A43-Rrn3 Komplexes abhängig. Die Phosphorylierung bzw. Dephosphorylierung von Pol I Untereinheiten ist wahrscheinlich an der Regulation dieser Komplexbildung beteiligt. Wir haben eine letale Pol I Mutante identifiziert, die diesen essenziellen Prozess möglicherweise beeinträchtigt, und anfänglich charakterisiert.

Bei weiterführenden Untersuchungen wurde die Mutation der Phosphorylierungsstelle S685 der Pol I Untereinheit A190 von Serin nach Aspartat nicht aber nach Alanin in Kombination mit der Deletion der nicht essenziellen Pol I Untereinheit A12.2 für synthetisch letal befunden. Unsere Daten suggerieren eine besondere Rolle der reversiblen Phosphorylierung an dieser Stelle für die Polymeraseassemblierung und –stabilität.

Desweiteren wurde ein letaler Phänotyp, resultierend aus einer Mutation in der TFIIS ähnlichen C-terminalen Domäne der nicht essenziellen Pol I Untereinheit A12.2, anfänglich *in vivo* charakterisiert.

Bislang ging man davon aus, dass die Regulation der rRNA Transkription durch die Verringerung der initiationskompetenten Pol I-Rrn3 Komplexe nach TOR Inaktivierung geschieht. Dieser Mechanismus ist jedoch zu träge, um die starken prä-rRNA

Prozessierungsdefekte zu erklären, die sehr schnell nach TOR Inaktivierung auftreten. Zur Klärung dieser Frage wurden die Pol I Transkription und rRNA Synthese kurz nach TOR Inaktivierung durch Rapamycin untersucht. Hierbei zeigte sich, dass die schnelle Herabregulation der Synthese der reifen rRNA stark mit prä-rRNA Prozessierungsdefekten korreliert und anschließenden RNA Abbau nach sich zieht. Die schnelle Herabregulation der r-Protein Synthese nach TOR Inaktivierung ist dabei ausreichend um die schweren prä-rRNA Prozessierungsdefekte zu erklären.

Zur Untersuchung der Pol I Elongation *in vivo* wurden über genetische Manipulation des gesamten endogenen rDNA Lokus mögliche Transkriptionsbarrieren für Pol I in jeder rDNA Einheit erzeugt. Desweiteren stellten wir Plasmide zur induzierbaren Expression der jeweiligen (artfremden) DNA Bindeproteine her. Wir konnten zeigen dass viele dieser Proteine an ihre verwandte DNA Bindesequenz innerhalb der transkribierten rDNA binden. Obwohl alle diese Proteine die Transkription *in vitro* blockieren, wird die Pol I Elongation *in vivo* durch einige dieser Proteine lediglich erschwert, jedoch nicht komplett verhindert. Das vorgestellte *in vivo* System erlaubt die Identifikation von Faktoren welche Pol I beim Überwinden verschiedener Barrieren unterstützen.

Zur Identifizierung spezifischer Faktoren, die an der Pol I Termination beteiligt sind, benutzten wir eine künstlich in jede rDNA Einheit eingeführte Terminatorregion. Dadurch konnten wir Ydr206c als Pol I Terminatorprotein identifizieren und charakterisieren. Interessanterweise ist dieser Faktor und nicht das zuvor veröffentlichte Reb1 mit der Reb1 Bindestelle am Terminator *in vivo* assoziiert und wird für die *in vivo* Pol I Termination benötigt. Unsere Daten suggerieren, dass ein `pause and release` Terminationsmechanismus ausreichend ist um die Pol I Termination *in vivo* zu fördern. Dies weist darauf hin, dass das vor kurzem vorgeschlagene `torpedo termination` Modell keine notwendige Voraussetzung für die Pol I Termination darstellt. Zusätzlich kann dieses *in vivo* System zur weiteren Charakterisierung der Pol I Termination genutzt werden.

5 MATERIAL AND METHODS

5.1 Material

5.1.1 *Saccharomyces cerevisiae* strains

Strain	Parent strain	Genotype	Reference of source
W303-1a		*mata ade2-1 can1-100 his3-11,-15 leu2-3,112 trp1-1 ura3-1*	(Thomas and Rothstein, 1989)
BY4741		*mata his3-1 leu2-0 met15-0 ura3-0*	EUROSCARF
BY4742		*mata his3-1 leu2-0 ura3-0 lys2-0*	EUROSCARF
D101-l2		*mata ade2-101 ura3-52 lys2-801 trp1-Δ63 his3-Δ200 leu2-Δ1 rpa43::LEU2 yCPA43 (URA3)*	(Thuriaux et al., 1995)
NOY222		*mata trp1-1 his4-401 leu2-3,112 ura3-52 can RPA190::URA3 pNOY20*	(Wittekind et al., 1988)
NOY989		*mata ade2-1 ura3-1 trp1-1 leu2-3,112 his3-11 can1-100 rdn::URA3/pNOY353*	(Wai et al., 2000)
NOY886		*mata ade2-1 ura3-1 his3-11,15 trp1-1 leu2-3,112 can1-100* rpa135-::LEU2 fob1::HIS pNOY117	(Cioci et al., 2003)
NOY1064		*mata ade2-1 ura3-1 his3-11 trp1-1 leu2-3,112 can1-100* fob1::HIS3	(Cioci et al., 2003)
NOY1071		*mata ade2-1 ura3-1 his3-11 trp1-1 leu2-3,112 can1-100 fob1::HIS3*	(Cioci et al., 2003)
YPH500		*mata ade2-101 his3-200 leu2-1 lys2-801 trp1-63 ura3-52*	(Sikorski and Hieter, 1989)
CARA	YPH500	*mata ade2-101 his3-200 leu2-1 lys2-801 trp1-63 ura3-52 RRN3::HIS5 RPA43::kan pGEN-RRN3-A43 (TRP1)*	(Laferté et al., 2006)
y532	D101-l2	*mata ade2-101 ura3-52 lys2-801 trp1-Δ63 his3-Δ200 leu2-Δ1 rpa43::LEU2 yCPA43 (URA3) RPA135-ProtA::kanMX6*	(Gerber, 2008)
y601	BY4741	*mata his3-1 leu2-0 met15-0 ura3-0 RPA12::KanMX4*	EUROSCARF
y612	D101-l2	*mata ade2-101 ura3-52 lys2-801 trp1-Δ63 his3-Δ200 leu2-Δ1 rpa43::LEU2 pRS314-rpa43-S208D (TRP1)*	(Gerber, 2008)
y658		*ura3-52 his3-Δ200 leu2-Δ1 trp1Δ63 lys2-801 ade2-101 prc1-1 RRN3::RRN3-TAP (URA3) RPA43::RPA43-HA$_3$ (HIS3)*	(Philippi, 2007)
y726	NOY222	*mata trp1-1 his4-401 leu2-3,112 ura3-52 can1-100 RPA190::URA3 RPA12::KanMX4 pNOY20*	(Reiter, 2007)
y1178	D101-l2	*mata ade2-101 ura3-52 lys2-801 trp1-Δ63 his3-Δ200 leu2-Δ1 rpa43::LEU2 pRS314-rpa43-S262D (TRP1)*	this study

y1179	D101-l2	*mata ade2-101 ura3-52 lys2-801 trp1-Δ63 his3-Δ200 leu2-Δ1 rpa43::LEU2 pRS314-rpa43-S263D (TRP1)*	this study
y1180	D101-l2	*mata ade2-101 ura3-52 lys2-801 trp1-Δ63 his3-Δ200 leu2-Δ1 rpa43::LEU2 pRS314-rpa43-S262/263D (TRP1)*	this study
y1181	D101-l2	*mata ade2-101 ura3-52 lys2-801 trp1-Δ63 his3-Δ200 leu2-Δ1 rpa43::LEU2 pRS314-rpa43-S262/285D (TRP1)*	this study
y1182	D101-l2	*mata ade2-101 ura3-52 lys2-801 trp1-Δ63 his3-Δ200 leu2-Δ1 rpa43::LEU2 pRS314-rpa43-S285D (TRP1)*	this study
y1183	D101-l2	*mata ade2-101 ura3-52 lys2-801 trp1-Δ63 his3-Δ200 leu2-Δ1 rpa43::LEU2 pRS314-rpa43-S220D (TRP1)*	this study
y1597	W303-1a	*mata ade2-1 can1-100 his3-11,-15 leu2-3,112 trp1-1 ura3-1 RPA12::KanMX4*	this study
y1598	NOY989	*mata ade2-1 ura3-1 trp1-1 leu2-3,112 his3-11 can1-100 rdn-3xLexA*	this study
y1599	NOY989	*mata ade2-1 ura3-1 trp1-1 leu2-3,112 his3-11 can1-100 rdn-WT*	this study
y1600	y726	*mata trp1-1 his4-401 leu2-3,112 ura3-52 can1-100 RPA190::URA3 RPA12::KanMX4 pRS314-RPA190-pGAL-RPA12*	this study
y1601	y726	*mata trp1-1 his4-401 leu2-3,112 ura3-52 can1-100 RPA190::URA3 RPA12::KanMX4 pRS314-rpa190 S685A-pGAL-RPA12*	this study
y1602	y726	*mata trp1-1 his4-401 leu2-3,112 ura3-52 can1-100 RPA190::URA3 RPA12::KanMX4 pRS314-rpa190 S685D-pGAL-RPA12*	this study
y1612	y1598	*mata ade2-1 ura3-1 trp1-1 leu2-3,112 his3-11 can1-100 rdn-3xLexA Δrpa12*	this study
y1615	y1599	*mata ade2-1 ura3-1 trp1-1 leu2-3,112 his3-11 can1-100 rdn-WT Δrpa49*	this study
y1618	y1599	*mata ade2-1 ura3-1 trp1-1 leu2-3,112 his3-11 can1-100 rdn-WT Δrpa12*	this study
y1620	y1599	*mata ade2-1 ura3-1 trp1-1 leu2-3,112 his3-11 can1-100 rdn-WT RPA190-MNase-3xHA::KanMX6*	this study
y1697	y206	*mata his3-1 leu2-0 met15-0 ura3-0 RRP6::kanMX4*	EUROSCARF
y2034	NOY989	*mata ade2-1 ura3-1 trp1-1 leu2-3,112 his3-11 can1-100 rdn-LacR*	this study
y2036	NOY989	*mata ade2-1 ura3-1 trp1-1 leu2-3,112 his3-11 can1-100 rdn-1x601*	this study
y2037	NOY989	*mata ade2-1 ura3-1 trp1-1 leu2-3,112 his3-11 can1-100 rdn-2x601*	this study
y2038	NOY989	*mata ade2-1 ura3-1 trp1-1 leu2-3,112 his3-11 can1-100 rdn-TTF-I*	this study
y2039	NOY989	*mata ade2-1 ura3-1 trp1-1 leu2-3,112 his3-11 can1-100 rdn-TTF-I-INVERT*	this study
y2042	NOY989	*mata ade2-1 ura3-1 trp1-1 leu2-3,112 his3-11 can1-100 rdn-ENH*	this study
y2043	y2088	*mata trp1-1 his4-401 leu2-3,112 ura3-52 can1-100 RPA190::URA3 RPA12::NatMX RPA135-ProtA::KanMX pRS314-RPA190-pGAL-RPA12*	this study
y2044	y2088	*mata trp1-1 his4-401 leu2-3,112 ura3-52 can1-100 RPA190::URA3 RPA12::NatMX RPA135-ProtA::KanMX pRS314-rpa190 S685A-pGAL-RPA12*	this study
y2045	y2088	*mata trp1-1 his4-401 leu2-3,112 ura3-52 can1-100 RPA190::URA3 RPA12::NatMX RPA135-ProtA::KanMX pRS314-rpa190 S685D-pGAL-RPA12*	this study

y2050	y1599	*mat*a *ade2-1 ura3-1 trp1-1 leu2-3,112 his3-11 can1-100* rdn-WT REB1-MNase-3xHA::KanMX6	this study
y2051	y1599	*mat*a *ade2-1 ura3-1 trp1-1 leu2-3,112 his3-11 can1-100* rdn-WT FOB1-MNase-3xHA::KanMX6	this study
y2054	y2042	*mat*a *ade2-1 ura3-1 trp1-1 leu2-3,112 his3-11 can1-100* rdn-ENH REB1-MNase-3xHA::KanMX6	this study
y2055	y2042	*mat*a *ade2-1 ura3-1 trp1-1 leu2-3,112 his3-11 can1-100* rdn-ENH FOB1-MNase-3xHA::KanMX6	this study
y2056	y2038	*mat*a *ade2-1 ura3-1 trp1-1 leu2-3,112 his3-11 can1-100* rdn-TTF-I RPA190-MNase-3xHA::KanMX6	this study
y2088		*mat*a *trp1-1 his4-401 leu2-3,112 ura3-52 can1-100* RPA190::URA3 RPA12::NatMX pNOY20	this study
y2089	D101-I2	*mat*a *ade2-101 ura3-52 lys2-801 trp1-Δ63 his3-Δ200 leu2-Δ1* rpa43::LEU2 yCPA43 (URA3) RRN3-TEV-ProtA::kanMX6	this study
y2090	y1599	*mat*a *ade2-1 ura3-1 trp1-1 leu2-3,112 his3-11 can1-100* rdn-WT YDR026c-MNase-3xHA::KanMX6	this study
y2093	y2042	*mat*a *ade2-1 ura3-1 trp1-1 leu2-3,112 his3-11 can1-100* rdn-ENH YDR026c-MNase-3xHA::KanMX6	this study
y2094	y2042	*mat*a *ade2-1 ura3-1 trp1-1 leu2-3,112 his3-11 can1-100* rdn-ENH RPA190-MNase-3xHA::KanMX6	this study
y2229	y2276	*mat*a *ade2-1 ura3-1 trp1-1 leu2-3,112 his3-11 can1-100* rdn-WT *ydr026c::klTRP1* RPA190-MNase-3xHA::KanMX6	this study
y2231	y2275	*mat*a *ade2-1 ura3-1 trp1-1 leu2-3,112 his3-11 can1-100* rdn-WT *fob1::klTRP1* YDR026c-MNase-3xHA::KanMX6	this study
y2232	y2276	*mat*a *ade2-1 ura3-1 trp1-1 leu2-3,112 his3-11 can1-100* rdn-WT *ydr026c::klTRP1* FOB1-MNase-3xHA::KanMX6	this study
y2234	y2281	*mat*a *ade2-1 ura3-1 trp1-1 leu2-3,112 his3-11 can1-100* rdn-ENH *ydr026c::klTRP1* RPA190-MNase-3xHA::KanMX6	this study
y2236	y2280	*mat*a *ade2-1 ura3-1 trp1-1 leu2-3,112 his3-11 can1-100* rdn-ENH *fob1::klTRP1* YDR026c-MNase-3xHA::KanMX6	this study
y2237	y2281	*mat*a *ade2-1 ura3-1 trp1-1 leu2-3,112 his3-11 can1-100* rdn-ENH *ydr026c::klTRP1* FOB1-MNase-3xHA::KanMX6	this study
y2238	y2273	*mat*a *ade2-1 ura3-1 trp1-1 leu2-3,112 his3-11 can1-100* rdn-ENH T-rich FOB1-MNase-3xHA::KanMX6	this study
y2239	y2273	*mat*a *ade2-1 ura3-1 trp1-1 leu2-3,112 his3-11 can1-100* rdn-ENH T-rich YDR026c-MNase-3xHA::KanMX6	this study
y2240	y2274	*mat*a *ade2-1 ura3-1 trp1-1 leu2-3,112 his3-11 can1-100* rdn-ENH mut1 FOB1-MNase-3xHA::KanMX6	this study
y2241	y2274	*mat*a *ade2-1 ura3-1 trp1-1 leu2-3,112 his3-11 can1-100* rdn-ENH mut1 YDR026c-MNase-3xHA::KanMX6	this study
y2273	NOY989	*mat*a *ade2-1 ura3-1 trp1-1 leu2-3,112 his3-11 can1-100* rdn-ENH T-rich	this study
y2274	NOY989	*mat*a *ade2-1 ura3-1 trp1-1 leu2-3,112 his3-11 can1-100* rdn-ENH mut1	this study
y2275	y1599	*mat*a *ade2-1 ura3-1 trp1-1 leu2-3,112 his3-11 can1-100* rdn-WT *fob1::klTRP1*	this study

y2276	y1599	*mata ade2-1 ura3-1 trp1-1 leu2-3,112 his3-11 can1-100* rdn-WT *ydr026c::klTRP1*	this study
y2280	y2042	*mata ade2-1 ura3-1 trp1-1 leu2-3,112 his3-11 can1-100* rdn-ENH *fob1::klTRP1*	this study
y2281	y2042	*mata ade2-1 ura3-1 trp1-1 leu2-3,112 his3-11 can1-100* rdn-ENH *ydr026c::klTRP1*	this study
y2285	y2034	*mata ade2-1 ura3-1 trp1-1 leu2-3,112 his3-11 can1-100* rdn-LacR *Δrpa12*	this study
y2286	y2034	*mata ade2-1 ura3-1 trp1-1 leu2-3,112 his3-11 can1-100* rdn-LacR *Δrpa49*	this study
y2287	y2038	*mata ade2-1 ura3-1 trp1-1 leu2-3,112 his3-11 can1-100* rdn-TTF-I *Δrpa12*	this study
y2288	y2038	*mata ade2-1 ura3-1 trp1-1 leu2-3,112 his3-11 can1-100* rdn-TTF-I *Δrpa49*	this study
y2289	y2039	*mata ade2-1 ura3-1 trp1-1 leu2-3,112 his3-11 can1-100* rdn-TTF-I-INVERT *Δrpa12*	this study
y2290	y2039	*mata ade2-1 ura3-1 trp1-1 leu2-3,112 his3-11 can1-100* rdn-TTF-I-INVERT *Δrpa49*	this study
y2313	D101-l2	*mata ade2-101 ura3-52 lys2-801 trp1-Δ63 his3-Δ200 leu2-Δ1 rpa43::LEU2 pRS314-rpa43-S208/220/262/263A (TRP1)*	this study
y2314	D101-l2	*mata ade2-101 ura3-52 lys2-801 trp1-Δ63 his3-Δ200 leu2-Δ1 rpa43::LEU2 pRS314-rpa43-S208/220/262/263/285A (TRP1)*	this study
y2315	D101-l2	*mata ade2-101 ura3-52 lys2-801 trp1-Δ63 his3-Δ200 leu2-Δ1 rpa43::LEU2 pRS314-rpa43-S220/262/263D (TRP1)*	this study
y2316	D101-l2	*mata ade2-101 ura3-52 lys2-801 trp1-Δ63 his3-Δ200 leu2-Δ1 rpa43::LEU2 pRS314-rpa43-S208/220/262/263D (TRP1)*	this study
y2317	D101-l2	*mata ade2-101 ura3-52 lys2-801 trp1-Δ63 his3-Δ200 leu2-Δ1 rpa43::LEU2 pRS314-rpa43-S208/220/262/263/285D (TRP1)*	this study
y2323	NOY989	*mata ade2-1 ura3-1 trp1-1 leu2-3,112 his3-11 can1-100* rdn-5`-ENH fwd	this study
y2325	y2323	*mata ade2-1 ura3-1 trp1-1 leu2-3,112 his3-11 can1-100* rdn-5`-ENH fwd YDR026c-MNase-3xHA::KanMX6	this study
y2326	y2323	*mata ade2-1 ura3-1 trp1-1 leu2-3,112 his3-11 can1-100* rdn-5`-ENH fwd FOB1-MNase-3xHA::KanMX6	this study
y2327	NOY989	*mata ade2-1 ura3-1 trp1-1 leu2-3,112 his3-11 can1-100* rdn-5`-ENH rev	this study
y2329	y2327	*mata ade2-1 ura3-1 trp1-1 leu2-3,112 his3-11 can1-100* rdn-5`-ENH rev YDR026c-MNase-3xHA::KanMX6	this study
y2330	y2327	*mata ade2-1 ura3-1 trp1-1 leu2-3,112 his3-11 can1-100* rdn-5`-ENH rev FOB1-MNase-3xHA::KanMX6	this study
y2331	NOY989	*mata ade2-1 ura3-1 trp1-1 leu2-3,112 his3-11 can1-100* rdn-3`-ENH fwd	this study
y2333	y2331	*mata ade2-1 ura3-1 trp1-1 leu2-3,112 his3-11 can1-100* rdn-3`-ENH fwd YDR026c-MNase-3xHA::KanMX6	this study

y2334	y2331	*mat*a *ade2-1 ura3-1 trp1-1 leu2-3,112 his3-11 can1-100* rdn-3`-ENH fwd FOB1-MNase-3xHA::KanMX6	this study
y2335	NOY989	*mat*a *ade2-1 ura3-1 trp1-1 leu2-3,112 his3-11 can1-100* rdn-3`-ENH rev	this study
y2337	y2335	*mat*a *ade2-1 ura3-1 trp1-1 leu2-3,112 his3-11 can1-100* rdn-3`-ENH rev YDR026c-MNase-3xHA::KanMX6	this study
y2338	y2335	*mat*a *ade2-1 ura3-1 trp1-1 leu2-3,112 his3-11 can1-100* rdn-3`-ENH rev FOB1-MNase-3xHA::KanMX6	this study
Y2339	NOY989	*mat*a *ade2-1 ura3-1 trp1-1 leu2-3,112 his3-11 can1-100* rdn-ENH mut2	this study

5.1.2 *Escherichia coli* strains

Name	Genotype	Origin
XL1-blue	*endA1 gyrA96(nal^R) thi-1 recA1 relA1 lac glnV44 F'[::Tn10 proAB$^+$ lacI^q Δ(lacZ)M15] hsdR17(r$_K^-$ m$_K^+$)*	Stratagene
BL21 (DE3)	*F$^-$ ompT gal dcm lon hsdS$_B$(r$_B^-$ m$_B^-$) λ(DE3 [lacI lacUV5-T7 gene 1 ind1 sam7 nin5])*	Stratagene

5.1.3 Plasmids

#	Name	Gene	Marker	Features	Origin
48	YCplac22-pGAL		AmpR, TRP1	CEN4, ARS1	Hurt E.
230	YCplac111-pGAL		AmpR, Leu2	CEN4, ARS1	Milkereit P.
231	YCplac111-pGAL-FLAG		AmpR, Leu2	CEN4, ARS1	Milkereit P.
375	pT11	*rRNA*	AmpR		(Wild, 2005)
652	pKM18	*RPA190*	AmpR, KanMX6		Merz K.
774	pR3	*LEXA*	AmpR, LEU2	CEN4, ARS1	(Reiter, 2007)
825	pAG2.1	*REB1*	AmpR, KanMX6		Merz K.
839	pAG24	*FOB1*	AmpR, KanMX6		Griesenbeck J.
840	pAG25	*YDR026c*	AmpR, KanMX6		Griesenbeck J.
936	pAG36	kl. TRP1	AmpR		Griesenbeck J.
1785	pT11-WT	*rRNA*	AmpR		this study
1786	pT11-3xLexA	*rRNA*	AmpR		this study
1787	pT11-TTF1	*rRNA*	AmpR		this study
1788	pT11-TTF1-invert	*rRNA*	AmpR		this study
1789	pT11-1x LacI	*rRNA*	AmpR		this study
1791	pT11-1x 601	*rRNA*	AmpR		this study

1792	pT11-2x 601	*rRNA*	AmpR		this study
1793	pT11-ENH	*rRNA*	AmpR		this study
1794	pT11-5`-ENH fwd	*rRNA*	AmpR		this study
1795	pT11-5`-ENH rev	*rRNA*	AmpR		this study
1796	pT11-3`-ENH fwd	*rRNA*	AmpR		this study
1797	pT11-3`-ENH rev	*rRNA*	AmpR		this study
1798	pT11-ENH-T-rich	*rRNA*	AmpR		this study
1800	pT11-ENH-mut1	*rRNA*	AmpR		this study
1801	pT11-ENH-mut2	*rRNA*	AmpR		this study
1802	YCplac111-pGAL-FOB1	*FOB1*	AmpR, LEU2	CEN4, ARS1	this study
1803	YCplac111-pGAL-YDR026c	*YDR026c*	AmpR, LEU2	CEN4, ARS1	this study
1804	YCplac111-pGAL-REB1	*REB1*	AmpR, LEU2	CEN4, ARS1	this study
1805	YCplac111-pGAL-LexA	*LEXA*	AmpR, LEU2	CEN4, ARS1	this study
1806	YCplac111-pGAL-LexA-MNase	*LEXA*	AmpR, LEU2	CEN4, ARS1	this study
1807	YCplac111-pGAL-TTF-I	*TTF-I*	AmpR, LEU2	CEN4, ARS1	this study
1808	YCplac111-pGAL-TTF-I-MNase	*TTF-I*	AmpR, LEU2	CEN4, ARS1	this study
1809	YCplac111-pGAL-LacI	*LACI*	AmpR, LEU2	CEN4, ARS1	this study
1810	YCplac111-pGAL-LacI-MNase	*LACI*	AmpR, LEU2	CEN4, ARS1	this study
1811	pRS314-rpa43 (S208D)	*RPA43*	AmpR, TRP1	CEN6, ARSH4	this study
1812	pRS314-rpa43 (S220D)	*RPA43*	AmpR, TRP1	CEN6, ARSH4	this study
1813	pRS314-rpa43 (S262D)	*RPA43*	AmpR, TRP1	CEN6, ARSH4	this study
1814	pRS314-rpa43 (S263D)	*RPA43*	AmpR, TRP1	CEN6, ARSH4	this study
1815	pRS314-rpa43 (S262/263D)	*RPA43*	AmpR, TRP1	CEN6, ARSH4	this study
1816	pRS314-rpa43 (S285D)	*RPA43*	AmpR, TRP1	CEN6, ARSH4	this study
1817	pRS314-rpa43 (S262/285D)	*RPA43*	AmpR, TRP1	CEN6, ARSH4	this study
1818	pRS314-rpa43 (S208/220/262/263A)	*RPA43*	AmpR, TRP1	CEN6, ARSH4	this study
1819	pRS314-rpa43 (S208/220/262/263/285A)	*RPA43*	AmpR, TRP1	CEN6, ARSH4	this study
1820	pRS314-rpa43 (S220/262/263D)	*RPA43*	AmpR, TRP1	CEN6, ARSH4	this study
1821	pRS314-rpa43 (S208/220/262/263D)	*RPA43*	AmpR, TRP1	CEN6, ARSH4	this study

1822	pRS314-rpa43 (S208/220/262/263/285D)	*RPA43*	AmpR, TRP1	CEN6, ARSH4	this study
1823	pRS314-rpa43 (S48A)	*RPA43*	AmpR, TRP1	CEN6, ARSH4	this study
1824	pRS314-rpa43 (S141A)	*RPA43*	AmpR, TRP1	CEN6, ARSH4	this study
1825	pRS314-rpa43 (S143A)	*RPA43*	AmpR, TRP1	CEN6, ARSH4	this study
1826	pRS314-rpa43 (S141/143A)	*RPA43*	AmpR, TRP1	CEN6, ARSH4	this study
1827	pRS314-rpa43 (S156A)	*RPA43*	AmpR, TRP1	CEN6, ARSH4	this study
1828	pRS314-rpa43 (S213A)	*RPA43*	AmpR, TRP1	CEN6, ARSH4	this study
1829	pRS314-rpa43 (S244A)	*RPA43*	AmpR, TRP1	CEN6, ARSH4	this study
1830	pRS314-rpa43 (S48D)	*RPA43*	AmpR, TRP1	CEN6, ARSH4	this study
1831	pRS314-rpa43 (S141D)	*RPA43*	AmpR, TRP1	CEN6, ARSH4	this study
1832	pRS314-rpa43 (S143D)	*RPA43*	AmpR, TRP1	CEN6, ARSH4	this study
1833	pRS314-rpa43 (S141/143D)	*RPA43*	AmpR, TRP1	CEN6, ARSH4	this study
1834	pRS314-rpa43 (S156D)	*RPA43*	AmpR, TRP1	CEN6, ARSH4	this study
1835	pRS314-rpa43 (S213D)	*RPA43*	AmpR, TRP1	CEN6, ARSH4	this study
1836	pRS314-rpa43 (S244D)	*RPA43*	AmpR, TRP1	CEN6, ARSH4	this study
1837	pCM182-Leu		AmpR, LEU2	CEN4, ARS1	this study
1838	pCM182-Leu-RPA12	*RPA12*	AmpR, LEU2	CEN4, ARS1	this study
1839	pCM182-Leu-rpa12 (1-69) (rpa12ΔC)	*RPA12*	AmpR, LEU2	CEN4, ARS1	this study
1840	pCM182-Leu-rpa12 (69-125) (rpa12ΔN)	*RPA12*	AmpR, LEU2	CEN4, ARS1	this study
1841	YCplac111-pGAL-RPA12	*RPA12*	AmpR, LEU2	CEN4, ARS1	(Gerber, 2008)
1842	YCplac111-pGAL-rpa12 (D105A)	*RPA12*	AmpR, LEU2	CEN4, ARS1	this study
1843	YCplac111-pGAL-rpa12 (E106A)	*RPA12*	AmpR, LEU2	CEN4, ARS1	this study
1844	YCplac111-pGAL-rpa12 (DE/AA)	*RPA12*	AmpR, LEU2	CEN4, ARS1	(Gerber, 2008)
1845	YCplac111-pGAL-FLAG-RPA12	*RPA12*	AmpR, LEU2	CEN4, ARS1	this study
1846	YCplac111-pGAL-FLAG-rpa12 (D105A)	*RPA12*	AmpR, LEU2	CEN4, ARS1	this study
1847	YCplac111-pGAL-FLAG-rpa12 (E106A)	*RPA12*	AmpR, LEU2	CEN4, ARS1	this study
1848	YCplac111-pGAL-FLAG-rpa12 (DE/AA)	*RPA12*	AmpR, LEU2	CEN4, ARS1	this study

1849	YCplac111-pGAL-RPA12-FLAG	*RPA12*	AmpR, LEU2	CEN4, ARS1	this study
1850	YCplac111-pGAL-rpa12 (DE/AA)-FLAG	*RPA12*	AmpR, LEU2	CEN4, ARS1	this study
1861	pRS314-RPA190-pGAL-RPA12	*RPA190, RPA12*	AmpR, TRP1	CEN6, ARSH4	this study
1862	pRS314-rpa190-S685A-pGAL-RPA12	*RPA190, RPA12*	AmpR, TRP1	CEN6, ARSH4	this study
1863	pRS314-rpa190-S685D-pGAL-RPA12	*RPA190, RPA12*	AmpR, TRP1	CEN6, ARSH4	this study
1864	YCplac22-pGAL-RPA43	*RPA43*	AmpR, TRP1	CEN4, ARS1	this study
1865	YCplac22-pGAL-rpa43 (S141/143A)	*RPA43*	AmpR, TRP1	CEN4, ARS1	this study
1866	YCplac22-pGAL-rpa43 (S141/143D)	*RPA43*	AmpR, TRP1	CEN4, ARS1	this study
1867	YCplac22-pGAL-FLAG		AmpR, TRP1	CEN4, ARS1	this study
1868	YCplac22-pGAL-FLAG-RPA43	*RPA43*	AmpR, TRP1	CEN4, ARS1	this study
1869	YCplac22-pGAL-FLAG-rpa43 (S141/143A)	*RPA43*	AmpR, TRP1	CEN4, ARS1	this study
1870	YCplac22-pGAL-FLAG-rpa43 (S141/143D)	*RPA43*	AmpR, TRP1	CEN4, ARS1	this study
1871	YCplac22-pGAL-RPA43-FLAG	*RPA43*	AmpR, TRP1	CEN4, ARS1	this study
1872	YCplac22-pGAL-rpa43 (S141/143A)-FLAG	*RPA43*	AmpR, TRP1	CEN4, ARS1	this study
1873	YCplac22-pGAL-rpa43 (S141/143D)-FLAG	*RPA43*	AmpR, TRP1	CEN4, ARS1	this study
1874	pET21b-A14/A43	*RPA14, RPA43*	AmpR	pBR322 origin, f1 origin	(Geiger et al., 2008)
1876	pET21b-A14/A43 (S141/143A)	*RPA14, RPA43*	AmpR	pBR322 origin, f1 origin	this study
1877	pET21b-A14/A43 (S141/143D)	*RPA14, RPA43*	AmpR	pBR322 origin, f1 origin	this study
1884	pRS314-RPA43-pGAL-RPA43	*RPA43*	AmpR, TRP1	CEN6, ARSH4	this study
1885	pRS314-rpa43 (S141/143A) -pGAL-RPA43	*RPA43*	AmpR, TRP1	CEN6, ARSH4	this study
1886	pRS314-rpa43 (S141/143D)-pGAL-RPA43	*RPA43*	AmpR, TRP1	CEN6, ARSH4	this study

1887	pRS314-RPA43-pGAL-FLAG-RPA43	*RPA43*	AmpR, TRP1	CEN6, ARSH4	this study
1888	pRS314-rpa43 (S141/143A)-pGAL-FLAG-RPA43	*RPA43*	AmpR, TRP1	CEN6, ARSH4	this study
1889	pRS314-rpa43 (S141/143D)-pGAL-FLAG-RPA43	*RPA43*	AmpR, TRP1	CEN6, ARSH4	this study
	pRset-deltaNTTF	*TTF-I*	AmpR	pUC ori, f1 origin	(Németh et al., 2004)

5.1.4 Oligonucleotides

#	Name	Sequence	Gene/locus
683	No6	TCCGTATTTTCCGCTTCCGC	rDNA
698	fob1_A	TTCATCATACCTAACATTGTGATCG	*FOB1*
710	M1	TGGAGCAAAGAAATCACCGC	rDNA
711	M2	CCGCTGGATTATGGCTGAAC	rDNA
712	M3	GAGTCCTTGTGGCTCTTGGC	rDNA
713	M4	AATACTGATGCCCCCGACC	rDNA
817	rDNA-709_for	GAGGGACGGTTGAAAGTG	rDNA
818	rDNA-461_rev	ATACGCTTCAGAGACCCTAA	rDNA
920	5S ChIP-F1	GCCATATCTACCAGAAAGCACC	5S
921	5S ChIP-R1	GATTGCAGCACCTGAGTTTCG	5S
969	Prom ChIP-F2	TCATGGAGTACAAGTGTGAGGA	rDNA
970	Prom ChIP-R1	TAACGAACGACAAGCCTACTC	rDNA
1049	R25	GCTTAGAGAAGGGGGCAACT	rDNA
1056	fob1_D	GCCTCTTGTAATATTGTTCAAGGAA	*FOB1*
1064	3_LEXA_up	CAGATATCCTTAAGGCCGAAAGATTAAAATCAACG	LexA-BS
1065	3_LEXA_down	CAGATATCCTTAAGCGGGTCGACTCTAGAGGATCT	LexA-BS
1191	Kpn_sonde_up	TGAGCGTCATTTCCTTCTCA	rDNA
1192	Kpn_sonde_down	ATCCCGGTTGGTTTCTTTTC	rDNA
1199	RPA49for	GCATAGAATAAGAACTTGACC	*RPA49*
1200	RPA49rev	TCACCTATATAACACGTTGG	*RPA49*
1203	RPA135-pYM-for	CTATCCGCAATGGGTATAAGATTGCGTTATAATGTAGAGCCCAAACGTACGCTGCAGGTCGAC	pYM

1204	RPA135-pYM-rev	CCTTCATTTACCATTCTATATCAATTTGGAAAGA AGGGTATTTCTATCGATGAATTCGAGCTC	pYM
1600	Mnase-lexa-for-1	ATTCAAGCTGTACAGTACATATGTCGTACGCTG CAGG	MNase (pKM9)
1601	Mnase-lexa-rev	ATTCAAGCTGTACAGTACATATGTCGTACGCTG CAGG	MNase (pKM9)
1603	RPA43-down	CTACGTATGCAGGACTATTGAT	*RPA43*
1604	RPA43-208-Asp-up	GGGCAAATTTGACTTTGGAAAC	*RPA43*
1605	RPA43-208-Asp-do	GTTTCCAAAGTCAAATTTGCCC	*RPA43*
1606	RPA43-220-Asp-up	CTGGGTAGATGATAATGGTGAA	*RPA43*
1607	RPA43-220-Asp-do	TTCACCATTATCATCTACCCAG	*RPA43*
1608	RPA43-262-Asp-up	ATGGCTATAACGACTCTCGTTC	*RPA43*
1609	RPA43-262-Asp-do	GAACGAGAGTCGTTATAGCCAT	*RPA43*
1610	RPA43-263-Asp-up	CTATAACAGCGATCGTTCCCAA	*RPA43*
1611	RPA43-263-Asp-do	TTGGGAACGATCGCTGTTATAG	*RPA43*
1612	RPA43-262/63-Asp-up	GCTATAACGACGATCGTTCCCA	*RPA43*
1613	RPA43-262/63-Asp-do	TGGGAACGATCGTCGTTATAGC	*RPA43*
1614	RPA43-285-Asp-up	GACGAAGTTGATATCGAAAAC	*RPA43*
1615	RPA43-285-Asp-do	GTTTTCGATATCAACTTCGTC	*RPA43*
1617	RPA43-262/63-Ala-up	GCTATAACGCCGCTCGTTCCCA	*RPA43*
1618	RPA43-262/63-Ala-do	TGGGAACGAGCGGCGTTATAGC	*RPA43*
1619	RPA43-285-Ala-up	GACGAAGTTGCAATCGAAAAC	*RPA43*
1620	RPA43-285-Ala-do	GTTTTCGATTGCAACTTCGTC	*RPA43*
1621	A190-AhdI-up	AGATGGTAAGCCCTCCCGTAT	*RPA190*
1622	A190-EcoRI-up	CAAGCTCGGAATTCACCCTCACTAAA	*RPA190*
1623	A190-EcoRI-do	TTTAGTGAGGGTGAATTCCGAGCTTG	*RPA190*
1624	A190-BamHI-do	CCGTAGGATTGGTAATTTGCT	*RPA190*
1626	A43-S48Ala-up	CTCTATGTTGCTTTGGCACCAA	*RPA43*
1627	A43-S48Ala-do	TTGGTGCCAAAGCAACATAGAG	*RPA43*
1628	A43-S48Asp-up	CTCTATGTTGATTTGGCACCAA	*RPA43*
1630	A43-S141Ala-up	TTTCATTCAAGCCGCCTCACAC	*RPA43*
1631	A43-S141Ala-do	GTGTGAGGCGGCTTGAATGAAA	*RPA43*
1632	A43-S141Asp-up	TTTCATTCAAGACGCCTCACAC	*RPA43*
1634	A43-S143Ala-up	TCAATCCGCCGCACACATTGGT	*RPA43*

1635	A43-S143Ala-do	ACCAATGTGTGCGGCGGATTGA	*RPA43*
1636	A43-S143Asp-up	TCAATCCGCCGATCACATTGGT	*RPA43*
1638	A43-S141/43Ala-up	CATTCAAGCCGCCGCACACATT	*RPA43*
1639	A43-S141/43Ala-do	AATGTGTGCGGCGGCTTGAATG	*RPA43*
1640	A43-S141/43Asp-up	CATTCAAGACGCCGATCACATT	*RPA43*
1642	A43-S156Ala-up	GTTTAATGCTGCTATCAAAAAG	*RPA43*
1643	A43-S156Ala-do	CTTTTTGATAGCAGCATTAAAC	*RPA43*
1644	A43-S156Asp-up	GTTTAATGCTGATATCAAAAAG	*RPA43*
1646	A43-S213Ala-up	TGGAAACAGAGCTTTGGGCCAC	*RPA43*
1647	A43-S213Ala-do	GTGGCCCAAAGCTCTGTTTCCA	*RPA43*
1648	A43-S213Asp-up	TGGAAACAGAGATTTGGGCCAC	*RPA43*
1650	A43-S244Ala-up	AAGAGTTGTTGCTGTGGACGGT	*RPA43*
1651	A43-S244Ala-do	ACCGTCCACAGCAACAACTCTT	*RPA43*
1652	A43-S244Asp-up	AAGAGTTGTTGATGTGGACGGT	*RPA43*
1729	FOB1_KO_f	TTAAGCCTTCAGGGGGGAGAACAATTTAACGAT TGTGTGAGTGTGAATTTCGTACGCTGCAGGTCG AC	*klTRP1*
1731	YDR026C_KO_f	AGAGCAAGCAGCCGTTTCTTGTCTGCGTCAAGA AGAAAGATAAAGGTAGACGTACGCTGCAGGTC GAC	*klTRP1*
1738	YDR026C_A	TGAAGAAATGATCAAACAATGAAGA	*YDR026c*
1739	YDR026C_D	AGCTGGTTATGAATCAGCATAAGAC	*YDR026c*
1745	FOB1_r	CTACCGCGGTTTTTTTTTCACCTATGGTGACTCC TCCTTTCATTCTATCCTACATATTAATCGATGAA TTCGAGCTCG	*klTRP1*
1747	YDRC026C_r	CTACCGCGGAATATGCTTTTATCTATTGGGTCTG TATATGTTTGGGAAAGTAACCCTTCATCGATGA ATTCGAGCTCG	*klTRP1*
2099	5S_probe_fwd	TGTCCTCCACCCATAACACC	rDNA
2100	5S_probe_rev	ATTTAGCATAGGAAGCCAAG	rDNA
2731	Flag-up	CCCCGGATCGGATCCATGTCTGTT	*RPA12*
2732	Flag-do	CCTTGCATGCTCACTTATCGTCGTCATCCTTGTA ATCATTGTTGGTACGGAACTTGTAACC	*RPA12*
2733	Ndel-up	GCAAGGATACGATCTGATCATATGC	*RPA43*
2734	S48D-do	ACATTGGTGCCAAATCAACATAGAG	*RPA43*
2735	S141D-do	AATGTGTGAGGCGTCTTGAATGAAA	*RPA43*
2736	S143D-do	AAGACCAATGTGATCGGCGGATTGA	*RPA43*
2737	S141/43D-do	ACCAATGTGATCGGCGTCTTGAATG	*RPA43*

2738	S156D-do	ATTCTTTTTGATATCAGCATTAAAC	*RPA43*
2739	S213D-do	CCAGTGGCCCAAATCTCTGTTTCCA	*RPA43*
2740	S244D-do	TGTACCGTCCACATCAACAACTCTT	*RPA43*
2744	A43-pET-do	CAACGTCAAAGGGCGAAAAACC	*RPA43*
2745	A43-141/43A-do	ACCAATGTGTGCGGCGGCTTGAATG	*RPA43*
2746	A43-141/43D-do	AGACCAATGTGATCGGCGTCTTGAATGAA	*RPA43*
2748	A43-pET-up1	CGAGATCTCGATCCCGCGAAATTAATAC	*RPA43*
2759	A43-BamHI-up	CGGATCGGATCCATGTCACAAGTAAAAAG	*RPA43*
2760	A43-SphI-do	CCGTAGCATGCCTACTAATCACTATCACTCG	*RPA43*
2761	A43-Flag-do	CCTTGCATGCTCACTTATCGTCGTCATCCTTGTA ATCATCACTATCACTCGATTCACCAT	*RPA43*
2764	A12-up-BamHI	CGGATCGGATCCATGTCTGTTGTA	*RPA12*
2765	A12-D105A-up	TAAGATCTGCAGCTGAAGGTGCTAC	*RPA12*
2766	A12-D105A-do	GTAGCACCTTCAGCTGCAGATCTTA	*RPA12*
2767	A12-E106A-up	GATCTGCAGATGCAGGTGCTACTGT	*RPA12*
2768	A12-E106A-do	ACAGTAGCACCTGCATCTGCAGATC	*RPA12*
2769	A12-do-SphI	ATTACGCCAAGCTTGCATGCGGAT	*RPA12*
2770	A12-up-new	AAGTGAAGGGCATTGCATGGCAA	*RPA12*
2771	A12-do-new	GATGTTCACATGATGAAAGCGGG	*RPA12*
2794	A12-69/125-BamHI-up	GATGCGGATCCATGTCTTTGAAGAAGAACGAA CTGAAA	*RPA12*
2797	601-up-AflII	GATGCACTTAAGGAATTCGAGCTCGGTACCCG GGTG	601-NPS
2798	601-do-AflII	GATGCACTTAAGGGATCCCCGGGATGTATATAT CTGA	601-NPS
2801	1xTTF1-up-AflII	TTAAGACTTCGGAGGTCGACCAGTACTCCGC	TTF-I-BS
2802	1xTTF1-do-AflII	TTAAGCGGAGTACTGGTCGACCTCCGAAGTC	TTF-I-BS
2803	1xlacR-up-AflII	TTAAGTGTGGAATTGTGAGCGGATAACAATTTC ACAC	LacR-BS
2804	1xlacR-do-AflII	TTAAGTGTGAAATTGTTATCCGCTCACAATTCCA CAC	LacR-BS
2807	A12-1/69-NotI-do	GATGCGCGGCCGCTCAAGTTTTAACCACGGATT TCTTGGCTCT	*RPA12*
2808	A12-69/125-NotI-do	GATGCGCGGCCGCTCAACAACCCAATCAATTGT TGGTACGGAA	*RPA12*
2811	Enh-AflII-up	GATGCACTTAAGAATTCTATGATCCGGGTAAAA ACA	rDNA
2814	RFB-AflII-do	GATGCACTTAAGTCAATTCTCTAAACTTATACAA G	rDNA

100

2815	pLacI-BamHI-up	GATGCGGATCCATGGTGAAACCAGTAACGTTAT ACGAT	*LacI*
2816	pLacI-XbaI-do	GATGCTCTAGACTGCCCGCTTTCCAGTCGGGAA AC	*LacI*
2817	MNase-XbaI-up	GATGCTCTAGAGAATTCAAAATGCCCAAGAAG AAG	MNase
2818	MNase-SbfI-do	GATGCCCTGCAGGTCATTACCGGTAGCGTAGTC TGGAACG	MNase
2820	dNTTF1-BamHI-up	GATGCGGATCCATGGAGAGCACCAAAGAATCC CACAGT	TTF-I (pRset-deltaNTTF)
2821	dNTTF1-XbaI-do	GATGCTCTAGACTGCACATCAGAGGCGCTGGG CTC	TTF-I (pRset-deltaNTTF)
2825	A43-PstI-DO	GATGCCTGCAGATCACTATCACTCGATTCACCA TC	*RPA43*
2826	A43-PstI-stop-DO	GATGCCTGCAGCTAATCACTATCACTCGATTCA CCATC	*RPA43*
2827	pLacI-XbaI-stop	GATGCTCTAGATCACTGCCCGCTTTCCAGTCGG GAAAC	*LacI*
2828	dNTTF1-XbaI-stop	GATGCTCTAGATCACTGCACATCAGAGGCGCTG GGCTC	TTF-I (pRset-deltaNTTF)
2829	LexA-BamHI-up	GATGCGGATCCATGAAAGCGTTAACGGCCAGG CAA	pR3
2830	LexA-XbaI-stop	GATGCTCTAGATCACAGCCAGTCGCCGTTGCGA ATAA	pR3
2832	SOE-NheI-up	CGAGACCTTAACCTACTAAATAGTG	rDNA
2833	SOE-XhoI-do	AACCCTCACTAAAGGGAACAAAAGCT	rDNA
2836	Reb1-BS-a-up	AATTCTATGATCCTTGTAAAAACATGT	rDNA
2837	Reb1-BS-a-do	ACATGTTTTTACAAGGATCATAGAATT	rDNA
2838	Reb1-BS-b-up	ATGATCCGGGTAACCCCATGTATTGTA	rDNA
2839	Reb1-BS-b-do	TACAATACATGGGGTTACCCGGATCAT	rDNA
2840	FOB1-Bam-up	GATGCGGATCCATGACGAAACCGCGTTACAAT GACGT	*FOB1*
2841	FOB1-Xba-do	GATGCTCTAGATCATTATTACAATTCCATTGATG TGCCAA	*FOB1*
2842	YDR026c-Bam-up	GATGCGGATCCATGGACAGCGTGTCAAACCTTA AGAG	*YDR026c*
2843	YDR026c-Xba-do	GATGCTCTAGATCATTAATTGATTTGTTCCAACA ATGAA	*YDR026c*
2847	E-T-rich-do	ACAAATAAAATTTATAGAGACCGCAGGCCCGG CTGGACTCTCCATC	rDNA
2848	E-T-rich-up	GTCTCTATAAATTTTATTTGTCTTAAGAATTCTAT GATCCGGGTAA	rDNA

101

2851	GAL-EcoRI-up	CAGTGAATTCTTATATTGAATTTTC	*GAL1*
2852	A43-Xho-do	GACACTCGAGCTAATCACTATCACTCGATTCAC CAT	*RPA43*
2863	R25-rev-q	CGGCTGGACTCTCCATCTCT	rDNA
2864	IGS2-up-q	GCATGCCTGTTTGAGCGTC	rDNA
2865	IGS2-do-q	CGACCGTACTTGCATTATACC	rDNA
2874	REB1-prom-do1	CCGAGATCATATCACTGTGG	pT11
2877	Enh-AflII-do2	GATGCACTTAAGGTAACTTACATACATTAGTAA ATGG	rDNA
2878	RFB-AflII-up2	GATGCACTTAAGTTCGTTGCAAAGATGGGTTGA AAG	rDNA
2879	RFB-AflII-do2	GATGCACTTAAGTGTTAACTATAGGAAATGAGC TTTT	rDNA
2882	25S-Jo-up	ATCATTTGTATACGACTTAGATGTACAACG	rDNA
2883	25S-Jo-do	AACAAATCAGACAACAAAGGCTTAATC	rDNA
2884	3`-REB-Jo-up	TACGATGAGGATGATAGTGTGTAAGAGTG	rDNA
2885	3`-REB-Jo-do	TACGATGAGGATGATAGTGTGTAAGAGTG	rDNA
2886	Fob-bs-Jo-up	GAGAAAAGCTCATTTCCTATAGTTAACAG	rDNA
2887	Fob-bs-Jo-do	TTCACTTGTCTCTTACATCTTTCTTGG	rDNA
2997	REB1-TER-do	CACTCTTACACACTATCATCCTCATCGTA	rDNA
2998	REB1-TER-up	GCCTAGTTTAGAGAGAAGTAGACTGAACA	rDNA

5.1.5 Southern Probes

Name	Synthesis	Locus	Restriction enzyme	Fragment size
KpnI-probe	PCR from genomic DNA using primers #1191/#1192	rDNA	KpnI	10.3kb
25S-18S-probe	NcoI digestion of pNOY373 and purification of a 3.4kb fragment	rDNA	EcoRI	3.4kb
5S-probe	PCR from genomic DNA using primers #2099/#2100	rDNA	AlwNI	5.4kb
XcmI-prom-probe	PCR from genomic DNA using primers #817/#818	rDNA	XcmI	4.9kb

5.1.6 Northern probes

#	Name	Sequence
204	o1-5'A0	GGTCTCTCTGCTGCCGG
205	o2-18S	CATGGCTTAATCTTTGAGAC
212	o9-25S	CTCCGCTTATTGATATGC
1819	ext_ITS1_2	GTAAAAGCTCTCATGCTCTTGCC
2880	AflIII-A2-probe1	ACTTACAAGCCTAGCAAGACCG

5.1.7 Antibodies

Antibody	Species	Dilution	Origin
α-A43	rabbit	1:50000	A. Sentenac, Paris (Buhler et al., 1980)
α-A135	rabbit	1:50000	A. Sentenac, Paris (Buhler et al., 1980)
α-HA (3F10)	rat	1:5000	Roche
α-mouse IgG (H+L) (peroxidase-conjugated)	goat	1:5000	Jackson IR/Dianova
α-rabbit IgG (H+L) (peroxidase-conjugated)	goat	1:5000	Jackson IR/Dianova
α-rat IgG+IgM (H+L) (peroxidase-conjugated)	goat	1:5000	Jackson IR/Dianova
PAP (peroxidase anti-peroxidase)	rabbit	1:5000	DakoCytomation

5.1.8 Enzymes

Enzyme	Origin
Antarctic Phosphatase	New England Biolabs
HotStarTaq DNA Polymerase	Qiagen
iProof High-Fidelity DNA Polymerase	Bio-Rad
Restriction Endonucleases	New England Biolabs
T4 DNA Ligase	New England Biolabs
Taq DNA Polymerase	New England Biolabs
Go Taq DNA Polymerase	Promega
Trypsin, sequencing grade	Roche
RNase A	Invitrogen
Proteinase K	Sigma-Aldrich
Zymolyase 100T	Seikagaku Corporation

5.1.9 Kits

Kit	Origin
PureLink™ PCR Purification Kit	Invitrogen
PureLink™ Quick Gel Extraction Kit	Invitrogen
PureLink™ Quick Plasmid Miniprep Kit	Invitrogen
RadPrime DNA Labeling System	Invitrogen

5.1.10 Media

Medium	Composition
YPD (yeast extract, peptone, dextrose)	1% (w/v) yeast extract 2% (w/v) peptone 2% (w/v) glucose
YPD+gen/+hyg (YPD plus geneticin/hygromycin B)	YPD + 200 µg/ml geneticin (G418) / + 300 µg/ml hygromycin B
YPAD (YPD plus adenine)	YPD + 100 mg/l adenine
YPUD (YPD plus uracil)	YPD + 2 mg/ml uracil

YPD+dox (YPD plus doxycycline)	YPD + 10 µg/ml doxycycline 2% (w/v) agar
YPG (yeast extract, peptone, galactose)	1% (w/v) yeast extract 2% (w/v) peptone 2% (w/v) galactose
YPUG (YPG plus uracil)	YPG + 2 mg/ml uracil
YPG+gen/+hyg (YPG plus geneticin/hygromycin B)	YPG + 200 µg/ml geneticin (G418) / + 300 µg/ml hygromycin B
YPG+dox (YPG plus doxycycline)	YPG + 10 µg/ml doxycycline 2% (w/v) agar
SCD (synthetic complete dextrose)	0.67% (w/v) YNB + nitrogen 0.062% (w/v) CSM-his-leu-trp 2% (w/v) glucose + 20 mg/l L-histidine + 100 mg/l L-leucine + 50 mg/l L-tryptophan
SCD-leu/-trp (SCD minus leucine/tryptophan)	0.67% (w/v) YNB + nitrogen 0.062% (w/v) CSM-his-leu-trp 2% (w/v) glucose + 20 mg/l L-histidine + 50 mg/l L-tryptophan / + 100 mg/l L-leucine
SCD-arg-trp	0.67% (w/v) YNB + nitrogen 0,006% (w/v) CSM-arg-his-lys-trp-ura 2% (w/v) glucose + 20 mg/l L-histidine + 50 mg/l L-lysine + 20 mg/l uracil
SCD-arg-trp + CAN	SCD-arg-trp + 6 mg/l L-canavanine
SCD-leu+5FOA (SCD minus leucin plus 5-FOA)	SCD-leu + 0.1% (w/v) 5-FOA
SCD-trp+5FOA (SCD minus tryptophan plus 5-FOA)	SCD-trp + 0.1% (w/v) 5-FOA
SCG (synthetic complete galactose)	0.67% (w/v) YNB + nitrogen 0.062% (w/v) CSM-his-leu-trp 2% (w/v) galactose + 20 mg/l L-histidine + 100 mg/l L-leucine + 50 mg/l L-tryptophan

SCG-leu (SCG minus leucine)	0.67% (w/v) YNB + nitrogen 0.062% (w/v) CSM-his-leu-trp 2% (w/v) galactose + 20 mg/l L-histidine + 50 mg/l L-tryptophan
SCR (synthetic complete raffinose)	0.67% (w/v) YNB + nitrogen 0.13% AAM-leu-ura-his + 100 mg/l L-leucine + 20 mg/l L-uracil + 20 mg/l L-histidine + 2% (w/v) raffinose
SCR-leu (SCR minus leucine)	0.67% (w/v) YNB + nitrogen 0.13% AAM-leu-ura-his + 20 mg/l L-uracil + 20 mg/l L-histidine + 2% (w/v) raffinose
SCR-leu+gal (SCR minus leucine plus galactose)	SCR-leu + 2% (w/v) galactose
LB (luria broth)	1% (w/v) tryptone 0.5% (w/v) yeast extract 0.5% (w/v) NaCl
LB+amp (LB plus ampicillin)	LB + 100 µg/ml ampicillin

The solvent is H_2O, if not indicated otherwise. The pH values were measured at room temperature (RT).

5.1.11 Buffers

Buffer	Ingredients	Concentration
5x TBE buffer	Tris	445mM
	Boric acid	445mM
	EDTA	10mM
10x DNA loading buffer	Bromphenol blue	0,25%
	Xylen cyanol	0,25%
	Glycerine	40%
10x MOPS buffer	Sodium acetate trihydrate	20mM
	MOPS (Fluka)	0,2M
	EDTA pH8	10mM
	pH7 with NaOH	

MATERIAL AND METHODS

RNA hybridisation buffer	Formamide deionised	50%
	SSC	5x
	SDS	0,5%
	H_2O	10%
	Denhards	5x
50x Denhards	Ficoll (Typ 400)	10 mg/ml
	Polyvinylpyrolidone	10 mg/ml
	BSA (Fraction 5)	10 mg/ml
	Store at -20°C	
RNA solubilisation buffer	Formamide	50%
	Formaldehyde	8%
	MOPS buffer	1x
	H_2O	18%
Buffer R	Glucose	2%
	Peptone	1%
	Malt extract	0,6%
	Yeast extract	0,01%
	Mannitol	12%
	Magnesium acetate	17,8mM
20x SSC	NaCl	3M
	Tri-sodium citrate dehydrate	0,3M
	pH7 with HCl	
Protease inhibitors 100x	Benzamidine	33 mg/ml
	PMSF	17 mg/ml
10x Electrophoresis buffer	Tris	250mM
	Glycine	192mM
	SDS	1%
Transfer buffer (Western Blot)	Tris	25mM
	Glycine	192mM
	Methanol	20%
4x Upper Tris	Tris	0,5M
	SDS	0,4%
	Bromphenol blue	
	pH 6,8 with HCl	
4x Lower Tris	Tris	1,5M
	SDS	0,4%
	pH 8,8 with HCl	
HU buffer	SDS	5%
	Tris-HCl pH 6,8	200mM
	EDTA	1mM
	β-mercapto-ethanol	1,5%
	Urea	8M
	Bromphenol blue, store at -20°C	
TELit	LiOAc	100mM
	Tris-HCl pH 8	10mM
	EDTA pH 8	1mM
	pH 8 with HOAc	

LitSorb	Sorbitol	1M
	Dissolved in TELit	
	sterile filtration, store at 4°C	
Buffer A200	Tris-HCl pH 8	20mM
	KCl	200mM
	MgAc	5mM
	Triton X-100	0,2%
	DTT	1mM
	Protease inhibitors	1x
Buffer MB	Tris-HCl pH 8	20mM
	KCl	200mM
	MgAc	5mM
	Protease inhibitors	1x
AE buffer	NaOAc pH 5,3	50mM
	EDTA pH 8	10mM
	Xylene cyanol FF (Sigma)	0,025%
	Bromphenole blue	0,025%
5x MaBS	Maleic acid	0,5M
	NaCl	0,75M
	pH 7,5	
IRN buffer	Tris-HCl pH 8	50mM
	EDTA	20mM
	NaCl	0,5M
Buffer A (ChEC)	Tris-HCl pH 7,4	15mM
	Spermine	0,2mM
	Spermidine	0,5mM
	KCl	80mM
	EDTA	4mM
Buffer Ag (ChEC)	Buffer A without EDTA	
	EGTA	0,1mM
10x PBS	NaCl	1,37M
	KCl	27mM
	Na_2HPO_4 x$2H_2O$	10mM
	KH_2PO_4	20mM
	pH 7,4 with HCl or NaOH	
PBST	PBS	1x
	Tween 20	0,05%
ChIP Lysis buffer	Hepes pH 7,5	50mM
	NaCl	140mM
	EDTA	5mM
	EGTA	5mM
	Triton X-100	1%
	DOC	0,1%
ChIP Wash buffer I	Hepes pH 7,5	50mM
	NaCl	500mM
	EDTA	2mM
	Triton X-100	1%
	DOC	0,1%

ChIP Wash buffer II	Tris-HCl pH 8	10mM
	LiCl	250mM
	EDTA	2mM
	Nonidet P40	0,5%
	DOC	0,5%
PEG	LiOAc	100mM
	Tris-HCl pH 8	10mM
	EDTA	1mM
	PEG3350	40%

The solvent is H_2O, if not indicated otherwise. The pH values were measured at room temperature (RT).

5.1.12 Chemicals

Chemicals were purchased at the highest purity available from Sigma-Aldrich, Merck, Fluka, Roth or J.T.Baker, except 5-FOA (Toronto Research Chemicals), electrophoresis-grade agarose (Invitrogen), bromophenol blue (Serva), G418/Geneticin (Gibco), milk powder (Sukofin), Nonidet P40 (NP40) (USB Corporation), Tris ultrapure (USB Corporation) and Tween 20 (T20) (Serva).

Ingredients for growth media were purchased from BD Becton, Dickinson and Co. (agar, peptone, tryptone and yeast extract), Qbiogene, Bio101 or Sunrise Science Products (complete supplement mixtures (CSM), yeast nitrogen base (YNB), amino acids and adenine), Sigma-Aldrich (D(+)-glucose, D(+)-galactose, amino acids and uracil), PerkinElmer (5',6'-[^{3}H] uracil) and Hartmann Analytic (α-[^{32}P]-ATP, γ-[^{32}P]-ATP). Water was always purified with an Elga Purelab Ultra device prior to use.

5.1.13 Other materials

Material	Origin
Protein Marker, Broad Range (2-212 kDa)	New England Biolabs
ColorPlus Prestained Protein Marker, Broad Range (7-175 kDa)	New England Biolabs
1 kb DNA ladder	New England Biolabs
100 bp DNA ladder	New England Biolabs
Salmon Sperm DNA (10 mg/ml)	Invitrogen
yeast genomic DNA (strain S288C)	Invitrogen
Immobilion-P Membrane PVDF 0,45 µm	Millipore
Membrane Positive^{TM}	MP Biomedicals

Blotting papers MN 827 B	Millipore
Extra Thick Blot Paper	Bio-Rad
BM Chemiluminescence Blotting Substrate (POD)	Roche
SimplyBlue™ SafeStain	Invitrogen
IgG Sepharose™ 6 Fast Flow	GE Healthcare
Protein G Sepharose™ 4 Fast Flow	GE Healthcare
Protein Assay Dye Reagent Concentrate	Bio-Rad
SYBR Safe DNA Gel Stain	Invitrogen
SYBR Green	Roche
glass beads ($\varnothing$ 0.75-1 mm)	Roth
BioMax MS Film	Sigma-Aldrich
EN³HANCE Spray Surface Autoradiography Enhancer	PerkinElmer

5.1.14 Equipment

Device	Manufacturer
4700 Proteomics Analyser MALDI-TOF/TOF	Applied Biosystems
4800 Proteomics Analyser MALDI-TOF/TOF	Applied Biosystems
Biofuge Fresco refrigerated tabletop centrifuge	Hereaus
Biofuge Pico tabletop centrifuge	Hereaus
C412 centrifuge	Jouan
Centrikon T-324 centrifuge	Kontron Instruments
CT422 refrigerated centrifuge	Jouan
Electrophoresis system model 45-2010-i	Peqlab Biotechnologie GmbH
FastPrep Instrument	Qbiogene
Gel Max UV transilluminator	Intas
IKA-Vibrax VXR	IKA
Incubators	Memmert
LAS-3000 chemiluminescence imager	Fujifilm
MicroPulser electroporation apparatus	Bio-Rad
NanoDrop ND-1000 spectrophotometer	Peqlab Biotechnologie GmbH
Avanti J-20 XP centrifuge	Beckman Coulter
Optima L-80 X ultracentrifuge	Beckman Coulter
PCR Sprint thermocycler	Hybaid

Power Pac 3000 power supplies	Bio-Rad
Roto-Shake Genie	Scientific Industries
Shake incubators Multitron / Minitron	Infors
Speed Vac Concentrator	Savant
Thermomixer compact	Eppendorf
Trans-Blot SD Semi-Dry Transfer Cell	Bio-Rad
Ultrospec 3100pro spectrophotometer	Amersham
XCell SureLock Mini-Cell electrophoresis system	Invitrogen
AxioCam MR CCD camera	Zeiss
Axiovert 200M microscope	Zeiss
Rotor-Gene 3000	Corbett Research
Sonifier 250	Branson
Mono Q PC 1.6/5	Pharmacia Biotech
Superose 12 PC 3.2/30	GE Healthcare
FLA-3000 phosphor imager	Fujifilm

5.1.15 Software

Software	Producer
4000 Series Explorer v.3.6	Applied Biosystems
Acrobat 7.0 Professional v.7.0.9	Adobe
Data Explorer v.4.5 C	Applied Biosystems
GPS Explorer v.3.5	Applied Biosystems
Image Reader LAS-3000 V2.2	Fujifilm
Mascot	Matrix Science
Microsoft Office 2007	Microsoft
ND-1000 v.3.5.2	Peqlab Biotechnologie GmbH
Photoshop CS v.8.0.1	Adobe
Illustrator CS3	Adobe
Axiovision V 4.7.1.0	Zeiss
Multi Gauge V3.0	Fujifilm
Rotor-Gene V6.1	Corbett Research
Image Reader FLA-3000 V1.8	Fujifilm

5.2 Methods

5.2.1 Work with *Saccharomyces cerevisiae*

5.2.1.1 Cultivation of yeast strains

Saccharomyces cerevisiae strains were cultivated using standard microbiological methods (Sherman, 2002).

Liquid cultures were grown in the appropriate medium usually at 30°C, except for temperature-sensitive mutants (24°C), or stated otherwise. Cell growth was monitored by measuring the optical density at 600 nm (OD_{600}).

For cultivation on solid agar plates containing the appropriate medium, single colonies or small aliquots of glycerol stocks were striked out using sterile disposable inoculation loops in order to obtain colonies derived from single yeast cells. Plates were incubated upside down at the respective temperatures for 1-5 days. Short-term storage of yeast strains was accomplished by keeping the agar plates at 4°C.

5.2.1.2 Preparation of competent yeast cells

50 ml of a logarithmically growing yeast culture (OD_{600} ~ 0.5-0.7) were harvested by centrifugation for 5 min at 4000 rpm and RT. Cells were washed with 25 ml sterile H_2O and 5 ml LitSorb before resuspending in 360 µl LitSorb. 40 µl of denatured Salmon Sperm DNA were added to the cell suspension. After mixing, 50 µl aliquots were transferred to 1.5 ml tubes before storage at -80°C.

5.2.1.3 Transformation of competent yeast cells

Competent yeast cells were thawed on ice. DNA (100 ng of plasmid DNA or 5-10 µg of linear DNA, respectively) was added and the sample was mixed. Six volumes of LitPEG were added and the suspension was again mixed thoroughly and incubated for 30 min at RT on a turning wheel. The sample was mixed with 1/9 total volume of sterile DMSO followed by a heat-shock at 42°C for 15 min and centrifugation for 1 min at 3000 rpm and RT.

When selecting for auxotrophic markers the cell pellet was directly resuspended in 100 µl sterile H_2O and plated on SCD- or SCG-plates, respectively, lacking the corresponding amino acid.

If selection for antibiotic resistance was required, the cell pellet was resuspended in 5 ml YPD or YPG, respectively, and incubated for 3-6 h at 30°C while shaking to allow the expression of the marker before plating on the respective selection media. Since selection for antibiotic resistance often results in a high number of transient transformants, these plates were replica-plated on fresh selection plates to identify positive clones.

5.2.1.4 Formaldehyde-Crosslinking of yeast cells

Logarithmically growing cells from 50 ml liquid culture were crosslinked by adding 1,35 ml 37% (v/v) formaldehyde and subsequent incubation for additional 15 min at the respective growth temperature while shaking. Crosslinking was quenched by adding 2.5 ml 2.5 M glycine. The culture was further incubated at growth temperature for additional 5 min. Cells were harvested by centrifugation in a 50 ml tube for 3 min at 3000 rpm and 4°C. The cell pellet was washed with cold water, transferred to a 1.5 ml tube, and frozen in liquid nitrogen before storage at -80°C.

5.2.1.5 Yeast plasmid shuffle

Plasmid shuffle yeast-strains were used to replace the essential RPA-genes for the mutant alleles. In these strains the chromosomal locus of the gene of interest is knocked-out with a marker gene and the deletion complemented by a wild-type copy of the gene of interest on a plasmid containing a counterselectable marker. The mutant copy is introduced on another plasmid and the strain grown on the corresponding selection-medium. If the mutant allele is able to complement the chromosomal deletion, the plasmid containing the wild-type copy can be lost during cultivation. Finally growth on the respective counterselection medium is lethal for all cells still containing the wild-type plasmid.

Single clones derived from LiAc-transformations of the mutant vectors (see 5.2.1.3) into the corresponding shuffle-yeast strains were striked on the counterselection-plates with sterile disposable inoculation loops (Sarstedt). A portion of the same clones was striked on control-plates containing the same medium except for the counterselection drug. Transformants of the RPA190-shuffle strain NOY222 (Wittekind et al., 1988) were cultivated on plates containing L-canavanine to select against the Can^S-allele of the CAN1-gene which codes for a functional arginine permease and thus allows for the uptake and incorporation of this lethal arginine-derivate (Grenson et al., 1966; Whelan et al., 1979; Broach et al., 1979). The transformants of all other RPA-shuffle strains were cultivated on plates with 5-FOA (5-Fluoro-orotic acid) which facilitates counterselection against strains carrying a functional URA3 gene. URA3 codes for the enzyme orotidin-5'-phosphate decarboxylase of the uracil-biosynthesis pathway which also converts 5-FOA into the toxic 5-fluorouracil (Boeke et al., 1984, 1987).

Single clones were controlled for i) the presence of the mutant vector, ii) the loss of the wild-type plasmid and iii) the maintenance of the chromosomal deletion via the respective auxotrophic markers. Single clones were further cultivated on YPD plates to obtain the mutant strains listed in 5.1.1.

5.2.1.6 Construction of yeast strains with integrated protein binding sites in the rDNA locus

Protein binding sites were either PCR-amplified (601, 3x LexA, ENH) or obtained through oligo annealing (TTF-I, LacR) and cloned into the pT28 vector (composed of the 18S rRNA gene and the complete ITS1 sequence) at the AflII restriction site. From these pT28 variants, fragments containing the protein binding sites were subcloned in several steps into the final vector pT11, consisting of the whole rDNA locus flanked by sequences for homologous recombination. SpeI-linearized pT11 was transformed in NOY989 for endogenous integration through homologous recombination and expansion of the rDNA locus as described in (Wai et al., 2000). Correct integration of the rDNA unit and maintenance of the artificially integrated sequence downstream of the 18S rRNA gene was confirmed by PCR of genomic DNA. Integrated regions 3` of the 18S rRNA gene were sequenced from a PCR of genomic DNA to check for mutations.

5.2.1.7 Spot test analysis of yeast strains

Overnight cultures of yeast strains were diluted in sterile 96 well plates to $OD_{600} = 0.2$ with sterile H_2O. 7-10 µl of this cell suspension and of serial 1:10, 1:100 and 1:1000 dilutions with sterile H_2O were spotted on the appropriate test plates. Phenotypes were monitored after incubation for 2-4 days at 16°C, 24°C, 30°C and 37°C, respectively.

5.2.1.8 Growth kinetic analysis of yeast strains

Cultures of yeast strains were grown to stationary phase overnight. From these pre-cultures fresh cultures were inoculated to $OD_{600} = 0.1$ in the appropriate medium and growth at 30°C was monitored by measuring the OD_{600} in 1h intervals. Dilution with the respective media has to be taken into account for growth kinetics calculations.

5.2.1.9 Long-term storage of yeast strains

2 ml of an overnight culture of the yeast strain were mixed with 1 ml sterile 50% (v/v) glycerol and separated into two aliquots. Glycerol stocks were stored at -80°C.

5.2.2 Work with *Escherichia coli*

5.2.2.1 Cultivation of bacterial strains

Liquid cultures were grown in LB_{amp} medium at 37°C. Cell growth was monitored by measuring the optical density at 600 nm (OD_{600}). For cultivation on agar plates containing LB_{amp} medium, single colonies or small aliquots of glycerol stocks were striked out using sterile disposable inoculation loops in order to obtain colonies derived from single bacterial cells. Plates were

incubated upside down at 37°C for 1 day. Short term storage of bacterial strains was accomplished by keeping the agar plates at 4°C.

5.2.2.2 Preparation of competent bacterial cells for electroporation

The XL1-Blue strain was used as a host for amplification of plasmid DNA. In order to increase the efficiency of plasmid DNA uptake, competent cells for electroporation were prepared. Cells were grown in 400 ml SOB medium at 37°C to mid-log phase (OD_{600} ~ 0.35-0.6), chilled on ice for 15 min and centrifuged for 10 min at 6000 rpm and 4°C.

Cells were washed 3x with cold sterile H_2O and 1x with sterile 10% (v/v) glycerol. After resuspending the cells in 1.5 ml sterile 10% (v/v) glycerol, 50 µl aliquots were transferred to 1.5 ml tubes before storage at -80°C.

5.2.2.3 Transformation of competent bacterial cells by electroporation

Competent bacterial cells were thawed on ice. DNA (1 ng of plasmid DNA or up to 3 µl of a ligation sample) was added and the sample was mixed. Pulsing was performed with program EC2 in a MicroPulser electroporation apparatus after pipetting the suspension into a cold 0.2 cm electroporation cuvette. 1 ml LB medium was added immediately after the pulse and the sample was transferred to a 1.5 ml tube following incubation for 30-60 min at 37°C. 50 µl of the cell suspension were plated on LB_{amp} and incubated overnight at 37°C. The residual cells were centrifuged for 1 min at 5000 rpm and RT. About 900 µl of the supernatant were discarded and the pellet was resuspended in the remaining liquid, plated on LB_{amp} and incubated overnight at 37°C.

5.2.2.4 Protein-purification from *E. coli*

A14/A43 heterodimer purification and purification of respective A43 mutants was performed basically as described in (Kuhn et al., 2007).

The genes for A14 and A43 were cloned sequentially into vector pET21b (Novagen), resulting in a thrombin-cleavable N-terminal hexahistidine tag on A14. A ribosomal binding site was introduced before A43 to enable bicistronic expression. A14/43 was expressed for 18 h at 18°C in *E. coli* BL21 (DE3) RIL cells (Stratagene) in 1 L of LB medium. Cells were harvested by centrifugation, resuspended in 100 ml buffer A (100 mM NaCl, 20 mM Tris pH 8.0, 10 mM β-mercaptoethanol, 1 mM protease inhibitor mix: 1 mM PMSF, 1 mM benzamidine, 200 mM pepstatin, and 60 mM leupeptin) and lysed by sonication. After centrifugation, the supernatant was loaded onto a 3 ml Ni-NTA column equilibrated with buffer A. After washing, proteins were eluted with buffer A containing 100 mM imidazole. A Mono Q 10/10 GL anion exchange column was equilibrated with buffer B (100 mM NaCl, 20 mM Tris pH 8.0, 5 mM DTT),

and proteins were eluted with a linear gradient from 100mM to 1M NaCl. A14/ 43 eluted at 220 mM NaCl.

5.2.3 Work with DNA

5.2.3.1 Phenol-chloroform extraction

One volume of a phenol:chloroform:isoamyl alcohol-mixture (25:24:1) was added to the sample. The samples were mixed by vortexing until the solution was milky. After centrifugation for 5 min at 13000 rpm and RT, an aliquot of the upper aqueous phase was transferred to a 1.5 ml tube.

5.2.3.2 Ethanol precipitation of DNA

DNA was precipitated from aqueous solution by mixing the sample with 1/10 volume of 3 M NaOAc pH 5.3 and 2.5 volumes of ethanol following incubation for at least 20 min at -20°C. Samples were centrifuged for 20 min at 13000 rpm and 4°C. To eliminate salt, the pellet was washed with cold 70% (v/v) ethanol. After removal of the supernatant, the nucleic acid pellet was dried at RT and solubilized in an appropriate volume of water or TE buffer.

5.2.3.3 DNA quantification using UV spectroscopy

Concentration of pure DNA samples was measured by UV spectroscopy at 260 nm (1 OD_{260} = 50 μg/ml) using a NanoDrop ND-1000 spectrophotometer. To determine contamination with proteins, absorbance was concomitantly measured at 280 nm. The ratio of OD_{260}/OD_{280} of pure DNA is between 1.8 and 2.0.

5.2.3.4 Pulse-field gel electrophoresis (PFGE)

Pellet cells by centrifuging at 3000 rpm (Falcon tubes, eppendorf centrifuge) 5 min at 4°C. Discard the supernatant and wash the cells twice in 0,05M EDTA (pH 7.5). When resuspending pellets after the final wash keep in mind that this solution will be diluted 1:1 into agarose. Calculate cell concentration and resuspension volume accordingly. Heat a 1.2% solution of LMP agarose in 0.125 M EDTA (pH 7.5) and equilibrate to 42–50°C in a waterbath. This solution can be held until ready for use.

Mix the cells with an equal amount of agarose. Also add 15.5 μl of Zymolyase solution per ml of agarose:cell suspension. Warm the cell suspension briefly in a 37°C in a waterbath before mixing with agarose. When mixing, take care to pipette thoroughly but slowly, to avoid damaging the cells and shearing the DNA.

Pipette the agarose:cell suspension into a casting mold, taking care to avoid air bubbles. Allow the molds to set at 4°C until the agarose has gelled. Unmold the solidified inserts and incubate

the inserts in 0.5 M EDTA containing 7.5% β-mercaptoethanol overnight at 37°C to create spheroplasts, disrupt membranes and digest other cellular debris.

Drain the buffer from the tube and replace with NDSK. Incubate overnight in NDSK at 50°C. Change NDSK buffer with TE containing 0.01mM PMSF. Incubate overnight at 4°C or 25°C. Dialyse the inserts into a larger volume of TE.

Load samples on a gel and perform PFGE overnight.

(adapted from Herschleb et al., 2007)

5.2.3.5 Native agarose gel electrophoresis

Native agarose gel electrophoresis was used to separate DNA fragments. Electrophoresis was performed routinely with gels composed of 1.0-1.2% (w/v) agarose and 1x TBE and containing 1x SYBR Safe DNA Gel Stain. 1x TBE was used as electrophoresis buffer and gels were run at 100-150 V. For length determination, 0.5 μg of a DNA standard (1 kb ladder or 100 bp ladder) was used in a concentration of 50 μg/ml in 2.5x DNA loading buffer. DNA fragments could be visualized by exposing the gel to blue light (470 nm).

5.2.3.6 Southern Blot (passive capillary transfer)

Separated DNA fragments were transferred and immobilized on a positively charged membrane using the passive capillary transfer method. Prior to the transfer, the agarose gel was incubated for 20 min in 0,25M HCl on a shaker followed by 2x 15 min in 0.5 M NaOH/1.5 M NaCl to denature double-stranded DNA. Subsequently, the gel was incubated for 2x 15 min in 1 M NH_4OAc. Transfer of the DNA fragments from the agarose gel to the membrane was then achieved overnight by drawing the transfer buffer (1 M NH_4OAc) from the reservoir through the gel and the membrane into a stack of paper towels. The DNA fragments were deposited onto the positively charged membrane. After the transfer, the DNA fragments were crosslinked to the dried membrane by exposition for 30 sec to UV light (0.3 J/cm^2).

5.2.3.7 Radioactive probe labeling, hybridization and detection

Probes were radioactively labeled with α-[^{32}P]-ATP using the RadPrime DNA Labeling System as indicated by the manufacturer.

The membranes, separated by meshes in a hybridization tube, were pre-hybridized for 1 h at hybridization temperature (65°C) with 50 ml hybridization buffer. For hybridization, the membranes were incubated in fresh 15 ml hybridization buffer. The labeled probe was mixed with 150 μl Salmon Sperm DNA, incubated for 5 min at 95°C, immediately chilled on ice and added to the hybridization tube. Hybridization occurred overnight at hybridization temperature with tubes rotating in a hybridization oven. The membranes were rinsed 1x with

30 ml 3x SSC/0.1% (w/v) SDS and subsequently washed in each case for 2x 15 min with 30 ml 0.3x SSC/0.1% (w/v) SDS, 0.1x SSC/0.1% (w/v) SDS and 0.1x SSC/1.5% (w/v) SDS at hybridization temperature. Membranes were dried and covered with an erased phosphor-imaging plate in a cassette. The time of exposure depended on the intensity of the radioactive signal. The phosphor-imaging plate was scanned by a FLA-3000 phosphor imager using Image Reader FLA-3000 V1.8 followed by quantitative analysis using Multi Gauge V3.0.

5.2.3.8 Polymerase Chain Reaction (PCR)

For amplification of DNA fragments for integration in the yeast genome, PCR was performed with yeast genomic DNA or plasmid DNA (50-100 ng) as templates in 50 µl reactions [20 mM Tris-HCl pH 8.8, 10 mM $(NH_4)_2SO_4$, 10 mM KCl, 2 mM $MgSO_4$, 0.1% (v/v) Triton X-100, 0.25 µM of forward and reverse primers, 0.25 mM dNTPs, 2.5-5 U Taq Polymerase]. The main PCR program used in this work was as following:

95°C	5 min	(1x)
95°C	1 min	
54°C	1 min	(35x)
72°C	2 min	
72°C	10 min	(1x)

For amplification of DNA fragments used for cloning, PCR was performed with yeast genomic DNA or plasmid DNA (50-100 ng) as templates in a 50 µl reaction [1x iProof HF Buffer, 0.5 µM of forward and reverse primers, 0.2 mM dNTPs, 2 U iProof High-Fidelity DNA Polymerase]. The PCR program was designed as indicated by the manufacturer.

10% of the reactions were analysed by native agarose gel electrophoresis. The PCR product was purified with a PCR Purification Kit according to the manufacturer.

5.2.3.9 Mutagenesis through SOE-PCR

Mutagenesis by PCR is accomplished by incorporating desired genetic changes into custom-made primers used in amplification reactions. Because these mutagenizing primers have terminal complementarity, two separate DNA fragments amplified from a target gene can be fused into a single product by primer extension without relying on restriction endonuclease sites or ligation reactions. Briefly, mutagenesis is achieved by performing PCR with specially designed oligonucleotide primers that include the desired substitutions, insertions, or deletions in their sequence. The two overlapping fragments are fused together in a subsequent extension reaction. The inclusion of outside primers in the extension reaction amplifies the fused product by PCR. Theoretically, the primers can be moved anywhere along the targeted gene to introduce mutations. A limitation of SOE is the difficulty of manipulating large DNA segments (i.e., >1-2 kb). To circumvent this, a cassette system can be targeted,

modified by SOE, and reinserted using restriction endonuclease sites designed into the cassette structure. This approach also allows easy shuffling or replacement of gene segments. (protocol from Vallejo et al., 2008)
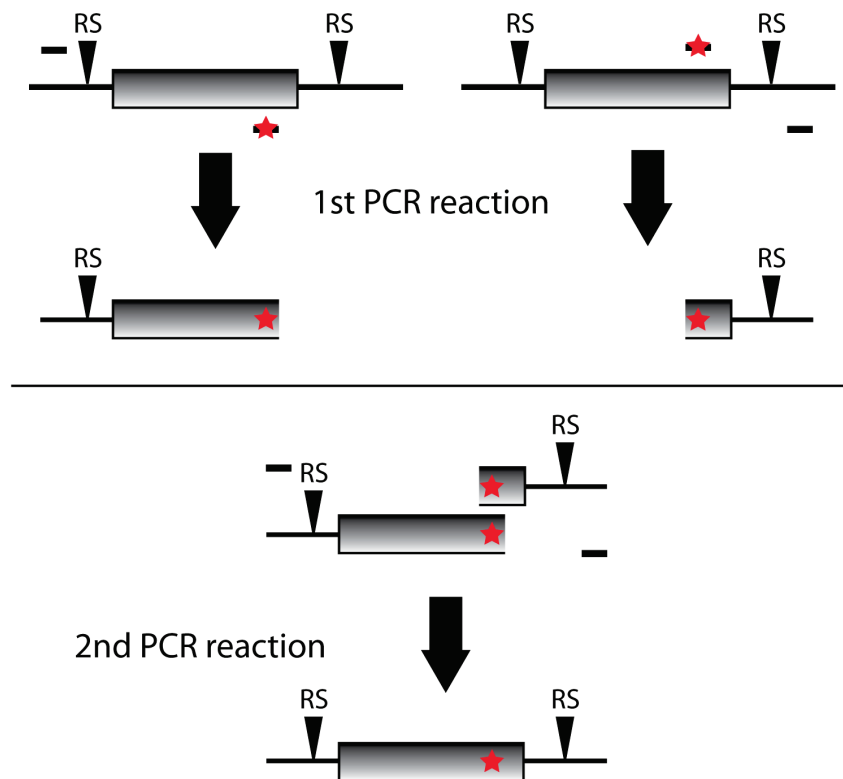

Figure 45. Schematic representation of the mutagenesis strategy using SOE-PCR

SOE-PCR mutagenesis strategy: The grey rectangle represents the gene to be mutated. PCR-primers are shown as short black lines. Restriction sites (RS) and the site to be mutated (red star) are indicated.

5.2.3.10 Quantitative real-time Polymerase Chain Reaction (qPCR)

Quantitative real-time PCR was used to measure a specific DNA fragment with high accuracy. The amount of DNA present at the end of each single PCR cycle was detected by measuring the fluorescence of SYBR Green. SYBR Green is a dye that exhibits fluorescence when bound to double-stranded DNA, but not in solution. Therefore, the intensity of the fluorescence signal allows direct measurement of the actual amount of DNA present in the sample. Quantitative real-time PCR reactions were performed in 0.1 ml tubes, the reaction volume was 20 µl. The reaction contained 4 µl of DNA sample and 16 µl of master mix. The master mix contained 4 pmol of both the forward and the reverse primer, 0.25 µl of a 1:400000 SYBR Green stock solution in DMSO, 0.4 U HotStarTaq DNA Polymerase and a premix. The premix was composed of $MgCl_2$ (final concentration in the reaction: 2.5 mM), dNTPs (final concentration in the reaction: 0.2 mM) and 10x PCR buffer (final concentration in the reaction: 1x). Quantitative

real-time PCR was performed in a Rotor-Gene 3000. The data were analysed with Rotor-Gene V6.1.

5.2.3.11 Digestion of DNA with restriction endonucleases

A variety of restriction endonucleases were used to digest DNA in order to prepare defined DNA fragments for cloning or to check for presence and correct orientation of inserted DNA fragments. Restriction endonucleases were essentially used as suggested by the manufacturer.

5.2.3.12 DNA ligation

In order to clone DNA sequences into yeast/bacterial plasmids, the quantity of purified DNA fragments digested with restriction endonucleases was measured by UV spectroscopy (see section 5.2.3.3). A fourfold molar excess of insert DNA compared to the plasmid DNA fragment was incubated in a 20 µl ligase reaction (50 mM Tris-HCl pH 7.5, 10 mM $MgCl_2$, 1 mM ATP, 10 mM DTT, 400 U T4 DNA Ligase) for 1 h at RT or overnight at 16°C. Up to 3 µl of the ligation reaction were used for transformation of competent bacterial cells (see section 5.2.2.3).

5.2.3.13 DNA sequencing and oligonucleotide synthesis

DNA sequencing was performed by GENEART and the service of primer synthesis was provided by Eurofins MWG Operon. Oligonucleotides used in this work are listed in section 5.1.4.

5.2.4 Work with RNA

5.2.4.1 Analysis of neo-synthesized RNA

For each sample 1 OD_{600} of cells was centrifuged for 1 min at 10000 rpm and RT before the cell pellets were resuspended in 100 µl buffer R, respectively. Depending on the experiment 60 µCi or 20 µCi of 5',6'-[^{3}H]-uracil were added and the cells were incubated for 5 min at 30°C (pulse prior to chase) or 20 min at 30°C (pulse), before one volume of YPUD was added and cells were incubated either for additional 4 min, 8 min, and 16 min at 30°C (chase). Immediately after the treatment, the samples were chilled on ice and centrifuged for 1 min at 13000 rpm and 4°C. The supernatants were discarded and the cell pellets were stored at -20°C. Total RNA was extracted as described (see section 5.2.4.2), same amounts of samples were separated by denaturing agarose gel electrophoresis as described (see section 5.2.4.3), transferred to a membrane as described (see section 5.2.4.4), and analysed as described (see section 5.2.4.5).

5.2.4.2 RNA extraction

RNA extractions were essentially performed as described previously (Schmitt et al., 1990). Cell pellets were resuspended in 500 µl AE buffer and mixed with 500 µl phenol equilibrated in AE buffer and 50 µl of 10% (w/v) SDS. The samples were incubated in a thermomixer for 5 min at 1400 rpm and 65°C and afterwards chilled on ice for 2 min. After centrifugation for 2 min at 13000 rpm and RT, 3x 150 µl of the aqueous phase was collected and mixed with 500 µl phenol equilibrated in AE buffer by vortexing. The samples were again centrifuged and 3x 120 µl of the supernatant were mixed with 500 µl chloroform by vortexing. Phases were separated by centrifugation and the RNA in 3x 100 µl of the supernatant was precipitated by addition of 1/10 volume of 3 M NaOAc pH 5.3 and 2.5 volumes of ethanol and incubation for 30 min at -20°C. The precipitated RNA, when used for denaturing agarose gel electrophoresis, was solubilized in RNA solubilization buffer, denatured by incubation for 15 min at 65°C and stored at -20°C.

5.2.4.3 Denaturing agarose gel electrophoresis

Denaturing agarose gel electrophoresis was used to separate longer RNA species. Electrophoresis was performed routinely with gels composed of 1.3% (w/v) agarose, 2% (v/v) formaldehyde and 1x MOPS containing 0.5 µg/ml ethidium bromide. The electrophoresis buffer was composed of 1x MOPS and 2% (v/v) formaldehyde. Gels were run for 14-16 h at 40 V.

5.2.4.4 Northern blot (passiv capillary transfer)

Separated [^{3}H]-labeled RNAs were transferred and immobilized on a positively charged membrane using the passive capillary transfer method. Prior to the transfer, the agarose gel was washed for 5 min in H_2O, for 30 min in 50 mM NaOH to hydrolyze the RNAs and facilitate the transfer of larger RNAs, and was further equilibrated for 2x 20 min in 10x SSC. Transfer of the RNA fragments from the agarose gel to the membrane was achieved overnight by drawing the transfer buffer (10x SSC) from the reservoir through the gel and the membrane into a stack of paper towels. The RNA fragments were deposited onto the positively charged membrane. After the transfer, the RNAs were crosslinked to the dried membrane by exposition for 1 min to UV light (254 nm/312 nm).

5.2.4.5 Radioactive probe labelling and detection

Different RNA species immobilised on solid supports can be detected using specific DNA probes. Probes used in this work are listed in 5.1.6. 5' ends of all oligo-probes were labelled with [^{32}P]. Ten pmol of oligo-probe were incubated with 50mCi of γ-[^{32}P]-ATP (Amersham), in

1xPNK buffer (70mM Tris-HCl, 10mM $MgCl_2$, 5mM DTT) and 10 U of T4 polynucleotide kinase (NEB) for 30-45min at 37°C. Reactions were stopped by addition of 1ml of 0.5M EDTA pH 8. Labelled probes were purified from the non-incorporated nucleotides by gel exclusion column (Spin6-Biorad). Incorporated radioactivity was estimated by counting 1μl of purified-labelled probes using a scintillation counter (1600TR-Packard). Membranes were prehybridised at least 1 h at 30°C in RNA hybridisation buffer. Membranes were then incubated at 30°C over-night after addition of $1-2x10^6$ cpm of radiolabelled oligo-probe per blot. The membranes were washed twice 15 min in 2xSSC at 30°C. Signals were acquired exposing the membrane to a Phosphoimager screen and / or BioMax MS/MR film (Fujifilm).

5.2.4.6 Detection of [³H]-labeled RNAs

The membrane was covered with an erased tritium-imaging plate (TIP) in a cassette. The time of exposure depended on the intensity of the radioactive signal. The TIP was scanned with a resolution of 100 μm by a FLA-3000 phosphor imager using Image Reader FLA-3000 V1.8 followed by quantitative analysis using Multi Gauge V3.0.

Alternatively or subsequently, the membrane was sprayed with EN³HANCE solution and subjected to autoradiography.

5.2.5 Work with proteins

5.2.5.1 Preparation of yeast whole cell extract (WCE)

For whole cell extract preparation, logarithmically growing cells from 50 ml liquid culture of $OD_{600} \sim 0.8$ were harvested by centrifugation in a 50 ml tube for 3 min at 3000 rpm and 4°C. The cells were washed with 1 ml cold H_2O and transferred to a 1.5 ml tube. After resuspending the cell pellet in an equal volume of high-salt extraction buffer [150 mM HEPES pH 7.6, 400 mM $(NH_4)_2SO_4$, 10 mM $MgCl_2$, 20% (v/v) glycerol, 5 mM β-mercaptoethanol, 2 mM benzamidine, 1 mM PMSF], an equal volume of cold glass beads ($\varnothing$ 0.75-1 mm) was added to the suspension and the tube was vigorously shaken either on an IKA-Vibrax VXR for 3x 15 min at 2200 rpm and 4°C or in a FastPrep Instrument for 2x 40 sec at 5.5 m/s and 4°C. The tube was pierced on the bottom and on the lid with a hot needle and placed in a 15 ml tube to remove the glass beads from the cell extract by centrifugation for 2 min at 2000 rpm and 4°C. The cell extract was transferred to a 1.5 ml tube and centrifuged again for 1 min at 13000 rpm and 4°C to remove cell debris. The cleared supernatant (WCE) was transferred to a 1.5 ml tube and appropriate amounts were supplemented with 4x SDS sample buffer, incubated for 5 min at 99°C and analysed as described (see sections 5.2.5.6, 5.2.5.7, and 5.2.5.8) or if required frozen in liquid nitrogen before storage at -80°C. Protein concentration was determined using the Bradford assay (Bradford, 1976).

5.2.5.2 Determination of protein concentration

Protein concentrations were determined using the Bio-Rad Protein Assay which is based on the method by Bradford (Bradford, 1976). 1-5 µl of the protein solution to be tested were mixed with 1 ml protein assay dye after diluting the reagent to the working concentration according to the instructions of the manufacturer. The approximate protein concentrations in µg/µl were calculated by dividing the absorbance at 595 nm by the sample volume and multiplying with the factor 23 which was determined using a BSA standard curve.

5.2.5.3 TCA precipitation

The volume of the protein sample to be analysed was adjusted to 100 µl with cold H_2O prior to mixing with 10 µl cold 100% (w/v) TCA and 2 µl 2% (w/v) DOC (Bensadoun and Weinstein, 1976). After incubation for 30 min at 4°C, the precipitated proteins were pelleted by centrifugation for 15 min at 13000 rpm and 4°C. The supernatant was discarded and the pellet was solubilized in an adequate volume of SDS sample buffer. The pH of the sample was neutralized using NH_3 gas if necessary. Proteins were denatured by incubating the sample for 5 min at 99°C for subsequent separation by SDS-PAGE.

5.2.5.4 Methanol-chloroform precipitation

Protein precipitation for subsequent mass spectrometric analyses was performed using the methanol-chloroform precipitation method (Wessel and Flügge, 1984). The volume of the sample was adjusted to 150 µl with H_2O, followed by the addition of four volumes of methanol (600 µl), one volume of chloroform (150 µl), and three volumes of H_2O (450 µl). After each of these steps the sample was mixed well by vortexing. After incubation for 5 min at 4°C, the sample was centrifuged for 5 min at 13000 rpm and 4°C. The supernatant was discarded without disturbing the interphase which contains the precipitated proteins. Upon addition of another three volumes of methanol (450 µl) and vortexing, the sample was incubated for 5 min at 4°C before centrifugation for 5 min at 13000 rpm and 4°C. The supernatant was completely removed and the protein pellet dried for 10 min in a Speed Vac Concentrator.

5.2.5.5 Denaturing protein extraction

Cell pellets were resuspended in 1 ml cold H_2O, mixed with 150 µl pre-treatment solution [1.85 M NaOH, 1 M β-mercaptoethanol] and incubated for 15 min at 4°C. Proteins were precipitated with 150 µl 55% (w/v) TCA for 15 min at 4°C and pelleted by centrifugation for 10 min at 13000 rpm and 4°C. The supernatant was discarded and the pellet was resuspended in 50 µl HU buffer. The pH of the sample was neutralized using NH_3 gas if necessary. Proteins

were denatured by incubating the sample for 10 min at 65°C for subsequent separation by SDS-PAGE.

5.2.5.6 SDS-polyacrylamide gel electrophoresis (SDS-PAGE)

Proteins were separated according to their molecular weight using the vertical discontinuous SDS-polyacrylamide gel electrophoresis method by Laemmli (Laemmli, 1970). The discontinuous system consists of a lower separating gel composed of 8-12% acrylamide, 375 mM Tris-HCl pH 8.8 and 0.1% (w/v) SDS and an upper stacking gel composed of 4% acrylamide, 125 mM Tris-HCl pH 6.8 and 0.1% (w/v) SDS.

Gels were run for 1.5-2.5 h at 50 mA and 180 V in 1x electrophoresis buffer. Molecular weights of the different proteins were estimated using protein markers of known molecular weight.

5.2.5.7 Western Blot

Separated proteins were transferred to a PVDF membrane using a Trans-Blot SD Semi-Dry Transfer Cell. The gel and the PVDF membrane, pretreated with methanol, were placed in the transfer cell between two piles of three blotting papers soaked with transfer buffer. Transfer was performed for 1 h at 24 V.

To control the blotting of the proteins before immunodetection, the total protein content was reversibly stained with Ponceau S by incubating the membrane in ponceau staining solution for 2 min and subsequent destaining with H_2O until the protein bands were visible.

5.2.5.8 Detection of proteins by chemiluminescence

Prior to specific immunodetection of defined proteins, the membrane was blocked with non-related proteins from bovine milk to avoid unspecific binding of the antibodies by incubating the membrane in 5% (w/v) milk powder in 1x PBS for 1 h at RT or overnight at 4°C on a shaker. The antibodies were diluted to an adequate working concentration in 5% (w/v) milk powder in 1x PBST. The incubations were performed in small bags made of sealed plastic foils on a turning wheel for 1 h (primary antibodies) or 30 min (secondary antibodies) at RT. The membrane was washed in 1x PBST for 3x 5 min on a shaker following each antibody incubation step.

In order to detect the specifically bound antibodies, the membrane was incubated for 1 min at RT with 2-4 ml BM Chemiluminescence Blotting Substrate (POD) which was prepared according to the instructions of the manufacturer. This reagent contains hydrogen peroxide and luminol which is a substrate for the horseradish peroxidase conjugated to the secondary antibodies used in this work. The light, which is emitted during this reaction at the corresponding specific positions on the membrane, was detected with a LAS-3000

chemiluminescence imager using Image Reader LAS-3000 V2.2 followed by quantitative analysis using Multi Gauge V3.0.

5.2.5.9 Coomassie staining

The polyacrylamide gel was stained with Coomassie Brilliant Blue R-250 in order to visualize the total protein content.

The gel was stained in coomassie staining solution for 30 min on a shaker at RT. Destaining was performed by incubating the gel in destaining solution for 3-4x 30 min until protein bands showed up significantly over the background staining. Optionally, the gel could be dried in a vacuum gel dryer system for 2 h at 80°C or bands could be excised for subsequent protein identification using mass spectrometry.

5.2.5.10 Analysis of neo-synthezised protein

Cells were grown in SCD medium depleted of methionine and cysteine at 30°C and further cultivated either in the absence or in the presence of rapamycin or cycloheximide, respectively. For each sample 2 OD_{600} of cells were centrifuged for 1 min at 10000 rpm and RT before the cell pellets were resuspended in 200 µl SCD-met-cys. 15 µCi of [^{35}S]-met/cys were added and the cells were incubated for 5 min at 30°C (pulse). Immediately after the treatment, the samples were centrifuged for 1 min at 13000 rpm and 4°C. The supernatants were discarded and the cell pellets were stored at -20°C. Total protein was extracted as described (see section 5.2.5.5), same amounts of samples were separated by SDS-polyacrylamide gel electrophoresis as described (see section 5.2.5.6) and coomassie staining was performed as described (see section 5.2.5.9). The dried gel was subjected to autoradiography.

5.2.6 I-TRAQ analyses (semi-quantitative MALDI mass spectrometry)

5.2.6.1 Trypsin digest and iTRAQ labelling

The lyophilised protein samples were resuspended in 20 µl dissolution buffer (iTRAQ^{TM} labelling kit, Invitrogen) and reduced with 5 mM Tris-(2-carboxyethyl)-phosphine at 60°C for 1 h. Cysteins were blocked with 10 mM methyl-methanethiosulfonate (MMTS) at room temperature for 10 min. After trypsin digest for 20 h at 37°C, tryptic peptides of the purifications of interest were labelled with different combinations of the four iTRAQ^{TM} reagents according to the manufacturer (Invitrogen). The differentially labelled peptides were combined and lyophilised (Ross et al., 2004).

5.2.6.2 Peptide separation and automated spotting of the peptide fractions

The combined differently labelled peptides were dissolved for 2 h in 0.1% TFA and loaded on a nano-flow HPLC-system (Dionex) harbouring a C18-Pep-Mep column (LC-Packings). The peptides were separated by a gradient of 5% to 95% of buffer B (80% acetonitrile/0.05% TFA) and fractions were mixed with 5 volumes of CHCA (alpha-cyano-4-hydroxy cinnamic acid; Sigma) matrix (2 mg/ml in 70% acetonitrile/0.1% TFA) and spotted online via the Probot system (Dionex) on a MALDI-target.

5.2.6.3 MALDI TOF/TOF analysis

MS/MS analyses were performed on an Applied Biosystems 4700 or 4800 Proteomics Analyser MALDI-TOF/TOF mass spectrometer operated in positive ion reflector mode and evaluated by searching the NCBInr protein sequence database with the Mascot search engine (Matrix Science) implemented in the GPS Explorer software (Applied Biosystems). Laser intensity was adjusted due to laser condition and sample concentration. The eight most intense peptide peaks per spot detected in the MS mode were further fragmented yielding the respective MS/MS spectra.

5.2.6.4 iTRAQ data evaluation

Only proteins identified by at least two nonredundant peptides with a Confidence Interval >95% were included in the analysis. The peak area for iTRAQ™ reporter ions were interpreted and corrected by the GPS-Explorer software (Applied Biosystems) and Excel (Microsoft). An iTRAQ ratio average of all peptides of a given protein was calculated and outliers were deleted by manual evaluation. The iTRAQ ratios of the co-purifying proteins were normalised to the ratio of the bait protein.

5.2.7 Additional biochemical methods

5.2.7.1 Chromatin immunoprecipitation (ChIP)

Chromatin immunoprecipitation was performed in three independent experiments for each protein mainly as described (Hecht and Grunstein, 1999). Cells from 50 ml liquid culture were crosslinked with formaldehyde as described (see section 5.2.1.4), washed with 500 µl cold ChIP lysis buffer [50 mM HEPES pH 7.5, 140 mM NaCl, 5 mM EDTA pH 8.0, 5 mM EGTA pH 8.0, 1% (v/v) Triton X-100, 0.1% (w/v) DOC] and resuspended in an equal volume of cold ChIP lysis buffer. An equal volume of cold glass beads (∅ 0.75-1 mm) was added to the suspension and the tube was vigorously shaken on an IKA-Vibrax VXR for 3x 15 min at 2200 rpm and 4°C. The tube was pierced on the bottom and on the lid with a hot needle and placed in a 15 ml tube to remove the glass beads from the cell extract by centrifugation for 1 min at 1000 rpm and 4°C.

Cold ChIP lysis buffer was added to a final volume of 1 ml and the DNA in the suspension was sonicated using a Sonifier 250 to obtain an average DNA fragment size of 500-1000 bp. Cell debris were removed by centrifugation for 20 min at 13000 rpm and 4°C. The chromatin extracts were split into three aliquots. 40 µl of each aliquot served as an input control. 200 µl of each aliquot were incubated either with 3 µg of a monoclonal α-HA antibody (3F10) and 50 µl equilibrated Protein G Sepharose or with 50 µl equilibrated IgG Sepharose for 2 h at 4°C to enrich either HA$_3$-tagged proteins or Prot.A-tagged proteins. After immunoprecipitation, the beads were washed 3x with cold ChIP lysis buffer, 2x with cold ChIP washing buffer I [50 mM HEPES pH 7.5, 500 mM NaCl, 2 mM EDTA pH 8.0, 1% (v/v) Triton X-100, 0.1% (w/v) DOC], and 2x with cold ChIP washing buffer II [10 mM Tris-HCl pH 8.0, 250 mM LiCl, 2 mM EDTA pH 8.0, 0.5% (v/v) Nonidet P40, 0.5% (w/v) DOC] followed by a final washing step with TE buffer [10 mM Tris-HCl pH 8.0, 1 mM EDTA pH 8.0]. 250 µl IRN buffer [50 mM Tris-HCl pH 8.0, 20 mM EDTA pH 8.0, 500 mM NaCl] were added to the input (IN) and to the beads (IP) samples. RNA in the samples was digested with 2 µl RNase A (20 mg/ml) for 1 h at 37°C. Afterwards, 0.5% (w/v) SDS and 2 µl Proteinase K (20 mg/ml) were added to the samples followed by incubation for 1 h at 56°C. The formaldehyde crosslink was reversed overnight by incubation at 65°C. DNA was isolated by phenol-chloroform extraction as described (see section 5.2.3.1), precipitated with ethanol as described (see section 5.2.3.2) and resuspended in 50 µl sterile water.

DNA amounts present in IN and IP samples were determined by quantitative real-time PCR as described (see section 5.2.3.8). Primer pairs for amplification used in this work are listed in section 5.1.4. IN DNA was diluted 1:1000 and IP DNA was diluted 1:200 prior to analysis. Retention of specific DNA fragments was calculated as the fraction of the total input DNA. The mean values and error bars were derived from independent ChIP experiments analysed in triplicate quantitative real-time PCR reactions.

5.2.7.2 Chromatin endogenous cleavage (ChEC)

Chromatin endogenous cleavage was performed mainly as described (Schmid et al., 2004). Cells from 50 ml liquid culture were crosslinked with formaldehyde as described (see section 5.2.1.4), washed 3x with 500 µl cold ChEC buffer A (+ 1x PIs) and resuspended in 350 µl cold ChEC buffer A (+ 1x PIs). An equal volume of cold glass beads (⌀ 0.75-1 mm) was added to the suspension and the tube was vigorously shaken on an IKA-Vibrax VXR for 10 min at 2200 rpm and 4°C. The tube was pierced on the bottom and on the lid with a hot needle and placed in a 15 ml tube to remove the glass beads from the cell extract by centrifugation for 1 min at 1000 rpm and 4°C. The cell lysate was transferred to a 1.5 ml tube and centrifuged again for 2 min at 13000 rpm and 4°C. The supernatant was discarded. The lysate pellet containing intact nuclei was washed with 500 µl cold ChEC buffer A (+ 1x PIs) and resuspended in 350 µl cold

ChEC buffer Ag (+ 1x PIs). The sample was incubated in a thermomixer at 700 rpm and 30°C. One aliquot (0 min, untreated) of the well-mixed sample was taken (80 μl). MNase digestion was started by adding 10 μl 100 mM (w/v) $CaCl_2$. Aliquots were taken at the chosen time points (80 μl). The digestion reaction was immediately stopped by pipetting the aliquot into 100 μl IRN buffer [50 mM Tris-HCl pH 8.0, 20 mM EDTA pH 8.0, 500 mM NaCl]. Before taking an aliquot, the sample should be mixed at higher rotation rates since nuclei sediment. Stopped aliquots could be kept at RT. When the time course was complete, 100 μl IRN buffer was added to the 0 min aliquots. RNA in the aliquots was digested with 2 μl RNase A (20 mg/ml) for 1 h at 37°C. Afterwards, 0.5% (w/v) SDS and 2 μl Proteinase K (20 mg/ml) were added to the aliquots followed by incubation for 1 h at 56°C. The formaldehyde crosslink was reversed overnight by incubation at 65°C. DNA was isolated by phenol-chloroform extraction as described (see section 5.2.3.1), precipitated with ethanol as described (see section 5.2.3.2), and resuspended in 30 μl sterile water.

10 μl of the DNA sample were digested with the appropriate restriction endonuclease for the experiment in a 20 μl reaction overnight at 37°C. Total DNA of the digestion reaction was separated by native agarose gel electrophoresis as described (see section 5.2.3.4), transferred to a membrane as described (see section 5.2.3.5), and analysed as described (see section 5.2.3.6).

5.2.7.3 Psoralen treatment

Psoralen crosslinking was performed on nuclei. Nuclei were suspended in 1 ml buffer Ag/IRN (1:1). 200 μl of this suspension were incubated with psoralen and another 200 μl were treated with ethanol as a control. The remaining nuclei were pelleted, frozen in liquid nitrogen and stored at -80°C. All samples were pipetted into the wells of a 24 tissue culture plate (for suspension cells). To each sample 10 μl of trimethylpsoralen (TMP, 0.2 mg/ml in ethanol) or ethanol was added, mixed and stored on ice in the dark for 5 minutes. Then, samples were irradiated with long-wavelength UV light (288 nm) for 5 minutes. The addition of psoralen and irradiation was repeated four times in total. Tissue plates were kept on a metal plate on ice during the irradiation. During irradiation it was important to remove the plastic cover of the 24 well plates. Then, samples were transferred to reaction tubes and subjected to further DNA workup. For this the RNA was digested with 2 μl RNAseA (20 mg/ml) for 1 h at 37°C. Afterwards, SDS (final concentration 0.5%) was added together with 2 μl of proteinase K (20 mg/ml stock) and incubated for 1 h at 56°C. The formaldehyde crosslink was reversed by incubation at 65°C overnight or for at least 8 h. DNA was isolated by phenol-chloroform extraction, precipitated with ethanol and resuspended in 30 μl sterile water.

To obtain slow-migrating band (s-band) or fast-migrating band (f-band) profiles from psoralen analyses, signal intensities in each lane were normalized to the respective peak values and

plotted against the distance of migration in the gel. Raw data were processed with the PeakFit software (Systat Software Inc.) using a Gaussian basis function (r^2 values fit $\geq$0.98).

5.2.7.4 Miller chromatin spreads

Chromatin spreading was performed as described in (Osheim et al., 2009) with minor modifications. Carbon-coated grids were made hydrophilic by glow discharge instead of ethanol treatment. Depending on the contrast of the spread chromatin, counterstaining with heavy metal can be avoided. Negatively stained chromatin was obtained by short incubation with heavy metal followed by quick drying of the sample.

5.2.7.5 Affinity purification using IgG coupled magnetic beads

The cell pellet corresponding to 1 L yeast culture with OD_{600}=0.8-1.0 was resuspended in 1.5 ml of cold buffer MB with 1 mM DTT and 0.04 U/µl RNasin per 1 g cell pellet. 800 µl of this cell suspension was added to 1.4 ml glass beads (Ø 0.75 – 1mm) and divided into 2 ml reaction tubes. A cell lysate was prepared by vigorous shaking of the cell suspension in a Vibrax shaker for 20 min, followed by 2 min on ice. This procedure was repeated twice. The cell lysate was cleared from cell debris by two centrifugation steps, 1x 5 min at 14000 rpm and 1x 10 min at 14000 rpm. The protein concentration of the cleared lysate was determined using the Bradford assay. Triton X-100 (0.5%) and Tween 20 (0.1%) was added to the cell lysate. The whole amount of cell lysate (typically 2.0-2.4 ml with 120 – 180 mg of total protein) was incubated with 250 µl of equilibrated (3x washing with buffer A200 with 1x protease inhibitors) IgG coupled magnetic beads slurry and rotated for 1 h at 4°C. The beads were washed 7 times (1x 1 ml, 5x 2 ml and 1x 10 ml) with cold buffer MB with 0.5% Triton X-100 and 0.1% Tween 20 in a BioRad 10 ml column. Bound proteins were eluted 2x with 500 µl of freshly prepared 500 mM NH_4OH solution and rotation for 20 min at RT. Both supernatants were pooled in an original Eppendorf 1.5 ml reaction tube and lyophilised over night and e.g. further used for iTRAQ analyses.

6 REFERENCES

Abovich, N., Gritz, L., Tung, L., and Rosbash, M. (1985). Effect of RP51 gene dosage alterations on ribosome synthesis in Saccharomyces cerevisiae. Mol. Cell. Biol *5*, 3429-3435.

Albert, B., Léger-Silvestre, I., Normand, C., Ostermaier, M. K., Pérez-Fernández, J., Panov, K. I., Zomerdijk, J. C. B. M., Schultz, P., and Gadal, O. (2011). RNA polymerase I-specific subunits promote polymerase clustering to enhance the rRNA gene transcription cycle. J. Cell Biol *192*, 277-293.

Anderson, S. J., Sikes, M. L., Zhang, Y., French, S. L., Salgia, S., Beyer, A. L., Nomura, M., and Schneider, D. A. (2011). The transcription elongation factor Spt5 influences transcription by RNA polymerase I positively and negatively. J Biol Chem. Available at: http://www.ncbi.nlm.nih.gov/pubmed/21467039 [Accessed April 13, 2011].

Archambault, J., Lacroute, F., Ruet, A., and Friesen, J. D. (1992). Genetic interaction between transcription elongation factor TFIIS and RNA polymerase II. Mol. Cell. Biol *12*, 4142-4152.

Armache, K.-J., Kettenberger, H., and Cramer, P. (2003). Architecture of initiation-competent 12-subunit RNA polymerase II. Proc. Natl. Acad. Sci. U.S.A *100*, 6964-6968.

Armache, K.-J., Mitterweger, S., Meinhart, A., and Cramer, P. (2005). Structures of complete RNA polymerase II and its subcomplex, Rpb4/7. J. Biol. Chem *280*, 7131-7134.

Barbet, N. C., Schneider, U., Helliwell, S. B., Stansfield, I., Tuite, M. F., and Hall, M. N. (1996). TOR controls translation initiation and early G1 progression in yeast. Mol. Biol. Cell *7*, 25-42.

Baron, U., and Bujard, H. (2000). Tet repressor-based system for regulated gene expression in eukaryotic cells: principles and advances. Meth. Enzymol *327*, 401-421.

Beckouet, F., Labarre-Mariotte, S., Albert, B., Imazawa, Y., Werner, M., Gadal, O., Nogi, Y., and Thuriaux, P. (2008). Two RNA polymerase I subunits control the binding and release of Rrn3 during transcription. Mol. Cell. Biol *28*, 1596-1605.

Bell, G. I., Valenzuela, P., and Rutter, W. J. (1976). Phosphorylation of yeast RNA polymerases. Nature *261*, 429-431.

Beltrame, M., and Tollervey, D. (1992). Identification and functional analysis of two U3 binding sites on yeast pre-ribosomal RNA. EMBO J *11*, 1531-1542.

Bensadoun, A., and Weinstein, D. (1976). Assay of proteins in the presence of interfering materials. Anal. Biochem *70*, 241-250.

Berger, A. B., Decourty, L., Badis, G., Nehrbass, U., Jacquier, A., and Gadal, O. (2007). Hmo1 is required for TOR-dependent regulation of ribosomal protein gene transcription. Mol. Cell. Biol *27*, 8015-8026.

Berset, C., Trachsel, H., and Altmann, M. (1998). The TOR (target of rapamycin) signal transduction pathway regulates the stability of translation initiation factor eIF4G in the yeast Saccharomyces cerevisiae. Proc. Natl. Acad. Sci. U.S.A *95*, 4264-4269.

Bier, M., Fath, S., and Tschochner, H. (2004). The composition of the RNA polymerase I transcription machinery switches from initiation to elongation mode. FEBS Lett *564*, 41-46.

Bischler, N., Brino, L., Carles, C., Riva, M., Tschochner, H., Mallouh, V., and Schultz, P. (2002). Localization of the yeast RNA polymerase I-specific subunits. EMBO J *21*, 4136-4144.

Boeke, J. D., LaCroute, F., and Fink, G. R. (1984). A positive selection for mutants lacking orotidine-5'-phosphate decarboxylase activity in yeast: 5-fluoro-orotic acid resistance. Mol. Gen. Genet *197*, 345-346.

Boeke, J. D., Trueheart, J., Natsoulis, G., and Fink, G. R. (1987). 5-Fluoroorotic acid as a selective agent in yeast molecular genetics. Meth. Enzymol *154*, 164-175.

Borukhov, S., and Nudler, E. (2008). RNA polymerase: the vehicle of transcription. Trends Microbiol *16*, 126-134.

Bradford, M. M. (1976). A rapid and sensitive method for the quantitation of microgram quantities of protein utilizing the principle of protein-dye binding. Anal. Biochem *72*, 248-254.

Braglia, P., Heindl, K., Schleiffer, A., Martinez, J., and Proudfoot, N. J. (2010a). Role of the RNA/DNA kinase Grc3 in transcription termination by RNA polymerase I. EMBO Rep *11*, 758-764.

Braglia, P., Kawauchi, J., and Proudfoot, N. J. (2010b). Co-transcriptional RNA cleavage provides a failsafe termination mechanism for yeast RNA polymerase I. Nucleic Acids Res. Available at: http://www.ncbi.nlm.nih.gov/pubmed/20972219 [Accessed December 2, 2010].

Bréant, B., Buhler, J. M., Sentenac, A., and Fromageot, P. (1983). On the phosphorylation of yeast RNA polymerases A and B. Eur. J. Biochem *130*, 247-251.

Brewer, B. J., and Fangman, W. L. (1988). A replication fork barrier at the 3' end of yeast ribosomal RNA genes. Cell *55*, 637-643.

Brewer, B. J., Lockshon, D., and Fangman, W. L. (1992). The arrest of replication forks in the rDNA of yeast occurs independently of transcription. Cell *71*, 267-276.

Broach, J. R., Strathern, J. N., and Hicks, J. B. (1979). Transformation in yeast: development of a hybrid cloning vector and isolation of the CAN1 gene. Gene *8*, 121-133.

Buhler, J. M., Huet, J., Davies, K. E., Sentenac, A., and Fromageot, P. (1980). Immunological studies of yeast nuclear RNA polymerases at the subunit level. J. Biol. Chem *255*, 9949-9954.

Buhler, J. M., Iborra, F., Sentenac, A., and Fromageot, P. (1976a). Structural studies on yeast RNA polymerases. Existence of common subunits in RNA polymerases A(I) and B(II). J. Biol. Chem *251*, 1712-1717.

REFERENCES

Buhler, J. M., Iborra, F., Sentenac, A., and Fromageot, P. (1976b). The presence of phosphorylated subunits in yeast RNA polymerases A and B. FEBS Lett *72*, 37-41.

Burkhalter, M. D., and Sogo, J. M. (2004). rDNA enhancer affects replication initiation and mitotic recombination: Fob1 mediates nucleolytic processing independently of replication. Mol. Cell *15*, 409-421.

Cardenas, M. E., Cutler, N. S., Lorenz, M. C., Di Como, C. J., and Heitman, J. (1999). The TOR signaling cascade regulates gene expression in response to nutrients. Genes Dev *13*, 3271-3279.

Carles, C., Treich, I., Bouet, F., Riva, M., and Sentenac, A. (1991). Two additional common subunits, ABC10 alpha and ABC10 beta, are shared by yeast RNA polymerases. J. Biol. Chem *266*, 24092-24096.

De Carlo, S., Carles, C., Riva, M., and Schultz, P. (2003). Cryo-negative staining reveals conformational flexibility within yeast RNA polymerase I. J. Mol. Biol *329*, 891-902.

Carmen, A. A., and Holland, M. J. (1994). The upstream repression sequence from the yeast enolase gene ENO1 is a complex regulatory element that binds multiple trans-acting factors including REB1. J. Biol. Chem *269*, 9790-9797.

Chédin, S., Riva, M., Schultz, P., Sentenac, A., and Carles, C. (1998). The RNA cleavage activity of RNA polymerase III is mediated by an essential TFIIS-like subunit and is important for transcription termination. Genes Dev *12*, 3857-3871.

Cherkasova, V. A., and Hinnebusch, A. G. (2003). Translational control by TOR and TAP42 through dephosphorylation of eIF2alpha kinase GCN2. Genes Dev *17*, 859-872.

Cioci, F., Vu, L., Eliason, K., Oakes, M., Siddiqi, I. N., and Nomura, M. (2003). Silencing in yeast rDNA chromatin: reciprocal relationship in gene expression between RNA polymerase I and II. Mol. Cell *12*, 135-145.

Claypool, J. A., French, S. L., Johzuka, K., Eliason, K., Vu, L., Dodd, J. A., Beyer, A. L., and Nomura, M. (2004). Tor pathway regulates Rrn3p-dependent recruitment of yeast RNA polymerase I to the promoter but does not participate in alteration of the number of active genes. Mol. Biol. Cell *15*, 946-956.

Cmarko, D., Verschure, P. J., Rothblum, L. I., Hernandez-Verdun, D., Amalric, F., van Driel, R., and Fakan, S. (2000). Ultrastructural analysis of nucleolar transcription in cells microinjected with 5-bromo-UTP. Histochem. Cell Biol *113*, 181-187.

Cohen, P. (2002). The origins of protein phosphorylation. Nat. Cell Biol *4*, E127-130.

Conconi, A., Widmer, R. M., Koller, T., and Sogo, J. M. (1989). Two different chromatin structures coexist in ribosomal RNA genes throughout the cell cycle. Cell *57*, 753-761.

Cramer, P., Bushnell, D. A., and Kornberg, R. D. (2001). Structural basis of transcription: RNA polymerase II at 2.8 angstrom resolution. Science *292*, 1863-1876.

Cramer, P., Bushnell, D. A., Fu, J., Gnatt, A. L., Maier-Davis, B., Thompson, N. E., Burgess, R. R., Edwards, A. M., David, P. R., and Kornberg, R. D. (2000). Architecture of RNA polymerase II and implications for the transcription mechanism. Science *288*, 640-649.

Cramer, P. (2002). Multisubunit RNA polymerases. Curr. Opin. Struct. Biol *12*, 89-97.

Crews, C. M. (2003). Feeding the machine: mechanisms of proteasome-catalyzed degradation of ubiquitinated proteins. Curr Opin Chem Biol *7*, 534-539.

Cybulski, N., and Hall, M. N. (2009). TOR complex 2: a signaling pathway of its own. Trends Biochem. Sci *34*, 620-627.

Decourty, L., Saveanu, C., Zemam, K., Hantraye, F., Frachon, E., Rousselle, J.-C., Fromont-Racine, M., and Jacquier, A. (2008). Linking functionally related genes by sensitive and quantitative characterization of genetic interaction profiles. Proc. Natl. Acad. Sci. U.S.A *105*, 5821-5826.

Dequard-Chablat, M., Riva, M., Carles, C., and Sentenac, A. (1991). RPC19, the gene for a subunit common to yeast RNA polymerases A (I) and C (III). J. Biol. Chem *266*, 15300-15307.

Deutschbauer, A. M., Jaramillo, D. F., Proctor, M., Kumm, J., Hillenmeyer, M. E., Davis, R. W., Nislow, C., and Giaever, G. (2005). Mechanisms of haploinsufficiency revealed by genome-wide profiling in yeast. Genetics *169*, 1915-1925.

Dez, C., Houseley, J., and Tollervey, D. (2006). Surveillance of nuclear-restricted pre-ribosomes within a subnucleolar region of Saccharomyces cerevisiae. EMBO J *25*, 1534-1546.

Drouin, G., and de Sá, M. M. (1995). The concerted evolution of 5S ribosomal genes linked to the repeat units of other multigene families. Mol. Biol. Evol *12*, 481-493.

El Hage, A., Koper, M., Kufel, J., and Tollervey, D. (2008). Efficient termination of transcription by RNA polymerase I requires the 5' exonuclease Rat1 in yeast. Genes Dev *22*, 1069-1081.

Elion, E. A., and Warner, J. R. (1986). An RNA polymerase I enhancer in Saccharomyces cerevisiae. Mol. Cell. Biol *6*, 2089-2097.

Elion, E. A., and Warner, J. R. (1984). The major promoter element of rRNA transcription in yeast lies 2 kb upstream. Cell *39*, 663-673.

Epshtein, V., and Nudler, E. (2003). Cooperation between RNA polymerase molecules in transcription elongation. Science *300*, 801-805.

Epshtein, V., Toulmé, F., Rahmouni, A. R., Borukhov, S., and Nudler, E. (2003). Transcription through the roadblocks: the role of RNA polymerase cooperation. EMBO J *22*, 4719-4727.

Exinger, F., and Lacroute, F. (1992). 6-Azauracil inhibition of GTP biosynthesis in Saccharomyces cerevisiae. Curr. Genet *22*, 9-11.

Fangman, W. L., and Brewer, B. J. (1992). A question of time: replication origins of eukaryotic chromosomes. Cell *71*, 363-366.

Fath, S., Milkereit, P., Peyroche, G., Riva, M., Carles, C., and Tschochner, H. (2001). Differential roles of phosphorylation in the formation of transcriptional active RNA polymerase I. Proc. Natl. Acad. Sci. U.S.A *98*, 14334-14339.

Fath, S., Kobor, M. S., Philippi, A., Greenblatt, J., and Tschochner, H. (2004). Dephosphorylation of RNA polymerase I by Fcp1p is required for efficient rRNA synthesis. J. Biol. Chem *279*, 25251-25259.

Felixberger, J. (2009). Analysevon Phosphorylierungsmutantender RNA-Polymerase I.

Ferreira-Cerca, S., Pöll, G., Gleizes, P.-E., Tschochner, H., and Milkereit, P. (2005). Roles of eukaryotic ribosomal proteins in maturation and transport of pre-18S rRNA and ribosome function. Mol. Cell *20*, 263-275.

Ferreira-Cerca, S., Pöll, G., Kühn, H., Neueder, A., Jakob, S., Tschochner, H., and Milkereit, P. (2007). Analysis of the in vivo assembly pathway of eukaryotic 40S ribosomal proteins. Mol. Cell *28*, 446-457.

Ficarro, S. B., McCleland, M. L., Stukenberg, P. T., Burke, D. J., Ross, M. M., Shabanowitz, J., Hunt, D. F., and White, F. M. (2002). Phosphoproteome analysis by mass spectrometry and its application to Saccharomyces cerevisiae. Nat. Biotechnol *20*, 301-305.

Fischer, E. H., and Krebs, E. G. (1955). Conversion of phosphorylase b to phosphorylase a in muscle extracts. J. Biol. Chem *216*, 121-132.

Fish, R. N., and Kane, C. M. (2002). Promoting elongation with transcript cleavage stimulatory factors. Biochim. Biophys. Acta *1577*, 287-307.

Flores, A., Briand, J. F., Gadal, O., Andrau, J. C., Rubbi, L., Van Mullem, V., Boschiero, C., Goussot, M., Marck, C., Carles, C., et al. (1999). A protein-protein interaction map of yeast RNA polymerase III. Proc. Natl. Acad. Sci. U.S.A *96*, 7815-7820.

French, S. L., Osheim, Y. N., Cioci, F., Nomura, M., and Beyer, A. L. (2003). In exponentially growing Saccharomyces cerevisiae cells, rRNA synthesis is determined by the summed RNA polymerase I loading rate rather than by the number of active genes. Mol. Cell. Biol *23*, 1558-1568.

Fromont-Racine, M., Senger, B., Saveanu, C., and Fasiolo, F. (2003). Ribosome assembly in eukaryotes. Gene *313*, 17-42.

Gadal, O., Mariotte-Labarre, S., Chedin, S., Quemeneur, E., Carles, C., Sentenac, A., and Thuriaux, P. (1997). A34.5, a nonessential component of yeast RNA polymerase I, cooperates with subunit A14 and DNA topoisomerase I to produce a functional rRNA synthesis machine. Mol. Cell. Biol *17*, 1787-1795.

Gadal, O., Shpakovski, G. V., and Thuriaux, P. (1999). Mutants in ABC10beta, a conserved subunit shared by all three yeast RNA polymerases, specifically affect RNA polymerase I assembly. J. Biol. Chem *274*, 8421-8427.

Gallagher, J. E. G., Dunbar, D. A., Granneman, S., Mitchell, B. M., Osheim, Y., Beyer, A. L., and Baserga, S. J. (2004). RNA polymerase I transcription and pre-rRNA processing are linked by specific SSU processome components. Genes Dev *18*, 2506-2517.

Ganley, A. R. D., Hayashi, K., Horiuchi, T., and Kobayashi, T. (2005). Identifying gene-independent noncoding functional elements in the yeast ribosomal DNA by phylogenetic footprinting. Proc. Natl. Acad. Sci. U.S.A *102*, 11787-11792.

Garí, E., Piedrafita, L., Aldea, M., and Herrero, E. (1997). A set of vectors with a tetracycline-regulatable promoter system for modulated gene expression in Saccharomyces cerevisiae. Yeast *13*, 837-848.

Geiduschek, E. P., and Kassavetis, G. A. (2001). The RNA polymerase III transcription apparatus. J. Mol. Biol *310*, 1-26.

Geiger, S. R., Kuhn, C. D., Leidig, C., Renkawitz, J., and Cramer, P. (2008). Crystallization of RNA polymerase I subcomplex A14/A43 by iterative prediction, probing and removal of flexible regions. Acta Crystallogr. Sect. F Struct. Biol. Cryst. Commun *64*, 413-418.

Geiger, S. R., Lorenzen, K., Schreieck, A., Hanecker, P., Kostrewa, D., Heck, A. J. R., and Cramer, P. (2010). RNA polymerase I contains a TFIIF-related DNA-binding subcomplex. Mol. Cell *39*, 583-594.

Gerber, J. K., Gögel, E., Berger, C., Wallisch, M., Müller, F., Grummt, I., and Grummt, F. (1997). Termination of mammalian rDNA replication: polar arrest of replication fork movement by transcription termination factor TTF-I. Cell *90*, 559-567.

Gerber, J. (2008). Site-specific phosphorylation of yeast RNA polymerase I.

Gerber, J., Reiter, A., Steinbauer, R., Jakob, S., Kuhn, C.-D., Cramer, P., Griesenbeck, J., Milkereit, P., and Tschochner, H. (2008). Site specific phosphorylation of yeast RNA polymerase I. Nucleic Acids Res *36*, 793-802.

Ghosh, P., Ishihama, A., and Chatterji, D. (2001). Escherichia coli RNA polymerase subunit omega and its N-terminal domain bind full-length beta' to facilitate incorporation into the alpha2beta subassembly. Eur. J. Biochem *268*, 4621-4627.

Gorenstein, C., and Warner, J. R. (1977). Synthesis and turnover of ribosomal proteins in the absence of 60S subunit assembly in Saccharomyces cerevisiae. Mol. Gen. Genet *157*, 327-332.

Gossen, M., and Bujard, H. (1992). Tight control of gene expression in mammalian cells by tetracycline-responsive promoters. Proc. Natl. Acad. Sci. U.S.A *89*, 5547-5551.

Graham, I. R., and Chambers, A. (1994). A Reb1p-binding site is required for efficient activation of the yeast RAP1 gene, but multiple binding sites for Rap1p are not essential. Mol. Microbiol *12*, 931-940.

Granneman, S., and Baserga, S. J. (2005). Crosstalk in gene expression: coupling and co-regulation of rDNA transcription, pre-ribosome assembly and pre-rRNA processing. Curr. Opin. Cell Biol *17*, 281-286.

Grenson, M., Mousset, M., Wiame, J. M., and Bechet, J. (1966). Multiplicity of the amino acid permeases in Saccharomyces cerevisiae. I. Evidence for a specific arginine-transporting system. Biochim. Biophys. Acta *127*, 325-338.

Grummt, I., Smith, V. A., and Grummt, F. (1976). Amino acid starvation affects the initiation frequency of nucleolar RNA polymerase. Cell *7*, 439-445.

Hampsey, M. (1997). A review of phenotypes in Saccharomyces cerevisiae. Yeast *13*, 1099-1133.

Hartwell, L. H., McLaughlin, C. S., and Warner, J. R. (1970). Identification of ten genes that control ribosome formation in yeast. Mol. Gen. Genet *109*, 42-56.

Hausner, W., Lange, U., and Musfeldt, M. (2000). Transcription factor S, a cleavage induction factor of the archaeal RNA polymerase. J. Biol. Chem *275*, 12393-12399.

Hecht, A., and Grunstein, M. (1999). Mapping DNA interaction sites of chromosomal proteins using immunoprecipitation and polymerase chain reaction. Meth. Enzymol *304*, 399-414.

Hedtke, B., Börner, T., and Weihe, A. (1997). Mitochondrial and chloroplast phage-type RNA polymerases in Arabidopsis. Science *277*, 809-811.

Henderson, S., and Sollner-Webb, B. (1986). A transcriptional terminator is a novel element of the promoter of the mouse ribosomal RNA gene. Cell *47*, 891-900.

Henras, A. K., Soudet, J., Gérus, M., Lebaron, S., Caizergues-Ferrer, M., Mougin, A., and Henry, Y. (2008). The post-transcriptional steps of eukaryotic ribosome biogenesis. Cell. Mol. Life Sci *65*, 2334-2359.

Henras, A. K., Bertrand, E., and Chanfreau, G. (2004). A cotranscriptional model for 3'-end processing of the Saccharomyces cerevisiae pre-ribosomal RNA precursor. RNA *10*, 1572-1585.

Herr, A. J., Jensen, M. B., Dalmay, T., and Baulcombe, D. C. (2005). RNA polymerase IV directs silencing of endogenous DNA. Science *308*, 118-120.

Herschleb, J., Ananiev, G., and Schwartz, D. C. (2007). Pulsed-field gel electrophoresis. Nat Protoc *2*, 677-684.

Hirata, A., Klein, B. J., and Murakami, K. S. (2008). The X-ray crystal structure of RNA polymerase from Archaea. Nature *451*, 851-854.

Holzer, H., and Duntze, W. (1971). Metabolic regulation by chemical modification of enzymes. Annu. Rev. Biochem *40*, 345-374.

Honma, Y., Kitamura, A., Shioda, R., Maruyama, H., Ozaki, K., Oda, Y., Mini, T., Jenö, P., Maki, Y., Yonezawa, K., et al. (2006). TOR regulates late steps of ribosome maturation in the nucleoplasm via Nog1 in response to nutrients. EMBO J *25*, 3832-3842.

Hontz, R. D., Niederer, R. O., Johnson, J. M., and Smith, J. S. (2009). Genetic identification of factors that modulate ribosomal DNA transcription in Saccharomyces cerevisiae. Genetics *182*, 105-119.

Horton, R. M., Hunt, H. D., Ho, S. N., Pullen, J. K., and Pease, L. R. (1989). Engineering hybrid genes without the use of restriction enzymes: gene splicing by overlap extension. Gene *77*, 61-68.

Houseley, J., Kotovic, K., El Hage, A., and Tollervey, D. (2007). Trf4 targets ncRNAs from telomeric and rDNA spacer regions and functions in rDNA copy number control. EMBO J *26*, 4996-5006.

Huet, J., Buhler, J. M., Sentenac, A., and Fromageot, P. (1975). Dissociation of two polypeptide chains from yeast RNA polymerase A. Proc. Natl. Acad. Sci. U.S.A *72*, 3034-3038.

Hughes, J. M., and Ares, M., Jr (1991). Depletion of U3 small nucleolar RNA inhibits cleavage in the 5′ external transcribed spacer of yeast pre-ribosomal RNA and impairs formation of 18S ribosomal RNA. EMBO J *10*, 4231-4239.

Huh, W.-K., Falvo, J. V., Gerke, L. C., Carroll, A. S., Howson, R. W., Weissman, J. S., and O'Shea, E. K. (2003). Global analysis of protein localization in budding yeast. Nature *425*, 686-691.

Huibregtse, J. M., Yang, J. C., and Beaudenon, S. L. (1997). The large subunit of RNA polymerase II is a substrate of the Rsp5 ubiquitin-protein ligase. Proc. Natl. Acad. Sci. U.S.A *94*, 3656-3661.

Ide, S., Miyazaki, T., Maki, H., and Kobayashi, T. (2010). Abundance of ribosomal RNA gene copies maintains genome integrity. Science *327*, 693-696.

Ishihama, A. (1981). Subunit of assembly of Escherichia coli RNA polymerase. Adv. Biophys *14*, 1-35.

Jansa, P., and Grummt, I. (1999). Mechanism of transcription termination: PTRF interacts with the largest subunit of RNA polymerase I and dissociates paused transcription complexes from yeast and mouse. Mol. Gen. Genet *262*, 508-514.

Jasiak, A. J., Armache, K.-J., Martens, B., Jansen, R.-P., and Cramer, P. (2006). Structural biology of RNA polymerase III: subcomplex C17/25 X-ray structure and 11 subunit enzyme model. Mol. Cell *23*, 71-81.

Jeon, C., Yoon, H., and Agarwal, K. (1994). The transcription factor TFIIS zinc ribbon dipeptide Asp-Glu is critical for stimulation of elongation and RNA cleavage by RNA polymerase II. Proc. Natl. Acad. Sci. U.S.A *91*, 9106-9110.

Jeong, S. W., Lang, W. H., and Reeder, R. H. (1995). The release element of the yeast polymerase I transcription terminator can function independently of Reb1p. Mol. Cell. Biol *15*, 5929-5936.

Johnson, L. N., and Lewis, R. J. (2001). Structural basis for control by phosphorylation. Chem. Rev *101*, 2209-2242.

Johnson, L. N., and O'Reilly, M. (1996). Control by phosphorylation. Curr. Opin. Struct. Biol *6*, 762-769.

Jorgensen, P., Nishikawa, J. L., Breitkreutz, B.-J., and Tyers, M. (2002). Systematic identification of pathways that couple cell growth and division in yeast. Science *297*, 395-400.

Jorgensen, P., Rupes, I., Sharom, J. R., Schneper, L., Broach, J. R., and Tyers, M. (2004). A dynamic transcriptional network communicates growth potential to ribosome synthesis and critical cell size. Genes Dev *18*, 2491-2505.

Ju, Q. D., Morrow, B. E., and Warner, J. R. (1990). REB1, a yeast DNA-binding protein with many targets, is essential for growth and bears some resemblance to the oncogene myb. Mol. Cell. Biol *10*, 5226-5234.

Kawauchi, J., Mischo, H., Braglia, P., Rondon, A., and Proudfoot, N. J. (2008). Budding yeast RNA polymerases I and II employ parallel mechanisms of transcriptional termination. Genes Dev *22*, 1082-1092.

Keener, J., Dodd, J. A., Lalo, D., and Nomura, M. (1997). Histones H3 and H4 are components of upstream activation factor required for the high-level transcription of yeast rDNA by RNA polymerase I. Proc. Natl. Acad. Sci. U.S.A *94*, 13458-13462.

Keener, J., Josaitis, C. A., Dodd, J. A., and Nomura, M. (1998). Reconstitution of yeast RNA polymerase I transcription in vitro from purified components. TATA-binding protein is not required for basal transcription. J. Biol. Chem *273*, 33795-33802.

Kettenberger, H., Armache, K.-J., and Cramer, P. (2003). Architecture of the RNA polymerase II-TFIIS complex and implications for mRNA cleavage. Cell *114*, 347-357.

Keys, D. A., Lee, B. S., Dodd, J. A., Nguyen, T. T., Vu, L., Fantino, E., Burson, L. M., Nogi, Y., and Nomura, M. (1996). Multiprotein transcription factor UAF interacts with the upstream element of the yeast RNA polymerase I promoter and forms a stable preinitiation complex. Genes Dev *10*, 887-903.

Keys, D. A., Vu, L., Steffan, J. S., Dodd, J. A., Yamamoto, R. T., Nogi, Y., and Nomura, M. (1994). RRN6 and RRN7 encode subunits of a multiprotein complex essential for the initiation of rDNA transcription by RNA polymerase I in Saccharomyces cerevisiae. Genes Dev *8*, 2349-2362.

Klinger, C., Huet, J., Song, D., Petersen, G., Riva, M., Bautz, E. K., Sentenac, A., Oudet, P., and Schultz, P. (1996). Localization of yeast RNA polymerase I core subunits by immunoelectron microscopy. EMBO J *15*, 4643-4653.

de Kloet, S. R. (1966). Ribonucleic acid synthesis in yeast. The effect of cycloheximide on the synthesis of ribonucleic acid in Saccharomyces carlsbergensis. Biochem. J *99*, 566-581.

Knop, M., Siegers, K., Pereira, G., Zachariae, W., Winsor, B., Nasmyth, K., and Schiebel, E. (1999). Epitope tagging of yeast genes using a PCR-based strategy: more tags and improved practical routines. Yeast *15*, 963-972.

Kobayashi, T., and Horiuchi, T. (1996). A yeast gene product, Fob1 protein, required for both replication fork blocking and recombinational hotspot activities. Genes Cells *1*, 465-474.

Kobayashi, T., Heck, D. J., Nomura, M., and Horiuchi, T. (1998). Expansion and contraction of ribosomal DNA repeats in Saccharomyces cerevisiae: requirement of replication fork blocking (Fob1) protein and the role of RNA polymerase I. Genes Dev *12*, 3821-3830.

Kobayashi, T., Hidaka, M., Nishizawa, M., and Horiuchi, T. (1992). Identification of a site required for DNA replication fork blocking activity in the rRNA gene cluster in Saccharomyces cerevisiae. Mol. Gen. Genet *233*, 355-362.

Kobayashi, T., Nomura, M., and Horiuchi, T. (2001). Identification of DNA cis elements essential for expansion of ribosomal DNA repeats in Saccharomyces cerevisiae. Mol. Cell. Biol *21*, 136-147.

Kobayashi, T. (2003). The replication fork barrier site forms a unique structure with Fob1p and inhibits the replication fork. Mol. Cell. Biol *23*, 9178-9188.

Kobayashi, T., Horiuchi, T., Tongaonkar, P., Vu, L., and Nomura, M. (2004). SIR2 regulates recombination between different rDNA repeats, but not recombination within individual rRNA genes in yeast. Cell *117*, 441-453.

Kos, M., and Tollervey, D. (2010). Yeast pre-rRNA processing and modification occur cotranscriptionally. Mol. Cell *37*, 809-820.

Kruiswijk, T., Planta, R. J., and Krop, J. M. (1978). The course of the assembly of ribosomal subunits in yeast. Biochim. Biophys. Acta *517*, 378-389.

Kufel, J., Dichtl, B., and Tollervey, D. (1999). Yeast Rnt1p is required for cleavage of the pre-ribosomal RNA in the 3' ETS but not the 5' ETS. RNA *5*, 909-917.

Kuhn, A., Bartsch, I., and Grummt, I. (1990). Specific interaction of the murine transcription termination factor TTF I with class-I RNA polymerases. Nature *344*, 559-562.

Kuhn, C.-D., Geiger, S. R., Baumli, S., Gartmann, M., Gerber, J., Jennebach, S., Mielke, T., Tschochner, H., Beckmann, R., and Cramer, P. (2007). Functional architecture of RNA polymerase I. Cell *131*, 1260-1272.

Kulkens, T., Riggs, D. L., Heck, J. D., Planta, R. J., and Nomura, M. (1991). The yeast RNA polymerase I promoter: ribosomal DNA sequences involved in transcription initiation and complex formation in vitro. Nucleic Acids Res *19*, 5363-5370.

Laemmli, U. K. (1970). Cleavage of structural proteins during the assembly of the head of bacteriophage T4. Nature *227*, 680-685.

Laferté, A., Favry, E., Sentenac, A., Riva, M., Carles, C., and Chédin, S. (2006). The transcriptional activity of RNA polymerase I is a key determinant for the level of all ribosome components. Genes Dev *20*, 2030-2040.

Lalo, D., Carles, C., Sentenac, A., and Thuriaux, P. (1993). Interactions between three common subunits of yeast RNA polymerases I and III. Proc. Natl. Acad. Sci. U.S.A *90*, 5524-5528.

Lalo, D., Steffan, J. S., Dodd, J. A., and Nomura, M. (1996). RRN11 encodes the third subunit of the complex containing Rrn6p and Rrn7p that is essential for the initiation of rDNA transcription by yeast RNA polymerase I. J. Biol. Chem *271*, 21062-21067.

Landrieux, E., Alic, N., Ducrot, C., Acker, J., Riva, M., and Carles, C. (2006). A subcomplex of RNA polymerase III subunits involved in transcription termination and reinitiation. EMBO J *25*, 118-128.

Lang, W. H., and Reeder, R. H. (1993). The REB1 site is an essential component of a terminator for RNA polymerase I in Saccharomyces cerevisiae. Mol. Cell. Biol *13*, 649-658.

Lang, W. H., and Reeder, R. H. (1995). Transcription termination of RNA polymerase I due to a T-rich element interacting with Reb1p. Proc. Natl. Acad. Sci. U.S.A *92*, 9781-9785.

REFERENCES

Lanzendörfer, M., Smid, A., Klinger, C., Schultz, P., Sentenac, A., Carles, C., and Riva, M. (1997). A shared subunit belongs to the eukaryotic core RNA polymerase. Genes Dev *11*, 1037-1047.

Lee, Y., Kim, M., Han, J., Yeom, K.-H., Lee, S., Baek, S. H., and Kim, V. N. (2004). MicroRNA genes are transcribed by RNA polymerase II. EMBO J *23*, 4051-4060.

Léger-Silvestre, I., Trumtel, S., Noaillac-Depeyre, J., and Gas, N. (1999). Functional compartmentalization of the nucleus in the budding yeast Saccharomyces cerevisiae. Chromosoma *108*, 103-113.

Lempiäinen, H., and Shore, D. (2009). Growth control and ribosome biogenesis. Curr. Opin. Cell Biol *21*, 855-863.

Li, B., Carey, M., and Workman, J. L. (2007a). The role of chromatin during transcription. Cell *128*, 707-719.

Li, H., Tsang, C. K., Watkins, M., Bertram, P. G., and Zheng, X. F. S. (2006). Nutrient regulates Tor1 nuclear localization and association with rDNA promoter. Nature *442*, 1058-1061.

Li, X., Gerber, S. A., Rudner, A. D., Beausoleil, S. A., Haas, W., Villén, J., Elias, J. E., and Gygi, S. P. (2007b). Large-scale phosphorylation analysis of alpha-factor-arrested Saccharomyces cerevisiae. J. Proteome Res *6*, 1190-1197.

Liaw, P. C., and Brandl, C. J. (1994). Defining the sequence specificity of the Saccharomyces cerevisiae DNA binding protein REB1p by selecting binding sites from random-sequence oligonucleotides. Yeast *10*, 771-787.

Liljelund, P., Mariotte, S., Buhler, J. M., and Sentenac, A. (1992). Characterization and mutagenesis of the gene encoding the A49 subunit of RNA polymerase A in Saccharomyces cerevisiae. Proc. Natl. Acad. Sci. U.S.A *89*, 9302-9305.

Linskens, M. H., and Huberman, J. A. (1988). Organization of replication of ribosomal DNA in Saccharomyces cerevisiae. Mol. Cell. Biol *8*, 4927-4935.

Lowary, P. T., and Widom, J. (1998). New DNA sequence rules for high affinity binding to histone octamer and sequence-directed nucleosome positioning. J. Mol. Biol *276*, 19-42.

Lucioli, A., Presutti, C., Ciafrè, S., Caffarelli, E., Fragapane, P., and Bozzoni, I. (1988). Gene dosage alteration of L2 ribosomal protein genes in Saccharomyces cerevisiae: effects on ribosome synthesis. Mol. Cell. Biol *8*, 4792-4798.

Magnusson, L. U., Farewell, A., and Nyström, T. (2005). ppGpp: a global regulator in Escherichia coli. Trends Microbiol *13*, 236-242.

Makeyev, E. V., and Bamford, D. H. (2002). Cellular RNA-dependent RNA polymerase involved in posttranscriptional gene silencing has two distinct activity modes. Mol. Cell *10*, 1417-1427.

Mann, C., Buhler, J. M., Treich, I., and Sentenac, A. (1987). RPC40, a unique gene for a subunit shared between yeast RNA polymerases A and C. Cell *48*, 627-637.

Marion, R. M., Regev, A., Segal, E., Barash, Y., Koller, D., Friedman, N., and O'Shea, E. K. (2004). Sfp1 is a stress- and nutrient-sensitive regulator of ribosomal protein gene expression. Proc. Natl. Acad. Sci. U.S.A *101*, 14315-14322.

Mason, P. B., and Struhl, K. (2005). Distinction and relationship between elongation rate and processivity of RNA polymerase II in vivo. Mol. Cell *17*, 831-840.

Mason, S. W., Sander, E. E., and Grummt, I. (1997a). Identification of a transcript release activity acting on ternary transcription complexes containing murine RNA polymerase I. EMBO J *16*, 163-172.

Mason, S. W., Wallisch, M., and Grummt, I. (1997b). RNA polymerase I transcription termination: similar mechanisms are employed by yeast and mammals. J. Mol. Biol *268*, 229-234.

Mémet, S., Gouy, M., Marck, C., Sentenac, A., and Buhler, J. M. (1988). RPA190, the gene coding for the largest subunit of yeast RNA polymerase A. J. Biol. Chem *263*, 2830-2839.

Merz, K., Hondele, M., Goetze, H., Gmelch, K., Stoeckl, U., and Griesenbeck, J. (2008). Actively transcribed rRNA genes in S. cerevisiae are organized in a specialized chromatin associated with the high-mobility group protein Hmo1 and are largely devoid of histone molecules. Genes Dev *22*, 1190-1204.

Milkereit, P., and Tschochner, H. (1998). A specialized form of RNA polymerase I, essential for initiation and growth-dependent regulation of rRNA synthesis, is disrupted during transcription. EMBO J *17*, 3692-3703.

Minakhin, L., Bhagat, S., Brunning, A., Campbell, E. A., Darst, S. A., Ebright, R. H., and Severinov, K. (2001). Bacterial RNA polymerase subunit omega and eukaryotic RNA polymerase subunit RPB6 are sequence, structural, and functional homologs and promote RNA polymerase assembly. Proc. Natl. Acad. Sci. U.S.A *98*, 892-897.

Mitchell, P., Petfalski, E., Shevchenko, A., Mann, M., and Tollervey, D. (1997). The exosome: a conserved eukaryotic RNA processing complex containing multiple 3'-->5' exoribonucleases. Cell *91*, 457-466.

Mohanty, B. K., and Bastia, D. (2004). Binding of the replication terminator protein Fob1p to the Ter sites of yeast causes polar fork arrest. J. Biol. Chem *279*, 1932-1941.

Moss, T. (2004). At the crossroads of growth control; making ribosomal RNA. Curr. Opin. Genet. Dev *14*, 210-217.

Muhlrad, D., Hunter, R., and Parker, R. (1992). A rapid method for localized mutagenesis of yeast genes. Yeast *8*, 79-82.

Mullem, V. V., Landrieux, E., Vandenhaute, J., and Thuriaux, P. (2002). Rpa12p, a conserved RNA polymerase I subunit with two functional domains. Molecular Microbiology *43*, 1105-1113.

Musters, W., Knol, J., Maas, P., Dekker, A. F., van Heerikhuizen, H., and Planta, R. J. (1989). Linker scanning of the yeast RNA polymerase I promoter. Nucleic Acids Res *17*, 9661-9678.

Nazar, R. N. (2004). Ribosomal RNA processing and ribosome biogenesis in eukaryotes. IUBMB Life *56*, 457-465.

Németh, A., Strohner, R., Grummt, I., and Längst, G. (2004). The chromatin remodeling complex NoRC and TTF-I cooperate in the regulation of the mammalian rRNA genes in vivo. Nucleic Acids Res *32*, 4091-4099.

Nogi, Y., Yano, R., Dodd, J., Carles, C., and Nomura, M. (1993). Gene RRN4 in Saccharomyces cerevisiae encodes the A12.2 subunit of RNA polymerase I and is essential only at high temperatures. Mol. Cell. Biol *13*, 114-122.

Nouraini, S., Archambault, J., and Friesen, J. D. (1996). Rpo26p, a subunit common to yeast RNA polymerases, is essential for the assembly of RNA polymerases I and II and for the stability of the largest subunits of these enzymes. Mol. Cell. Biol *16*, 5985-5996.

O'Donohue, M.-F., Choesmel, V., Faubladier, M., Fichant, G., and Gleizes, P.-E. (2010). Functional dichotomy of ribosomal proteins during the synthesis of mammalian 40S ribosomal subunits. J. Cell Biol *190*, 853-866.

Osheim, Y. N., French, S. L., Keck, K. M., Champion, E. A., Spasov, K., Dragon, F., Baserga, S. J., and Beyer, A. L. (2004). Pre-18S ribosomal RNA is structurally compacted into the SSU processome prior to being cleaved from nascent transcripts in Saccharomyces cerevisiae. Mol. Cell *16*, 943-954.

Osheim, Y. N., French, S. L., Sikes, M. L., and Beyer, A. L. (2009). Electron microscope visualization of RNA transcription and processing in Saccharomyces cerevisiae by Miller chromatin spreading. Methods Mol. Biol *464*, 55-69.

Panse, V. G., Hardeland, U., Werner, T., Kuster, B., and Hurt, E. (2004). A proteome-wide approach identifies sumoylated substrate proteins in yeast. J. Biol. Chem *279*, 41346-41351.

Paule, M. R. (1999). Transcription of Ribosomal RNA Genes by Eukaryotic RNA Polymerase I (Springer, Berlin).

Pazin, M. J., and Kadonaga, J. T. (1997). What's up and down with histone deacetylation and transcription? Cell *89*, 325-328.

Petes, T. D. (1979). Yeast ribosomal DNA genes are located on chromosome XII. Proc. Natl. Acad. Sci. U.S.A *76*, 410-414.

Peyroche, G., Milkereit, P., Bischler, N., Tschochner, H., Schultz, P., Sentenac, A., Carles, C., and Riva, M. (2000). The recruitment of RNA polymerase I on rDNA is mediated by the interaction of the A43 subunit with Rrn3. EMBO J *19*, 5473-5482.

Peyroche, G., Levillain, E., Siaut, M., Callebaut, I., Schultz, P., Sentenac, A., Riva, M., and Carles, C. (2002). The A14-A43 heterodimer subunit in yeast RNA pol I and their relationship to Rpb4-Rpb7 pol II subunits. Proc. Natl. Acad. Sci. U.S.A *99*, 14670-14675.

Phatnani, H. P., and Greenleaf, A. L. (2006). Phosphorylation and functions of the RNA polymerase II CTD. Genes Dev *20*, 2922-2936.

Philippi, A. (2007). Untersuchungen zur Rolle des Transkriptionsfaktors Rrn3p in der wachstumsabhängigen Regulation der rRNA-Synthese.

Philippi, A., Steinbauer, R., Reiter, A., Fath, S., Leger-Silvestre, I., Milkereit, P., Griesenbeck, J., and Tschochner, H. (2010). TOR-dependent reduction in the expression level of Rrn3p lowers the activity of the yeast RNA Pol I machinery, but does not account for the strong inhibition of rRNA production. Nucleic Acids Res *38*, 5315-5326.

Philippsen, P., Thomas, M., Kramer, R. A., and Davis, R. W. (1978). Unique arrangement of coding sequences for 5 S, 5.8 S, 18 S and 25 S ribosomal RNA in Saccharomyces cerevisiae as determined by R-loop and hybridization analysis. J. Mol. Biol *123*, 387-404.

Pilsl, M. (2010). Analyse von RNA-Polymerase I - Mutanten.

Pleiss, J. A., Whitworth, G. B., Bergkessel, M., and Guthrie, C. (2007). Rapid, transcript-specific changes in splicing in response to environmental stress. Mol. Cell *27*, 928-937.

Pogulis, R. J., Vallejo, A. N., and Pease, L. R. (1996). In vitro recombination and mutagenesis by overlap extension PCR. Methods Mol. Biol *57*, 167-176.

Pöll, G., Braun, T., Jakovljevic, J., Neueder, A., Jakob, S., Woolford, J. L., Jr, Tschochner, H., and Milkereit, P. (2009). rRNA maturation in yeast cells depleted of large ribosomal subunit proteins. PLoS ONE *4*, e8249.

Powers, T., and Walter, P. (1999). Regulation of ribosome biogenesis by the rapamycin-sensitive TOR-signaling pathway in Saccharomyces cerevisiae. Mol. Biol. Cell *10*, 987-1000.

Prescott, E. M., Osheim, Y. N., Jones, H. S., Alen, C. M., Roan, J. G., Reeder, R. H., Beyer, A. L., and Proudfoot, N. J. (2004). Transcriptional termination by RNA polymerase I requires the small subunit Rpa12p. Proc. Natl. Acad. Sci. U.S.A *101*, 6068-6073.

Prieto, J.-L., and McStay, B. (2007). Recruitment of factors linking transcription and processing of pre-rRNA to NOR chromatin is UBF-dependent and occurs independent of transcription in human cells. Genes Dev *21*, 2041-2054.

Reeder, R. H., and Lang, W. H. (1997). Terminating transcription in eukaryotes: lessons learned from RNA polymerase I. Trends Biochem. Sci *22*, 473-477.

Reeder, R. H., Guevara, P., and Roan, J. G. (1999). Saccharomyces cerevisiae RNA polymerase I terminates transcription at the Reb1 terminator in vivo. Mol. Cell. Biol *19*, 7369-7376.

Reinberg, D., and Sims, R. J., 3rd (2006). de FACTo nucleosome dynamics. J. Biol. Chem *281*, 23297-23301.

Reines, D., and Mote, J., Jr (1993). Elongation factor SII-dependent transcription by RNA polymerase II through a sequence-specific DNA-binding protein. Proc. Natl. Acad. Sci. U.S.A *90*, 1917-1921.

Reiter, A. (2007). In vitro- und in vivo-Analysen von RNA-Polymerase I Mutanten.

Reiter, A., Steinbauer, R., Philippi, A., Gerber, J., Tschochner, H., Milkereit, P., and Griesenbeck, J. (2011). Reduction in ribosomal protein synthesis is sufficient to explain major effects on ribosome production after short-term TOR inactivation in Saccharomyces cerevisiae. Mol. Cell. Biol *31*, 803-817.

Remacle, J. E., and Holmberg, S. (1992). A REB1-binding site is required for GCN4-independent ILV1 basal level transcription and can be functionally replaced by an ABF1-binding site. Mol. Cell. Biol *12*, 5516-5526.

Robledo, S., Idol, R. A., Crimmins, D. L., Ladenson, J. H., Mason, P. J., and Bessler, M. (2008). The role of human ribosomal proteins in the maturation of rRNA and ribosome production. RNA *14*, 1918-1929.

Roeder, R. G., and Rutter, W. J. (1969). Multiple forms of DNA-dependent RNA polymerase in eukaryotic organisms. Nature *224*, 234-237.

Rosbash, M., Harris, P. K., Woolford, J. L., Jr, and Teem, J. L. (1981). The effect of temperature-sensitive RNA mutants on the transcription products from cloned ribosomal protein genes of yeast. Cell *24*, 679-686.

Ross, P. L., Huang, Y. N., Marchese, J. N., Williamson, B., Parker, K., Hattan, S., Khainovski, N., Pillai, S., Dey, S., Daniels, S., et al. (2004). Multiplexed protein quantitation in Saccharomyces cerevisiae using amine-reactive isobaric tagging reagents. Mol. Cell Proteomics *3*, 1154-1169.

Ruan, W., Lehmann, E., Thomm, M., Kostrewa, D., and Cramer, P. (2011). Evolution of two modes of intrinsic RNA polymerase transcript cleavage. J Biol Chem. Available at: http://www.ncbi.nlm.nih.gov/pubmed/21454497 [Accessed May 4, 2011].

Rubbi, L., Labarre-Mariotte, S., Chédin, S., and Thuriaux, P. (1999). Functional characterization of ABC10alpha, an essential polypeptide shared by all three forms of eukaryotic DNA-dependent RNA polymerases. J. Biol. Chem *274*, 31485-31492.

Rubin, G. M., and Sulston, J. E. (1973). Physical linkage of the 5 S cistrons to the 18 S and 28 S ribosomal RNA cistrons in Saccharomyces cerevisiae. J. Mol. Biol *79*, 521-530.

Rudra, D., Zhao, Y., and Warner, J. R. (2005). Central role of Ifh1p-Fhl1p interaction in the synthesis of yeast ribosomal proteins. EMBO J *24*, 533-542.

Santillán, M., and Mackey, M. C. (2008). Quantitative approaches to the study of bistability in the lac operon of Escherichia coli. J R Soc Interface *5 Suppl 1*, S29-39.

Schawalder, S. B., Kabani, M., Howald, I., Choudhury, U., Werner, M., and Shore, D. (2004). Growth-regulated recruitment of the essential yeast ribosomal protein gene activator Ifh1. Nature *432*, 1058-1061.

Schmid, M., Durussel, T., and Laemmli, U. K. (2004). ChIC and ChEC; genomic mapping of chromatin proteins. Mol. Cell *16*, 147-157.

Schmitt, M. E., Brown, T. A., and Trumpower, B. L. (1990). A rapid and simple method for preparation of RNA from Saccharomyces cerevisiae. Nucleic Acids Res *18*, 3091-3092.

Schneider, D. A., French, S. L., Osheim, Y. N., Bailey, A. O., Vu, L., Dodd, J., Yates, J. R., Beyer, A. L., and Nomura, M. (2006). RNA polymerase II elongation factors Spt4p and Spt5p play roles in transcription elongation by RNA polymerase I and rRNA processing. Proc. Natl. Acad. Sci. U.S.A *103*, 12707-12712.

Schneider, D. A., Michel, A., Sikes, M. L., Vu, L., Dodd, J. A., Salgia, S., Osheim, Y. N., Beyer, A. L., and Nomura, M. (2007). Transcription elongation by RNA polymerase I is linked to efficient rRNA processing and ribosome assembly. Mol. Cell *26*, 217-229.

Schultz, P., Célia, H., Riva, M., Sentenac, A., and Oudet, P. (1993). Three-dimensional model of yeast RNA polymerase I determined by electron microscopy of two-dimensional crystals. EMBO J *12*, 2601-2607.

Schwarzacher, H. G., and Wachtler, F. (1993). The nucleolus. Anat. Embryol *188*, 515-536.

Schweizer, E., and Halvorson, H. O. (1969). On the regulation of ribosomal RNA synthesis in yeast. Exp. Cell Res *56*, 239-244.

Sherman, F. (2002). Getting started with yeast. Meth. Enzymol *350*, 3-41.

Shilatifard, A. (2004). Transcriptional elongation control by RNA polymerase II: a new frontier. Biochim. Biophys. Acta *1677*, 79-86.

Siddiqi, I. N., Dodd, J. A., Vu, L., Eliason, K., Oakes, M. L., Keener, J., Moore, R., Young, M. K., and Nomura, M. (2001). Transcription of chromosomal rRNA genes by both RNA polymerase I and II in yeast uaf30 mutants lacking the 30 kDa subunit of transcription factor UAF. EMBO J *20*, 4512-4521.

Sigurdsson, S., Dirac-Svejstrup, A. B., and Svejstrup, J. Q. (2010). Evidence that transcript cleavage is essential for RNA polymerase II transcription and cell viability. Mol. Cell *38*, 202-210.

Sikorski, R. S., and Boeke, J. D. (1991). In vitro mutagenesis and plasmid shuffling: from cloned gene to mutant yeast. Meth. Enzymol *194*, 302-318.

Sikorski, R. S., and Hieter, P. (1989). A system of shuttle vectors and yeast host strains designed for efficient manipulation of DNA in Saccharomyces cerevisiae. Genetics *122*, 19-27.

Smid, A., Riva, M., Bouet, F., Sentenac, A., and Carles, C. (1995). The association of three subunits with yeast RNA polymerase is stabilized by A14. J. Biol. Chem *270*, 13534-13540.

Somesh, B. P., Reid, J., Liu, W.-F., Søgaard, T. M. M., Erdjument-Bromage, H., Tempst, P., and Svejstrup, J. Q. (2005). Multiple mechanisms confining RNA polymerase II ubiquitylation to polymerases undergoing transcriptional arrest. Cell *121*, 913-923.

Somesh, B. P., Sigurdsson, S., Saeki, H., Erdjument-Bromage, H., Tempst, P., and Svejstrup, J. Q. (2007). Communication between distant sites in RNA polymerase II through ubiquitylation factors and the polymerase CTD. Cell *129*, 57-68.

Song, J. M., Cheung, E., and Rabinowitz, J. C. (1996). Organization and characterization of the two yeast ribosomal protein YL19 genes. Curr. Genet *30*, 273-278.

Song, X., and Nazar, R. N. (2002). Modification of rRNA as a "quality control mechanism" in ribosome biogenesis. FEBS Lett *523*, 182-186.

Spingola, M., Grate, L., Haussler, D., and Ares, M., Jr (1999). Genome-wide bioinformatic and molecular analysis of introns in Saccharomyces cerevisiae. RNA *5*, 221-234.

Stefanovsky, V., Langlois, F., Gagnon-Kugler, T., Rothblum, L. I., and Moss, T. (2006). Growth factor signaling regulates elongation of RNA polymerase I transcription in mammals via UBF phosphorylation and r-chromatin remodeling. Mol. Cell *21*, 629-639.

Steffan, J. S., Keys, D. A., Dodd, J. A., and Nomura, M. (1996). The role of TBP in rDNA transcription by RNA polymerase I in Saccharomyces cerevisiae: TBP is required for upstream activation factor-dependent recruitment of core factor. Genes Dev *10*, 2551-2563.

Steffan, J. S., Keys, D. A., Vu, L., and Nomura, M. (1998). Interaction of TATA-binding protein with upstream activation factor is required for activated transcription of ribosomal DNA by RNA polymerase I in Saccharomyces cerevisiae in vivo. Mol. Cell. Biol *18*, 3752-3761.

Steinbauer, R. (2010). Growth-dependent regulation of ribosome biogenesis and the role of Rrn3p in RNA polymerase I transcription.

Suthers, P. F., Gourse, R. L., and Yin, J. (2007). Rapid responses of ribosomal RNA synthesis to nutrient shifts. Biotechnol. Bioeng *97*, 1230-1245.

Svejstrup, J. Q. (2007). Contending with transcriptional arrest during RNAPII transcript elongation. Trends Biochem. Sci *32*, 165-171.

Thomas, B. J., and Rothstein, R. (1989). Elevated recombination rates in transcriptionally active DNA. Cell *56*, 619-630.

Thuriaux, P., Mariotte, S., Buhler, J. M., Sentenac, A., Vu, L., Lee, B. S., and Nomura, M. (1995). Gene RPA43 in Saccharomyces cerevisiae encodes an essential subunit of RNA polymerase I. J. Biol. Chem *270*, 24252-24257.

Toulmé, F., Mosrin-Huaman, C., Sparkowski, J., Das, A., Leng, M., and Rahmouni, A. R. (2000). GreA and GreB proteins revive backtracked RNA polymerase in vivo by promoting transcript trimming. EMBO J *19*, 6853-6859.

Treich, I., Carles, C., Riva, M., and Sentenac, A. (1992). RPC10 encodes a new mini subunit shared by yeast nuclear RNA polymerases. Gene Expr *2*, 31-37.

Tschochner, H., and Hurt, E. (2003). Pre-ribosomes on the road from the nucleolus to the cytoplasm. Trends Cell Biol *13*, 255-263.

Udem, S. A., and Warner, J. R. (1972). Ribosomal RNA synthesis in Saccharomyces cerevisiae. J. Mol. Biol *65*, 227-242.

Vallejo, A. N., Pogulis, R. J., and Pease, L. R. (2008). PCR Mutagenesis by Overlap Extension and Gene SOE. Cold Spring Harb Protoc *2008*, pdb.prot4861.

Vanrobays, E., Leplus, A., Osheim, Y. N., Beyer, A. L., Wacheul, L., and Lafontaine, D. L. J. (2008). TOR regulates the subcellular distribution of DIM2, a KH domain protein required for cotranscriptional ribosome assembly and pre-40S ribosome export. RNA *14*, 2061-2073.

Vassylyev, D. G., Sekine, S.-ichi, Laptenko, O., Lee, J., Vassylyeva, M. N., Borukhov, S., and Yokoyama, S. (2002). Crystal structure of a bacterial RNA polymerase holoenzyme at 2.6 A resolution. Nature *417*, 712-719.

Venema, J., and Tollervey, D. (1995). Processing of pre-ribosomal RNA in Saccharomyces cerevisiae. Yeast *11*, 1629-1650.

Viktorovskaya, O. V., Appling, F. D., and Schneider, D. A. (2011). Yeast transcription elongation factor SPT5 associates with RNA polymerase I and RNA polymerase II directly. J Biol Chem. Available at: http://www.ncbi.nlm.nih.gov/pubmed/21467036 [Accessed April 13, 2011].

Wagner, R. (2002). Regulation of ribosomal RNA synthesis in E. coli: effects of the global regulator guanosine tetraphosphate (ppGpp). J. Mol. Microbiol. Biotechnol *4*, 331-340.

Wai, H. H., Vu, L., Oakes, M., and Nomura, M. (2000). Complete deletion of yeast chromosomal rDNA repeats and integration of a new rDNA repeat: use of rDNA deletion strains for functional analysis of rDNA promoter elements in vivo. Nucleic Acids Res *28*, 3524-3534.

Wang, K. L., and Warner, J. R. (1998). Positive and negative autoregulation of REB1 transcription in Saccharomyces cerevisiae. Mol. Cell. Biol *18*, 4368-4376.

Warner, J. R. (1989). Synthesis of ribosomes in Saccharomyces cerevisiae. Microbiol. Rev *53*, 256-271.

Warner, J. R. (1999). The economics of ribosome biosynthesis in yeast. Trends Biochem. Sci *24*, 437-440.

Warner, J. R., and Gorenstein, C. (1978). Yeast has a true stringent response. Nature *275*, 338-339.

Warner, J. R., and Udem, S. A. (1972). Temperature sensitive mutations affecting ribosome synthesis in Saccharomyces cerevisiae. J. Mol. Biol *65*, 243-257.

Weiss, S. B. (1960). Enzymatic incorporation of ribonucleoside triphosphates into the interpolynucleotide linkages of ribonucleic acid. Proc. Natl. Acad. Sci. U.S.A *46*, 1020-1030.

Wery, M., Ruidant, S., Schillewaert, S., Leporé, N., and Lafontaine, D. L. J. (2009). The nuclear poly(A) polymerase and Exosome cofactor Trf5 is recruited cotranscriptionally to nucleolar surveillance. RNA *15*, 406-419.

Wessel, D., and Flügge, U. I. (1984). A method for the quantitative recovery of protein in dilute solution in the presence of detergents and lipids. Anal. Biochem *138*, 141-143.

Whelan, W. L., Gocke, E., and Manney, T. R. (1979). The CAN1 locus of Saccharomyces cerevisiae: fine-structure analysis and forward mutation rates. Genetics *91*, 35-51.

Wierzbicki, A. T., Ream, T. S., Haag, J. R., and Pikaard, C. S. (2009). RNA polymerase V transcription guides ARGONAUTE4 to chromatin. Nat. Genet *41*, 630-634.

Wild, T. (2005). Modifizierung des endogenen rDNA Lokuses in Saccharomyces cerevisiae zur biochemischen Analyse der Chromatinstruktur.

Willis, I. M. (1993). RNA polymerase III. Genes, factors and transcriptional specificity. Eur. J. Biochem *212*, 1-11.

REFERENCES

Wittekind, M., Dodd, J., Vu, L., Kolb, J. M., Buhler, J. M., Sentenac, A., and Nomura, M. (1988). Isolation and characterization of temperature-sensitive mutations in RPA190, the gene encoding the largest subunit of RNA polymerase I from Saccharomyces cerevisiae. Mol. Cell. Biol *8*, 3997-4008.

Wittekind, M., Kolb, J. M., Dodd, J., Yamagishi, M., Mémet, S., Buhler, J. M., and Nomura, M. (1990). Conditional expression of RPA190, the gene encoding the largest subunit of yeast RNA polymerase I: effects of decreased rRNA synthesis on ribosomal protein synthesis. Mol. Cell. Biol *10*, 2049-2059.

Wittner, M., Hamperl, S., Stöckl, U., Seufert, W., Tschochner, H., Milkereit, P., and Griesenbeck, J. (2011). Establishment and maintenance of alternative chromatin States at a multicopy gene locus. Cell *145*, 543-554.

Woychik, N. A., Lane, W. S., and Young, R. A. (1991). Yeast RNA polymerase II subunit RPB9 is essential for growth at temperature extremes. J. Biol. Chem *266*, 19053-19055.

Woychik, N. A., Liao, S. M., Kolodziej, P. A., and Young, R. A. (1990). Subunits shared by eukaryotic nuclear RNA polymerases. Genes Dev *4*, 313-323.

Yamamoto, R. T., Nogi, Y., Dodd, J. A., and Nomura, M. (1996). RRN3 gene of Saccharomyces cerevisiae encodes an essential RNA polymerase I transcription factor which interacts with the polymerase independently of DNA template. EMBO J *15*, 3964-3973.

Yamazaki, K., Aso, T., Ohnishi, Y., Ohno, M., Tamura, K., Shuin, T., Kitajima, S., and Nakabeppu, Y. (2003). Mammalian elongin A is not essential for cell viability but is required for proper cell cycle progression with limited alteration of gene expression. J. Biol. Chem *278*, 13585-13589.

Yano, R., and Nomura, M. (1991). Suppressor analysis of temperature-sensitive mutations of the largest subunit of RNA polymerase I in Saccharomyces cerevisiae: a suppressor gene encodes the second-largest subunit of RNA polymerase I. Mol. Cell. Biol *11*, 754-764.

Zaragoza, D., Ghavidel, A., Heitman, J., and Schultz, M. C. (1998). Rapamycin induces the G0 program of transcriptional repression in yeast by interfering with the TOR signaling pathway. Mol. Cell. Biol *18*, 4463-4470.

Zebarjadian, Y., King, T., Fournier, M. J., Clarke, L., and Carbon, J. (1999). Point mutations in yeast CBF5 can abolish in vivo pseudouridylation of rRNA. Mol. Cell. Biol *19*, 7461-7472.

Zhang, G., Campbell, E. A., Minakhin, L., Richter, C., Severinov, K., and Darst, S. A. (1999). Crystal structure of Thermus aquaticus core RNA polymerase at 3.3 A resolution. Cell *98*, 811-824.

Zhang, Y., Sikes, M. L., Beyer, A. L., and Schneider, D. A. (2009). The Paf1 complex is required for efficient transcription elongation by RNA polymerase I. Proc. Natl. Acad. Sci. U.S.A *106*, 2153-2158.

Zhang, Y., Smith, A. D., 4th, Renfrow, M. B., and Schneider, D. A. (2010). The RNA polymerase-associated factor 1 complex (Paf1C) directly increases the elongation rate of RNA polymerase I and is required for efficient regulation of rRNA synthesis. J. Biol. Chem *285*, 14152-14159.

7 PUBLICATIONS

Reiter, A., Hamperl, S., Leger-Silvestre, I., Perez-Fernandez, J., Milkereit, P., Griesenbeck, J., Tschochner, H. (2011). Binding of the Reb1-homolog Tfr1 to the rDNA termination region is sufficient to terminate Pol I transcription *in vivo*. (manuscript in preparation)

Reiter*, A., Steinbauer*, R., Philippi*, A., Gerber, J., Tschochner, H., Milkereit, P., Griesenbeck, J. (2011). Reduction in ribosomal protein synthesis is sufficient to explain major effects on ribosome production after short-term TOR inactivation in Saccharomyces cerevisiae. Mol Cell Biol. 31, 803-817

Philippi*, A., Steinbauer*, R., Reiter*, A., Fath, S., Leger-Silvestre, I., Milkereit, P., Griesenbeck, J., Tschochner, H. (2010). TOR-dependent reduction in the expression level of Rrn3 lowers the activity of the yeast RNA Pol I machinery, but does not account for the strong inhibition of rRNA production. Nucleic Acids Research 38, 5315-5326

Gerber, J., Reiter, A., Steinbauer, R., Jakob, S., Kuhn, C., Cramer, P., Griesenbeck, J., Milkereit, P., Tschochner, H. (2008). Site specific phosphorylation of yeast RNA polymerase I. Nucleic Acids Research 36, 793-802

*   contributed equally

8 ABBREVIATIONS

A	ampere
Å	angstrom
amp	ampicillin
A/C	autonomous replication sequence/centromere (single copy)
ATP	adenosin triphosphate
bp	base pair(s)
CE/Core	core element
CF	core factor
ChEC	chromatin endogenous cleavage
ChIP	chromatin immunoprecipitation
CHX	cycloheximide
CoIP	co-immunoprecipitation
CSM	complete supplement mixture
C-terminal	carboxy-terminal
Da	dalton
DNA	desoxyribonucleic acid
dNTP	desoxyribonucleoside-5'-triphosphate
dox	doxycycline
E. coli	Escherichia coli
EDTA	ethylene diamine tetra acetate
EGTA	ethylene glycol tetraacetic acid
EtBr	ethidium bromide
ETS	external transcribed spacer
g	gram(s)
GAL	galactose
gen	geneticin
GLC	glucose
h	hour(s)
HA_3	triple hemagglutinin
HMG	high mobility group
hyg	hygromycin B
IGS	intergenic spacer
IN	input
IP	immunoprecipitation
iTRAQ	isobaric tag for relative and absolute quantitation

ITS	internal transcribed spacer
kb	kilo base pair(s)
l	liter(s)
LB	luria broth
LSU	large ribosomal subunit
m	milli / meter
M	molar (mol/l)
MALDI	matrix assisted laser desorption/ionization
min	minute(s)
MNase	micrococcal nuclease
mRNA	messenger RNA
MS	mass spectrometry
MW	molecular weight
n	nano
NTS	non-transcribed spacer
OD$_{600}$	optical density at 600 nm
PAGE	polyacrylamide gel electrophoresis
PCR	polymerase chain reaction
PEG	poly ethylene glycol
pGAL	galactose-inducible promoter (in this work usually GAL1-promoter)
pH	negative decadic logarithm [H$^+$]
PIP	phosphor-imaging plate
PKA	protein kinase A
PMSF	phenylmethylsulfonyl fluoride
Pol I	RNA polymerase I
Pol II	RNA polymerase II
Pol III	RNA polymerase III
Prot.A	protein A
qPCR	quantitative PCR
rDNA	ribosomal DNA
RAPA	rapamycin
RNA	ribonucleic acid
RNP	ribonucleoprotein particle
r-protein/RPs	ribosomal protein
rpm	rotations per minute
rRNA	ribosomal RNA
RT	room temperature
S	sedimentation coefficient

S. cerevisiae	Saccharomyces cerevisiae
SDC	synthetic dextrose complete
sec	second(s)
SGC	synthetic galactose complete
snoRNA	small nucleolar RNA
snoRNP	small nucleolar RNP
SOB	super optimal broth
SOE	splicing by overlap extension
SRC	synthetic raffinose complete
SSU	small ribosomal subunit
Taq	thermus aquaticus
TAP	tandem affinity tag
TBP	TATA-binding protein
TCA	tri chloro acetic acid
TEMED	tetramethylethylenediamine
TIP	tritium-imaging plate
TOR	target of rapamycin
TORC	target of rapamycin complex
ts	temperature sensitive
U	unit(s)
UAF	upstream activation factor
UE	upstream element
V	volt
v/v	volume/volume
WCE	whole cell extract
WT	wild type
w/v	weight/volume
YNB	yeast nitrogen base
YPD	yeast extract / peptone / dextrose
YPG	yeast extract / peptone / galactose
μ	micro
2μ	2 micron (multi copy)
5-FOA	5-fluoroorotic acid

Acknowledgments